

**The impact of yeast metabolites on the strain-dependent
rheological behavior of the polymeric wheat dough system in
relation to fermentation time and hydrothermal treatment**

Thekla Katharina Alpers

Vollständiger Abdruck der von der TUM School of Life Sciences der Technischen Universität München zur Erlangung einer

Doktorin der Ingenieurwissenschaften (Dr.-Ing.)
genehmigten Dissertation.

Vorsitz: Prof. Dr. Ute Weisz

Prüfende der Dissertation:

1. Prof. Dr.-Ing. Thomas Becker
2. Prof. Dr. Katharina Scherf
3. Prof. Dr.-Ing. Jörg Hinrichs

Die Dissertation wurde am 07.10.2024 bei der Technischen Universität München eingereicht
und durch die TUM School of Life Sciences am 12.03.2025 angenommen.

Acknowledgements

First, I thank Prof. Dr. Thomas Becker, who continuously offered advice and systematic guidance. His focus on the common thread of the thesis and his critical questions provided a valuable framework for this work. I appreciate the opportunities given during my graduation, where the unconstraint working environment was both challenging and empowering.

I would like to thank Prof. Dr. Mario Jekle for his supervision. His guidance, trust, and inspiration during our countless discussions paved the way for the development of the scope and methodology of this thesis. He enabled me to develop a scientific mindset and encouraged my personal development.

I would like to thank Prof. Dr. Katharina Scherf and Prof. Dr.-Ing. Jörg Hinrichs for reviewing and evaluating this thesis and Prof. Dr. Ute Weisz for accepting the assignment as chairperson.

Throughout the whole duration of my graduation, my colleagues from the Chair of Brewing and Beverage Technology were continuously supportive. I value the scientific, executive, and emotional support and advice given from all previous and current companions met along the way. The Research Group Cereal Process Engineering, in particular, stood close and was always supportive, making work always enjoyable.

A valuable source of emotional support originated from my friends, who hopefully grant pardon for my missing engagement during the final time invested in this thesis. Their belief was a strong pillar for this thesis.

Special thanks to my parents for their encouragement and enduring support. Our time together will always be a source of motivation and energy. Thank you for being patient and always standing by me.

I would like to express my deepest gratitude to Rola, who was an everlasting source of motivation. His believe in my skills gave me confidence and he provided selfless and unconditional support during all this time.

Preface

The practical work of this thesis was conducted at the Technical University of Munich, Chair of Brewing and Beverage Technology, Research Group Cereal Process Engineering from 2016 to 2021.

Peer-Reviewed Publications

The following **peer reviewed publications** (shown in chronological order) were generated in the period of work:

1. Alpers, T., Tauscher, V., Steglich, T., Becker, T. & Jekle, M. (2021). The self-enforcing starch–gluten system—Strain–dependent effects of yeast metabolites on the polymeric matrix. *Polymers*. 13(1), 30.
<https://doi.org/10.3390/polym13010030>
2. Alpers, T., Olma, J., Jekle, M. & Becker, T. (2022). Relation between polymer transitions and the extensional viscosity of dough systems during thermal stabilization assessed by lubricated squeezing flow. *Food Chemistry*. 389, 133048.
<https://doi.org/10.1016/j.foodchem.2022.133048>
3. Alpers, T., Becker, T. & Jekle, M. (2023). Strain-dependent assessment of dough's polymer structure and functionality during the baking process. *PLoS One*. 18(3), e0282670. <https://doi.org/10.1371/journal.pone.0282670>
4. Alpers, T., Panoch, D., Jekle, M. & Becker, T. (2024). New insights into crumb formation in model systems: Effects of yeast metabolites and hydration level by means of multiwave rheology. *Food Hydrocolloids*. 155, 110184.
<https://doi.org/10.1016/j.foodhyd.2024.110184>

Table of contents

| | | |
|--|---|-----------|
| Acknowledgements..... | II | |
| Preface | III | |
| Peer-Reviewed Publications..... | III | |
| Table of contents..... | IV | |
| Abbreviations | VI | |
| Summary..... | 1 | |
| Zusammenfassung..... | 3 | |
| 1 | Introduction | 6 |
| 1.1 | The polymeric wheat dough matrix | 7 |
| 1.2 | Deformations occurring during the bread making process | 11 |
| 1.3 | Rheology in cereal technology and its relevance for the bread making process | 13 |
| 1.4 | Structural and functional changes of the wheat dough matrix along the bread making process | 18 |
| 1.4.1 | Yeast-induced changes on the microscopic length scale during proofing | 18 |
| 1.4.2 | The formation of primary and secondary yeast metabolites during proofing and their impact on the dough's molecular structure..... | 22 |
| 1.4.3 | The effect of yeast metabolites on the processibility of wheat dough | 26 |
| 1.4.4 | Thermally induced changes on the molecular and microscopic length scale during baking..... | 27 |
| 1.5 | Thesis outline | 30 |
| 2 | Methods overview | 33 |
| 2.1 | Dough and model system preparation | 33 |
| 2.2 | Rheological characterization..... | 33 |
| 2.3 | Characterization of the wheat dough's polymers..... | 34 |
| 2.3.1 | Gluten characterization..... | 34 |
| 2.3.2 | Starch..... | 35 |
| 2.3.3 | Assessment of polymer hydration..... | 35 |

| | | |
|----------|--|------------|
| 2.4 | Baking trials | 35 |
| 2.5 | Assessment of wheat dough acidification | 36 |
| 2.6 | Statistical analysis | 37 |
| 3 | Results | 38 |
| 3.1 | Summary of thesis publications | 38 |
| 3.2 | The self-enforcing starch-gluten system – Strain-dependent effects of yeast metabolites on the polymeric matrix..... | 42 |
| 3.3 | Relation between polymer transitions and extensional viscosity of dough systems during thermal stabilization assessed by lubricated squeezing flow . | 57 |
| 3.4 | Strain-dependent assessment of dough's polymer structure and functionality during the baking process..... | 69 |
| 3.5 | New insights into crumb formation in model systems: Effects of yeast metabolites and hydration level by means of multiwave rheology | 88 |
| 4 | Discussion | 100 |
| 5 | Outlook..... | 114 |
| 6 | References | 117 |
| 7 | Appendix | 133 |
| 7.1 | Reviewed paper..... | 133 |
| 7.2 | Oral presentations | 133 |

Abbreviations

General abbreviations

| | |
|------------------|--|
| 3D | Three-dimensional |
| AACCI | American Association of Cereal Chemists international |
| ANOVA | Analysis of variance |
| CLSM | Confocal Laser Scanning Microscope |
| CPMG | Carr-Purcell-Meiboom-Gill |
| db | Dry basis |
| DSC | Differential Scanning Calorimetry |
| FAD | Flavin adenine dinucleotide |
| FID | Free induction decay |
| FT-IR | Fourier-Transform Infrared Spectroscopy |
| GMP | Glutenin macropolymer |
| GSH | Glutathione |
| HMW | High molecular weight |
| HOG | High osmolarity glycerol |
| ICC | International Association of Cereal Science and Technology |
| LAOS | Large amplitude oscillatory shear |
| LMW | Low molecular weight |
| LSF | Lubricated Squeezing Flow |
| LVE | Linear viscoelastic |
| N | Nitrogen content |
| NAD ⁺ | Nicotinamide adenine dinucleotide |
| NADPH | Reduced nicotinamide adenine dinucleotide phosphate |
| NMR | Nuclear Magnetic Resonance |
| p | p-value |
| PNA | Protein network analysis |
| SAOS | Small amplitude oscillatory shear |
| SDS | Sodium dodecyl sulfate |
| SH | Strain hardening |
| TCA cycle | Tricarboxylic acid cycle |
| Tx | Time of porosity |
| US\$ | US dollar |

Latin abbreviations

| | | |
|-----------|---|---------------|
| $ G^* $ | Complex modulus | Pa |
| F_N | Normal force | N |
| G' | Storage modulus | Pa |
| G'' | Loss modulus | Pa |
| H | Test statistic of Kruskal-Wallis test | - |
| h | Height | m |
| M_r | Relative molecular weight | kDa |
| n | Number of observations | - |
| p | Laplace pressure | Pa |
| r | Gas cell radius | μm |
| r_p | Plate radius | m |
| rh | Relative humidity | % |
| SHI | Strain hardening index | In(Pa) |
| T_2 | Spin-spin (or transverse) relaxation time | ms |
| t | Test time | s |
| \bar{X} | Mean | |

Greek abbreviations

| | | |
|-----------------------|--|------------------|
| γ | Surface tension | N/m |
| $\dot{\gamma}$ | Shear rate | s^{-1} |
| ε | Hencky strain | - |
| ε_b | Biaxial strain | - |
| $\dot{\varepsilon}_b$ | Biaxial extension rate | s^{-1} |
| $\dot{\varepsilon}$ | Extension rate | s^{-1} |
| η | Shear viscosity | Pas |
| η_b | Biaxial viscosity | Pas |
| η_b^* | Apparent biaxial extensional viscosity | Pas |
| η_e | Uniaxial viscosity | Pas |
| η_p | Planar viscosity | Pas |
| λ | Wavelength | nm |
| ν | Poisson's ratio | - |
| $T_{rr} - T_{zz}$ | Normal stress difference | N/m ² |

Summary

The bread making process consists of diverse processing steps, each exerting different types of strain on the wheat dough. Complexity is added as the dough matrix changes due to time-dependent biological reactions and hydrothermally induced physicochemical changes of the polymers. In this regard, baker's yeast receives growing interest with respect to the impact of its metabolites on the structure and functionality of dough polymers. Besides the leavening effect of carbon dioxide (CO_2), ethanol, and succinic acid have been reported to directly affect the wheat dough functionality by changing the structure of the dough's polymers. Yeast metabolites are categorized into primary (CO_2 and ethanol) and secondary (succinic acid) metabolites according to their relation to the energy metabolism. The individual contribution of the single metabolites to the overall change in the processibility of yeasted wheat dough is widely unknown. Thus, the scope of this work was to identify their impact on the structure and functionality of the wheat dough matrix under process-relevant strain types.

Among the yeast metabolites, gaseous CO_2 was found to majorly impact the small and large range interactions within the dough matrix. Contrarily, the single presence of the chemical stressors ethanol and succinic acid did not affect the structure and functionality of the dough matrix in a comparable manner as the whole metabolome of *Saccharomyces cerevisiae* itself. The yeast-induced alteration of the dough functionality was related to changes in the protein microstructure, where yeast-induced degradation was revealed. Being most relevant for the bread making process, the strain-rate dependent strain hardening (SH) behavior of the yeast-fermented and the yeast metabolites-spiked matrices was evaluated additionally. SH of yeasted dough was successfully linked to the dough matrix's stress memory, the condition of the protein microstructure, and the spatial distribution of the matrix components. Regarding the latter, a starch depletion of the gas cells surrounding lamella was suggested, leading to an accumulation of starch granules in the nodes and an increase in SH.

Following the process chain, thermal treatment during the baking step represents a major impact on the structure and functionality of the wheat dough matrix due to the initiation of starch gelatinization, protein denaturation, and polymerization. Therefore, the impact of yeast on these physicochemical changes was elucidated. A differentiation of the yeast-induced effects into metabolite-induced effects (direct) and indirect effects was aimed. Additionally, the contribution of hydrothermally induced polymer transitions to the overall course of the extensional viscosity in leavened and non-leavened doughs was addressed. On this functional level, gaseous CO_2 strongly impacts the solidification behavior of the dough matrix during the thermal treatment. The extensional viscosity of leavened dough matrices gradually rose, while the non-leavened dough matrix adhered to the renowned starch-induced sharp rise in viscosity. Reasons for the delayed increase in the extensional viscosity of the yeasted wheat dough matrix were seen in a degradation of the gluten network on a microscopic length scale and limited heat-induced molecular polymerization. The latter was assumed to be related to the existence of gluten fragments and sterically inhibited gluten crosslinking. Contrarily, the

slightly premature onset of starch gelatinization in the yeasted wheat dough did not majorly impact the course of the extensional viscosity of the dough matrix. Higher mobility of weakly bound water in the yeasted dough and a starch depletion in the gas cell-surrounding lamella were suggested to cause an excess hydration of starch granules in the yeasted dough, resulting in an early onset of starch gelatinization.

A better understanding of the polymer functionality during heating in dependency on their molecular and microscopic structure was developed for two dough systems with different gluten network structures: a highly branched non-yeasted wheat dough and a microstructurally degraded yeasted wheat dough. Yeasted dough systems revealed a higher share of gluten functionality as the CO₂-induced expansion of the matrix favored the occurrence of larger deformation behavior. Due to the same reason, a greater extent of SH was observed for yeasted doughs throughout the baking process, resulting in a higher consistency of the yeasted dough matrix. The greater extent of SH was further claimed to be responsible for the higher gas holding capacity. Despite protein interactions were reduced on a molecular and microstructural level.

Artificial model systems were reconstituted to further elucidate the impact of yeast metabolites on the physicochemical changes of starch and gluten during hydrothermal treatment. In contrast to the previous works, metabolite formation was restricted to proofing and the dough samples were partially degassed before the rheological measurements in this work. The results confirm the previous findings, showing that yeast metabolites are destabilizing the wheat dough matrix. However, the presence of chemical stressors did not affect the solidification point. Nevertheless, the magnitude of the solidification process in the wheat starch-gluten model system increased in the fermented dough systems, highlighting the importance of water availability during the solidification process. In the semi-inert, gluten-based model system, a degrading effect of yeast metabolites was observed along the whole baking process, underlining the degrading impact of yeast on the gluten network. It was further revealed that the highest extent of gluten polymerization was facilitated in non-starch-based model systems, supporting the hypothesis of the spatial hindered polymerization in the presence of gas cells.

This work generated new insights into the impact of single yeast metabolites on the structure and functionality of dough polymers during process-relevant deformations. The mechanical stressor CO₂ was found to induce structural alterations on a molecular and microscopic length scale, which are held responsible for the observed changes in the rheological behavior in yeasted dough. Although the chemical stressors (ethanol and succinic acid) do not majorly affect the structure or functionality of the dough matrix, dough polymer transition processes were found to be influenced by the indirect effects of the primary mechanical stressor (CO₂). The extension of the protein matrix resulted in an altered rheological behavior, an effect on the hydration equilibrium of the dough polymers, and an influence of the spatial conditions, which are regarded as influential on the extent of polymer-polymer interactions within the yeasted wheat dough matrix.

Zusammenfassung

Der Herstellungsprozess von Backwaren besteht aus mehreren Teilschritten, innerhalb welchen verschiedenste Deformationen auf die Teigmatrix ausgeübt werden. Neben externen Kräften unterliegt die Teigmatrix aufgrund des Ablaufes von biologischen Prozessen und hydrothermisch induzierten, physikochemischen Veränderungen der Teigpolymere während des Herstellungsverfahrens weiteren Transformationsprozessen. Unten den biologischen Prozessen beeinflusst insbesondere Bäckerhefe die Teigstruktur und –funktionalität entlang des Backprozesses wesentlich. Neben dem eigentlichen, lockernden Einfluss von Bäckerhefe, welcher auf der Bildung von gasförmigem Kohlenstoffdioxid (CO_2) basiert, beeinflussen auch Ethanol und Bernsteinsäure die Funktionalität der Teigmatrix. Anhand ihrer Rolle im Energiestoffwechsel von *S. cerevisiae* werden die Metabolite in primäre (Ethanol und CO_2) und sekundäre Metabolite (Bernsteinsäure) unterteilt. Bereits bekannt ist, dass der Einfluss der genannten Metabolite auf die Teigfunktionalität auf ihrer Fähigkeit beruht, die Struktur oder Löslichkeit der Polymere der Teigmatrix zu verändern. Allerdings ist das Ausmaß der individuellen Beiträge von einzelnen Hefemetaboliten zur globalen Funktionalitätsänderung in Hefeteigen bisher unbekannt. Die Ursache für die funktionellen Änderungen wurde in der Mikrostruktur des Proteinnetzwerkes gefunden, welches insbesondere durch mechanisch wirkende Hefemetabolite geschwächt wurde. Um den Beitrag der genannten Hefemetabolite auf die veränderten mechanischen Materialeigenschaften der Teigmatrix aufzuklären, wurde der Einfluss einzelner Metabolite analysiert. Dieser vergleichende Ansatz zeigte, dass gasförmiges CO_2 unter den betrachteten Hefemetaboliten den größten Einfluss auf die Teigmatrix hat. Dabei beeinflusste gasförmiges CO_2 sowohl die Interaktionen der Teigpolymere über kurze als auch über lange Distanz. Mit den Effekten, welche durch die Zugabe der chemischen Stressoren Ethanol und Bernsteinsäure zu Weizenteigen verursacht wurden, konnten hingegen nicht die hefeinduzierten strukturellen Änderungen in hefegelockerten Teigen im Vergleich zu ungelockerten Teigen erklärt werden. Neben der Untersuchung der strukturellen Änderungen in hefegelockerten Teigen lag ein weiterer Fokus der Arbeit auf der Analyse des Einflusses der genannten Hefemetabolite auf dem dehnratenabhängigen *strain hardening* Verhalten. Dieser Fokus erklärt sich durch die hohe Relevanz dieses Phänomens für den Backprozess. Das *strain hardening* Verhalten von hefegelockerten Teigen konnte erfolgreich auf das Stressgedächtnis der Teigmatrix, den Zustand des Proteinnetzwerkes sowie der räumlichen Anordnung der Teigpolymere zurückgeführt werden. In Bezug auf Letzteres wurde vermutet, dass insbesondere die Verdrängung von Stärkegranula aus den Lamellen des Proteinfilmes zu einem verstärkten *strain hardening* beitrug.

In der weiteren Prozesskette folgt nach der Gare die thermische Behandlung der Teigmatrix während des Backprozesses. Dabei wird in der Teigmatrix eine Kaskade an physikochemischen Veränderungen ausgelöst, welche die Struktur und Funktionalität der Teigpolymere verändert. Zu diesen Prozessen zählen die Stärkeverkleisterung,

Proteindenaturierung sowie deren anschließende Polymerisierung, welche den Verlauf der Dehnviskosität von Teigen während des Backprozess beeinflussen. Die Abhängigkeit der Dehnviskosität vom Ausmaß des Ablaufes dieser Prozesse, sowie der Einfluss von Hefemetaboliten auf den Ablauf dieser Prozesse, verblieben allerdings bisher unbekannt und wurden in dieser Arbeit betrachtet. Wie bereits im ersten Teil der Arbeit wurde insbesondere für gasförmiges CO_2 ein großer funktioneller Einfluss quantifiziert. Für CO_2 -gelockerte Teigsysteme stieg die Dehnviskosität lediglich sukzessiv, wohingegen durch die Teiglockerung ein steiler Anstieg zu beobachten war, wie er auch für reine Stärkesuspensionen beobachtet werden kann. Ursachen für dieses veränderte Verfestigungsverhalten wurden in der veränderten Proteinmikrostruktur, welche durch die Anwesenheit von Gasblasen schlechter vernetzt ist, und in einer Limitierung des Ausmaßes der Proteinpolymerisierung auf molekularer Ebene gefunden. Für Letzteres wird ebenfalls eine sterische Inhibierung der Vernetzung durch die Anwesenheit von Gasblasen in der Teigmatrix ursächlich gemacht. Im Gegensatz zum Einfluss der teilweise inhibierten Proteinpolymerisierung wirkt sich das leicht verfrühte Einsetzen der Stärkeverkleisterung nicht auf den Verlauf der Dehnviskosität aus. Vermutlich führen eine höhere Wasserverfügbarkeit für Stärke und die bessere Stärkezugänglichkeit zu diesem früheren Einsetzen des Verkleisterungsprozesses. Die Ursache für Letzteres wird in der bereits zuvor beschriebenen Verdrängung der Stärkegranula aus den Lamellen, welche die sich ausdehnenden Gasblasen umgeben, vermutet.

Im Hinblick auf die Prozessrelevanz wurde anschließend der Effekt des veränderten Ablaufes der Stärkeverkleisterung und Proteinpolymerisierung auf das *strain hardening* Verhalten betrachtet. Hierzu wurden zwei molekular- und mikrostrukturell verschiedene Systeme miteinander verglichen: ein gut vernetzter, nicht hefegelockerter Weizenteig und ein hefegelockerter Weizenteig, in welchem die Hefemetabolite die Struktur des Proteinnetzwerkes schwächen. Trotz des geschwächten Proteinnetzwerkes in hefegelockerten Teigen zeigte die Glutenfunktionalität im hefegelockerten Teig einen größeren Beitrag zum rheologischen Verhalten des Teigsystems. So zeigte das hefegelockerte Teigsystem bereits unter geringer Verformung deutlich ein Verhalten, welches sonst nur unter großer Deformation beobachtet wird. Dies wurde auf die CO_2 -induzierte Vordehnung der Matrix zurückgeführt. Auf demselben Grund wurde auch das verstärkte Auftreten von *strain hardening* über den gesamten Backprozess zurückgeführt. Somit zeigte die hefegelockte Teigmatrix, trotz der eingeschränkten Proteininteraktionen auf molekularer und mikrostruktureller Ebene, ein gesteigertes Gashaltevermögen im Vergleich zur ungelockerten Teigmatrix.

Abschließend wurden die, bislang lediglich hypothetischen, Ursachen für den veränderten Ablauf der physikochemischen Veränderungen von Stärke und Gluten näher betrachtet. Um den Einfluss von Hefemetaboliten auf die jeweiligen Weizenteigpolymere und deren hitzeinduziertes Verfestigungsverhalten differenziert zu betrachten, wurde ein Modellsystem konstituiert. Im Gegensatz zu den vorangegangenen Arbeiten wurde die Bildung von

Hefemetaboliten durch ein mildes, thermisches Inaktivierungsverfahren auf den Zeitraum der Gare beschränkt und die Teigmatrix vor den rheometrischen Tests partial entgast. Weder im Modellsystem, noch im Weizenteig, konnte ein Einfluss der verbliebenen chemischen Stressoren auf den Ablauf des Verfestigungsprozesses gefunden werden. Allerdings konnte gezeigt werden, dass das Ausmaß des Verfestigungsprozesses in stärkebasierten Systemen durch die vorangegangene Hefefermentation gesteigert wurde. Ursächlich hierfür wird die verbesserte Hydratation von Stärke gesehen, welche durch die Verdrängung der Granula aus den gasblasenumgebenden Lamellen verursacht wird. In rein glutenbasierten Matrices wurde hingegen über den gesamten Backprozess eine hefeinduzierte Destabilisierung beobachtet, welche auf die zuvor beschriebene molekulare und mikrostrukturelle Degradation des Proteinnetzwerkes während der vorangegangenen Gare zurückgeführt wurde. In diesen stärke-freien Systemen wurde zudem das höchste Ausmaß der Proteinpolymerisierung beobachtet, was die zuvor angestellte Hypothese der eingeschränkten Proteinpolymerisierung durch eine sterische Inhibierung bestärkt.

Zusammengefasst ermöglichte diese Arbeit neue, differenzierte Einsichten in den Einfluss einzelner Hefemetabolite auf die Struktur und Funktionalität der Teigpolymere unter prozessrelevanten Bedingungen und Deformationen. Hefeinduzierte Veränderungen auf molekularer und mikrostruktureller Ebene konnten erfolgreich mit dem veränderten rheologischen Verhalten von hefegelockerten Weizenteigen in Zusammenhang gestellt werden. Dabei zeigten die chemischen Stressoren Ethanol und Bernsteinsäure keinen wesentlichen Einfluss auf die Weizenteigmatrix, wohingegen gasförmiges CO₂ als primärer mechanischer Stressor die Funktionalität der polymeren Matrix wesentlich beeinflusste. Dies basiert auf der CO₂-induzierten Vordehnung der Proteinmatrix, welche zu wesentlichen Veränderungen im dehn-rheologischen Verhalten der Teige sowie der räumlichen Anordnung der Teigpolymere führte. Letzteres wirkte sich dabei insbesondere auf den Ablauf der Stärkeverkleisterung und der Proteinpolymerisierung während des Erhitzungsprozesses und den, damit in Zusammenhang stehenden, Ablauf des Verfestigungsprozesses der Teigmatrix aus.

1 Introduction

Wheat represents one of the most important staple foods worldwide, serving as a raw material for bread making, as well as for pasta and noodles production, pastry making, manufacturing of snack foods, and breakfast cereals production. For bread making, wheat flour has been used for centuries. The unique functionality of the hydrated wheat flour polymers was vital for the development of the bread making process, a process whose worldwide volume is nowadays amounting to 266.33 billion US\$ a year (The Insight Partners, 2023).

The essential functionalities of the dough matrix involve plasticity for shaping operations, elasticity for the gas holding capacity, and thermally induced solidification during the baking process. They can be related to the underlying wheat dough structure. On a microscopic length scale, the matrix comprises of a three-dimensional (3D) gluten network filled with an actively interacting starch-water phase and dispersed gas cells (Jekle & Becker, 2015). Furthermore, constituents like minerals and enzymes represent a minor mass fraction with a strong functional impact. The functionality of the dough matrix during the bread making process is mainly related to the material properties of the constituting polymers. Wheat gluten and starch, accounting for more than 90% of the wheat flour dry mass, depict particular rheological properties. Gluten proteins, the storage proteins of wheat (*Triticum aestivum* L.), form a viscoelastic network upon hydration and plays a key role in the gas retention capacity of the dough matrix until thermal treatment. Wheat starch, which water binding capacity is limited in the cold stage, gains importance during the thermal treatment, as starch gelatinization contributes to the solidification during the dough-to-crumb transition process. Taken together, the heterogeneous dough matrix forms a functional system based on various interactions and repulsions of the involved polymers. Hence, the heterogeneous network configuration shows a complex rheological behavior, which, as non-Newtonian material, strongly depends on the type, amplitude, and rate of the applied strain.

As diverse processing conditions are applied during the bread making process, the knowledge of the time- and temperature-dependent behavior of the consisting dough polymers is further emphasized. Biochemical reactions and relaxation processes are known to change the structure and functionality of the dough matrix during kneading and proofing. During baking, thermally induced physicochemical changes of the wheat dough's polymers alter their structure and functionality, and, consequently, the rheological behavior of the dough matrix. Furthermore, the usage of baker's yeast results in the inclusion of an additional element of complexity. Baker's yeast, or *Saccharomyces cerevisiae*, is used as a biological leavening agent in the bread making process and resembles a century-old bread making ingredient. Despite its primary use as a rising agent, the time-dependent release of yeast metabolites into the matrix alters the dough matrix's functionality (Aslankoohi et al., 2015; Jayaram, Cuyvers, et al., 2014; Jayaram, Rezaei, et al., 2014; Meerts, Vaes, et al., 2018; Verheyen et al., 2014). Hence, different time- (relaxation processes and yeast fermentation) and temperature-dependent (physicochemical changes of the wheat dough's polymers) processes alter the

rheological behavior of wheat dough along the bread making process and, thus, affect its processibility.

This thesis focuses on the impact of yeast- and thermally induced changes as well as their combined effect on the structure and functionality of the wheat dough matrix. As an introduction, the current state of the art regarding the impact of yeast-induced and thermally induced changes of the rheological behavior of wheat dough matrix, as well as their impact on the processibility of wheat dough, will be reviewed, and open questions will be identified. Subsequently, the suitability of various rheological methods, commonly used in cereal technology to determine bread making process-relevant material properties, will be considered in this context before the thesis outline is introduced.

1.1 The polymeric wheat dough matrix

Following the approach of Vilgis (2015), who defined food materials in the context of soft matter, it is crucial to be familiar with the underlying structures in wheat dough on different length scales to understand its processing behavior. Wheat dough comprises diverse components and structures from the molecular to the macroscopic length scale, thus representing a heterogeneous polymeric system (Jekle & Becker, 2015; Schiedt et al., 2013). The wheat dough matrix is developed during the hydration of flour with simultaneous input of mechanical energy during the mixing step. Many wheat dough's properties were ascribed to one of its main constituting polymers: gluten. Gluten proteins, which compromise the non-water- and salt-soluble wheat proteins, represent the major storage proteins in wheat and are located in the endosperm (He et al., 2013). The required water-insolubility results from a particularly low content of charged amino acids in the amino acid composition of gluten proteins (Morel et al., 2002; Herbert Wieser, 2007). Gluten proteins can be categorized into monomeric gliadins and polymeric glutenins, which occur in a relation of 65/45 w/w% in gluten (Herbert Wieser et al., 2023b). Glutenins can be subdivided into high molecular weight (HMW) glutenins (relative molecular weight (M_r): 80 kDa – 120 kDa (Lagrain et al., 2012; Schalk et al., 2017)) and low molecular weight (LMW) glutenins (M_r = 32 kDa – 45 kDa (Lagrain et al., 2012; Schalk et al., 2017)), which share ~20 w/w% and ~10 w/w% of gluten proteins (H. Wieser & Kieffer, 2001). The greatest proportion of gluten proteins represent gliadins, composed of α -, γ - and ω -gliadins (M_r = 30 kDa, 35 kDa, 50 kDa – 55 kDa, respectively (Schmid et al., 2016)). HMW, further categorized as x- and y-type HMW glutenin proteins, and LMW glutenin proteins interact via disulfide bonds between cysteine residues. Additionally, Lefebvre et al. (2000) highlighted the importance of intermolecular interactions via β -sheets in glutamine-rich, repetitive domains of glutenins (Lefebvre et al., 2000). Contrarily, HMW glutenin and gliadin interactions are only facilitated via hydrogen bonds, electrostatic interactions, hydrophobic interactions, and van-der-Waals-forces (Wellner et al., 2005). The relevance of electrostatic interactions within these interactions is restricted, as charged amino acids share a small percentage in the amino acid composition of gluten (Létang et al., 1999).

Due to its chemical composition, gluten proteins form a non-conventional, transient network upon hydration and energy input (Mann et al., 2014; Schiedt et al., 2013). Hydration induces the swelling of the gluten proteins, where the increase of the radius of gyration can be up to 400% in the case of HMW glutenins (Mann et al., 2014). This is based on the assumption that good solvent conditions are given and no clustering of the proteins is induced due to an incompatible solvent (Hong & Lei, 2009). Furthermore, the shear and extensional forces induced by the kneading process favor the unfolding of the proteins (Létang et al., 1999). Hence, kneading promotes proteins to interact and the gluten network to develop. Campos et al. (1997) highlighted the importance of mechanical energy input, as undeveloped dough did not result in an appropriate network development. The authors relate this to a lack of alignment of the formed protein fibrils in the absence of mechanical energy input (Campos et al., 1997). On the contrary, well-connected networks can be established upon mechanical energy input. In this case, hydrated and unfolded x- and y-type HMW glutenins form the backbone of glutenin. With a size of ~800 amino acids and cysteine residues in the C- and N-terminal domain, HMW glutenins interact via disulfide bonds to form a basic mesh (Vilgis, 2015; Herbert Wieser, 2007). Also, LMW glutenins interact with these head-to-tail linked chains via disulfide bonds (Herbert Wieser et al., 2023a), forming a cohesive glutenin structure. This structure contributes the elastic properties to wheat dough (Létang et al., 1999).

Belton's loop and train model can be used to relate the elastic properties to structural building blocks of the glutenin structure (Belton, 1999). In a relaxed state, non-interacting repetitive β -turn structures of glutenin form so-called loop regions and regions, which interact with other molecules via intermolecular β -sheet structures, resemble train regions (Belton, 1999; Herbert Wieser et al., 2023a). Upon extension, loops are stretched until they come into contact with other molecules and intermolecular β -sheet structures are formed. A further extension would result in rupture of the protein strands. If the protein strands experience relaxation instead, the structure returns to its equilibrium configuration and the energy is restored (Belton, 1999; Kim et al., 2008; Herbert Wieser et al., 2023b). Using Rheo-Fourier-Transform Infrared Spectroscopy (FT-IR) measurements, Wellner et al. (2005) revised the original idea of complete structural recovery as the authors observed an increase in intermolecular β -sheets and a decrease in β -turns and unordered structures after repeated large amplitude extensional deformation. According to these observations, it becomes evident that gluten possesses a memory for its processing history, which impedes its elastic character upon repeated deformation (Herbert Wieser et al., 2023a).

The second building blocks of the gluten network are gliadins, which are non-covalently bound to the glutenin backbone (Wellner et al., 2005). They reduce the network's stiffness and increase the wheat dough's extensibility (Létang et al., 1999).

As mentioned above, the kneading process resembles an integral part of dough development. It enables the polymerization of the gluten proteins to form the gluten network, even though it can also cause depolymerization of the gluten structure upon overmixing (Dreese et al., 1988; Kim et al., 2008; Létang et al., 1999). The kneading process generally results in a high level of

alignment of the comprising proteins. Therefore, several authors highlighted the importance of resting time after kneading for structural relaxation to re-establish an entangled system (Brandner et al., 2022a; Kim et al., 2008).

Gluten quantity and quality are commonly correlated to gas holding capacity during leavening, which is a major quality criterion in bread making, as it represents the basis for the loose and soft crumb structure (Færgestad et al., 2000; Roels et al., 1993; Tronsmo, Magnus, Færgestad, et al., 2003). The growth of gas cells results in a large amplitude biaxial extension of the dough matrix. The high stability of the dough matrix towards this deformation is a unique property, which has been attributed to the strain hardening (SH) of the gluten polymer. This behavior, commonly known in polymer science, can typically be seen as the J-shaped behavior of the extensional viscosity with increasing strain at constant strain rates (Stading, 2008; Wikström & Bohlin, 1999b). SH is observed only for branched polymers, as entanglements are formed between branches while the main chain is extended (Dobraszczyk & Morgenstern, 2003). Sliwinski et al. found the SH behavior of pure gluten to be more pronounced than for wheat doughs and to be dependent on the originating cultivar. Based on these observations, the authors concluded that gluten is the primary source of SH behavior (Sliwinski et al., 2004). Belton (2005) explained the SH phenomena in the context of the loop and train model. According to this, SH is caused when the structure cannot respond anymore by further disentanglement of any loops. Consequently, regions with more pronounced intermolecular interactions need to be stretched to enable further extension, which requires additional energy input (Belton, 2005). In agreement with this model, Sroan et al. (2009) underlined the relevance of glutenins for SH behaviour. The strain hardening index (SHI) was observed to decrease by increasing the proportion of monomeric gliadins. Contrarily, adding glutenin-rich fractions increased the SHI until the optimum glutenin proportion was exceeded and excessive entanglements reduced the extensibility of the system (Sroan et al., 2009). In general, SH behavior is unique for wheat among other cereal cultivars and accounts for a high gas retention capacity and high specific volumes. While fermentation and oven rise, SH avoids several foam destabilization mechanisms, such as Ostwald ripening and coalescence. Thus, SH allows the extension of the dough matrix in the lamella around the gas cells (Van Vliet et al., 1992).

Even though the origins of the functionality of the dough matrix during the bread making process can be found in the structure of gluten on a molecular and microscopic length scale, the behavior of the dough matrix differs greatly from that of wheat dough (Georgopoulos et al., 2004; Tronsmo, Magnus, Baardseth, et al., 2003; Uthayakumaran et al., 2002). Besides gluten, starch represents a major component in wheat dough, accounting for a volume fraction of ~85w/w% (Meerts et al., 2017). Native starch is organized in granules. Unique for starch from the *Triticeae* tribe is the bimodal granule size distribution. A smaller weight percentage of starch is present as small B-type granules (2 – 5 µm, spherical shape) and a greater share as larger A-type granules (10 – 40 µm, lenticular shape) (Wenhao et al., 2013). All granules are organized in amorphous and crystalline shells (Jenkins et al., 1993). These structures arise due to the two different polymers, that built up starch: amylose and amylopectin. While amylose

is a mainly linear polymer composed of 500 – 6000 glucose residues, amylopectin represents a branched polymer consisting of 3×10^5 – 3×10^6 glucose units. Amylopectin forms double helices, representing the crystalline structures in the granule's structure, while amylose and non-crystalline amylopectin form amorphous regions (Goesaert et al., 2005). Due to this densely packed structure and its semi-crystalline character, native starch has a limited water binding capacity. Therefore, wheat starch is suspended in the liquid dough phase during dough kneading and embedded in the strongly connected, protein strand-based gluten phase (Jekle & Becker, 2015).

The role of starch in the polymeric wheat dough system has been intensively discussed. In general, incorporating rigid particles into polymeric systems is known to increase the stress of the system. According to Edwards (1990), who investigated carbon black-filled elastomer systems, such particle-filled systems differ significantly in their strain-dependent stress answer from pure elastomer systems. Pure elastomers show a strong elastic behavior but a low stress answer, whereas a reinforcing effect can be observed in the presence of filler particles, as the stress-strain behavior changes significantly. Similar behavior can be observed when comparing the rheological behavior of pure gluten to a wheat dough under oscillatory shear strain (Wehrli et al., 2023). Watanabe et al. (2002) concluded that this effect would result from friction within the starch granules and Edwards (1990) also explained the importance of abrasion resistance.

Besides the absolute stress answer, another major difference between pure gluten systems and wheat dough is the increasing sensitivity to deformation with increasing starch volume fractions (Khatkar & David Schofield, 2002; Meerts et al., 2017; Schiedt et al., 2013; Uthayakumaran et al., 2002). Schiedt et al. (2013) related this behavior to the "Payne effect", a collapse of the filler network, which has an increasing impact on the matrix as the starch volume fraction increases (Payne, 1962). The starch network, stabilized by short range interactions (such as non-covalent molecular interactions), is increasingly dominating the behavior of the dough matrix with increasing starch volume fraction and is responsible for the reduction of the linear viscoelastic (LVE) range, as with larger amplitudes, starch granules will be displaced and the deformation turns invasive. This interpretation of dough as a particle-based system, consisting of a highly connected polymeric gluten network and actively interacting filling starch particles, has received increasing attention. Bridging from polymer science to natural dough systems, Brandner et al. (2021) found further evidence for the importance of a rigid particle network in semi-artificial glass beads – gluten systems and pleaded for the existence of a particle-filled network in wheat dough. Also, Schiedt et al. (2013) highlighted the active involvement of starch granules in the dough matrix via interactions between the starch granule surface and the gluten proteins. Here, starch granule surface-associated molecules are of particular importance and are known to affect the functionality of starch granules during processing (Baldwin, 2001). Brandner et al. (2022, 2021) elucidated the role of various starch granule surface-associated molecules by imitating the functionality of different starch granule surface-associated molecules in large amplitude deformation

experiments. Within this scope, the best agreement with wheat dough functionality was found for the imitation of surface-associated protein. Therefore, the authors emphasized that starch surface-associated proteins increase the stability of the wheat dough system: strong gluten-starch granule interactions were suggested to endure after the breakdown of the particle network, as energy can be dissipated by sliding of starch-gluten-groupings along each other before the gluten matrix is deformed (Brandner et al., 2022b).

Along with gluten and starch as the main wheat dough's polymers, several minor components are involved in the wheat dough system. In this regard, lipids, non-starch polysaccharides, and endogenous enzymes can have a major impact on the development and functionality of the gluten network as well as on the structure of starch and non-starch polymers (Döring et al., 2015; Dornez et al., 2007; Rouillé et al., 2005). Even though these minor fractions can have major impacts on the rheological behavior of the wheat dough system, this thesis focuses on gluten and starch. In short, it can be summarized that wheat dough represents an inhomogeneous polymeric, multiphasic system with diverse interactions on molecular to microscopic length scale. Hence, the behavior strongly depends on the applied deformation as different length scales respond to different types and amplitudes of strain.

1.2 Deformations occurring during the bread making process

A thorough understanding of the steps involved in the bread manufacturing process is vital to know the stress exerted on wheat dough. The bread making process is a series of several sub-processes, varying in time, intensity, and order. As a basic example, the straight dough method is depicted in Figure 1. The process starts with a kneading step, followed by a relaxation step, and then a shaping process. Before the final baking process, the expansion of the dough is initiated during the proofing step.

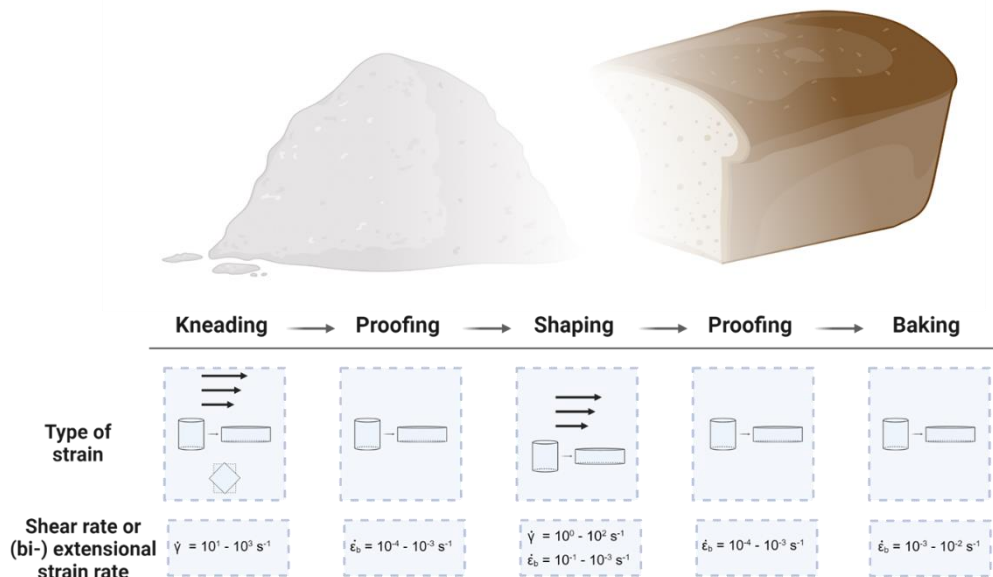


Figure 1: Overview of types of strains and strain rates occurring during the bread making process. Data from (Bloksma, 1990; Connelly & Kokini, 2006; Della Valle et al., 2014; Jongen et al., 2003). Created with Biorender.

The main goals of the kneading step are to distribute and hydrate the dough ingredients homogeneously and to develop the polymeric gluten network through a progressive sequence of stress and relaxation steps (Vidal et al., 2022). The types of strain applied during this processing step are diverse and vary over several magnitudes in terms of strain rates. A combination of high shear rates ($\dot{\gamma} = 10^1 \text{ s}^{-1} - 10^2 \text{ s}^{-1}$, quantified in a z blade mixer, filled with 0.11% Carbopol with shear-thinning properties), elongational and rotational stress acts on the dough during kneading, where the proportions between the types of strain may widely vary according to the geometry of the mixer (Connelly & Kokini, 2006; Jongen et al., 2003). The kneading step is followed by a resting step, allowing the highly aligned network to encounter conformational relaxation (Brandner et al., 2022a). To create a basis for the soft crumb of the final baked good, gas nuclei formed during the kneading step need to expand and to be redistributed during the following processing steps. As CO_2 is formed and diffuses to the gas cells, their growth is induced exerting extensional stress on the dough matrix. The extension is of a biaxial nature as the surrounding dough matrix is tangentially extended in two directions and uniaxial compressed in the radial direction. Biaxial extension rates occurring during proofing range from 10^{-4} s^{-1} to 10^{-3} s^{-1} , depending on the initial gas cell size (Babin et al., 2006; Turbin-Orger et al., 2015). While Babin et al. (2006) focused on exponential gas cell growth during the initial proofing phase, Weegels et al. traced coalescence processes and reported extensional strain rates in the magnitudes of $\dot{\varepsilon} = 10^1 \text{ s}^{-1} - 10^2 \text{ s}^{-1}$ (Peter L. Weegels et al., 2003).

During the subsequent shaping processing, the dough undergoes further shearing ($\dot{\gamma} = 10^0 \text{ s}^{-1} - 10^2 \text{ s}^{-1}$) and extension ($\dot{\varepsilon} = 10^{-3} \text{ s}^{-1} - 10^{-1} \text{ s}^{-1}$) (Della Valle et al., 2014). Throughout the baking step, deformation again is mostly originated from gas cell growth, where extensional strain rates are, compared to the proofing step, increasing to $\dot{\varepsilon}_b = 10^{-3} \text{ s}^{-1} - 10^{-2} \text{ s}^{-1}$, due to the thermally induced acceleration of gas cell expansion (Bloksma, 1990).

In summary, deformations during the bread making process can be categorized into two sections: external shear forces that induce large deformations during kneading and shaping and large deformations due to endogenic forces induced by the growth of gas cells. The leavening process causes relative deformations of the dough matrix around the growing gas cells (ε_b) of up to 1.3 at slow biaxial extensional strain rates ($\dot{\varepsilon}_b = 10^{-4} \text{ s}^{-1}$ to 10^{-2} s^{-1} (Babin et al., 2006; Bloksma, 1990)) during proofing and baking (Vliet et al., 1992). Therefore, this work focuses on the behavior of the wheat dough matrix during the proofing and baking process, where the biaxial extension process prevails. Hence, different methods used to characterize the behavior of the wheat dough matrix during such deformations will be revised in the following chapter.

1.3 Rheology in cereal technology and its relevance for the bread making process

The capacity to form a highly aerated foam is particularly important among the different functionalities of the dough matrix during the bread making process. Gas cells are stabilized in the semisolid dough matrix until the solidification of the system is initiated during the baking process. Inappropriate material properties can cause undesired product characteristics, such as a dense crumb structure due to a firm network or crumb collapse due to the failure of large gas cells (Dedey et al., 2021). The rheological behavior of the dough matrix is of strong interest in predicting the stability of the dough matrix against the deformations arising during proofing. For this reason, a wide range of analytical procedures has been implemented in the field of cereal technology. Rheometry is generally used to gain information on mechanical properties, material structure, and processing behavior. Thus, rheometry is widely used in food technology (Fischer & Windhab, 2011). In the field of cereal technology, empirical rheological approaches are commonly found due to their close relation to the bread making process.

Based on the processes occurring during bread making, tests have been developed to downscale the bread making process and enable the recording of quantitative measures of the analyzed dough systems. Besides some subjective manual tests, such as the windowpane test or the poke or ripe test, which are performed to judge either dough development or the status of dough during proofing, respectively, a broad set of instrumental standard tests has become parts of the state of the art methods filed by the leading associations for cereal science and technology (Van Boeckstaele, 2011). Noteworthy examples of instrumental approaches are z blade kneaders (Farinograph, DoughLAB), dough extensibility testers (Extensograph, Kieffer Dough Extensibility Rig, Alveograph), or rotational viscometers (Rapid Visco Analyzer, Viscoquick, ViscoQC).

Extensibility measurements for flour or gluten are widely used to predict loaf volume (Abang Zaidel et al., 2008; Dunnewind et al., 2003; Janssen, Vliet, et al., 1996; Kieffer et al., 1998; Tronsmo, Magnus, Baardseth, et al., 2003). In this context, it should be mentioned that Huen et al. found no significant correlation between any analytical value from empirical characterization methods of commercial wheat flours and the specific bread volume resulting from a baking procedure, which was held close to industrial methods (Huen et al., 2018). Thus, the generalized explanatory power of empirical methods, such as Extensograph or Alveograph, needs to be put into question. Bloksma (1972) found the rate of deformation occurring during Extensograph and Alveograph testing to be several magnitudes higher than during proofing or baking (Bloksma, 1972), which might limit the transferability of the results to the real bread making process and explain their restricted potential to serve as process predictors. Even though not in the desired magnitude, several authors suggested conversions to extract fundamental data from empirical tests for dough extensibility tests (Bloksma, 1972; M. Charalambides et al., 2002; M. N. Charalambides et al., 2002; Maude Dufour et al., 2024; Dunnewind et al., 2003). However, the often complex geometries of the probes used for

empirical tests induce poorly defined deformations on the samples. Thus, information or control of the applied strain and strain rates are limited and, therefore, the information to attain on the strain rate-dependent behavior as well.

To bridge this gap, fundamental rheology is receiving growing interest as a tool to extract superior information on the structure of the analyzed system. The impact of various ingredients and processing technologies on the structure and functionality of wheat dough has been determined using fundamental rheometry (Alvarez-Ramirez et al., 2019; Campos et al., 1997; Clarke et al., 2004; Fu et al., 1997; Steffe, 1996; Verheyen et al., 2015). Similarly, rheology has been applied to investigate the changes in structure and functionality of the cereal polymers during the thermal stabilization process during baking (Bloksma, 1979; Bloksma & Nieman, 1975; Campos et al., 1997; Jekle et al., 2016; Salvador et al., 2006; Vanin et al., 2018; Xu et al., 2017). Fundamental rheological techniques can roughly be distinguished between shear and elongational techniques, as well as small and large deformation testing. Measurements under small deformation are performed to preserve structural integrity (Létang et al., 1999). As Steffe (1996) highlighted, the characterized material behavior is strongly dependent on the applied type of flow. Being subjected to shear flow, molecules can rotate to avoid being stretched. Contrarily, pure extensional flow leads to an orientation of the molecules in the direction of the flow resulting in forced stretching (Steffe, 1996). In the case of Newtonian fluids, shear and elongational viscosity can be converted into each other using Trouton's ratio (Sliwinski et al., 2004). However, this convertibility is restricted in wheat dough due to its non-Newtonian nature.

Shear rheological techniques using rotational rheometers have been widely implemented to study the viscoelastic behavior of the dough matrix, from which oscillatory, stress-relaxation, and shear measurements are widely used. Extensive research has been performed using techniques within the LVE range of dough, where (complex) stress and (oscillatory) strain behave linearly. This non-invasive deformation is used to characterize short range interactions in the polymeric network, such as starch-starch interactions (Schiedt et al., 2013). In the case of larger strain amplitudes, the deformation becomes invasive as starch granules are displaced and the initial polymer interactions are interrupted (Schiedt et al., 2013). Hence, large amplitude deformation techniques are used to characterize the rheological behavior of gluten, while starch-protein interactions respond to intermediate deformations (Schiedt et al., 2013). When the applied strain does not exceed the LVE range, structural information can be extracted from the frequency-dependent behavior of a tested material. Gabriele et al. (2001) suggested a power law fit of the frequency-dependency of the complex modulus to characterize the "rheological structure" of weak gels. This approach has been applied to wheat dough to analyze the strength and interactions of the polymeric dough network as impacted by raw materials (Caramanico et al., 2018; Meerts et al., 2017), ingredients (Fu et al., 1997; Georgopoulos et al., 2004; Li et al., 2021; Lucas et al., 2019; Upadhyay et al., 2012) and processes (Gabriele et al., 2001; Létang et al., 1999; Vidal et al., 2022).

Lately, developments in devices and software have enabled the widespread use of multiwave testing, where more than one single frequency can be tested at a time. Fourier transform mechanical spectroscopy can provide complex rheological information within short measurement times due the application of a superimposed strain function (Dörr et al., 2020). By combining several sine waves of various frequencies into one complex sinusoidal wave, Holly et al. implemented multiwave rheology as a new analyzing tool for viscoelastic materials within a short measurement time (Holly et al., 1988). This method has been applied to a range of viscoelastic materials to quantify mainly time- (Meerts, Vaes, et al., 2018), temperature- (Alpers et al., 2023; Ma et al., 2014; Palla et al., 2019; Seighalani et al., 2021; Udyarajan et al., 2007), or process-induced (Vidal et al., 2022) changes in material properties.

The suitability of oscillatory rheological testing for predicting processibility was shown to depend on the applied amplitude. Although a strong link between small amplitude oscillatory shear (SAOS) rheological behavior and the protein microstructure has been proven (Jekle & Becker, 2015; Lucas et al., 2019), moderate to no correlations were mostly found with the final baking quality (e.g., loaf volume) (Dobraszczyk & Morgenstern, 2003; Tronsmo, Magnus, Baardseth, et al., 2003). Contrarily, structurally invasive large deformation rheological tests showed good to very high correlations (Dobraszczyk & Morgenstern, 2003). Considering this non-linear region, initial attempts have been conducted where the storage modulus G' was fitted with the power law model to quantify the strain dependency of the drop of G' (Hwang & Gunasekaran, 2001; Mann et al., 2014). Hwang and Gunasekaran (2001) observed a dependency of these power law parameters on the dough development time. The authors concluded that the power law model in the non-linear region can be used to analyze the gluten network structure. Lately, large amplitude oscillatory shear rheology (LAOS) has emerged to analyze the response of dough structures under non-linear, large deformation testing (Alvarez-Ramirez et al., 2019; Wehrli et al., 2023; Yazar et al., 2016a, 2016b; Yildirim-Mavis et al., 2019). The functionality assessed under large deformation can explain wheat dough functionality under deformation processes occurring during the bread making process (Alvarez-Ramirez et al., 2019; Yazar et al., 2016a) and reveal gluten functionality (Schiedt et al., 2013).

Besides shear tests, extensional tests represent the second main category of rheological testing. Here, three different types of extension can be distinguished. Uniaxial extension is caused by an elongation process along one axis, resulting in a contraction along the two other axes. In accordance with that, biaxial extension is the equal extension process along two axes resulting in the compression along one axis. A third case represents the planar extension, where the material is extended in one axis and compressed in a second axis while the third axis remains neutral (Haward et al., 2023). The abovementioned cases assume the Poisson's ratio of the material to be positive ($\nu > 0$), meaning that the material contracts along the axis being orthogonal to the applied tensile stress. In regards to the bread making process, the dough matrix is subjected to biaxial extensional deformation, mostly occurring during proofing and oven rise, as mentioned above. Being subjected to extensional flow, SH can occur in

polymeric materials. As previously introduced, gluten is subjected to this phenomenon, whose extent has been found to define the bread making performance of wheat flour (Dobraszczyk & Morgenstern, 2003; Sroan et al., 2009). Shear rheological measurements are, therefore, not appropriate tools for the quantification of SH.

Several fundamental extensional techniques have been developed in the past decades, either from initio or by converting data from empirical tests (M. N. Charalambides et al., 2002; Maude Dufour et al., 2024; Dunnewind et al., 2003; Launay et al., 1977). For high viscous materials like wheat dough, those techniques compromise the Meißner extensional rheometer (Meißner, 1969), the filament stretching rheometer (Matta & Tytus, 1990), hyperbolic contraction flow (Stading & Bohlin, 2001; Wikström & Bohlin, 1999b), or the Sentmanat extensional rheometer (Sentmanat, 2004) as uniaxial extensional techniques and Lubricated Squeezing Flow (LSF) (Chatraei et al., 1981) and bubble inflation (Launay et al., 1977) as biaxial extension techniques. Most of the mentioned techniques originate from the polymer industry, as extrusion and film forming processes are common practices that require knowledge of the extensional rheological behavior. The reviewed techniques for fundamental extensional rheometry compromise a broad spectrum of different techniques. Suitability for the application in wheat dough rheometry has been proven without exclusion, raising the need for additional factors to be considered. Setting the scope of the rheological measurements to the characterization of wheat dough behavior for deformations as they occur during the production process, the type of extension as well as the achievable strain amplitude and strain rate are gaining importance. Regarding the former, the differentiation between uniaxial and biaxial extensional techniques is crucial. In the case of Newtonian fluids, the Trouton ratio can be applied to convert shear viscosity η to uniaxial (η_e), planar (η_p), and biaxial extensional viscosity (η_b) (Petrie, 2006). For viscoelastic materials, this conversion becomes invalid for high strain rates and any predictability of suitable conversions decreases with increasing polymer concentrations as intermolecular interactions increase (Haward et al., 2023). Comparing the stress values retrieved from uni- and biaxial extension tests with wheat dough and gluten samples, Sliwinski et al. (2004) found, as to be expected, higher stress levels in uniaxial extension tests and related this to an increased orientation of glutenins in the direction of the flow. Even though uniaxial testing was performed with a Kieffer Extensibility rig, which was previously shown to cause a mix of shear and extensional flow, the authors were able to highlight the importance of the induced flow type. Hence, it is essential to characterize materials under process-relevant types of strain to retrieve information on the processing behavior in the imitated processes. Therefore, bubble inflation and LSF as biaxial extensional techniques are potential methods to imitate bread making-relevant deformations. In the case of the bubble inflation test, a conversion, as suggested by Blokasma (1957), needs to be applied to extract $\eta_b(\dot{\varepsilon})$. Following this approach, Charalambides et al. (2006) found stress and strain to be overestimated at large amplitude strain. The authors further suggested that the bubble inflation test must be complemented with supplementary data to extract fundamental values, increasing the testing procedure's complexity. Thus, LSF represents the most applicable technique for wheat dough

analysis due to the applied biaxial extension, achievable strain and strain rates as well as the almost complete negligibility of shear due to applying lubrication (Launay & Michon, 2008). The fundamentals of this technique will, therefore, be introduced in the following section.

During LSF, a cylindrical sample is compressed between two lubricated plates and is subjected to a radial squeezing flow. The term “lubricated” originates from the lubricant used to enable a “perfect slip scenario” between the sample and the plates (Engmann et al., 2005), avoiding shear stress between the plates and the sample. The technique was introduced by Chatraei et al., who theoretically and practically introduced the squeezing flow experiment. Beneficiating from the perfect slip assumption, Hencky strain ε can be calculated according to Equation 1 (Chatraei et al., 1981):

$$\varepsilon = \ln\left(\frac{h_t}{h_0}\right) \quad \text{Equation 1}$$

where h_0 refers to the initial sample height and h_t is the sample height at the test time t .

Derivation by time yields the strain rate $\dot{\varepsilon}$ defined by Equation 2 (Chatraei et al., 1981).

$$\dot{\varepsilon} = \frac{d\varepsilon}{dt} = \frac{\dot{h}}{h_0} \quad \text{Equation 2}$$

with \dot{h} being the compression speed.

Taking into account the velocity field, the related biaxial strain ε_b and biaxial extension rate $\dot{\varepsilon}_b$ are then defined by Equation 3 and Equation 4 (Vanin et al., 2018):

$$\varepsilon_b = \frac{1}{2} \ln\left(\frac{h_t}{h_0}\right) \quad \text{Equation 3}$$

$$\dot{\varepsilon}_b = \frac{1}{2} \dot{\varepsilon} = \frac{\dot{h}}{2h_0} \quad \text{Equation 4}$$

Furthermore, the LSF setup allows the calculation of the apparent biaxial extensional viscosity η_b^* as the contact area within the sample and the plates remains constant during the whole experiment. Using the normal stress difference $(T_{rr} - T_{zz})$, η_b^* can be calculated according to Equation 5,

$$\eta_b^* = (T_{rr} - T_{zz})/\dot{\varepsilon}_b = \frac{F_{N,t}}{\pi r_p^2 \dot{\varepsilon}_b} \quad \text{Equation 5}$$

where $F_{N,t}$ is the normal force at the test time t and r_p the plate radius (Chatraei et al., 1981).

As Launay and Michon (2008) highlighted, lubrication is crucial in LSF. The viscosity of the lubricant is decisive as it may impede the measured extensional viscosity in two different scenarios: a) the viscosity of the lubricant is too high and may not be neglectable from the resulting viscosity or the depletion of lubricant on the interface of the sample and plates in scenario b) causes friction and impedes the zero-shear condition (Launay & Michon, 2008). To avoid depletion of the lubricant, the applied strain should be limited to $\varepsilon_b \approx 1.0 - 1.5$ (Launay & Michon, 2008). Considering these conditions, LSF represents a suitable tool for the fundamental characterization of the extensional behavior of wheat dough. On the downside,

Launay and Michon (2008) questioned the validity of the incompressibility boundary condition for dough, which could influence the calculated SHI.

LSF has been widely used to investigate the effect of raw materials (Janssen, Van Vliet, et al., 1996; Kokelaar et al., 1996; Sliwinski et al., 2004; Wikström & Bohlin, 1999a), ingredients (Arufe et al., 2017; Yue et al., 2020), and processing parameters (Kokelaar et al., 1996; Launay & Michon, 2008; Turbin-Orger et al., 2016; Vanin et al., 2018) on the rheological behavior of wheat dough. Most authors applied LSF to cold stage, non-proofed dough samples. A few exceptions represent Yue et al. (2020), who reported decreased SH ability for proofed wheat dough, and Launay & Michon (2008), Kokelaar et al. (1996), as well as Vanin et al. (2018), who considered the impact of thermal treatment on the flow behavior of wheat dough and gluten under biaxial extensional flow. Regarding the latter, all authors observed a marked drop in the flow behavior index when temperatures exceeded 42 °C for wheat dough and gluten samples. Kokelaar et al. (1996) also compared the SHI for wheat dough and gluten at 20 °C and 55 °C. The thermally induced change in SHI was inconsistent across the comparison between samples of different wheat varieties, limiting the interpretability. Furthermore, a relation of the observed changes to thermally induced structural changes of the dough-matrix-constituting polymers is largely lacking. This lack of knowledge is meant to be targeted within the framework of this thesis.

1.4 Structural and functional changes of the wheat dough matrix along the bread making process

This chapter will review the most important structural and functional changes of the wheat dough matrix occurring during proofing and baking. Following the bread making process, yeast-induced effects during the proofing step will be firstly discussed. Afterward, the effect of hydrothermal treatment, occurring during the latter baking process, on the cereal polymers will be reviewed.

1.4.1 Yeast-induced changes on the microscopic length scale during proofing

The processes of gas cell stabilization, growth, and destabilization must be comprehended to understand the complex changes in the mechanical material properties of the proofing dough matrix. Therefore, a closer look will be taken at these processes and the resulting structural changes in the wheat dough matrix.

In yeasted wheat dough, the gas void fraction increases gradually with the increase in fermentation time (Elmehdi et al., 2003; Verheyen et al., 2014). The origin of this process lies in the gradual release of CO₂ by yeast cells during proofing, being dissolved in the liquid dough phase until saturation is reached. As nucleation is an energy-intensive process that only occurs in a supersaturated medium (Pandiella et al., 1999), yeast-released CO₂ instead migrates into existent air cells as soon as the dough matrix is saturated with CO₂. These air cells originate from the mixing process where air pockets are entrapped during the mixing process (Mehta et

al., 2009). The geometric mean of the gas cell size distribution after kneading was reported to be $\sim 22 \mu\text{m}$, being homogeneously distributed in the dough matrix (Babin et al., 2006; Koksel et al., 2016; Rouillé et al., 2005). Furthermore, the gas cell sizes varied widely depending on the dough formulation. With increasing fermentation times, the size of gas cells increased. Quantitative data is given by Turbin-Orger et al., who reported volume mean values of the gas cell size distribution of $411 \pm 230 \mu\text{m}$ and $675 \pm 320 \mu\text{m}$ after 87 min and 166 min of fermentation, respectively, with a yeast concentration of 2% (w/flour weight) fresh compressed yeast. This data was confirmed by Rouillé et al., who further quantified gas cell sizes of up to $3000 \mu\text{m}$ after 133 min using 2.5% (w/flour weight) fresh compressed yeast (Rouillé et al., 2005).

In wheat dough, gas cells are stabilized in the 3D gluten network and surrounded by a thin liquid film of surface active proteins and lipids (Babin et al., 2006; Salt et al., 2006). From a mechanical perspective, this can be described by the superposition of the Laplace pressure, such as hydrostatic and viscous forces as described by Grenier et al. (2010). Thereby, the Laplace pressure (p) is determined by the surface tension γ and the radius r as described by the Young-Laplace equation (Equation 6):

$$p = \frac{2\gamma}{r} \quad \text{Equation 6}$$

According to the Young-Laplace equation, the pressure inside gas cells is always higher than in the surrounding dough matrix due to the surface tension and is indirectly proportional to the gas cell size. Surface active substances aid reducing the surface tension by surrounding the gas cell. In wheat dough, the aqueous phase is known to form a thin liquid film at the gas cell surfaces (Mills et al., 2003; Sroan & MacRitchie, 2009). As Mills et al. (2003) summarized, endogenous substances such as various dilute salt solution-soluble proteins, polar lipids, and arabinoxylans help to reduce the surface tension or stabilize the gas cell surrounding thin liquid film. Besides these wheat-descending surfactants (e.g., lipids (Sroan et al., 2009; Sroan & MacRitchie, 2009)), yeast metabolites could further contribute reducing the surface tension. Accordingly, ethanol, which surface tension-reducing effect is well documented in beer (Lynch & Bamforth, 2002), could also contribute to gas cell stabilization in wheat dough.

As mentioned above, hydrostatic pressure and viscous forces contribute to the pressure exerted on gas cells (D. Grenier et al., 2010). Depending on the hydration level in the wheat dough, surface tension contributed up to 30%-40% of the total pressure in the core of proofed bread dough with decreasing relevance in dough systems with lower hydration levels. In these cases, the contribution of viscous forces prevailed (D. Grenier et al., 2010).

As with any foam, the dough matrix is subjected to destabilization mechanisms. Koksel and Scanlon stated that disproportionation and coalescence are the main destabilization processes during proofing (Koksel & Scanlon, 2016). As the Laplace pressure is indirectly proportional to the gas cell size (see Equation 6), higher CO_2 concentrations arise in the surroundings of smaller gas cells, which are then diffusing towards larger gas cells to reach a pressure equilibrium. This diffusion process is referred to as disproportionation. Disproportionation was

observed in both, non-yeasted and in yeasted dough (Koksel et al., 2016; Shimiya & Nakamura, 1997; Shimiya & Yano, 1988).

The occurrence of destabilization processes contributes to the increase of the size of the gas cells and the heterogeneity of their size distribution with increasing proofing time (Turbin-Orger et al., 2012). The increasing heterogeneity results from the decrease in the proportion of small gas cells and a broadening of the distribution towards larger gas cell sizes, as observed by several authors (Shimiya & Nakamura, 1997; Turbin-Orger et al., 2012, 2015). Theoretical considerations of Shah et al. and Chiotellis and Campbell on the growth of gas cells in the absence of coalescence indicated that gas cells of all sizes are subjected to growth, even in dough systems with initially log-normal distributed gas cell sizes (Chiotellis & Campbell, 2003; Shah et al., 1998). The authors explained the privileged growth of smaller gas cells by the greater surface area and, hence, the higher mass transfer of smaller gas cells. This effect was found to be tantamount to the preferred growth of larger cells due to the lower internal pressure, thus initiating a uniform gas cell growth of all sizes (Chiotellis & Campbell, 2003). However, coalescence in real dough systems leads to a decreasing volumic fraction of small gas cell sizes with increasing fermentation time (Turbin-Orger et al., 2012, 2015).

The growth of the gas cells must result in a thinning of the surrounding gas cell walls. When a critical thickness is reached, the rupture of these cell walls can occur and cause the coalescence of the formerly separated gas cells (Koksel & Scanlon, 2016). In wheat dough systems, these gas cell walls are referred to as lamella. Grenier et al. (2010) reviewed several studies on the microscopic analysis of gas cell walls. Based on these results, the authors suggested a schematic representation of the gas cell walls, from which it becomes evident that the constitution of the material of the lamella is dynamic throughout the fermentation process. Initially, the lamella is composed of gluten with embedded starch granules surrounded by a thin liquid film (see Figure 2, left) (David Grenier et al., 2021; Sroan & MacRitchie, 2009). With increasing fermentation time, the composition of the material of the lamella transitions and, at some extremes, starch granules are partially excluded from the thinning gas cell walls (see Figure 2, right) (David Grenier et al., 2021).

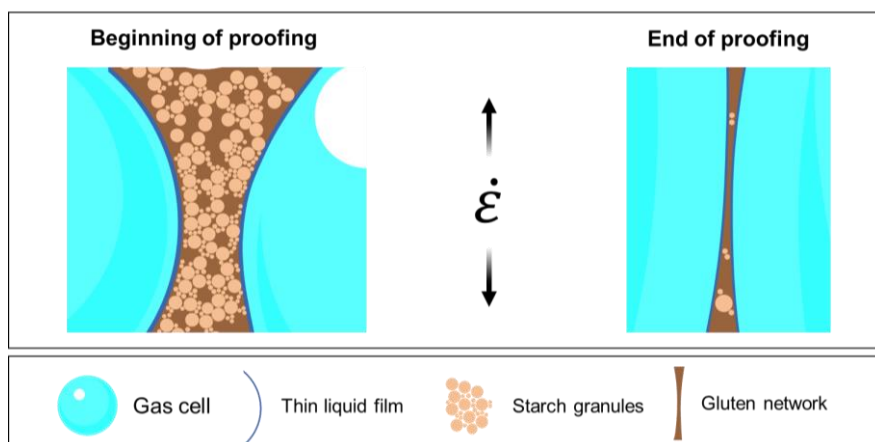


Figure 2: Schematic representation of the arrangement of the wheat dough's components in gas cell walls. Structure of a lamella at a microscopic length scale before thinning (left) and after thinning due to the growth of gas cells in the dough matrix (right). Figure adapted from David Grenier et al. (2021). Created with Biorender.

At the latter stages of dough proofing, thinning of the lamellas might result in discontinuities of the gluten-starch-lamella (Gan et al., 1990). In such cases, Gan et al. hypothesized the stabilization of gas cells to be reliant on a thin liquid film comprising surface-active substances, such as polar flour lipids, proteins, or pentosanes, which are actively stabilizing gas cells and enable their expansion.

To identify the effects of yeast metabolites on the dough matrix, several authors investigated the fermentation time-dependent rheological behavior of yeasted wheat flour doughs. Using fundamental SAOS rheometry, several authors observed a decreasing elastic behavior of the dough matrix with increasing fermentation time (Meerts, Vaes, et al., 2018; Verheyen et al., 2014). Similar behavior was observed for the extensional behavior as elasticity or resistance to extension decreased with increasing fermentation time and increasing yeast levels (Lee et al., 2004; Lee & Campanella, 2013; Salvador et al., 2006; Verheyen et al., 2014). Accordingly, Yue et al. (2020) found the SHI to decrease after wheat dough proofing. Overall, most authors ascribed the increasing viscous behavior to the production of CO_2 and, thereby, the decreasing dough density. The inverse relation of material density and moduli has been described for many other polymeric systems (Saint-Michel et al., 2006). In yeasted dough systems, the relation between dough density and the resulting mechanical properties of the dough matrix is rather complex to assess because the changes in the gas void fraction also impact the material properties. For instance, to reach a higher gas void fraction via leavening agents, biological or chemical leavening agents must be dosed in higher levels or react over a longer time. Therefore, an alteration of the material properties of the wheat dough matrix cannot be excluded and the changes in the rheological behavior of wheat doughs cannot be exclusively linked to changes in the gas void fraction.

Chin et al. (2005) conducted one of the rare attempts to control the gas void fraction of wheat dough via the mixing process to keep the material properties of the dough matrix constant while the gas void fraction was controlled. The authors found the SHI to decrease with an increasing gas void fraction, which was attributed to the gas cells causing a disjunction of the network (Chin et al., 2005). The results align with the findings of Yue et al. for fermented wheat dough, thus potentially indicating a significant impact of the gas void fraction on wheat dough functionality. When analyzing the impact of the yeast level on the wheat dough's rheological properties, Upadhyay et al. reported an increase in G' with increasing yeast levels (Upadhyay et al., 2012). The authors explained this tendency by observing the formation of smaller gas cell sizes with increasing yeast concentrations and suggested the occurrence of nucleation due to supersaturation in the presence of 10% (w/flour weight) dry yeast. The exceptionally high yeast level differs from the previously mentioned studies and could explain the discrepancy in the observed effects. However, the results underline the importance of the distribution of the gas cell size to the overall wheat dough's functionality. Contradictory observations were also made by Newberry et al. (2002), who found no difference in the rheological behavior of wheat dough prepared without or inactivated yeast. The contradictory observations of Newberry et al. might be explained by considering that the samples were

degassed due to the compressional forces exerted during the loading of the sample (Meerts, Ramirez Cervera, et al., 2018; Verheyen et al., 2014). A new pressure build-up in the dough during the measurement was prevented due to the previous inactivation of the yeast (Newberry et al., 2002).

In general, it can be summarized that the attempt to study the impact of an increasing gas void volume on the mechanical properties of the surrounding wheat dough matrix faces some challenges as (i) the gas void volume, (ii) the gas cell size distribution, and (iii) the lamella thickness of the proofing dough matrix. A differentiation between these factors has not been revealed yet in the literature, despite that these factors should be considered influential for the mechanical properties of fermented wheat dough. However, some authors found evidence that the decay of the dough's elasticity with decreasing density is not entirely related (Elmehdi et al., 2003; Meerts, Vaes, et al., 2018). Considering the reduced density as the main impact on the rheological behavior of the yeasted dough matrix, Elmehdi et al. (2003), Meerts et al. (2018), and Salvador et al. (2006) found indications that changes in the material properties of the gas cell surrounding the dough matrix are likewise changing the rheological behavior of yeasted dough. Thus, additional impact factors should also be considered: (iv) the lamella composition and (v) its mechanical material properties. One cause of structural and, thus, functional changes in the wheat dough matrix is the release of additional yeast metabolites besides CO₂ during proofing. The successful quantification of yeast metabolites in the fermented dough matrix has paved the way for research, providing insights into the effect of single yeast metabolites in the complex wheat flour dough matrix (Jayaram et al., 2013). Since then, numerous studies elucidated the effects of yeast metabolites on the structure and functionality of the dough matrix (Aslankoohi et al., 2015; Jayaram, Cuyvers, et al., 2014; Jayaram, Rezaei, et al., 2014; Meerts, Ramirez Cervera, et al., 2018; Rezaei et al., 2016). The origin and potential effect of these metabolites are meant to be reviewed in the following chapter.

1.4.2 The formation of primary and secondary yeast metabolites during proofing and their impact on the dough's molecular structure

The relevant metabolic pathways occurring during the fermentation of wheat dough must be considered to understand the metabolome of *S. cerevisiae* in wheat dough. The active metabolic pathways in *S. cerevisiae* during dough fermentation are strongly related to the conditions in the wheat dough. After only a short time, wheat dough is depleted of oxygen (Joye et al., 2012). Under these anaerobic conditions and in the presence of glucose, which initiates the Crabtree effect in high doses, fermentable short-chain sugars are converted to CO₂ and ethanol (Heitmann et al., 2018; Jayaram et al., 2013; Rezaei et al., 2014). Once in the cell, the metabolism of glucose starts with the glycolysis of glucose to pyruvate (Broach, 2012). Degradation of pyruvate in the fermentative pathway leads to the formation of acetaldehyde. Further reduction of acetaldehyde to ethanol aids in restoring the cell's redox balance by regenerating the coenzyme nicotinamide adenine dinucleotide (NAD⁺). Ethanol has

been studied regarding structure- and functionality-influencing interactions in wheat dough. The intensity of the effect of ethanol on the dough matrix functionality has been found to strongly depend on its concentration. Jayaram et al. quantified 15 mmol/100 g flour (equivalent to 0.69 g/100 g flour) to be released into the dough matrix by 1 (w/flour weight)% fresh compressed yeast (based on flour with 14% moisture) after 3 hours of fermentation. In the case of 3 (w/flour weight)% fresh compressed yeast (based on flour with 14% moisture), 35 mmol ethanol/100 g flour was quantified after 3 hours, which is in the same range as 29.3 ± 0.9 mmol ethanol/100 g dough, which was determined by Loveday and Winger for a compressed yeast level of 3.3 (w/flour weight)% (Jayaram et al., 2013; Loveday & Winger, 2008). Jayaram et al. found ethanol concentrations greater than 20 mmol/100 g flour to affect the extensional properties of dough and concentrations greater than 40 mmol/100 g flour to affect the dough spread. The authors related these changes to the ability of ethanol to act as a solvent for gliadins. The protein network was, therefore, expected to be more swollen and expanded. Consequently, the partial solubilization of gliadins was assumed to reduce the viscous properties, resulting in a more elastic but stiffer network (Jayaram, Rezaei, et al., 2014). However, an ethanol concentration of 40 mmol/100 g flour is only reached after long proofing times with comparably high yeast levels.

A second major category of yeast metabolites are organic acids, where acetate and succinic acid need to be mentioned. Acetate originates from the cytosolic pyruvate dehydrogenase bypass, which provides acetyl-coenzyme A for reactions in the cytosol synthesis such as lipid synthesis (Remize et al., 2000). The formation of acetate by the oxidation of acetaldehyde by acetaldehyde dehydrogenase yields reduced nicotinamide adenine dinucleotide phosphate (NADPH) and is, thus, helping to maintain the redox balance (Remize et al., 2000). Succinic acid represents a well-known metabolite originating from the respiration pathway under aerobic conditions. During the alcoholic fermentation, the tricarboxylic acid cycle (TCA cycle) is repressed and pyruvate is mainly transformed to CO_2 and ethanol (Camarasa et al., 2003; Dzialo et al., 2017). Still, as TCA-descended organic acids, such as malate and succinate, are produced during fermentation under oxygen-limited conditions, a residual TCA pathway activity was proved (Camarasa et al., 2003). The authors reported the production of succinate as the main product of the reductive branch of the TCA pathway during fermentation and assumed a critical role in the flavin adenine dinucleotide (FAD) supply of the yeast cell (Camarasa et al., 2003). Despite this generally accepted knowledge of the succinic acid production via the reductive branch of the TCA cycle during fermentation, Rezaei et al. also reported evidence on a residual activity of the TCA cycle of *S. cerevisiae* in wheat dough fermentation. The authors reported a significant reduction of the amounts of succinic acid produced in fermenting wheat dough when the respective genes for the expression of the enzymes involved in the steps 1-5 in the TCA pathway were deleted. Furthermore, a significant increase in succinic acid concentration was observed when repressing the succinate dehydrogenase (step 7 of the TCA pathway) (Rezaei, Aslankoohi, et al., 2015).

Functional effects of organic acids need to be considered as their formation, together with the formation of CO_2 , can affect the pH of the dough matrix. Jayaram et al. quantified concentrations of succinic acid in a yeasted dough of up to 1.6 mmol/100 g flour (equivalent to 0.19 g/100 g flour) after 3 hours of fermentation with 5.3 (w/flour weight)% fresh compressed yeast (based on flour with 14% moisture). In this case, succinic acid prevailed over acetic acid, quantified in a concentration of 0.25 mmol/100 g flour (equivalent to 0.02 g/100 g flour) under the same conditions (Jayaram et al., 2013). A faster and stronger acidification has been reported with higher levels of yeast (Verheyen et al., 2014).

The analysis of the origin of acidification in yeasted wheat dough, through the spiking of organic acids has been performed by several researchers. Jayaram et al., who employed a yeast strain in which the metabolome succinic acid dominates over acetic acid (ratio of succinic/acetic acid: 6.4), reported that spiking the amount of succinic acid quantified in a yeasted dough to a non-yeasted wheat dough resulted in a pH of 5.0 ± 0.1 (Jayaram et al., 2013). This pH value was close to the pH reached by yeast fermentation itself with the respective yeast level and fermentation time (pH = 4.8) (Jayaram et al., 2013). Based on this result, the authors related the pH drop in fermented wheat dough to the production of succinic acid when using a *S. cerevisiae* strain (Jayaram et al., 2013). Rezaei et al. studied a wide range of different *S. cerevisiae* strains with succinic acid to acetic acid ratios ranging from around 0.2 up to above 1. In their study, the pH value of fermented dough was successfully replicated when both, succinic and acetic acid, were spiked to a non-yeasted dough matrix in amounts as they were previously quantified in fermented wheat dough for four different fermented dough samples (Rezaei, Verstrepen, et al., 2015). Both studies attributed only a minor effect to the formation and dissociation of carbonic acid, which could originate from the solubilization of CO_2 in the liquid dough phase. Despite the abovementioned authors proofed that the sole presence of organic acids is sufficient to recreate the pH value in the yeast-leavened dough, the respective contribution of organic acids and carbonic acid remains unclear. For instance, Miller et al. (1994) attributed the origin of the occurring pH drop in the first 30 min of yeast fermentation purely to the formation and dissociation of carbonic acid (Miller et al., 1994). However, the authors did not quantify the concentration of organic acids.

Difficulties in allocating the contribution of organic acids and carbonic acid can be attributed to the buffer capacity of wheat dough. Even though the buffer capacity of wheat flour is relatively low compared to other protein-based food and feed, a residual buffer capacity can be attributed to the presence of minerals and proteins (Ji et al., 2005; Mennah-Govela & Bornhorst, 2021). Due to this buffer capacity, the initial addition of any acid may drop the pH value but into the buffer's working range of wheat flour. Thus, the further addition of acid would not change the pH value as the dough's buffer working range has been reached. Within this pH range, further acid does not significantly affect the pH of a buffered system. Similarly, yeasted dough can be considered a buffer system. As CO_2 is initially present in much higher quantities than organic acids (~ 20-fold amount (Jayaram et al., 2013)), the liquid dough phase might first be saturated with CO_2 . Hence, the formation and dissociation of carbonic acid might

be responsible for the pH drop during short fermentation times. With the additional release of organic acids, the yeasted wheat dough would reach the working range of the dough's buffer working range, leading to a disproportional response of the pH value to any additionally added amount of organic acid. Nevertheless, the extent of the initial pH drop due to the presence of carbonic acid has not been quantified for yeasted dough yet. Based on these information, it is hypothesized that the acidification of the dough matrix is a mixed effect of CO_2 and organic acids. However, this hypothesis has not been proven or disproven so far.

Generally, acids released into the dough matrix enhance elasticity and stiffness (Clarke et al., 2004; Jayaram, Cuyvers, et al., 2014). In the presence of greater amounts of acid, a positive net charge and conformational changes within the gluten polymer are enabled (Galal et al., 1978; Rezaei et al., 2016). Subsequently, fewer intermolecular interactions are present and disaggregation is initiated. This is based on an increased positive charge of ionizable side chains of amino acids of gluten upon a pH drop (Elmehdi et al., 2003). The resulting increased intermolecular electrostatic repulsive forces are hypothesized to cause a stiffer and more fragile dough structure. Wehrle et al. (1997) found lactic acid and acetic acid to cause a more elastic and firmer dough behavior (Wehrle et al., 1997). Also, Jayaram et al. (2014) reported succinic acid in a concentration of 0.8 mmol/100 g flour to reinforce the internal cohesion of dough, accompanied by decreasing dough extensibility, which was attributed to the unfolding and swelling of gluten proteins in the presence of succinic acid. Increasing interactions, caused by the greater accessibility upon the unfolding and elongation of the protein conformation, are assumed to enable the reinforcement of the dough structure. In addition to its impact on gluten, Barber et al. (1992) suspected the inducement of mild acid hydrolysis of starch in the presence of organic acids in sourdoughs (Barber et al., 1992), which has been shown to result in a relative increase of crystalline structures and therefore, in an increased gelatinization temperature (Ulbrich et al., 2014). The effect of organic acids on the dough structure is also strongly concentration-dependent. E.g., the potential effect of lower concentrations of succinic acid, as occurring during fermentation with lower amounts of compressed yeast (e.g., 0.5 mmol/100 g flour in a wheat dough containing 2 (w/flour weight)% fresh compressed yeast (based on flour with 14% moisture) after 3 h of fermentation), is yet unknown.

Glycerol, another amply produced secondary *S. cerevisiae* metabolite plays a vital role in yeast fermentation (Jayaram et al., 2013). Its production is initiated by the HOG (high osmolarity glycerol) signaling pathway to face the osmotic stress exerted by the low water activity in the dough matrix and to regenerate NAD^+ (Hohmann, 2002; Raab & Lang, 2011; Rezaei, Verstrepen, et al., 2015). The production of glycerol is reliant on the synthesis of glycerol-3-phosphate-dehydrogenase and glycerol-3-phosphatase by the expression of the encoding genes *GPD2* and *GPP1* under anaerobic conditions, which is vital for maintaining the redox balance (Tamás et al., 1999). The efflux of glycerol is regulated by osmolarity and conducted by plasma membrane channels (aquaglyceroporin, *Fps1p*) (Aslankoohi et al., 2015; Oliveira et al., 2003; Tamás et al., 1999).

Glycerol levels of up to 10 mmol/100 g flour (equivalent to 0.92 g/100 g flour) were quantified in yeasted wheat dough after 3 hours of fermentation with 5.3 (w/flour weight)% fresh compressed yeast (based on flour with 14% moisture) (Jayaram et al., 2013). Aslankoohi et al. found the gas retention capacity of wheat flour dough to be improved when using *GPD1*-overexpressing (encodes for glycerol-3-phosphate-dehydrogenase) mutants (Aslankoohi et al., 2015). Additionally, dough extensibility was found to be improved when spiking 1.5 mmol glycerol/100 g flour to non-yeasted wheat dough (Aslankoohi et al., 2015). The authors ascribed this observation to the dough softening effect of exogenous glycerol. Therefore, the technological relevance of glycerol might be imposed during dough fermentation.

Besides osmotic stress, thermal stress affects the yeast fermentation process. Deviations from the optimum in any unfavorable direction (cold and heat) affect the yeast metabolome. Trehalose and proline accumulation have been shown to enable freeze tolerance and superior viability in dry yeast (Lahue et al., 2020). Their impact on wheat dough structure and rheology will not be focused in this work as the protective mechanism involves intracellular accumulation rather than active transport out of the cell. However, in the case of the use of dry yeast, these metabolites need to be considered as the cell wall of yeast cells becomes porous upon cellular death and, thus, considerable amounts of, e.g., glutathione (GSH, 5.37 mg/g yeast (db) – 81.22 mg/g yeast (db)) can be found in commercial dry yeast preparations (Verheyen et al., 2015). GSH concentrations in this range were further shown to reduce significantly the specific bread volume (Verheyen et al., 2016). Furthermore, thermal stress is well-known to inactivate yeast cells during baking. Doppler et al. (2022) were the first ones to report the viability of yeast cells along the baking process. By utilizing three different techniques (Colony-forming unit counting, Fluorescence imaging, and Flow cytometry), the authors could quantify viable, dead, and inactive yeasts in a solid matrix, as is the case for wheat flour dough and crumb. Using an electrical resistance oven, a method benefitting from gradient-free heating, viability drastically reduced at 65.5 °C and nearly completely reduced at 81.3 °C (Doppler et al., 2022). Therefore, formerly enclosed yeast metabolites might be released during baking upon cell lysis depicting functional impact. However, quantitative data to underline this hypothesis is not available.

Besides the abovementioned metabolites, hydrogen peroxide has been hypothesized to represent an important yeast metabolite but was disproved to be produced in relevant amounts during fermentation with *S. cerevisiae* (Rezaei, Dornez, et al., 2015).

1.4.3 The effect of yeast metabolites on the processibility of wheat dough

The literature reviewed in the previous chapter suggests a significant functional impact of primary (CO₂ and ethanol) and secondary (organic acids and glycerol) yeast metabolites on the dough matrix. However, it remains unclear if the processibility of wheat dough is affected by the altered functionality of the wheat dough matrix and which sub-processes of the manifold steps of the bread making process would be affected by this. The latter is of particular interest

and requires the dough's material properties to be analyzed for the same type, amplitude, and rate of strain as occurring during the sub-processes of bread making itself. The need for such an approach can be seen in the dependency of the dough matrix functionality on the gas formation kinetics, as reported by Verheyen et al. (2016). The authors found the matrix-weakening impact of GSH to be reduced when high concentrations of chemical leavening agents were used. The authors concluded that higher gas formation kinetics would compensate for GSH-induced effects. Contrarily, the dry yeast concentration correlated negatively with the time of porosity and, therefore, the onset of CO₂ loss from the proofing dough matrix (Verheyen et al., 2016). Hence, a strain-dependent functionality for GSH might be concluded, as processes at large strain amplitudes and high strain rates (e.g., kneading) appeared less affected than processes inducing low strain rates, such as proofing.

Besides these empirical measures, initial attempts have been made to quantify the extent of SH on the strain rate. Using plain wheat dough, McCann et al. found no impact of the extension speed on the SHI of four commercial Australian wheat flours (McCann et al., 2016), while Sliwinski et al. (2004) reported that the fracture stress and strain increase with an increasing rate of deformation. Given that the extent of SH of wheat dough is strain rate-dependent, fundamental information on the SHI for the different strain rates occurring during kneading and proofing with various yeast levels during the bread making process would be needed to predict the processibility of wheat dough. Additionally, the impact of yeast metabolites in relevant amounts on the biaxial extension behavior of the wheat matrix needs to be considered when focusing on the wheat matrix's proofing and baking. The relevance of focusing on the yeast metabolites' impact on the biaxial extension behavior has been proven by Yue et al. (2020). The authors targeted the quantification of the strain hardening behavior of yeasted dough in a fundamental manner using LSF to analyze the SHI and η_b for proofing wheat dough (Yue et al., 2020). Upon verifying an impact of yeast metabolites on the functionality of the dough matrix under extensional deformation, the authors found a significant increase in the SHI after proofing. Hence, they hypothesized the origin in the stretching of the dough matrix during proofing. Additionally, the authors found η_b to decrease after proofing (Yue et al., 2020). However, attempts to differentiate along the impact of the different yeast metabolites have not been performed so far.

1.4.4 Thermally induced changes on the molecular and microscopic length scale during baking

Thermal processing is the second major impact on the dough matrix functionality during bread making. During the final processing step, the matrix undergoes thermally induced solidification. Gluten and starch are the driving factors for this process due to the thermal dependency of their functionality. The conformational and functional changes of the polymers occurring during hydrothermal treatment have been extensively investigated. Comprehensive literature can be found on characterizing the polymers in pure systems under isolated conditions. The key mechanisms and findings will be summarized in the following sections.

Hydrothermal treatment of gluten induces a stepwise change in the structure and functionality of the macromolecule. Up to 40 °C, structural and rheological changes are reversible upon cooling (Lefebvre et al., 2000). Above this temperature, irreversible transformations are caused as protein unfolding is initiated. As the strength of hydrogen bonds decreases with increasing temperature (Apichartsrangkoon et al., 1998; Defaye et al., 1995; Tang et al., 2002), structural changes are facilitated, such as a decrease of α -helical structures (P. Wang et al., 2018). Together with an increase in β -structures for temperatures from 50 °C onwards these conformational changes may be interpreted as the unfolding of the proteins (P. Wang et al., 2018). Accordingly, surface hydrophobicity increased from 45 °C and 50 °C onwards (Guerrieri et al., 1996; P. Wang et al., 2018). Furthermore, another indication of the exposure of hydrophobic regions is that water is excluded from the gluten network upon heating, as found by low-field ^1H -Nuclear Magnetic Resonance (NMR) studies (Bosmans et al., 2012).

With increasing protein denaturation, hydrophobic and thiol-rich regions are exposed. Due to its lower heat stability and molecular structure, glutenin is the first subunit to form large glutenin structures upon aggregation above 55 °C (Schofield et al., 1983). Extractability studies with sodium dodecyl sulfate (SDS) in combination with size exclusion chromatography revealed a decreasing extractability, which can be interpreted as an increase of aggregation (Redl et al., 2003) resulting in an increase of the glutenin molecular sizes in this temperature region (Schofield et al., 1983). This polymerization was found to be initiated by interactions via hydrophobic regions and disulfide bonds (Schofield et al., 1983). Accordingly, the amount of free thiol-groups decreases between 70 °C and 80 °C (Lagrain et al., 2005; Schofield et al., 1983), indicating polymerization via oxidation of thiol-groups (Lagrain et al., 2008). This increase in crosslinking of glutenins provokes changes in the functionality of gluten, as reported by Wehrli et al. (2021). In dependency on the gliadin content, which was reported as a measure of thermal stability of gluten, a first transition toward a more enhanced elastic behavior was found between 55 °C and 65 °C (Wehrli et al., 2021).

Gliadins were shown to be resilient up to 75 °C (Schofield et al., 1983). However, consecutive heating up to 95 °C or 100 °C led to a decreasing extractability of α - and γ -gliadins, whereas the level of extractable ω -gliadins was not found to be influenced by increasing temperatures up to 100 °C (Lagrain et al., 2005; Schofield et al., 1983). This divergent behavior originates from the polymerization through disulfide bonds, initiated by sulphhydryl-disulfide intercharge reactions within unfolded glutenins and sulphuric amino acid-containing α - and γ -gliadins. In contrast, ω -gliadins without sulphuric groups are not covalently integrated in the network structure (Lagrain et al., 2008; Schofield et al., 1983). The integration of gliadins induces a second change of functionality towards a more elastic behaviour. The onset of this functional change was found at temperatures around 80 °C accompanied by a change in β -turns, which was quantified for hydrothermal treatment to 85 °C (Wehrli et al., 2021). Interestingly, the mobility of gluten protons was not found to be majorly affected upon heat treatment (Alpers et al., 2024; Bosmans et al., 2012).

As water represents a plasticizer for gluten, the hydration level has a substantial impact on the structural and functional changes upon thermal treatment. A strong impact of the hydration level on the denaturation temperatures of gluten has been reported. With an increasing hydration level, an earlier onset and greater extent of the denaturation process were favored for glutenins (Leon et al., 2003). Accordingly, a decreasing SDS-extractability for glutenins after heating treatment was shown for moisture levels above 20% (P.L. Weegels et al., 1994). Thus, the contribution of thermally induced, physicochemical changes of gluten proteins to the solidification of the dough matrix depends on the hydration level of gluten in the dough matrix. In the case of wheat starch, gelatinization represents the primary driver for functional changes upon hydrothermal treatment. The pre-requisite for starch gelatinization is the presence of a plasticizer (e.g., water, glycerol, ethylene glycol, urea, and sorbitol (Perry & Donald, 2000; Van Soest et al., 1996; Zuo et al., 2015)) allowing sufficient chain mobility. Within the various plasticizers, water has superior functionality due to its low molecular weight and hydrogen bonding's capacity (Ai & Jane, 2015; Taghizadeh & Favis, 2013). Due to its relevance for the bread making process, water shall be exclusively considered a potential plasticizer in this chapter. Native wheat starch, with a limited water binding capacity, gradually increases its water binding capacity upon thermal treatment and in the presence of plasticizers. At first, the amorphous starch structures absorb water and increase the polymer's mobility (Ratnayake & Jackson, 2007). From this so-called swelling process, starch polymers in the amorphous regions form new interactions and reorganize. Continuous thermal treatment initiates further structural changes as the strength of intermolecular interactions along starch polymers decreases gradually (Ratnayake & Jackson, 2007). The authors concluded that the endothermic gelatinization process comprises the realignment of intermolecular interactions in the amorphous phase on the one hand and the melting of crystalline regions on the other hand (Ratnayake & Jackson, 2007).

Several intrinsic and extrinsic factors have been shown to impact the starch gelatinization process. When comparing the gelatinization process of starches from different botanical origins, a strong relation between the branch-chain length of amylopectin and the amylose content was revealed (Ai & Jane, 2015). Furthermore, a relation between the starch granule size and the gelatinization temperature was shown for starches from various botanical origins (Lin et al., 2015; Noda et al., 2005; Singh & Kaur, 2004). Within these, starch from members of the *Triticeae* tribe presents an exceptional case due to the existence of A-type and B-type granules, which display distinct gelatinization behaviors (Ao & Jane, 2007; Saccomanno et al., 2017). Thus, large A-type granules show lower gelatinization peak temperatures than small B-type granules (Ao & Jane, 2007; Chiotelli & Le Meste, 2002; Eliasson & Karlsson, 1983; Vermeylen et al., 2005). Small B-type granules' higher gelatinization temperature was related to a denser crystalline structure (Vermeylen et al., 2005). As extrinsic factors, besides low hydration levels, plasticizers different from water and increasing concentrations of sugars and salts are known to retard the onset of the gelatinization process (Ai & Jane, 2015).

The gelatinization process initializes extensive intermolecular interactions due to swelling and distortion of the granules. Therefore, an increase of viscosity with increasing temperature is observed as the granules are swelling. After reaching a peak viscosity, structural breakdown, alignment, and progressive melting of crystalline structures result in a decreasing viscosity with continuous thermal treatment (Keetels et al., 1996; Tsai et al., 1997).

Regarding the importance of the thermal transitions of gluten and starch for the bread making process, a layer of complexity is added when starch and gluten are combined in one system. Besides spatial effects, water distribution between the two polymers has a major impact on the functionality of the heterogeneous system. At room temperature, commercially isolated and dried vital gluten has a water absorption potential of ~158 w/w% (Schopf et al., 2021). In contrast, the hydration of native wheat starch is limited, as the water absorption potential was quantified to ~ 65 w/w% (Jakobi et al., 2018). During heating, the water distribution was then shown to shift in favor of starch (Eliasson, 1983). The impact of water availability and the starch/gluten ratio on solidification has been proven earlier (Campos et al., 1997; Champenois et al., 1998; Jekle et al., 2016). Therefore, the extent of the thermal transition processes of gluten and starch strongly depends on the availability of water for plasticizing the polymers, which is difficult to access in a differentiated manner for the heterogeneous dough matrix. Therefore, many researchers focused on the impact of the thermal processing of isolated cereal polymers rather than on elucidating structural and functional changes in the complex dough matrix (Mann et al., 2014).

Furthermore, most research was based on SAOS rheometry, whose results may not be directly translated to the behavior of the wheat dough matrix under large extensional deformation. However, this type of strain was identified as most relevant during baking. Only little data on the impact of temperature on the biaxial viscosity and flow behavior of wheat dough have been published for baking-related types of strain and strain rates (Vanin et al., 2018). Another level of complexity is added when additional ingredients are incorporated. The impact of yeast metabolites on the thermal transition behavior of gluten and starch, in general, is relatively unknown, even though there are indications for potential impacts such as mild acid hydrolysis of starch or deamination of gluten (Liao et al., 2010; Ulbrich et al., 2014). This is represented by the lack of publications on the impact of yeast metabolites on the course of the biaxial extensional viscosity or SHI during thermosetting.

1.5 Thesis outline

The previous chapter outlined the various impacts on wheat dough during bread making. As reviewed, its structure and functionality are altered due to several ingredient- and process-induced changes during processing. The main factors affecting the rheological behavior of wheat dough during bread making were previously identified as the release of yeast metabolites during proofing and thermally induced physicochemical changes of the main wheat dough's polymers during baking. These processes alter the structure of the dough polymers and, consequently, affect the processibility of the wheat dough matrix.

As the flow behavior of wheat dough is non-Newtonian, the rheological behavior of dough during the bread making procedure depends on the type, amplitude, and rate of strain exerted during each processing step. Thus, to predict and improve the processibility, the behavior of the transient polymeric system needs to be assessed under process-relevant conditions. In terms of processibility, the ability of the dough matrix to stabilize the expanding gas cells is of particular interest regarding bread quality. The biaxial extension was previously identified as the dominating strain type during proofing and baking. Generally, it is well-known that wheat dough greatly resists such large amplitude deformations. This resistance has been related to SH, thus, being the basis for the gas holding capacity of proofing wheat dough and during consecutive baking. However, endogenous and exogenous factors affecting this property have yet to be adequately evaluated.

Up to now, too little focus has been put on identifying functionally relevant yeast metabolites and their impact on the physicochemical changes of the wheat dough's polymers. Hence, the elucidation of the effect of yeast metabolites and thermally induced physicochemical changes of the wheat dough's polymers on the SH behavior of wheat dough remains a critical point. Additionally, a potential interaction of these two factors needs to be investigated as the impact of yeast metabolites might affect the solidification behavior of the wheat dough matrix during the dough-to-crumb-transition process. To elucidate the impact of individual yeast metabolites on the wheat dough matrix along the bread making process, this thesis bases on the following three hypotheses:

- The non-yeasted dough can behave similarly to its yeasted counterpart by spiking the primary (CO_2 and ethanol) and secondary (succinic acid) metabolites in their respective concentrations. The spiking of yeast metabolites is hypothesized to affect the rheological behavior of wheat dough in dependency on the applied type and rate of strain. Thus, the individual impact of single yeast metabolites on the functionality during the individual bread making sub-processes can be determined.
- The yeast metabolite-induced changes in the rheological behavior of the yeasted dough matrix are based on the alteration of the protein structure. They can be revealed on the molecular and microscopic length scale.
- The yeast-induced modification of the polymeric structures in wheat dough is further hypothesized to alter the thermally induced polymer transition processes. Consequently, the structural changes on the molecular and microscopic length scale alter the thermal dependency of the flow behavior and the solidification behavior of the wheat dough matrix during baking.

The following procedure was applied to evaluate these formulated hypotheses:

Following the above-stated hypotheses, it was intended to elucidate the effect of the most abundant primary (CO_2 and ethanol) and secondary (succinic acid) yeast metabolites on the rheological behavior and microstructure of the wheat dough matrix. The effect of single yeast metabolites on the behavior of the complex yeasted dough matrix was assessed by spiking yeast metabolites to a non-yeasted dough matrix. Using this approach, the impact of single

yeast metabolites on the behavior of wheat dough under small and large amplitude deformation was quantified. The origin of these functional changes was assessed on a microscopic length scale.

After identifying the structurally and functionally relevant metabolites, their impact on the rheological behavior during thermal processing was considered. Within this scope, the physicochemical changes of gluten and starch were traced along the baking process in the yeasted and non-yeasted dough matrix to reveal the impact of yeast metabolites on the extent and onset of starch gelatinization or gluten polymerization. The relation between these structural changes and the extensional viscosity along baking was evaluated. Due to the relevance for oven rise, the rheological behavior was assessed with a particular focus on the strain-rate dependent SH.

Finally, a resolution towards the impact of yeast metabolites on single wheat dough polymers was achieved by (semi-)artificial wheat dough systems. Artificial model systems, as used by Brandner et al., were reconstituted, (Brandner et al., 2018), to elucidate the impact of yeast metabolites on the single dough polymers. Re-engineered systems, composed of wheat starch and native gluten, as well as semi-inert model systems, were used in this regard. Additionally, water availability varied to represent multiple restrictive conditions. This approach elucidated the impact of yeast metabolites on single wheat dough polymers and their functionality during the bread making process. The strain-rate dependent assessment enabled the transfer to specific sub-processes, such as the slow growth of gas cells during proofing, intermediate strain rates occurring during baking, or fast deformation occurring during the coalescence of gas cells.

2 Methods overview

For a detailed description of the methods applied, the reader is referred to Chapter 4. A brief summary of the applied methods will be summarized in the following chapters.

2.1 Dough and model system preparation

Dough and model systems were prepared using a 50 g-scale z blade kneader. When using commercial German wheat flour, the wheat dough systems were mixed until optimally developed as defined by ICC 115/1. The dough systems were composed of wheat flour, distilled water and 1.5 (w/flour weight)% white sugar, where sugar was added to exclude a nutrient-related inhibition of yeast fermentation. The kneading process was also adapted for the (semi-)inert systems, which were composed of mildly isolated vital gluten (Wehrli et al., 2023) and commercial wheat starch or glass beads, whose composition has been adapted to the particle size distribution of native wheat starch (Alpers et al., 2024). The ratios of vital gluten to starch or glass beads were adjusted to represent the composition of the underlying wheat flour. The hydration level of the (semi-)inert systems was rheologically adjusted to wheat dough to reach comparable $|G^*|$ values at a defined deformation.

Yeast metabolites were either incorporated by yeast fermentation, where different levels of compressed yeast were applied, or by spiking yeast metabolites at relevant concentrations as previously reported (Jayaram et al., 2013). Alternatively, a gentle yeast inactivation method with slight modifications to the method suggested by Newberry et al. was used to incorporate yeast metabolites to a defined level during proofing but not during further processing or successive measurements (Alpers et al., 2024; Newberry et al., 2002). The wheat dough samples rested or proofed for defined fermentation times or 30 min in the case of spiked wheat dough samples until further processing or measurement at 30 °C in hermetically sealed cylinders or in the rheological equipment under comparable conditions.

2.2 Rheological characterization

Shear rheology was applied to the dough and model systems to reveal short-range starch-starch interactions. Using an AR-G2 rheometer (TA Instruments, New Castle, United States of America) equipped with 40 mm cross-hatched parallel plates, frequency sweeps (2 mm measurement gap, 20 °C, 10 min equilibration time followed by a 0.1% deformation at 0.1 Hz to 10 Hz) of the dough samples were performed. A modular compact rheometer (MRC 502, Anton Paar GmbH, Graz, Austria) with cross-hatched parallel plates with a 25 mm diameter was used to perform temperature sweeps with combined multiwave frequency sweeps testing. To avoid structural damage due to sample transfer after the proofing time, the samples were proofed in the rheometer under controlled temperature and humidity using a modular humidity generator (30 °C, 80% relative humidity). Uniaxial sample expansion was facilitated by applying a normal force-controlled gap adjustment with $F_N = 0.01$ N. After proofing, the baking process was imitated when heating the sample to 90 °C at a heating rate of 4.5 °C/min with

continued normal force-controlled gap adjustment. Multiwave frequency sweeps were conducted every 5 °C at a base frequency of 1 Hz and 0.05% deformation and disabled normal force-controlled gap adjustment. Besides the fundamental frequency, the 2nd, 3rd, 5th, 7th, 8th, and 10th multiple were performed simultaneously with a resulting amplitude of 0.082%, which was still quantified to be within the LVE range.

The frequency dependency of $|G^*|$ was fitted using the power law equation according to (Gabriele et al., 2001).

Fundamental extensional rheometry was performed using LSF conducted at a texture analyzer (TA.XT.Plus, Stable Microsystems, Godalming, United Kingdom) equipped with a 50 kg load cell. The samples were placed between two lubricated parallel plates, where the sample and plate diameter were equal. Compression of the samples was conducted after sample loading or after a defined resting/prooing time or baking time, where the temperature control was conducted as described by Alpers et al. (2022, 2023). The compression to 90% of the initial sample height was performed with compression speeds of 0.1, 1.0, 2.0, 5.0, and 10.0 mm/s. The biaxial strain ε_b , biaxial extension rate $\dot{\varepsilon}_b$, and apparent biaxial extensional viscosity η_b^* were calculated using Equation 1 - Equation 5. Additionally, the SHI was calculated by plotting the readings of the stress values for deformations of 0.3, 0.4, 0.5, 0.6, 0.7, 0.8, 0.9, and 1.0 for each displacement speed against the biaxial strain rate using a double logarithmic scale. The stress values for two biaxial strain rates (0.01 s^{-1} and 1.00 s^{-1}) were calculated by fitting the data with a linear model. The slope of a linear model of the stress-strain plot was calculated as SHI (Rouillé et al., 2005).

2.3 Characterization of the wheat dough's polymers

2.3.1 Gluten characterization

On a microscopic length scale, the gluten network was characterized using a Confocal Laser Scanning Microscope (CLSM, eclipse Ti-U inverted microscope with an e-C1 plus confocal system, Nikon GmbH, Düsseldorf, Germany). Proteins were stained with an aqueous Rhodamine B solution or Nile blue solution in ethanol and recorded in fluorescence micrographs ($\lambda_{\text{ex}} = 543\text{ nm}$ or $\lambda_{\text{ex}} = 633\text{ nm}$). The protein network configuration was quantified using the protein network analysis (PNA) approach suggested by Bernklau et al. (2016) in combination with the AngioTool64 software (Bernklau et al., 2016; Zudaire et al., 2011).

Gluten polymerization was indirectly assessed using SDS protein extraction, as suggested by Wilderjans et al. (2008). The quantification of SDS-soluble proteins can be used to gain information about the amount of non-crosslinked and low molecular weight proteins in the dough matrix (Redl et al., 2003). Therefore, heat-induced polymerization of gluten decreases the SDS-extractability of proteins in wheat-based systems (Wilderjans et al., 2008). The protein content of the extracts was determined using the Kjeldahl method ($\text{N} \times 5.7$).

2.3.2 Starch

Differential Scanning Calorimetry (DSC, DSC250, TA Instruments, New Castle, United States of America) was used to quantify the amount of native starch in dough samples and the effect of metabolites on the crystallinity of starch. For this purpose, dough or wheat starch samples were homogenized with an excess of distilled water (dough:water ratio - 1:3(w/w)) and weighted into pans before hermetically sealing these. The enthalpy needed for starch gelatinization was recorded during heating the samples from 20 °C – 90 °C with a heating rate of 10 °C/min in an inert nitrogen atmosphere using a heat flux DSC with Tzero™ technology.

2.3.3 Assessment of polymer hydration

To determine the effect of yeast metabolites and thermal treatment on the amount of bound water, the ratio between total water and the amount of freezable water was determined following a published method (Linlaud et al., 2011). Dough samples of known water content were weighted into pans and hermetically sealed. Starting from 20 °C, the samples were cooled to -30 °C at a cooling rate of 5 °C/min, held isothermally for 1 min, and were then heated to 25 °C at a 5°C/min heating rate. After integrating the endothermic peak at 0 °C, this area was used to calculate the amount of freezable water using the ice-melting constant of 333.5 J/g (Linlaud et al., 2011; Pérez et al., 2019; Yang & Mather, 2014).

Additionally, ¹H-NMR studies were conducted in order to resolve the distribution of water in the dough (Bosmans et al., 2012; Rondeau-Mouro et al., 2015). A low field ¹H-NMR (mq 20 NMR analyzer, Bruker BioSpin GmbH, Rheinstetten, Germany) was used to measure the transverse relaxation times (T_2) by applying a Carr-Purcell-Meiboom-Gill (CPMG) pulse sequence or a combination of free induction decay (FID) and CPMG. An exponential fit was performed in order to obtain the intensity and relaxation time of the two FID and three CPMG populations, as suggested by Rondeau-Mouro et al. (2015).

2.4 Baking trials

Baking trials were conducted with dough samples produced, as reported in Chapter 2.1. 220 g of dough was portioned, shaped, and placed into loaf pans. Proofing was conducted for the respective fermentation period at 28 °C and 80% relative humidity. Subsequently, baking was performed at 230 °C and 0.5 l steam for 18 min in a Matador 12.8 oven (Werner & Pfleiderer Lebensmitteltechnik GmbH, Dinkelsbühl, Germany). After allowing the structure to settle, the volume of the loaves was determined using a volumeter (Volscan BVM-L 370, TexVol Instruments, Viken, Sweden) and crumb hardness was measured using a Texture Analyzer (TVT-300 XP, TexVol Instruments, Viken, Sweden) following the AACCI method 74-09 with modifications as described by Brandner et al. (2022a).

2.5 Assessment of wheat dough acidification

To resolve the origin of the acidification in yeasted wheat dough, the concentrations of organic acids released during proofing were quantified using liquid chromatography tandem mass spectrometry (LC-MS/MS) as previously published by Bösl et al. (2023). 5 g fermented wheat dough were homogenized after 3 h of fermentation at 30 °C in 10 ml 50 (v/v)% acetonitrile/water using an Ultra Turrax (T25, IKA Labortechnik, Staufen, Germany). After 30 min of extraction under constant shaking, the solids were removed by centrifugation (4500xg, 20 °C, Rotina 420 R, Hettich GmbH & Co. KG, Tuttlingen, Germany) and membrane filtration (0.45 µm polyethersulfone syringe filter, Machery-Nagel GmbH & Co. KG, Düren, Germany). The resulting extract was diluted 1:10 (v/v) with 50 (v/v)% acetonitrile/water. To enhance the separation and fragmentation of the analyst (Bösl et al., 2023), derivatization was conducted following a published procedure (Amann et al., 2022).

The samples were injected into an LC-MS/MS system at an injection volume of 10 µl. The HPLC system (Agilent, Waldbronn, Germany), consisting of a HiP-ALS SL autosampler, a 1200 series bin pump module, a 1200 series degasser and a 1100 series column oven, was operated with a SecurityGuard™ ULTRA Cartridge Polar C18 (Phenomenex, Aschaffenburg, Germany) and a 100 Å Kinetex® C18 column, 150 × 2.1 mm, 2.6 µm particle size column (Phenomenex, Aschaffenburg, Germany) at a flow rate of 200 µl/min at 40 °C column temperature. The eluents used were 0.1% (v/v) formic acid in water (eluent A) and 0.1% (v/v) formic acid in acetonitrile (eluent B). The following gradient was followed: 1 min isocratic 15% B before a gradual increase to 35% B within 11 min, followed by an increase to 100% B within 1 min and 1 min 100% B. Initial conditions were restored by reducing the concentration of B to 15% within 1 min, followed by 2 min of isocratic elution. Detection was conducted using the coupled Triple Quad 4500 MS (AB Sciex Germany GmbH, Darmstadt, Germany) with the following settings: ion spray voltage was set to -4.500 V, the curtain gas pressure was set to 35 psi, the nebulizer gas pressure was 65 psi, the heater gas pressure was 55 psi and the turbogas temperature was set to 450 °C. The quantification was conducted using MultiQuant (version 3.0.2, AB Sciex Germany GmbH, Darmstadt, Germany). A correction of the quantified concentrations was performed based on the recovery of sorbic acid, which was added during the homogenization of the dough samples.

The quantified concentrations of succinic and acetic were spiked to a non-yeasted wheat dough during kneading in a UMSK 24 mixer (Stephan Machinery GmbH, Hameln, Germany). The combined effect of organic acids and solubilized CO₂ was quantified by exchanging the headspace atmosphere to CO₂ prior to mixing (evacuation to -800 mbar followed by re-equilibration to 1 bar with CO₂). Subsequently, mixing was performed for 3 min at a mixing speed of 300 rpm. The pH of the dough samples was assessed directly after mixing by a pH meter for solids (Testo-206, Testo SE & Co. KGaA, Lenzkirch, Germany).

2.6 Statistical analysis

If not stated differently, the measurements were performed with technical triplicates, where replication started from the dough preparation step in the measurement protocol. All data is reported as mean values with standard deviation. Where propagation of uncertainties was used to calculate the standard deviation of indirect measures, the standard error is stated along with the mean value. Significant differences between groups were tested with the parametric ANOVA test, followed by Tukey's test, and non-parametric Kruskal-Wallis test, followed by Dunn's test, on a significance level of $\alpha = 0.05$. Mathematical and statistical evaluations were performed using Matlab (R2018a, MathWorks Inc., Natick, United States of America) and Origin (2018b-2021, OriginLab Corporation, Northhampton, United States of America).

3 Results

3.1 Summary of thesis publications

The publications created within the scope of this dissertation are included as original copies.

| 1. The self-enforcing starch–gluten system — Strain–dependent effects of yeast metabolites on the polymeric matrix | Pages |
|---|---------|
| | 42 - 56 |

Chapter 3.1 focuses on the effect of yeast metabolites on the microstructure and rheological behavior of the wheat dough matrix. The material behavior needs to be assessed under process-relevant deformation types in relation to time to predict the impact of yeast fermentation on the behavior of the polymeric dough system during the decisive processing steps. The work was based on the hypothesis that a yeasted wheat dough can be considered an accumulation of yeast metabolites. Furthermore, these metabolites were expected to affect the protein microstructure and the rheological behavior. Thus, the effect of yeast metabolites on the rheological behavior of yeasted and metabolites-spiked wheat dough was assessed. The functionality of yeasted wheat dough was strongly related to the protein microstructure. Yeast fermentation resulted in shorter protein strands and was shown to impede interactions, which was linked to a decreasing consistency and flow index. SAOS measurements were performed to track these changes back to the impact of single metabolites. Here, CO₂ was found to majorly impact the functionality of the dough matrix. In contrast, ethanol and succinic acid did not affect the functionality of the network in the same way as observed in case of yeasted dough. A minor impact of these chemical stressors was also quantified on SH. On the contrary, the strain-rate dependent SH of chemically and biologically leavened dough matrices differed drastically from non-yeasted dough. The extent of SH was successfully linked to the deformation history of the dough matrix, the condition of the protein microstructure, and the spatial distribution of the matrix components. Here, a depletion of the gas cell surrounding lamella was suggested, leading to an accumulation of starch granules in the nodes, thereby causing increased SH. The fact that the SH behavior of the yeasted dough matrix was emphasized even though structural degradation was quantified on various structural levels led to the consideration of the yeasted dough matrix as a self-enforcing system. To summarize, a major impact on the dough's functionality was identified for CO₂, a mechanical stressor. In contrast, chemical stressors only minorly influenced the structure and functionality of wheat dough, especially at short fermentation times.

Contributions: The doctoral candidate created the design of the study, partially carried out analysis, interpreted data, performed statistical analysis as well as drafted and revised the article. V. Tauscher supported the optimization of the experimental setup and conducted the LSF measurements. Co-authors critically revised the design of the article and supported the evaluation and interpretation of the data. All authors critically reviewed and edited the manuscript of this article.

| | |
|--|----------------|
| 2. 3.3 Relation between polymer transitions and extensional viscosity of dough systems during thermal stabilization assessed by lubricated squeezing flow | Pages |
| | 57 - 68 |

Besides mechanical processing, bread making involves thermally induced polymer transitions. The hydrothermal treatment of the main dough polymers changes the structure and functionality due to starch gelatinization, protein denaturation, and protein polymerization. As shown in Chapter 3.1, CO₂ strongly alters the protein microstructure and matrix functionality in the non-heated dough matrix. Subsequently, the work presented in Chapter 3.2 elucidates the direct and indirect impact of yeast metabolites on the temperature-dependent polymer transitions during the baking process. Additionally, the outstanding question of the contribution of hydrothermally induced polymer transitions on the dough matrix components to the overall course of extensional viscosity in leavened and non-leavened doughs is addressed throughout the baking process. On this functional level, a strong impact of gaseous CO₂ in the dough matrix was found on the solidification behavior of the dough matrix during the thermal treatment. The extensional viscosity of leavened dough matrices gradually rose, whereas the non-leavened dough matrix adhered to the renowned, starch-induced sharp rise in viscosity. Due to the insufficient explanation for this behavior, the impact of CO₂ and chemical stressors on polymer transitions of the dough's polymers was characterized on a molecular and microscopic length scale. Explanations for the delayed increase of the extensional viscosity of the yeasted wheat dough matrix were found in a degrading impact of CO₂ gas cells on the gluten network, resulting in a wider meshed and less branched network. Through the entrapment of gas cells on a microscopic length scale, limited heat-induced molecular polymerization was quantified in the yeasted dough, which was related to the existence of gluten fragments and sterically inhibited crosslinking. Contrarily, the slightly premature onset of starch gelatinization in the yeasted wheat dough matrix does not appear to majorly impact the course of the extensional viscosity of the dough matrix. Higher mobility of weakly bound water in the yeasted dough and a starch depletion in the gas cell-surrounding lamella was suggested to cause an excess hydration of starch granules in the yeasted dough, which resulted in an early onset of starch gelatinization.

Contributions: The doctoral candidate created the design of the study, partially carried out analysis, interpreted data, performed statistical analysis as well as drafted and revised the article. J. Olma conducted the microscopic analysis, NMR measurements and extractability trials as well as parts of the calorimetric measurements. Co-authors critically revised the design of the work and supported the evaluation and interpretation of the data. All authors critically reviewed and edited the manuscript of this article.

| | |
|--|----------------|
| 3. Strain-dependent assessment of dough's polymer structure and functionality during the baking process | Pages |
| | 69 - 87 |

The behavior of the polymeric wheat dough matrix during the bread making process is strongly dependent on the interactions among the polymers. Based on the applied deformation, different structural elements respond strain-dependently. As described in Chapter 3.2, the conformation of the dough polymers changes throughout the baking process as the hydrothermal treatment and yeast metabolites affect the micro- and macrostructure of the polymeric matrix. As the bread making process comprises diverse deformations, the dough matrix's functionality must be examined under different deformations and types of strain. Particular attention should be devoted to large amplitude extensional deformation and the characterization of the strain-hardening behavior of the matrix, as the oven rise behavior and, therefore, the bread quality, is known to be strongly linked to these material characteristics. The aim of Chapter 3.3 was to elucidate the link between the rheological behavior upon different types and magnitudes of strain exerted and the oven rise behavior. The gained information allowed the development of a structural model for the dough polymers during baking, which was used to explain the oven rise behavior of yeasted and non-yeasted dough. Together with the results of Chapter 3.2, an understanding of polymer functionality on dependency of their molecular and microstructure was developed for two structurally different dough systems: a highly connected non-yeasted wheat dough and a less branched, microstructurally degraded yeasted wheat dough. Yeasted dough systems revealed a higher share of gluten functionality as the CO₂-induced expansion of the matrix favored the occurrence of large amplitude deformation behavior. For the same reason, a higher extent of SH was observed for yeasted dough at all temperatures, resulting in a higher consistency of the yeasted dough matrix. Although the protein connectivity was reduced on a molecular and microscopic length scale, the greater extent of SH further accounted for the higher gas holding capacity. Therefore, the self-enforcing nature of the yeasted wheat dough system was once more underlined, even though limitations were found to occur with the overall matrix solidification. Accordingly, oven rise was limited prematurely around 60 °C, where the maximum SH was observed.

Contributions: The doctoral candidate created the design of the study, carried out analysis, interpreted data, performed statistical analysis as well as drafted and revised the article. Co-authors critically revised the design of the work and supported the evaluation and interpretation of the data. All authors critically reviewed and edited the manuscript of this article.

4. New insights into crumb formation in model systems: Effects of yeast metabolites and hydration level by means of multiwave rheology **Pages 88 - 99**

Chapters 3.1 to 3.3 generated considerable knowledge on the structure and functionality of dough polymers in the presence of yeast metabolites along the bread making process. Due to the complexity of the wheat dough matrix, a final differentiation between the yeast-induced modifications in the transition behavior of starch and gluten was still limited and remained hypothetical. Therefore, this study addresses the impact of the presence of yeast metabolites on the solidification process in wheat dough by differentiating starch- and gluten-based impacts. Model systems were reconstituted to elucidate the impact of yeast metabolites on the single dough polymers. Wheat starch – native gluten mixtures and semi-inert model systems were created to trace the impact of yeast metabolites on the thermally induced transitions of dough polymers. Additionally, the availability of water was varied to represent multiple restrictive influences.

In wheat dough systems, a destabilizing effect of the present yeast metabolites was found, even though yeast metabolites did not affect the solidification point. Using the wheat starch-gluten model system, the temperature-dependent solidification behavior of wheat dough was successfully imitated. Similar to the wheat dough system, the onset of the solidification process was not affected by yeast. Nevertheless, the magnitude of the solidification process increased in the presence of yeast metabolites, suggesting the importance of water availability for the course of the solidification process. A similar effect was observed in the presence of a higher hydration level, which supports the importance of water availability. In the semi-inert gluten-based model system, a degrading effect of yeast metabolites was observed throughout baking, underlining the degrading impact of yeast on the gluten network. It was further revealed that the highest gluten polymerization was facilitated in a non-starch-based model system. This result supports the hypothesis from Chapter 3.2 on the spatial hindered polymerization in the presence of gas cells.

Contributions: The doctoral candidate created the design of the study, partially carried out analysis, interpreted data, performed statistical analysis, and drafted as well as revised the article. D. Panoch contributed to the development of the experimental setup, conducted all laboratory experiments except NMR measurements, and supported with the evaluation and interpretation of the data. The other co-authors critically revised the design of the work, and reviewed as well as edited the manuscript of this article.

3.2 The self-enforcing starch-gluten system – Strain-dependent effects of yeast metabolites on the polymeric matrix



Article

The Self-Enforcing Starch–Gluten System—Strain–Dependent Effects of Yeast Metabolites on the Polymeric Matrix

Thekla Alpers ¹, Viviane Tauscher ², Thomas Steglich ², Thomas Becker ¹ and Mario Jekle ^{1,*} 

¹ Research Group Cereal Technology and Process Engineering, Institute of Brewing and Beverage Technology, Technical University of Munich, 85354 Freising, Germany; thekla.alpers@tum.de (T.A.); tb@tum.de (T.B.)

² Dr. Oetker Technology Development Center, 19243 Wittenburg, Germany; viviane.tauscher@gmx.de (V.T.); thomas.steglich@oetker.com (T.S.)

* Correspondence: mjekle@tum.de; Tel.: +49-8161-71-3669

Abstract: The rheological behaviour of dough during the breadmaking process is strongly affected by the accumulation of yeast metabolites in the dough matrix. The impact of metabolites in yeasted dough-like concentrations on the rheology of dough has not been characterised yet for process-relevant deformation types and strain rates, nor has the effect of metabolites on strain hardening behaviour of dough been analysed. We used fundamental shear and elongational rheometry to study the impact of fermentation on the dough microstructure and functionality. Evaluating the influence of the main metabolites, the strongest impact was found for the presence of expanding gas cells due to the accumulation of the yeast metabolite CO_2 , which was shown to have a destabilising impact on the surrounding dough matrix. Throughout the fermentation process, the polymeric and entangled gluten microstructure was found to be degraded (-37.6% average vessel length, $+37.5\%$ end point rate). These microstructural changes were successfully linked to the changing rheological behaviour towards a highly mobile polymer system. An accelerated strain hardening behaviour ($+32.5\%$ SHI for yeasted dough) was promoted by the pre-extension of the gluten strands within the lamella around the gas cells. Further, a strain rate dependency was shown, as a lower strain hardening index was observed for slow extension processes. Fast extension seemed to influence the disruption of sterically interacting fragments, leading to entanglements and hindered extensibility.

Keywords: yeast fermentation; wheat dough; strain hardening properties; fundamental extensional rheology; lubricated squeezing flow; shear rheology; protein network analysis; CLSM



Citation: Alpers, T.; Tauscher, V.; Steglich, T.; Becker, T.; Jekle, M. The Self-Enforcing Starch–Gluten System—Strain–Dependent Effects of Yeast Metabolites on the Polymeric Matrix. *Polymers* **2021**, *13*, 30. <https://dx.doi.org/10.3390/polym13010030>

Received: 19 November 2020
Accepted: 21 December 2020
Published: 23 December 2020

Publisher's Note: MDPI stays neutral with regard to jurisdictional claims in published maps and institutional affiliations.



Copyright: © 2020 by the authors. Licensee MDPI, Basel, Switzerland. This article is an open access article distributed under the terms and conditions of the Creative Commons Attribution (CC BY) license (<https://creativecommons.org/licenses/by/4.0/>).

1. Introduction

The behaviour of wheat dough, considered as a non-Newtonian fluid, is strongly dependent on the type and strength of stress applied. The processability is thereby determined by the viscoelastic properties of wheat dough, resulting from different interactions among the major and minor dough components [1,2]. Due to the heterogeneous network configuration and the complex rheological behaviour, the response of the dough system is likely to depend on the type and strength of stress applied to the system. Especially during the complex breadmaking process, various types of deformation are applied. Beside the application of external forces (e.g., during kneading, sheeting or shaping), the dough is subjected to extension processes as the dough matrix is stretched during the fermentation process. Thereby, the dough matrix, considered as the material located in lamellas around the gas cells, is tangentially extended in two directions and uniaxially compressed in the radial direction while the gas cells increase in size. Different models were applied to estimate extension rates arising during the fermentation. Bloksma (1990) proposed a model consisting of gas-filled cylinders, embedded in the dough matrix phase, undergoing uniaxial extension as the volume of the gas phase increases during fermentation. The extensional strain rates, calculated based on the model of Bloksma (1990) (c.f. Equation (1)), are in the range of 10^{-4} – 10^{-3} s^{-1} [3].

$$\dot{\varepsilon} = \frac{1}{V_{rel}} \cdot \frac{dV_{rel}}{dt} \quad (1)$$

where V_{rel} is the relative volume ($V_{\text{gas} + \text{dough matrix phase}}/V_{\text{dough matrix phase}}$). In a different approach, van Vliet estimated the biaxial strain of the dough matrix phase around the gas cells [4]. Assuming a constant gas cell number with increasing size over time, the biaxial strain rate is then defined by Equation (2).

$$\dot{\varepsilon} = \frac{dV_{rel}}{3(V_{rel} - 1)dt} \quad (2)$$

The extensional strains found with this approach are comparable to Bloksma's approach and range from 1.3×10^{-4} to $1.1 \times 10^{-3} \text{ s}^{-1}$, decreasing with increasing fermentation time as the changes in the relative volume decrease [4]. A more practical approach was conducted by Weegels et al. (2016), who traced moving starch granules under the microscope, which were accelerated due to the coalescence of gas cells. Using this approach, maximum extension rates of 10^1 to 10^2 s^{-1} were found for proofing dough during the merging process of two gas cells [5]. The presented mathematical models represent an appropriated assumption regarding the overall fermentation process. Thus, as the merging process is part of the destabilisation processes of the dough matrix occurring during the fermentation process, it is necessary to characterise the rheological behaviour of the dough matrix for a broad range of extension rates.

Resisting these biaxial extension forces, the dough matrix is characterised by a high gas retention capacity. This capability is strongly correlated to gluten functionality and its strain hardening characteristics, preventing physical instabilities as coalescence of gas cells and disproportionation. Especially strain hardening behaviour, a phenomenon known in polymer science which can also be observed in dough, requires elongational deformation to be quantified. Undergoing increasing extensional strain, an overproportioned rise in stress is detected at constant strain rates with this phenomenon [4,6].

During the fermentation step, CO_2 and many secondary metabolites are generated by yeast cells and released into the dough matrix phase due to common metabolic activity, or, in case of osmotic stress, to maintain the internal redox balance [7]. An often-underestimated effect is the impact of secondary metabolites on the rheological properties of the dough matrix, clearly determining the manufacturing properties and end product characteristics [7–13]. Thus, the aim of the current study is to characterise the rheological behaviour of the fermenting dough matrix for relevant deformation types and strain rates occurring during the breadmaking process. As the behaviour of yeasted dough during the breadmaking procedure is dependent on the exerting load of the current process step and the fermentation-time-dependent metabolite concentration (e.g., CO_2 , acids and ethanol) released into the dough matrix, it is important to characterise dough's rheological behaviour for deformation types and loads relevant for the breadmaking process. These insights are used to integrate the knowledge of the effects of different yeast metabolites on the rheological behaviour of the dough matrix for the evaluation of strain hardening of fermenting dough at different strain rates. It is hypothesised, that the fermentation process can be considered as an accumulation of metabolites in the dough matrix and the rheological changes can therefore be described by the sum of the impact of each individual metabolite on the dough microstructure. This altered functionality in terms of rheological behaviour is assumed to result from the modified dough microstructure. Therefore, a standard wheat dough, a yeasted dough and a wheat dough spiked with metabolites in yeasted dough-like concentrations, were characterised using shear and elongational rheometry. As elongational deformation occurs during most of the dough processing steps, extensional rheometry provides promising knowledge on practice-related dough behaviour [14], exerting the same load as e.g., fermentation or baking. Lubricated squeezing flow, quantifying the biaxial extensional viscosity, is therefore used to analyse the behaviour of wheat dough and fermented wheat dough at various strain rates. As the

extensional strain rates occurring during the breadmaking process were shown to vary within several magnitudes, strain hardening properties were evaluated for a slow and high extension rate within the limits of the applied method. In addition to the rheological characterisation, quantitative microstructural analysis has been shown to be a powerful tool in predicting dough rheology [15]. Protein network analysis (PNA) was thus used to obtain insights into the relation between the rheological behaviour and the microstructural conformation. The obtained knowledge can help to achieve a better understanding of the influence of individual yeast metabolites on the process behaviour of dough during the breadmaking process and support for knowledge-based choice of fermentation parameters benefitting desirable dough properties.

2. Materials and Methods

2.1. Wheat Dough Composition

German commercial wheat flour Type 550 with 13.34 ± 0.11 g moisture per 100 g flour (AACCI 44-01), a protein content of 11.26 ± 0.10 g per 100 g dry flour (AACCI 46-16, N \times 5.7), 0.55 ± 0.05 g ash per 100 g dry flour (ICC 104/1) and 30.5 ± 0.1 g wet gluten per 100 g flour was used in this study. Dough resistance and water absorption were measured in a Z-kneader doughLAB (Perten Instruments AB, Hägersten, Sewden) according to AACCI 54-70.01 to determine the required kneading time.

2.2. Fundamental Shear Rheology

For the shear rheological measurements, 50 g flour (corrected to 14.00% moisture), 3 g white sugar/100 g flour (EC category II quality, Bäko, Nürnberg, Germany) and demineralised water were kneaded for 120 s at 63 rpm using a Z-kneader, equipped with a 50 g bowl. Yeasted doughs were prepared with fresh compressed yeast (*S. cerevisiae*, F.X. Wieninger GmbH, Passau, Germany) at levels of 1 and 2 g yeast/100 g flour. Sugar was added in order to enable unpressed fermentation by sufficient fermentable sugars. To recreate the level of different metabolites in dough, ethanol, succinic acid and CO₂ were incorporated in yeast-free doughs in amounts as found by [16]. Respectively 5, 10, 15 or 30 mmol/100 g flour Ethanol (absolute, VWR Chemicals, Darmstadt, Germany) or 0.2, 0.3, 0.4 or 0.5 mmol/100 g flour succinic acid (high purity grade, VWR Chemicals, Darmstadt, Germany) were added, representing the amounts produced by 2 g yeast/100 g flour in dough after 0.5, 1, 2 and 3 h fermentation. To simulate the amount of gaseous CO₂ released during fermentation, different concentrations of a mixture of Glucono-delta-lactone (Alfa Aesar GmbH & Co KG, Karlsruhe, Germany) and NaHCO₃ (Solvay GmbH, Hannover, Germany) were used as raising agent. The amount of NaHCO₃ needed for neutralisation was calculated according to Verheyen et al. (2016) [13]. To adjust the incorporated amount of CO₂, the volumes of chemically and biologically leavened doughs were compared in graduated cylinders in order to reach the same volume expansion.

After kneading, 7.5 g dough were moulded to sphere form and stored under closed atmosphere (to prevent dehydration) in a drying chamber at 30 °C for periods of 0.5, 1, 2 and 3 h until shear rheological measurements were performed. To standardise the extent of endogenous enzymatic activities and dough relaxation processes, the resting time for metabolite doughs was set to 0.5 h for all metabolite concentrations. Shear rheological measurements were performed using an AR-G2 rheometer (TA instruments, New Castle, DE, USA), equipped with parallel cross-hatched plates (40 mm diameter) at a constant gap of 2 mm. The temperature was constantly controlled to 20 °C by a smart swap peletier plate temperature system. Dough samples were placed centred on the lower plate and excess dough was removed after the gap was set. The cut surface was coated with paraffin oil to prevent dehydration. Subsequently, the sample was allowed to relax for an equilibration time of 10 min before a frequency sweep was performed in a range from 0.1 to 10 Hz at a

constant deformation of 0.1%. The obtained complex module data (G^*) were fitted to the power law equation (c.f. Equation (3)).

$$G^*(\omega) = A_f \omega^{1/z} \quad (3)$$

where ω is the angular frequency (s^{-1}), A_f refers to the network strength ($\text{Pa s}^{1/z}$) and z to the network connectivity ($-$) [17].

2.3. Elongation Properties by Lubricated Squeezing Flow

Due to the higher amount of dough needed for LSF measurements, the dough was prepared in a spiral kneader (KM-25, SINMAG Bakery Equipment, Zuijenkerke, Belgium). 2000 g flour (corrected to 14.00% moisture), 3 g white sugar/100 g flour (EC category II quality, Sweet family, Nordzucker AG, Braunschweig, Germany) and tap water were pre-mixed for 30 s and consequently kneaded at 280 rpm for 360 s. For the preparation of yeasted doughs, fresh compressed yeast (*S. cerevisiae*, Uniferm GmbH & Co., Werne, Germany) at levels of 1 and 2 g yeast/100 g flour was added. The dough was sheeted to a final height of 20 mm and cut to cylindrical pieces using lubricated cylindrical cutters (45 mm diameter). The moulded samples were placed into a fermentation chamber (28 °C, 71% rh). The dough samples of the reference and yeast doughs were measured after 0, 4, 7, 10, 30, 60, 120 and 180 min. The metabolite doughs were analysed after 30 min. The measurement was performed with a self-constructed rig for a texture analyser (TA.XT.Plus, Stable Microsystems, Godalming, UK) equipped with a 50 kg load cell based on the experimental procedure described by [18]. The sample was placed between two lubricated perspex plates of 45 mm diameter. The cylindrical sample had the same initial diameter as the upper and lower plate of the experimental setup and was subsequently compressed at displacement speeds of 0.1, 1, 2, 5 and 10 mm/s. The samples were compressed from an initial height of 20 mm to 2 mm, representing a final deformation of 90%. The biaxial strain ε_b and biaxial strain rate $\dot{\varepsilon}_b$ were calculated according to equations 4 and 5 [18],

$$\varepsilon_b = \frac{1}{2} \ln \frac{h_t}{h_0} \quad (4)$$

$$\dot{\varepsilon}_b = -\frac{\dot{h}}{2h_t} = -\frac{v}{2h_t} \quad (5)$$

where h_t and h_0 are the thickness at time t and the initial sample thickness and v is the compression speed. The apparent biaxial viscosity was calculated according to Equation (6) [1],

$$\eta_b^* = -\frac{F_t}{\pi r_p^2 \dot{\varepsilon}_b} \quad (6)$$

where F_t is the force recorded by the load cell at time t and r_p is the radius of the plates. The strain hardening index (SHI) was calculated as proposed by [1,19]. Therefore, the stress σ was calculated according to Equation (7),

$$\sigma = \frac{F}{A} \quad (7)$$

with A being defined as the plate area. Stress values for given deformations (0.3, 0.4, 0.5, 0.6, 0.7, 0.8, 0.9, 1.0) were extracted for each measurement at the five compression speeds and were plotted against the biaxial strain rate on a double logarithmic scale. The data for constant deformation was fitted applying a linear model. Using this regression models, stress values were calculated for given values of $\dot{\varepsilon}_b$ (0.001, 1.00) and plotted against the

deformation on a logarithmic scale. The slope of the linear fit of the plotted data is defined as the SHI, expressed by Equation (8) [1]:

$$SHI = \left(\frac{\delta \ln(\sigma)}{\delta \dot{\epsilon}_b} \right)_{\dot{\epsilon}_b=const.} \quad (8)$$

2.4. Microstructural Analysis

The protein microstructure was visualised using a confocal laser scanning microscope (eclipse Ti-U inverted microscope with an e-C1 plus confocal system, Nikon GmbH, Düsseldorf, Germany) with a Plan Apo VC $60 \times / 1.40$ oil objective. The dough was prepared according to the procedure described in Section 2.2 and stained according to the bulk water technique described by [20] using Rhodamine B (0.01 g/100 mL water, Sigma-Aldrich GmbH, Munich, Germany). Proteins were recorded in fluorescence micrographs ($\lambda_{ex} = 543$ nm, $\lambda_{em} = 590/50$ nm) with a 1024×1024 pixel resolution.

Image processing was performed using the method protein network analysis (PNA) as proposed by [21]. The software AngioTool64 version 0.6a (National Cancer Institute, National Institute of Health, MD, USA, [22]) was applied and the following morphological attributes were chosen for further discussion: Branching rate (number of junctions/protein area), end-point rate (number of end points/protein area), average protein length and width (length and width of a continuous protein strand) and lacunarity (a measure for gaps and irregularities).

2.5. Statistical Analysis

All measurements were performed in triplicates. The stated standard deviation accounts for the deviation between triplicates and, in case of modelling, the standard error of the estimates. The propagation of uncertainties was used according to Equation (9) to calculate the absolute error STD [23].

$$ST = \sqrt{\left(\frac{\delta f}{\delta x} \right)^2 STD_x^2 + \left(\frac{\delta f}{\delta y} \right)^2 STD_y^2 + \left(\frac{\delta f}{\delta z} \right)^2 STD_z^2} \quad (9)$$

where STD_x , STD_y , STD_z is the standard deviation of each measurand and $\left(\frac{\delta f}{\delta x} \right)$ is the partial derivation of the function according to each measurand. Mathematical and statistical evaluation was performed using Matlab (R2018a, MathWorks Inc., Natick, MA, USA) and Origin (2018b, OriginLab Corporation, Northampton, MA, USA). Kruskal-Wallis test as a non-parametric test followed by Dunn's Test as a post-hoc test were used to detect significant differences between groups on a significance level of $\alpha = 0.05$.

3. Results

3.1. Network Characterisation under Small Deformation

A frequency sweep at low deformation, within the linear-viscoelastic region (i.e., non-destructive/-structure invasive) was used to quantify the strength of short-range interactions as they occur among starch–starch and starch–gluten polymers [2]. The strength of the short-range interactions was quantified in terms of network strength A_f and network connectivity z . Those coefficients were obtained using the power law equation to fit the frequency dependency of the complex shear modulus G^* .

A standard wheat dough serves as a reference point since this corresponds to the untreated case. As shown in Figure 1, the rheological behaviour of standard wheat dough is shown to be dominated by relaxation processes of the gluten structure as a time-dependent weakening of the dough structure occurred during dough resting. The network connectivity, a measure for the extend of interactions within the structure, slightly decreased with increasing resting time. On a molecular level, this relaxation behaviour is attributed to the conformational changes occurring as the polymer matrix is attempted to reach a thermodynamically preferred equilibrium. Along those changes, occurring after the

termination of energy input throughout the kneading step, the proteins abandon their unfolded and extended conformation and return to a compact structure. Due to this process, the system has a decreasing ability to form intermolecular forces. After the kneading step, the protein strands are in a strongly aligned conformation and are forced to interact among shortrange interactions among the highly extended, densely packed strands. With increasing resting time, the loop-train structure is re-achieved and the high number of forced, low entropic interactions is replaced with fewer, more stable interactions. This was shown to prevail the re-polymerisation process upon the reformation of S-S-bonds, as the network connectivity shows an overall decrease during dough resting. Furthermore, the decreasing consistency was related to conformational changes during the relaxation process in terms of the re-formation of loop regions based on the loop and train model proposed by [24]. Additionally, endogenous enzymatic activity might contribute to the time-dependent behaviour of non-yeasted standard wheat dough [25].

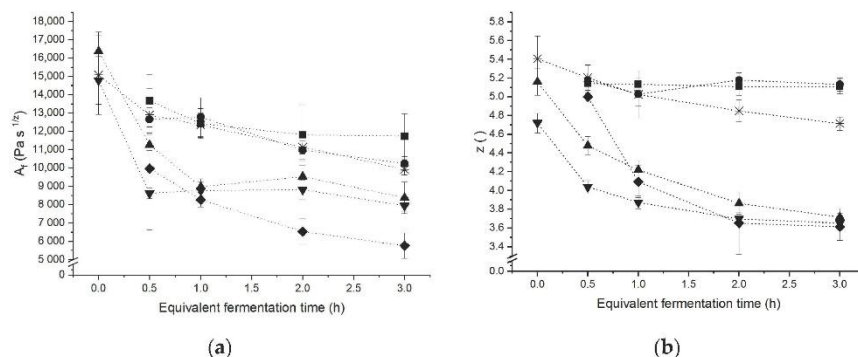


Figure 1. Effect of different yeast levels and yeast metabolites on power law constants during 3 h fermentation at 30 °C. (a) Network strength A_f . (b) Network connectivity z . (□) Reference without additives, (▲) 1 g yeast/100 g flour, (▼) 2 g yeast/100 g flour, (◆) CO_2 , (■) succinic acid, and (●) ethanol. The term equivalent fermentation time does not represent a real time for metabolite spiked doughs as those doughs contain the same amount of metabolites as [16] quantified in fermenting doughs (2 g yeast/100 g flour) at the marked time points, but rested for only 0.5 h after kneading. ($n = 3$, $\bar{X} \pm \text{STD}$).

As might be expected, the presence of yeast caused the dough network to turn considerable instable. The network structure appears less stable as the network branching and strength of the interactions are markedly lower. Those effects, comprising the structural degradation of the dough microstructure, were shown to be concentration dependent as the network is shown to be substantially more instable with a higher yeast level. The origin of the above-mentioned structural changes, causing the modified rheological behaviour, is assumed to be caused by the rupture of protein strands inside the gas cell-surrounding lamella due to the mechanical forces exerted by expanding gas cells [26]. To verify this assumption, different concentrations of yeast metabolites found during the fermentation process have been used in spiking experiments to reconstruct doughs in order to reformulate a fermenting dough. To reduce the complexity and enhance the validity, only one metabolite at once was used in the metabolite doughs.

Initiated by the presence of gaseous CO_2 in fermenting dough-like amounts, the frequency dependence was shown to be increased and the consistency was lowered like in yeasted dough as indicated in Figure 1. These findings are in agreement with Chin et al. (2005) who found the presence of CO_2 to decrease the load capacity of dough, especially the failure stress was shown to develop indirect proportional to the gas void fraction [27]. As the amount of CO_2 produced over time increases and gas cells increase in size, the increasing gas void fraction is leading to a growing spatial demand. Thus, the interactions

of dough polymers are sterically hindered by the presence of gaseous CO_2 in the raising dough matrix. Beside gaseous CO_2 as a main metabolite, it appeared that the presence of ethanol and organic acids caused only minor changes. Ethanol was found to affect the dough matrix behaviour only for high concentrations. This confirms the results of [9,10], who found ethanol to influence the dough structure at concentrations above 2 v/v%. Such an ethanol concentration would only be reached after 3 h at a yeast level of 5.3 g/100 g flour [16], which represents a rather high concentration for the production of baked goods. This indicates that this metabolite has no weakening influence on dough structure during the early fermentation state. The effects of this metabolite can only be seen in the latter fermentation state, where ethanol causes a slight increase in the number of interactions ($z \uparrow$). At the same time, the strength of the system was shown to be decreased ($A_f \downarrow$), which probably reflects the dilution effect caused by the increasing amount of liquid present in the system. According to the Osborne fractionation, ethanol acts as solvent for gliadins. Therefore, it is expected, that this gluten fraction shows a swelling behaviour which causes the reduction of the reinforcing effect of gliadins on the glutenin network as previously reported by [28]. For succinic acid, a re-enforcing effect on the dough matrix functionality has been observed. Succinic acid enabled a higher network connectivity and strength (z and $A_f \uparrow$). This matched the findings of Wehrle (1997), who found lactic acid and acetic acid to cause a more elastic and firmer dough behaviour [29]. Further, Jayaram (2014) reported succinic acid to stiffen the dough structure, accompanied by a decreasing dough extensibility. The authors attributed this behaviour to unfolding and swelling of the gluten proteins in presence of succinic acid. As the network connectivity z was shown to be markedly increased in presence of succinic acid, these conformational changes are considered to increase the number and strength of possible interactions due to the greater accessibility upon the unfolded and elongated protein conformation. This indicates that small amounts of acid, as present on fermented yeasted dough seem to strengthen the dough structure and increase the stability of the system.

The results of this section indicate that CO_2 has the greatest functional influence on the rheological behaviour of dough under small deformation. The destabilising effect of gas was shown to predominate over the reinforcing effect of acid in fermented dough.

3.2. Extensional Viscosity of Yeasted Wheat Dough

Beside the characterisation in the linear viscoelastic shear flow regime, an extensional flow technique was applied to analyse the extensional viscosity of the system (Figure 2). Dough as a polymeric system with gluten as three-dimensional entangled macromolecule is characterised by a high extensional viscosity [30]. Since the gained flow curves show a linear relation within extensional viscosity and extension rate ($R^2_{\text{adj}} = 0.99$), a power law model (c.f. equation 10) can be employed to analyse the flow behaviour

$$\eta_b(\dot{\varepsilon}) = K \cdot \dot{\varepsilon}^{(n-1)} \quad (10)$$

where K (Pa sⁿ) is the consistency index and n (-) is the flow index [31]. Seeing the flow index being lower than 1, the general dough elongational behaviour within the considered region can be described as extension thinning (Figure 3). Such a flow behaviour is well known for polymer solutions and can be contributed to orientation of the molecules along the flow direction. The spatial reorientation and partial collapse of the dough microstructure causes a decreasing stress with further extension as long as no stretching of the polymers occurs [32–34]. By extending the dough matrix, secondary bonds are broken and protein strands are able to slip past each other [35]. During further extension, rupture of gluten strands and the alignment and separation of starch granules within the gluten matrix contribute to the extension thinning flow behaviour of a standard wheat dough [36].

The presence of yeast was shown to reduce the extensional viscosity. The viscosity drop is even more pronounced with increasing fermentation time and a higher yeast level. Thus, the fermentation activity of yeast is considered to cause the system to be less connected or entangled. The re-orientation of the system according to the deformation

force is promoted, since the system has a higher mobility due to shifted polymeric structure. This alteration is presumably attributable to the occurrence of shorter chained polymers upon the rupture of gluten strands due to the fermenting activity, causing the polymeric structure to be less branched and entangled [34].

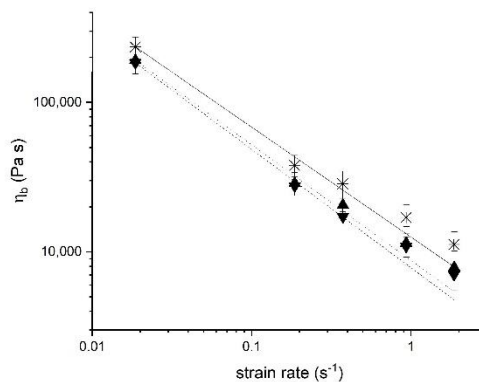


Figure 2. Extensional viscosity measured at $\varepsilon_b = 1.00$ after 3 h fermentation at $30\text{ }^\circ\text{C}$ presented as flow curve. Data were fitted according to Turbin-Orger et al. (2015) using a power law model ($\eta_b(\dot{\varepsilon}) = K \cdot \dot{\varepsilon}^{(n-1)}$). (—□—) Reference without additives, (—▲—) 1 g yeast/100 g flour, (—▼—) 2 g yeast/100 g flour. ($n = 3$, $\bar{X} \pm \text{STD}$).

3.3. Linkage between Extensional Rheological Properties and Protein Network Configuration

In order to validate the hypothesised correlation between the flow behaviour and the microstructure of the polymeric system, quantitative protein network analysis has been performed to address the microstructure of standard wheat dough and yeasted dough. In order to distinguish between yeast- and time-dependent effects, the effects of resting time and fermentation were evaluated (Table 1).

Table 1. Mean values of PNA results. The dough samples were stained with Rhodamine B using the bulk water technique and analysed by CLSM with $60 \times$ magnification. ($n = 3$, $\bar{X} \pm \text{STD}$).

| | Average Protein Vessel Length (μm) | Average Lacunarity (-) | Branching Rate (Junctions/ μm^2) | Endpoint Rate (End Points/ μm^2) | Protein Width (μm) |
|--|---|----------------------------|--|--|---------------------------------|
| Standard wheat dough without additives 0 h resting | $7217 \pm 2586^{\text{a}}$ | $0.35 \pm 0.04^{\text{a}}$ | $6.1 \cdot 10^{-5} \pm 0.4 \cdot 10^{-5}^{\text{a}}$ | $1.6 \cdot 10^{-5} \pm 0.2 \cdot 10^{-5}^{\text{a}}$ | $69.53 \pm 1.54^{\text{a}}$ |
| Standard wheat dough without additives 2 h resting | $5298 \pm 1307^{\text{a}}$ | $0.35 \pm 0.06^{\text{a}}$ | $5.8 \cdot 10^{-5} \pm 0.5 \cdot 10^{-5}^{\text{a}}$ | $2.1 \cdot 10^{-5} \pm 0.3 \cdot 10^{-5}^{\text{b}}$ | $66.07 \pm 0.66^{\text{b}}$ |
| 2 g yeast/100 g flour 2 h fermentation | $4503 \pm 1511^{\text{b}}$ | $0.41 \pm 0.12^{\text{a}}$ | $5.6 \cdot 10^{-5} \pm 0.4 \cdot 10^{-5}^{\text{b}}$ | $2.2 \cdot 10^{-5} \pm 0.4 \cdot 10^{-5}^{\text{b}}$ | $66.95 \pm 1.81^{\text{b}}$ |

a,b Mean values \pm STD labelled with a different letter in the same column are significantly different according to Dunn's Test on a significance level of $\alpha = 0.05$.

Directly after kneading, the dough microstructure appeared as a strongly interconnected network. Shear, elongational and rotational deformation forces during the kneading caused the formation of a highly aligned protein microstructure [37]. Especially the extension of strands during kneading forces the formation of additional shortrange interactions (e.g., hydrogen bonds) due to the more extended and unfolded protein configuration. Thus, the network appears dense and comprises wide and planar strands. Since the proteins were not allowed to regain their thermodynamic equilibrium conformation, the system appears in a strongly connected arrangement directly after the kneading process. After sufficient

resting time (cf. standard wheat dough without additives, 2 h resting), the conformational changes and rearrangement of protein strands cause a decreasing vessel length (−26.6%) due to the contraction of the protein threads. Further, the connectivity of the network was shown to be changed by relaxation processes. This relaxation processes include the continuous hydration of the dough system during resting and are emphasised to enable a higher molecular mobility and the formation of new interactions, supporting the regaining of a low entropy for the system. In contrast, the appearance of the system changed in presence of yeast. The most marked change was the reduced density and grown spatial separation of protein strands. During the fermentation step, the yeast metabolite CO_2 is known to dissolve from the liquid dough phase, leading to an increased gas void fraction. Thus, steric separation of protein structures and hindered interactions along protein strands reduce the width of protein threads due to compressive stress. Beside the compressive stress, the fermentation processes were shown to cause elongational strain leading to more pronounced restructuring processes and additional damage. In view of the reported data, this effect is represented by a significant decrease in number of junctions and an increase in end points. The observed changes can be summarised according to the classification scheme for gluten networks of [15]. It appears that yeast encourages the formation of a “particulate, dense network” where the proteins form clustered agglomerates and are densely arranged.

As abovementioned, the stress thinning behaviour suggest power law behaviour. The results of power law modelling are presented in Figure 3 in terms of flow and consistency index. The presented parameters underline the previously discussed changes. In general, the standard wheat dough without additives or yeast appears to decrease in consistency with increasing resting time, accompanied by an increase in crosslinks. This is expected to be caused by the rearrangement of the gluten network during the resting period, since the entropy changes during resting are known to increase the loop/train ratio. Contrary to that, the rheological behaviour of yeasted dough is marked by a decreasing consistency combined with decreasing flow index with increasing fermentation time, which has been associated to a higher mobility of biopolymers [38]. It is likely that the decreasing number of crosslinks provokes this altered flow behaviour. The drop is ascribed to the rupture of gluten strands due to the extensional load exerted from the growing steric demand of gas cells. Further, ethanol has been shown to reduce the strength of interactions within the system and could therefore contribute to the weakening of the system.

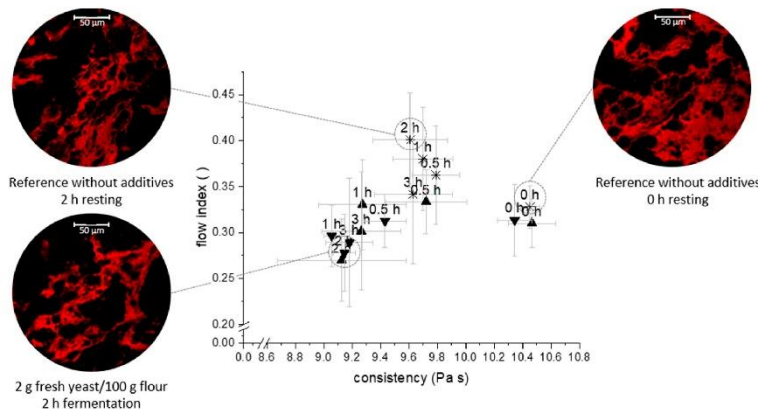


Figure 3. Time-dependent effect of fermentation on the flow index n and consistency index K for $\varepsilon_b = 1.00$. Selected micrographs (protein stained with Rhodamine B (red)) illustrate the corresponding dough microstructure. (□) Reference without additives, (▲) 1 g yeast/100 g flour, (▼) 2 g yeast/100 g flour. The CLSM images are shown at a scale of $\varnothing 225 \mu\text{m}$. ($n = 3$, $\bar{X} \pm \text{STD}$).

It is apparent that the flow behaviour is strongly linked to the functionality of the dough microstructure, as previously reported by other authors [15,39]. In the previous section, the impact of resting and fermentation processes on the dough microstructure and flow behaviour has been reported. As presented in Figure 3, the results indicate those processes to influence the functionality of the dough matrix considerable differently. During resting, relaxation processes occur, causing a stress reduction and enabling a higher deformability compared to unrested dough. This can be interpreted from the decaying values of K during the resting period of dough. The increase in the flow index n can be attributed to repolymerisation processes upon the reformation of S-S-bonds, providing a higher internal stability within the protein network than hydrogen bonds. In contrast to that, the fermentation process counteracts the formation of a stable, relaxed network arrangement. Additionally, the growing amount of gas impairs the protein strands (lacunarity \uparrow) and causes strand rupture (length \downarrow). Therefore, the amount and strength of interactions along the proteins decrease (branching rate \downarrow). The resulting fragments are more accessible to deformation upon mechanical exposure and the system has a lower yield strength.

3.4. Strain Hardening Behaviour of Yeasted Wheat Dough

The fermentation process has been shown previously to clearly impact the microstructure and functionality of the dough matrix. One of the most important functions of the dough matrix is the ability to retain and stabilise gas cells. As mentioned in the introduction, the gas holding capacity of dough is strongly correlated to the strain hardening phenomenon, which occurs in polymeric systems consequent to the exertion of extensional strain. To quantify the ability of a polymeric system to establish strain hardening behaviour, Jansen et al. and van Vliet et al. introduced the strain hardening index [4,40]. This was later adapted by Rouille et al., whose definition was applied for the present calculations [1]. In general, the strain hardening index (SHI, cf. equation 8) is defined as derivation of $\ln(\sigma)$ on ε_b at constant $\dot{\varepsilon}_b$. According to its mathematical definition, strain hardening occurs if $\frac{d\ln(\sigma)}{d\ln(\varepsilon)} > 1$ [4]. Regarding the underlying mechanism of this phenomenon, it is believed to be triggered by the formation of multi-branch structures in the gluten network. Those arrangements decrease the mobility of the system and give rise to an increased stress level during the deformation [36]. On a molecular scale, strain hardening was shown to result in extended HMW subunits, a higher β -sheet content and lower levels of turns [41]. Those changes were shown to be reversible but affected the rheological properties within the first minutes after extension. Further, an incomplete relaxation is assumed, as the extend of conformational changes increases with repeated deformation activity. The polymeric dough system is therefore assumed to serve from a stress memory. This memory behaviour is based on the non-reversible changes occurring in the protein network during the fermentation process. In order to evaluate the effects of yeast fermentation on the strain hardening behaviour of the dough matrix, the time-dependent SHIs were analysed for a standard wheat dough, yeasted doughs and metabolite-spiked doughs at two different strain rates. The chosen strain rates represent the lower and upper measuring limit of the method used and were chosen to reflect slow extension processes (e.g., fermentation) and processes at a high extension rate (e.g., oven rise during baking and shaping).

The data in Figure 4 illustrates that the strain hardening behaviour of a standard wheat dough is considerably affected by relaxation processes occurring during the resting of dough consecutive to the kneading process. Regardless the extension rate applied, particularly the first minutes after kneading led to a less dominant strain hardening behaviour. This decay is probably caused by the increase in the loop/train ratio during dough resting [24]. On the whole, the SHI was moderately higher upon the extension at high strain rates, compared to the deformation at a low extension rate. This discrepancy is initiated by the contrasting mechanisms arising from the different extension rates. During the extensional deformation at low extension rates, a breakage of secondary bonds causes the slippage of strands past each other, while at the high extension rate, the network breaks

into subunits which might entangle with each other and therefore show a higher resistance to extension. Further, separation and re-alignment of starch granules, acting as fillers within the extended gluten matrix, give rise to friction between starch granules originating in a higher resistance to extension.

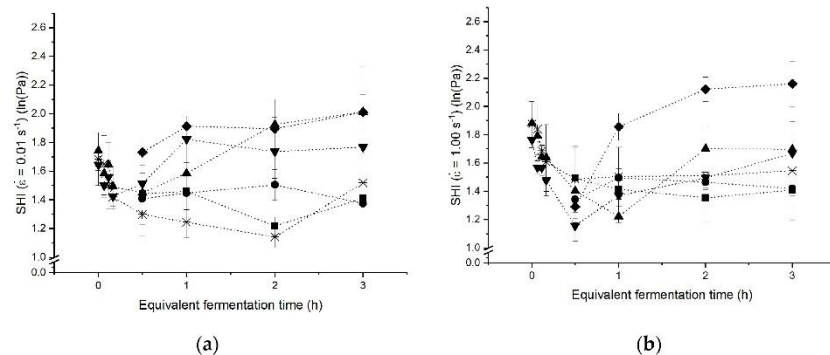


Figure 4. Strain hardening behaviour of yeasted dough with different yeast concentrations and yeast metabolites during 3 h fermentation at 30 °C. (a) Strain hardening index for an elongation rate of $\dot{\varepsilon}_b = 0.01 \text{ s}^{-1}$. (b) Strain hardening index for an elongation rate of $\dot{\varepsilon}_b = 1.00 \text{ s}^{-1}$. (□) Reference without additives, (▲) 1 g yeast/100 g flour, (▼) 2 g yeast/100 g flour, (◆) CO₂, (■) succinic acid, (●) ethanol. (n = 3, $\bar{x} \pm \text{STD}$).

It appears that the presence of acid or ethanol, representing the most common yeast metabolites, is not related to a clear functional influence on the strain hardening properties as the SHI obtained for those doughs do not differ significantly from the standard dough. Both metabolites showed no clear concentration dependent effect within the test range. Ethanol initiated a slightly enhanced strain hardening behaviour at a low strain rate. It can be assumed, that this behaviour results from lack of gliadins within the gluten network as gliadins are generally considered to contribute the viscose share to the viscoelastic dough properties. By lacking this fraction due to the increased solubilisation of this fraction within the liquid dough phase, the extension might be hindered as the elasticity of the system increases. Especially at higher concentrations of this metabolite and faster extension rates, the reinforcement of the system is limited, as the number of available binding sites is reduced. Succinic acid, representing the impact of organic acids on the dough matrix during fermentation, does not cause a clear overall trend. In line with the previous results, the protein conformation is assumed to be more open but simultaneously more connected as well. These contradictive processes contribute to the minor impact of this metabolite on the strain hardening functionality of the dough matrix during large deformation processes.

Unlike the previous discussed metabolites, yeasted and chemically leavened dough were substantially affecting the strain hardening behaviour. As both doughs are affected in the same manner, it appears that gaseous CO_2 is responsible for this effect. The presence of gas cells emphasises the SHI to increase considerably. It is assumed that this increase is due to gas serving as preload on the gluten network. Upon this initial load, the gluten strands are already in an extended conformation. Consequently, additional external elongational deformation cannot be tolerated to the same extend as in unleavened dough and, thus strain hardening occurs to a higher extend. As reported by Belton (2005), repeated extension of gluten leads to an increase of β -sheets. It is likely that these changes within the protein structure are promoted during the pre-extension of the system while fermentation and contribute to the accelerated strain hardening behaviour during further extension [41]. It is further hypothesised that starch granules are rearranged within the gluten matrix due to the increasing gas void fraction. Starch is therefore compressed and forms compartments within the gluten strands and gas cells. Thus, it is no longer homogeneously distributed

and causes higher local stress due to higher stiffness. The comparison within slow and fast extension rates reveals a more prominent strain hardening behaviour at a higher strain rate. This is in good agreement with the trend observed for unleavened standard wheat dough and traced back to the same underlying mechanism. As suggested earlier, slippage and intermediate stabilisation along protein strand occur at low strain rates, whereas structural break down is initiated at high deformation rates. As the presented data suggests a more pronounced strain hardening behaviour occurs during fast extension processes. The results indicate therefore that yeasted dough is a self-enforcing system, as (i) gas retention capacity requires strain hardening, and (ii) strain hardening is enhanced through fast gas formation (i.e., high strain rates). This observation is in good agreement with the result of Verheyen et al. [13]. The authors measured the gas holding capacity in dependency of the yeast level for fermenting dough by several macroscopic approaches, and found an enhanced retained CO_2 volume with higher CO_2 formation kinetics. Using a spiking-approach in combination with micro- and macrostructural analysis, it was possible to trace the mechanism behind this self-enforcement of yeasted dough systems back to the release of gaseous CO_2 into the dough matrix in the present study.

4. Discussion

Figure 5 proposes a schematic mechanism for extension processes of dough matrices. Two different scenarios are considered in this scheme: Unfermented dough with a gas void fraction of 0.1 and fermented dough with an increased gas void fraction of 0.75 and an increased gas cell size [42]. As stated previously, strain hardening was shown to be strongly dependent on the applied extension rate. In case of a slow extensional deformation, the gluten network can react to the deformation force by the extension of loop regions. Further, the slippage of gluten strands along each other is promoted due to the re-stabilisation ability among shortrange interactions. These interactions occur along gluten strands as well as along starch and gluten and enable an intermediate stabilisation while the extension process is conducted and prevent rupture of strands upon extension. Contrary, at a fast extension rate, intermediate stabilisation of the system is prevented due to the higher ratio of bond breakage to bond reformation. This results in the breakage of gluten strands and break apart of starch clusters. Fermentation was shown to cause a pre-load on the dough matrix. The stress memory of the gluten network is believed to be biased by the fermentation activity, which causes pre-extension and potential rupture of gluten strands due to the growing spatial demand of CO_2 cells, as stated in Section 3.3. Therefore, interactions within the dough polymers are sterically hindered and the strength of the gluten network is reduced. Similarly, as in the case of the unfermented dough, it is likely that at a low strain rate (Figure 5, left side, bottom), intermediate stabilisation via shortrange interactions among gluten–gluten, gluten–starch and starch–starch, results in a low strain hardening index. As starch is successfully stabilised within the gluten matrix via transitory shortrange interactions, the occurrence of friction within the compressed starch clusters and gluten strands is avoided and starch contributes to the stabilisation of the polymeric system during the extension process. In contrast to that, the potential mechanism for extension at a high strain rate (Figure 5, right side, bottom) is related to a breakdown of the network structure upon extension. The polymeric network fragments, caused by the pre-load of fermentation, remain entangled due to the fast extension process. The entrapped polymers cannot undergo a free slippage process and the resulting thinning process increase the resistance to extension. Further, the stabilisation of the system by intermediate polymer–filler-interactions is hindered. This is due to (i) the displacement of starch granules from the thinning dough matrix lamella around the growing gas cells during the fermentation process and (ii) the compression of starch granules into densely packed clusters, whose formation is promoted by (i). These clusters cause frictional forces between gluten and starch granules, resulting in additional load on the gluten strands. Consequently, higher resistance to extension is promoted and strain hardening is accelerated. Further, breakage of strands is enhanced due to the occurrence of locally high frictional

forces between starch clusters and gluten strands. In summary, our results suggest that the strain dependent behaviour is strongly affected by the stress memory of the gluten network. Fermentation causes irreversible changes in the polymeric structure, affecting the strain hardening behaviour of fermented dough system. The generated knowledge provides a fundamental understanding of the influence of yeast fermentation on the behaviour of dough during strain rate dependent extension processes. The obtained insights can be used to provide a base for the choice of fermentation parameters beneficiating desirable dough properties and a better understanding of processability of fermented dough during the breadmaking process.

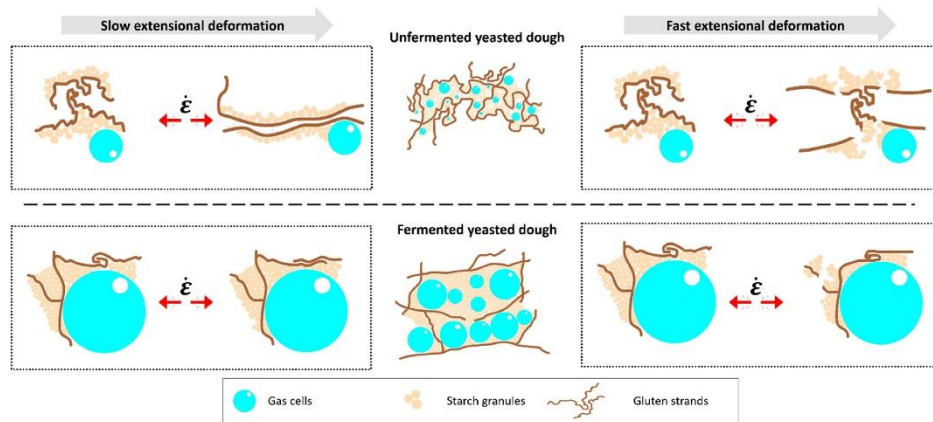


Figure 5. Schematic illustration presenting the hypothesised network model during extension processes for unfermented and fermented dough, describing the observed effects from Figure 4. The scheme illustrates the possible pathways for slow (left) and fast (right) extension rates ($\dot{\varepsilon}$) of unfermented (top) and fermented (bottom) dough matrix. The underlying information on the gas void fraction present in unfermented and fermented dough are 0.1 and 0.75, respectively [42].

5. Conclusions

The fermentation metabolite CO_2 had the strongest impact, as expanding gas cells destabilised the dough matrix. Thus, the extent and strength of interactions at all structural levels were reduced due to the growing steric demand of the gas void fraction. Dough incorporating gaseous CO_2 behaved highly complementary to fermenting dough. The gas void fraction thus mainly governs the properties of yeasted dough. Organic acids and ethanol had only a limited impact, especially during the first initial phase of the fermentation process. Therefore, the acidification and the accumulation of ethanol seem to influence the behaviour of yeasted dough only marginally.

The polymeric and entangled gluten structure, being quantitatively degraded throughout the fermentation process, defined the flow behaviour of fermenting dough. The microstructural destabilisation process was successfully related to the changing rheological behaviour towards a highly mobile polymer system, represented by a lower flow index. Besides the time-dependent changes during fermentation, the dependency on the load type and strain rate determined the rheological properties of fermenting dough. This includes extension-thinning behaviour and a dependency of the strain hardening behaviour on the applied strain rate. The dependency was mainly traced back to the presence of growing gas cells, which accelerated the strain hardening behaviour. This might be due to two reasons: (i) The growing steric demand of gas cells, causing a pre-extension of the gluten strands within the lamella around the gas cells and (ii) may be, as a side effect, starch granules accumulating and causing higher friction on the polymer strands around these

fillers. This second effect might occur even more pronounced at a high extension rate. In general, shortrange interactions contributed to the stabilisation of the polymeric system and therefore enabling a free slippage of elongated, disentangled strands at a low extension rate. At a high extension rate, the interference from broken-apart, sterically interacting fragments seems to accelerate the strain hardening behaviour of dough.

Author Contributions: Conceptualisation, T.A., M.J. and T.S.; methodology, T.A., V.T., M.J., and T.S.; software, T.A.; validation, T.A., and V.T.; formal analysis, T.A.; investigation, T.A. and V.T.; resources, M.J., T.S., and T.B.; writing—original draft preparation, T.A.; writing—review and editing, M.J., T.B., and T.S.; visualisation, T.A.; supervision, M.J., T.S., and T.B.; project administration, T.A., M.J., and T.S. All authors have read and agreed to the published version of the manuscript.

Funding: This research received no external funding.

Institutional Review Board Statement: Not applicable.

Informed Consent Statement: Not applicable.

Data Availability Statement: Data is contained within the article.

Conflicts of Interest: The authors declare no conflict of interest.

References

- Rouillé, J.; Della Valle, G.; Lefebvre, J.; Sliwinski, E.; Van Vliet, T. Shear and extensional properties of bread doughs affected by their minor components. *J. Cereal Sci.* **2005**, *42*, 45–57. [\[CrossRef\]](#)
- Schiedt, B.; Baumann, A.; Conde-Petit, B.; Vilgis, T.A. Short- and long-range interactions governing the viscoelastic properties during wheat dough and model dough development. *J. Texture Stud.* **2013**, *44*, 317–332. [\[CrossRef\]](#)
- Bloksma, A.H. Dough structure, dough rheology and baking quality. *Cereal Foods World* **1990**, *35*, 237–244.
- Van Vliet, T.; Janssen, A.M.; Bloksma, A.H.; Walstra, P. Strain hardening of dough as a requirement for gas retention. *J. Texture Stud.* **1992**, *23*, 439–460. [\[CrossRef\]](#)
- Weegels, P.L.; Groeneweg, F.; Esselink, E.; Smit, R.; Brown, R.; Ferdinando, D. Large and fast deformations crucial for the rheology of proofing dough. *Cereal Chem.* **2003**, *80*, 424–426. [\[CrossRef\]](#)
- Wikström, K.; Bohlin, L. Extensional flow studies of wheat flour dough. I. Experimental method for measurement in contraction flow geometry and application to flours varying in breadmaking performance. *J. Cereal Sci.* **1999**, *29*, 217–226. [\[CrossRef\]](#)
- Aslankoohi, E.; Rezaei, M.N.; Vervoort, Y.; Courtin, C.M.; Verstrepen, K.J. Glycerol production by fermenting yeast cells is essential for optimal bread dough fermentation. *PLoS ONE* **2015**, *10*, 1–13. [\[CrossRef\]](#)
- Jayaram, V.B.; Cuyvers, S.; Verstrepen, K.J.; Delcour, J.A.; Courtin, C.M. Succinic acid in levels produced by yeast (*Saccharomyces cerevisiae*) during fermentation strongly impacts wheat bread dough properties. *Food Chem.* **2014**, *151*, 421–428. [\[CrossRef\]](#)
- Jayaram, V.B.; Rezaei, M.N.; Cuyvers, S.; Verstrepen, K.J.; Delcour, J.A.; Courtin, C.M. Ethanol at levels produced by *Saccharomyces cerevisiae* during wheat dough fermentation has a strong impact on dough properties. *J. Agric. Food Chem.* **2014**, *62*, 9326–9335. [\[CrossRef\]](#)
- Meerts, M.; Ramirez Cervera, A.; Struyf, N.; Cardinaels, R.; Courtin, C.M.; Moldenaers, P. The effects of yeast metabolites on the rheological behaviour of the dough matrix in fermented wheat flour dough. *J. Cereal Sci.* **2018**, *82*, 183–189. [\[CrossRef\]](#)
- Meerts, M.; Vaes, D.; Botteldoorn, S.; Courtin, C.M.; Cardinaels, R.; Moldenaers, P. The time-dependent rheology of fermenting wheat flour dough: Effects of salt and sugar. *Rheol. Acta* **2018**, *57*, 813–827. [\[CrossRef\]](#)
- Rezaei, M.N.; Jayaram, V.B.; Verstrepen, K.J.; Courtin, C.M. The impact of yeast fermentation on dough matrix properties. *J. Sci. Food Agric.* **2016**, *96*, 3741–3748. [\[CrossRef\]](#) [\[PubMed\]](#)
- Verheyen, C.; Albrecht, A.; Becker, T.; Jekle, M. Destabilization of wheat dough: Interrelation between CO₂ and glutathione. *Innov. Food Sci. Emerg. Technol.* **2016**, *34*, 320–325. [\[CrossRef\]](#)
- Tronsmo, K.M.; Magnus, E.M.; Baardseth, P.; Schofield, J.D.; Aamodt, A.; Færgestad, E.M. Comparison of small and large deformation rheological properties of wheat dough and gluten. *Cereal Chem.* **2003**, *80*, 587–595. [\[CrossRef\]](#)
- Lucas, I.; Petermeier, H.; Becker, T.; Jekle, M. Definition of network types—Prediction of dough mechanical behaviour under shear by gluten microstructure. *Sci. Rep.* **2019**, *1*–13. [\[CrossRef\]](#) [\[PubMed\]](#)
- Jayaram, V.B.; Cuyvers, S.; Lagrain, B.; Verstrepen, K.J.; Delcour, J.A.; Courtin, C.M. Mapping of *saccharomyces cerevisiae* metabolites in fermenting wheat straight-dough reveals succinic acid as pH-determining factor. *Food Chem.* **2013**, *136*, 301–308. [\[CrossRef\]](#) [\[PubMed\]](#)
- Gabrielle, D.; de Cindio, B.; D'Antona, P. A weak gel model for foods. *Rheol. Acta* **2001**, *40*, 120–127. [\[CrossRef\]](#)
- Chatraei, S.; Macosko, C.W.; Winter, H.H. Lubricated squeezing flow: A new biaxial extensional rheometer. *J. Rheol.* **1981**, *25*, 433–443. [\[CrossRef\]](#)
- Kokelaar, J.J.; Van Vliet, T.; Prins, A. Strain hardening properties and extensibility of flour and gluten doughs in relation to breadmaking performance. *J. Cereal Sci.* **1996**, *24*, 199–214. [\[CrossRef\]](#)

20. Lucas, I.; Stauner, B.; Jekle, M.; Becker, T. Staining methods for dough systems—Impact on microstructure and functionality. *LWT* **2018**, *88*, 139–145. [[CrossRef](#)]
21. Bernklau, I.; Lucas, L.; Jekle, M.; Becker, T. Protein network analysis—A new approach for quantifying wheat dough microstructure. *Food Res. Int.* **2016**, *89*, 812–819. [[CrossRef](#)] [[PubMed](#)]
22. Zudaire, E.; Gambardella, L.; Kurcz, C.; Vermeren, S. A computational tool for quantitative analysis of vascular networks. *PLoS ONE* **2011**, *6*, e27385. [[CrossRef](#)] [[PubMed](#)]
23. Hering, E.; Martin, R.; Stohrer, M. Fehlerrechnung. In *Taschenbuch der Mathematik und Physik2*; Springer: Berlin, Germany, 2017; p. 114.
24. Belton, P.S. Mini review: On the elasticity of wheat gluten. *J. Cereal Sci.* **1999**, *29*, 103–107. [[CrossRef](#)]
25. Kawamura, Y.; Yonezawa, D. Wheat flour proteases and their action on gluten proteins in dilute acetic acid. *Agric. Biol. Chem.* **1982**, *46*, 767–773. [[CrossRef](#)]
26. Dobraszczyk, B.J. The physics of baking: Rheological and polymer molecular structure-function relationships in breadmaking. *J. Non-Newton. Fluid Mech.* **2004**, *124*, 61–69. [[CrossRef](#)]
27. Chin, N.L.; Martin, P.J.; Campbell, G.M. Dough aeration and rheology: Part 3. Effect of the presence of gas bubbles in bread dough on measured bulk rheology and work input rate. *J. Sci. Food Agric.* **2005**, *85*, 2203–2212. [[CrossRef](#)]
28. Robertson, G.H.; Cao, T.K.; Ong, I. Wheat gluten swelling and partial solubility with potential impact on starch-from-gluten separation by ethanol washing. *Cereal Chem.* **1999**, *76*, 843–845. [[CrossRef](#)]
29. Wehrle, K.; Grau, H.; Arendt, E.K. Effects of lactic acid, acetic acid, and table salt on fundamental rheological properties of wheat dough. *Cereal Chem.* **1997**, *74*, 739–744. [[CrossRef](#)]
30. Barnes, H.A.; Hutton, J.F.; Walters, K. Rheology of polymeric liquids. In *An introduction to Rheology*; Elsevier: Amsterdam, The Netherlands, 1989; pp. 97–114.
31. Turbin-Orger, A.; Boller, E.; Chaunier, L.; Chiron, H.; Della Valle, G.; Régueulle, A.L. Kinetics of bubble growth in wheat flour dough during proofing studied by computed X-ray micro-tomography. *J. Cereal Sci.* **2012**, *56*, 676–683. [[CrossRef](#)]
32. Weipert, D. The benefits of basic rheometry in studying dough rheology. *Cereal Chem.* **1990**, *67*, 311–317.
33. Lyu, M.-Y.; Lee, J.S.; Youlee, P. Study of mechanical and rheological behaviors of linear and branched polycarbonates blends. *J. Appl. Polym. Sci.* **2001**, *80*, 1814–1824. [[CrossRef](#)]
34. Dealy, J.M.; Read, D.J.; Larson, R.G. *Structure and Rheology of Molten Polymers: From Structure to Flow Behavior and Back Again*; Carl Hanser: Munich, Germany, 2018.
35. Singh, H.; Macritchie, F. Application of polymer science to properties of gluten. *J. Cereal Sci.* **2001**, *33*, 231–243. [[CrossRef](#)]
36. McCann, T.H.; Le Gall, M.; Day, L. Extensional dough rheology—Impact of flour composition and extension speed. *J. Cereal Sci.* **2016**, *69*, 228–237. [[CrossRef](#)]
37. Jongen, T.R.G.; Bruschke, M.V.; Dekker, J.G. Analysis of dough kneaders using numerical flow simulations. *Cereal Chem.* **2003**, *80*, 383–389. [[CrossRef](#)]
38. Turbin-Orger, A.; Shehzad, A.; Chaunier, L.; Chiron, H.; Della Valle, G. Elongational properties and proofing behaviour of wheat flour dough. *J. Food Eng.* **2016**, *168*, 129–136. [[CrossRef](#)]
39. Jekle, M.; Becker, T. Wheat dough microstructure: The relation between visual structure and mechanical behavior. *Crit. Rev. Food Sci. Nutr.* **2015**, *55*, 369–382. [[CrossRef](#)]
40. Janssen, A.M.; Van Vliet, T.; Vereijken, J.M. Fundamental and empirical rheological behaviour of wheat flour doughs and comparison with bread making performance. *J. Cereal Sci.* **1996**, *23*, 43–54. [[CrossRef](#)]
41. Belton, P.S. New approaches to study the molecular basis of the mechanical properties of gluten. *J. Cereal Sci.* **2005**, *41*, 203–211. [[CrossRef](#)]
42. Babin, P.; Della Valle, G.; Chiron, H.; Cloetens, P.; Hoszowska, J.; Pernot, P.; Régueulle, A.L.; Salvo, L.; Dendievel, R. In situ fast x-ray tomography study of the evaluation of cellular structure in bread dough during proving and baking. In *Bubbles in Food 2: Novelty, Health and Luxury*; Campbell, G.M., Scanlon, M.G., Pyle, D.L., Eds.; American Association of Cereal Chemists International: St. Paul, MN, USA, 2016; pp. 265–272, ISBN 9780128104590.

3.3 Relation between polymer transitions and extensional viscosity of dough systems during thermal stabilization assessed by lubricated squeezing flow

Food Chemistry 389 (2022) 133048



Relation between polymer transitions and the extensional viscosity of dough systems during thermal stabilization assessed by lubricated squeezing flow



Thekla Alpers^a, Johanna Olma^a, Mario Jekle^{a,b,*}, Thomas Becker^a

^a Research Group Cereal Technology and Process Engineering, Chair of Brewing and Beverage Technology, Technical University of Munich, 85354 Freising, Germany

^b Department of Plant-Based Foods, Institute of Food Science and Biotechnology, University of Hohenheim, 70599 Stuttgart, Germany

ARTICLE INFO

Keywords:

Starch gelatinization
Gluten polymerization
Fundamental elongational rheology
Baking
Wheat dough
Yeast fermentation

ABSTRACT

Polymer transitions occurring during the thermal processing of dough are defining the rheological behaviour of solidifying dough. Yeast, an essential ingredient in breadmaking, plays an important role in this transformation process, but its impact on the transitional behavior of the polymers remains unknown. Therefore, the aim of this study was to elucidate the impact of hydrothermally induced polymer transitions on the elongational rheological behavior of dough under process-relevant strain-strain-rate combinations: transitions in dependence of the presence of yeast. Using elongational rheology together with DSC, TD-NMR and microscopy, yeast-induced degradation on the microstructural level (average decrease of protein strand length of 46%) and microstructural level were shown to affect the course of the starch gelatinization process and the functionality of gluten while baking. These findings can be used to relate oven rise performance to fundamental rheological behavior based on occurring phase transitions, leading to a more comprehensive process understanding.

1. Introduction

Dough is a complex polymeric system, composed of gluten, starch, dispersed gas cells and minor flour components, such as surface-active substances and endogenous enzymes. The interactions of these polymers and phases on different structural levels shape the complex rheological behavior of dough (Schiedt et al., 2013). As a non-Newtonian fluid, the rheological behavior of wheat dough is strongly dependent on the type and strength of stress applied. Further, thermal processing during baking and, in case of yeasted dough, the release of metabolites into the dough matrix change the flow behaviour of the cereal system.

Temperature dependent structural and functional changes of cereal biopolymers are a major topic in cereal research. In case of gluten, the hydrothermal treatment causes a conformational change and polymerization. Denaturation causes the revelation of hydrophobic groups, leading to an increase of hydrophobic interactions and conformational changes (e.g. aggregation) (Weegels et al., 1994). Polymerization and the formation of covalent bonds within gliadins and glutenin are further contributing to a steady increase in shear viscosity of hydrated gluten during thermal treatment up to 90 °C or 95 °C (Lagrain et al., 2005, 2008; K. Q. Wang et al., 2016).

Starch, the second main polymer composing the dough matrix, undergoes several structural changes during the thermal treatment. Gelatinization occurs around 55–75 °C, depending on the moisture content and heating speed (Fukuoka et al., 2002). The viscosity of starch solutions during heating shows a parabolic course (Tsai et al., 1997). Tracing the pasting process with small deformation oscillatory measurements, the storage modulus is shown to increase with increasing temperature as the swollen granules occupy the available volume in the system and interact through intergranular interactions. The subsequent viscosity drop has successfully been attributed to the melting of crystalline structures and the breakdown and disentanglement of amylopectin structures as reported by Keetels et al. (1996) (Keetels et al., 1996; Tsai et al., 1997).

The abovementioned occurrence of polymer transitions and changes in functionality during the thermal treatment of dough is strongly influencing the resulting dough's rheological behavior. The temperature-dependency of the rheological behavior of dough itself has mainly been assessed through shear rheological measurements amongst others by Salvador et al. (2006). Despite the fact that extensional stress is the predominant deformation type occurring during fermentation and baking, few researchers have addressed the temperature-dependent

* Corresponding author at: Garbenstraße 25, 70599 Stuttgart, Germany.
E-mail address: mario.jekle@uni-hohenheim.de (M. Jekle).

viscosity of dough under extensional deformation. Vanin et al. (2018) recently addressed this lack using lubricated squeezing flow to access the extensional viscosity of a yeast free wheat dough. The course of the extensional viscosity differed markedly from those obtained by shear rheology. Vanin et al. (2018), as well as other authors suggested a more pronounced response of gluten structures to large scale extensional deformation in contrast to the response of starch-starch and starch-gluten interactions to small oscillatory deformations (Ameniya & Menjivar, 1992; Schiedt et al., 2013), but the connective link of changes in the extensional rheological behavior of dough to polymer transitions caused by thermal treatment during baking is still missing (Vanin et al., 2018). As reported by Jekle et al. (2016), the rheological behavior of starch-gluten systems cannot be described as the simple combination of starch and gluten functionality during hydrothermal treatment (Jekle et al., 2016). In fact, the rheological behavior or functionality of gluten-starch mixtures has been found to be a complex interaction of both polymers resulting from direct (molecular interactions or steric effects) or indirect effects, such as competitive hydration or barrier effects (Jekle et al., 2016). However, the contribution of hydrothermally induced polymer transitions of the dough matrix components to the overall viscosity course remains unclear. Besides that, the functionality of the dough matrix is further dependent on the release of yeast metabolites to the dough matrix. The impact of yeast fermentation and yeast metabolites are widely recognized as reported by Meerts et al. (2018). But the potential impact of yeast metabolites on the thermal induced polymer transitions and the hydration equilibrium during baking remains unclear.

The aim of the current study was to find relations between temperature induced polymer transitions and changes in the rheological behavior of yeasted and non-yeasted wheat flour dough and the dependency of these transitions. Based on the current literature, it was hypothesised that yeast fermentation activity affects structure and functionality of the gluten protein microstructure. The elongational rheological behavior of the dough matrix is therefore believed to be strongly affected by the presence of yeast and thermally induced polymerization could be altered. In contrast to that, clear temperature-dependent polymer transitions (starch gelatinization) and the hydration equilibrium of the dough polymers were not expected to be affected by yeast metabolites. For the first time, the present study uses a combination of methods to trace the structure-function relationship of polymer transitions during the thermal stabilization of dough. The functionality of the dough matrix was accessed by in-line elongational rheological measurements (LSF). In order to trace the extend of polymer transitions, differential scanning calorimetry (DSC) and SDS-protein extractability were used to cover the extend of molecular changes. Further, microscopic techniques (confocal laser scanning microscopy (CLSM) in combination with protein network analysis (PNA)) and low field ¹H NMR were used to elucidate changes on the microstructural scale and in proton mobility and hydration properties of different dough matrices.

2. Materials and methods

2.1. Wheat dough preparation

All experiments were conducted using a German commercial wheat flour Type 550 with 13.30 ± 0.17 g moisture per 100 g flour (AACCi 44-01), a protein content of 11.26 ± 0.10 g per 100 g dry flour (AACCi 46-16, N \times 5.7), 0.55 ± 0.05 g ash per 100 g dry flour (ICC 104/1) and 30.5 ± 0.1 g wet gluten per 100 g flour (AACCi 38-12A). Dough preparation was conducted according to the kneading time and water amount required for a resistance of 500 FU in a Z-kneader doughLAB (Perten Instruments AB, Hägersten, Sweden) following AACCi 54-70.01. Dough kneading was performed in a Z-kneader equipped with a 50 g bowl at 63 rpm using flour, demineralized water (according to the observed water absorption) and 3 g white sugar/100 g flour (EC

category II quality, Bäko, Nürnberg, Germany). Biologically leavened doughs were prepared with fresh compressed yeast (*S. cerevisiae*, F.X. Wieninger GmbH, Passau, Germany) using 1 g yeast/100 g flour. Chemically leavened doughs were produced using a mixture of Glucono-delta-lactone (Alfa Aesar GmbH & Co KG, Karlsruhe, Germany) and NaHCO₃ (Solvay GmbH, Hannover, Germany) as raising agent. The amount of NaHCO₃ needed for neutralization was calculated according to Verheyen et al. (2016). The amount of raising agent was adjusted in order to reach the same volume expansion in chemically and biologically leavened dough samples after 30 min of fermentation.

2.2. Elongation properties by lubricated squeezing flow

After kneading, the dough was sheeted to the height specified below and cut into cylindrical pieces using a cylindrical cutter (45 mm diameter). To compromise for different volume expansions caused by the different leavening agents, varied sheeting heights were applied: 20 mm, 10 mm or 12 mm in case of reference wheat dough, biologically leavened dough or chemically leavened dough. The chemically leavened dough was subjected to some initial gas formation during the kneading step and therefore sheeted to 12 mm instead of 10 mm. Both leavened dough systems reached a final height of 20 mm after the heating process and were therefore comparable in height to the reference dough. The molded and lubricated samples were immediately transferred into a self-constructed rig for a texture analyzer (TA.XT.Plus, Stable Microsystems, Godalming, United Kingdom) equipped with a 50 kg load cell, based on the experimental procedure described by Chatraei et al. (1981). An overview on the experimental setup is shown in the appendix (Fig. A.1). The samples were placed between two lubricated metal plates of 45 mm diameter, which were tempered using electric heating resistors (Aluminium housed fixed power wirewound resistor, 1 kΩ, 25 W, ATE Electronics, Giaveno, Italy) connected to a PID temperature controller (SYL-2342P, Auber Instruments, Alpharetta, GA, USA). The temperatures of the dough samples themselves were logged using a 1-Wire digital thermometer (DS18B20, Maxim Integrated Products, Inc., San Jose, CA, USA) connected to an Arduino microprocessor (Arduino Mega 2560, Arduino AG, Turin, Italy). The samples were transferred into the measuring cell immediately after kneading. To avoid biaxial extension, the cylindrical dough samples were jacketed with silicone (0.5 mm, Sahltec, Bremen, Germany) and a customized, 3D-printed shell (GreenTec Pro, Extrudr FD3D GmbH, Lauterach, Austria). After 60 min of resting/fermentation at 30 °C (in case of chemically leavened doughs 30 min due to the accelerated gas production rate), the dough samples were heated to the desired temperatures. During the fermentation and baking step, the samples were allowed to expand uniaxially as the upper plate was adjusted in order to keep the normal force on a constant level of 10 g. After reaching the desired baking temperature, the silicon jacket and 3D printed shell were removed. Subsequently, the samples were compressed at a displacement speed of 0.1 mm/s to a final compression of 90% of the initial height. The actual compression speed was adjusted to the final sample height and corrected to reach comparable strain-strain rate combinations. The resulting force-distance-curves were used to calculate the biaxial strain ϵ_b , the biaxial strain rate $\dot{\epsilon}_b$ and the apparent biaxial viscosity $\eta_b^*(\dot{\epsilon}_b)$ according to Alpers et al. (2021), Chatraei et al. (1981) and Rouillé et al. (2005). For further analyses, samples were taken from fermented and heated samples prior to compression. All measurements were performed in triplicate and average values are presented with standard deviation.

2.3. Differential scanning calorimetry

The gelatinization properties of dough samples were assessed using differential scanning calorimetry (DSC250, TA Instruments, New Castle, WA, USA) equipped with a RCS40 cooler system with nitrogen flow rate of 50 mL/min. Calibration of the system was performed for temperature

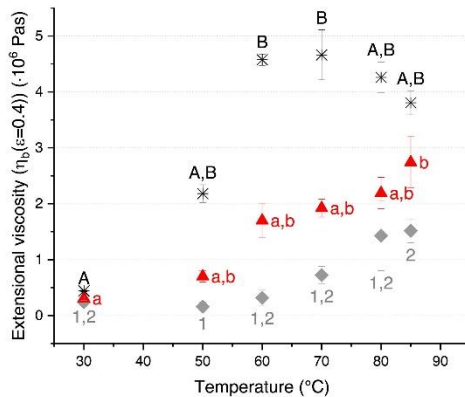


Fig. 1. Extensional viscosity measured at $\epsilon_b = 0.4$ after resting/fermentation at 30 °C and heating to the specified temperature. Viscosities of different dough systems are not quantitative comparable as the mass varied between the different dough systems in order to reach comparable strain - strain rate combinations. (♦) Reference without additives, (▲) biologically leavened dough (1% fresh yeast/100 g flour) and (◆) chemically leavened dough (CO_2). The amount of chemical leavening agent was adjusted in order to create the same dough volume expansion during the fermentation/resting phase as the biologically leavened doughs. Different letters or numbers indicate significant differences (Kruskal-Wallis and Dunn's test, $\alpha = 0.05$). ($n = 3, \bar{X} \pm \text{STD}$).

and heat flow using standard values for indium. Measurements were performed in accordance to Paulik et al. (2019) using hermetically sealed Tzero aluminum pans and lids filled with 15–25 mg sample (dough:water ratio = 1:3) (Paulik et al., 2019). In case of metabolite - starch mixtures, the wheat starch amount corresponding to a flour aliquot was diluted with 3 parts distilled water and the equivalent amounts of ethanol or succinic acid were added to the mixture. The samples and an empty reference were loaded at 20 °C and run at 10 K/min to 90 °C in an inert nitrogen atmosphere. The obtained heat flow diagrams were analyzed using the TMA software (V5.1.1, TA Instruments, New Castle, WA, USA) in terms of onset temperature, peak temperature and enthalpy change ΔH . Normalization of the enthalpy was performed using the sample dry mass which was obtained using a moisture analyzer (DAB 100-3/MLB 50-3, KERN & SOHN GmbH, Balingen, Germany). Measurements were performed in triplicate and average values are presented with standard deviation.

2.4. Protein extractability

Protein extractability was assessed using 2 g of dough homogenized in 40 mL SDS buffer solution (0.05 M sodium phosphate buffer (VWR LLC, Solon, OH, USA) with 2.0% (w/v) sodium dodecyl sulfate (VWR bvba, Leuven, Belgium), pH 6.8) following (Wilderjans et al., 2008). The homogenization was performed using an Ultra Turrax (T 25, Janke & Kunkel, Staufen, Germany). After 30 min of extraction, the samples were centrifuged (4600 $\times g$, 10 min, 20 °C, Rotina 420 R, Hettich GmbH & Co. KG, Tuttlingen, Germany). The supernatants of two consecutive extraction steps were used to determine the protein content by Kjeldahl analysis. Extractions were performed in triplicate and protein determination was performed in technical duplicates. Results are presented as average values with standard deviation.

2.5. Microstructural analysis

The protein microstructure was visualized using a confocal laser scanning microscope (eclipse Ti-U inverted microscope with an e-Cl

plus confocal system, Nikon GmbH, Düsseldorf, Germany) with a Plan Apo VC 60x/1.40 oil objective. The dough was stained according to the drop technique suggested by Lucas et al. (2018) using Rhodamine B (0.1 g/L water, Sigma-Aldrich GmbH Munich, Germany) and Nile blue (0.1 g/L ethanol, AppliChem Biochemica GmbH, Darmstadt, Germany) (Lucas et al., 2018). Proteins were recorded in fluorescence micrographs ($\lambda_{\text{ex}} = 543 \text{ nm}$ or $\lambda_{\text{ex}} = 633 \text{ nm}$) with a 1024 \times 1024 pixel resolution.

Image processing was performed using the method protein network analysis (PNA) according to Bernklau et al. (2016). The software AngioTool64 version 0.6a (National Cancer Institute, National Institute of Health, Bethesda MD, USA, (Zudaire et al., 2011)) was applied and the following morphological attributes were chosen for further discussion: Branching rate (number of junctions/protein area), end-point rate (number of end points/protein area), average protein length and width (length and width of a continuous protein strand) and lacunarity (a measure for gaps and heterogeneity). All measurements were performed in triplicate, whereby a minimum number of 5 images per sample was analyzed by image processing. Results are presented as average values with standard deviation.

2.6. Time domain NMR

Combined FID and CPMG measurements were performed using a low field ^1H NMR (mq 20 NMR analyzer, Bruker BioSpin GmbH, Rheinstetten, Germany). 1 g aliquots of dough were weighed in 8 mm inlays for 10 mm NMR tubes and equilibrated in the instrument for 15 min to ensure temperature stabilization. T_2 relaxation times were measured using a combination of free induction decay (FID) and the Carr-Purcell-Meiboom-Gill (CPMG) pulse sequence. The measurement settings were adapted from Bosmans et al. (2012) and Rondeau-Mouro et al. (2015) and optimized for the used systems (Bosmans et al., 2012; Rondeau-Mouro et al., 2015). The sampling rate for the acquisition of the FID signal was one point per 1.28 μs . The echo time in the CPMG sequence was 175 μs between the 90° and 180° pulses and 15,000 echoes were recorded. For an optimal signal-to-noise ratio, sixteen scans were performed with a recycle delay of 1 s. The obtained data were normalized for the actual sample weight and moisture content and processed using an exponential fit as suggested by Rondeau-Mouro et al. (2015). Measurements were performed in triplicate and average values are presented with standard deviation.

2.7. Statistical analysis

If not stated differently, all measurements were performed in triplicates. The stated standard deviation accounts for the deviation between triplicates. Mathematical and statistical evaluation was performed using OriginPro (2020, OriginLab Corporation, Northampton, MA, USA). Parametric ANOVA test followed by Tukey's test and Kruskal-Wallis test as a non-parametric test followed by Dunn's test as a post-hoc test were used to detect significant differences between groups on a significance level of $\alpha = 0.05$.

3. Results and Discussion

3.1. Impact of thermal treatment and yeast fermentation and fermentation metabolites on the elongational viscosity of dough

The elongational rheological behavior of dough during the baking process has been assessed by lubricated squeezing flow. As mentioned previously, elongational rheology should be the method of choice to investigate changes in the functionality of the dough matrix during the breadmaking process as extensional processes are the predominant load occurring during proofing and baking.

Fig. 1 presents the course of elongational rheology for three different dough systems during the baking process. It appears that the extensional viscosity of all three systems increases starting from 50 °C. This increase

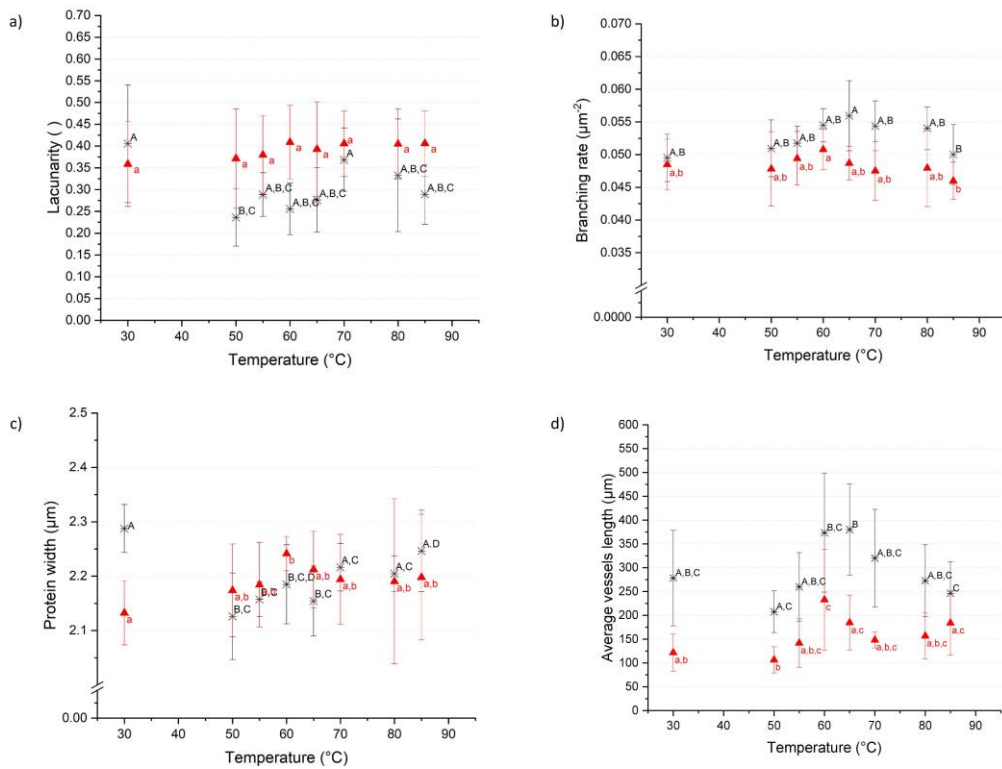


Fig. 2. Effect of yeast on the protein network microstructure during the baking process. a) Lacunarity. b) Branching rate. c) Protein width. d) Average vessel length. (●) Reference without additives, (▲) 1% fresh yeast/100 g flour. The doughs were rested/fermented for 1 h at 30 °C prior to the heating process. Different letters indicate significant differences (Kruskal-Wallis and Dunn's test, $\alpha = 0.05$). ($n = 3, \bar{X} \pm \text{STD}$).

is mainly attributed to the onset of starch gelatinization (Salvador et al., 2006). At a later stage, the slope of the viscosity curve reduces in dependence of the considered system. The unleavened reference dough system reaches the peak viscosity at 70 °C, which is likely to be determined by the termination of starch gelatinization process. Afterwards, the viscosity decreases with further heating. In contrast, the yeasted dough system undergoes a steady increase in viscosity up to 85 °C. The same behavior can be observed for chemically leavened dough systems.

It is apparent that both dough systems, leavened and unleavened, present markedly different viscosity trends during the baking process. In contrast to the reference dough system, the viscosity curves of the two leavened dough systems do not show a leveling off at temperatures above 70 °C but a steady increase till 85 °C. Surprisingly the course of the reference dough system slightly differs from the viscosity function obtained for a non-yeasted wheat dough system by Vanin et al. (2018), who used elongational rheology to quantify the rheological behavior as well. The authors did not report a viscosity drop above 70 °C, but reported a levelling off above 75 °C (Vanin et al., 2018). This different behavior might be related to bread improvers, which were part of the breadmaking formula of Vanin et al. (2018). The dough contained xylanase, α -amylase and several stabilizing ingredients, which might have contributed to the dough stability at evaluated temperatures. In any matter, the behavior of leavened dough systems appears to considerably differ from unleavened systems. The changes are likely to be able to be traced back to the impact of expending gas cells as the

behavior of a chemically leavened dough matrix is comparable to the behavior of a biologically leavened matrix. The chemically leavened dough system was thereby dimensioned in a way that the amount of gas released during the fermentation step is comparable to the one formed by the yeasted dough. The considerable difference in viscosity between the leavened and non-leavened dough systems during the later baking phase might occur due to the destabilizing impact of gas cells on the dough matrix, which probably prevent the reaching of the viscosity peak. Further, yeasted doughs might be subjected to a retardation of the starch gelatinization due to the impact of yeast metabolites on the starch granules (ethanol or organic acids). This effect might also impede the temperature dependency of the viscosity curve. This hypothesis is going to be verified in a following section (see Section 3.4). Methodical reasons leading to this greatly different behavior are likely to be excludable as the difference is not only in absolute numbers but also course related. In general, the viscosities of the different dough systems are not absolutely comparable as the absolute sample mass varied between the different dough systems. The leavened dough systems had a lower sample mass as the gas void fraction was significantly higher. Nevertheless, this divergence was accepted as it was essential to reach comparable heights immediately prior to the compression step to enable comparable strain-strain rate combinations.

In general, the results obtained for the unleavened reference dough system are in good agreement with those obtained by shear rheological measurements (Salvador et al., 2006). Furthermore, the course has a

high similarity to the course of starch suspensions during heating. The viscosity function of starch suspensions shows a parabolic shape with a maximum peak viscosity. This behavior has been related to the increasing disruption of crystallinity and the dissipation of the granular starch structure (Salvador et al., 2006; Xu et al., 2017), later followed by the breakdown and disentanglement of amylopectin structures (Keetels et al., 1996; Salvador et al., 2006; Tsai et al., 1997). In contrast to this, the temperature-dependency of the viscosity of hydrated gluten appears different. The viscosity curve of gluten during the hydrothermal treatment shows a steady increase. This behavior has been related to thermally induced polymerization effects (Lagrain et al., 2008; Wang et al., 2016). It is evident, that unleavened dough systems follow a starch-like viscosity trend, whereas leavened dough systems are more prone to show a gluten like viscosity behavior. This might be related to the pre-extension of the dough systems during the fermentation step, which is then already causing strain hardening of the lamella surrounding the expanding gas cells. The dough matrix within these lamellas is therefore already pre-extended, resulting in a higher stress response during additional elongational deformation. This behavior has already been observed in the unheated fermented dough matrix and has further been successfully traced back to the presence of gaseous CO_2 in the dough matrix (Alpers et al., 2021). Therefore, an increased share of gluten functionality due to the enhanced strain hardening effect might impact the viscosity of the leavened dough system during baking. This conclusion is further supported by the fact that the chemically leavened dough system shows a slower viscosity increase compared to the biologically leavened dough system. In case of yeast-leavened dough, a remarkable increase of the extensional viscosity becomes evident between 50 and 60 °C, whereas in chemically leavened dough systems, an accelerated increase in the extensional viscosity occurs between 60 °C and 70 °C. This is likely to be caused by the retarded gas formation in chemically leavened dough systems, where the gas formation is accelerated with temperature during baking, whereas in yeast-leavened dough systems, gas production occurs during fermentation and the early baking phase. In order to further elucidate the importance of polymer transitions on the viscosity function during the baking process, the impact of yeast fermentation on the thermal dependency of polymer transitions will be explained in detail in the following sections.

3.2. Impact of thermal treatment and yeast fermentation on the protein microstructure of dough

The observed functional changes are likely to arise from structural alterations. During baking, the protein network, which is mainly defining the rheological properties of dough, is subjected to conformational changes and polymerization. In order to quantify these structural reorganizations in dependence of the baking temperature, confocal laser scanning microscopy in combination with PNA was applied. Furthermore, the impact of yeast on these modifications was addressed by comparing a reference wheat dough and a yeasted wheat dough. The morphological attributes used to quantify the protein network in this study can be seen in Fig. 2. Both systems, the yeasted dough and the non-yeasted reference system, exhibit a comparable temperature dependency. It is apparent that the microstructure of the yeasted dough system is already affected by the gas formation which was released into the dough matrix during fermentation. The fermentative activity resulted in a degraded network structure reflected by shorter strands and a lower branching rate. The extended gas cells further cause a higher lacunarity due to the higher heterogeneity of the system. Further changes occurring during the baking process are discussed in the following section.

The course of the lacunarity during the baking process is shown in Fig. 2 a) and demonstrates a slight increase till 70 °C for the reference dough system. It is likely that entrapped gas cells are expanding recognizable, leading to a higher inhomogeneity of the system as the density of the dough matrix decreases. In case of yeasted dough, a slight

increase can be observed especially during the initial baking phase. This is believed to be triggered by the accelerated yeast activity, leading to an enhanced gas formation rate, until thermal inactivation around temperatures of 50 °C is accelerated (Graumlich & Stevenson, 1979; López-Malo et al., 1999; Reveron et al., 2003). Throughout the latter baking phase, no further increase of lacunarity is observed, which is believed to be caused by reaching the limits of the gas holding capacity of the dough matrix. Overall, the lacunarity of yeasted dough systems was tendentially higher at any time due to the presence of growing gas cells.

In case of the reference dough system, a slight decrease of the lacunarity is found for temperatures above 70 °C, which are known to initiate thermally induced polymerization of the gluten molecules. The increasing connectivity of the gluten strands is therefore believed to reduce the lacunarity as the gluten structure becomes more homogeneous. In case of yeasted doughs, the lacunarity drop is not as distinct as for the reference dough system. This might be caused by the fact that the expanded gas cells might hinder the polymerization as the reactive volume of adjacent protein strands is reduced. Extension of the strands due to the extension of the lamella within the gas cells enlarged the surface area of the protein strands. As polymerization is limited on the gas cell surface, a less pronounced polymerization reaction is expected for yeasted wheat doughs. In general, the values for lacunarity are rather constant. This might be owned to the high resolution chosen as the aim of the CLSM technique is to focus on protein structures. Furthermore, polymerization causes a more regular structure, distinguished by a higher continuity. Thus, this increasing homogeneity is counteracting the increasing porosity and possibly leading to fairly minor changes of the lacunarity throughout the baking process.

The branching rate (see Fig. 2 b)) increases up to temperatures of 60 °C – 65 °C followed by levelling off in case of yeasted doughs or even a decrease in case of the reference dough. This initial increase is likely to be caused by the formation of a highly branched, homogenous network with an increased number of branching points due to conformational changes occurring above temperatures of 45 °C. Above these temperatures, polymerization is known to continue and dominate, but it is not seen as increasing connectivity on a microstructural level after a certain level. Comparable observations have been reported by Verbauwheide et al. (2020), who explained this behavior by an increasing viscosity of the system due to the progressing starch gelatinization, which causes a lower mobility of polymers within the network. Hence, the movability of proteins is limited at higher temperatures and only a limited number of SH-SS-exchange reactions can become involved in the polymerization of the network, given that it is sterically favored (Verbauwheide et al., 2020).

The branching rate of the reference dough results overall in higher values compared to those of yeasted dough. The standard wheat dough system has therefore a higher connectivity. In contrast to that, the network of yeasted dough is subjected to degradation processes as the released CO_2 leads to the expansion of gas cells. Exceeding a certain extension, gluten strands are prone to rupture and, thus, to decrease the branching rate. This degradation process even prevails the polymerization process as yeasted doughs do not show a significant increase in connectivity till 65 °C. Further, the early decay of the branching rate of yeasted doughs for temperatures above 60 °C might be favored due to the release of glutathione into the dough matrix. The tripeptide is known to interfere gluten-crosslinking disulphide bridges (Verheyen et al., 2016). This cleavage is affecting the secondary structure of the gluten proteins, weakens hydrogen bonds and therefore destabilizes the gluten network (Guo et al., 2021).

The effect of yeast fermentation can further be seen in the results of protein width and length (see Fig. 2 c) + d)). Yeasted doughs have a lower initial vessel length as the network was already subjected to degradation during the fermentation step. Yeasted dough then shows an initial thinning due to the growth of incorporated gas cells. Similar behavior was observed for the average vessel length, as yeasted doughs do also show a length increase during the early baking phase. This is

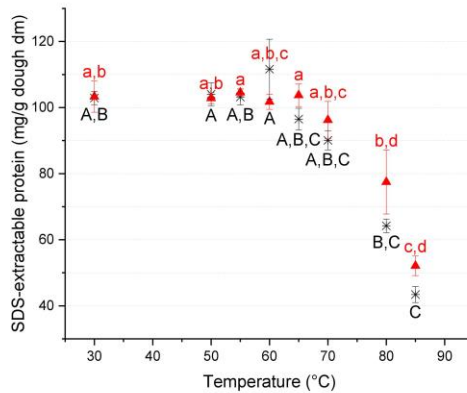


Fig. 3. Effect of thermal treatment on protein extractability of yeasted and non-yeasted dough during the baking process. (▲) Reference without additives, (▲) 1% fresh yeast/100 g flour. The doughs were rested/fermented for 1 h at 30 °C prior to the heating process. Different letters indicate significant differences (Kruskal-Wallis and Dunn's test, $\alpha = 0.05$). (n = 3, $X \pm \text{STD}$).

caused by the extension of the proteins within the lamella around the growing gas cells. Resulting from this extension processes, a thinner and higher branched network structure occurs as protein strands become separated and more dispersed. Over the whole baking process, the protein width was shown to increase after an initial reduction, which is likely to be caused by the polymerization of the gluten strands. This thickening can be observed for both dough systems, yeasted and non-yeasted. Simultaneously, the average vessel length is decreasing as well for temperatures above 60 °C/65 °C. Hence, polymerization is noticeable influencing the protein strand length as more crosslinks are progressively decreasing the vessel length.

The presented microstructural network attributes provide a clear overview on the processes occurring during the baking process. In case of a standard wheat dough system (reference dough), the initial network appears as a wide meshed network of thick vessels. Thermal treatment leads to a more pronounced branching and more regular structures. The overall network character changes into a fine meshed, highly connected network, which is in agreement with the observations of Verbauwheide et al. (2020). With progressive heating, polymerization triggers a thickening of the vessels for temperatures above 60 °C. Using PNA, an overall decrease of the vessel length and simultaneous increase of the thickness was detected. An increase in connectivity as a clear measure for polymerization is not visible on a microstructural level. In contrast, yeasted doughs are characterized by a wider meshed network through the enclosed of gas cells. The quantitative evaluation of the network morphology reveals a reduced vessel length and higher lacunarity. Protein strands are thinner and show less pronounced thickening upon thermal treatment. Therefore, yeasted doughs are prone to degradation of the protein network due to yeast metabolite on a microstructural level which is hypothesized to further limit the possible extend of polymerization within the system. The extend of the polymerization was therefore further analyzed using an extraction method.

3.3. Impact of hydrothermal treatment and yeast fermentation on the gluten polymerization

Beside the microstructural characterization, the connectivity of the protein network was further analyzed using SDS extraction. SDS-soluble protein can provide information on the amount of non-crosslinked proteins within the dough matrix (Wilderjans et al., 2008). As described by Redl et al. (2003), the quantification of SDS-soluble protein

can provide information on the amount of non-crosslinked proteins and low molecular weight gluten within the dough matrix (Redl et al., 2003). Gluten molecules become SDS-insoluble if increasing covalent interactions form larger molecules.

The amount of SDS-extractable protein remains rather constant up to temperatures of 60 °C – 65 °C (see Fig. 3). During this initial baking phase, gluten is mainly subjected to conformational changes. These changes include the reformation of hydrogen bonds and lead to the exposure of hydrophobic sites. These alterations do not affect SDS extractability of proteins as SDS is able to disrupt non-covalent bonds. A decreasing extractability is then triggered with increasing thermal treatment above temperatures of 65 °C (reference dough) and 70 °C (yeasted doughs). Therefore, we concluded that these temperatures are inducing the polymerization of proteins in the reference dough system and yeasted dough system, respectively. These findings are supported by the results of other authors, who reported a decreasing extractability resulting from the polymerization process (Wilderjans et al., 2010). Further, the marked decrease of extractability above 70 °C matches to the reported decrease of the level of free SH-groups (Lagrain et al., 2005). The amount of free SH-groups decreases rapidly due to the polymerization of glutenin by oxidation of SH-groups above temperatures of 70 °C provoked by disulfide/sulphydryl exchange reactions (Lagrain et al., 2005).

Overall, the comparison of yeasted and non-yeasted doughs reveals a slightly higher extractability for yeasted doughs. This is likely to be caused by the degrading impact of yeast on the gluten network. The rupture of gluten strands in lamella around expanding gas cells causes formation of low molecular weight fragments, which are more likely to be extracted by SDS. In this regard, it is noticeable that the level of extractable proteins during the initial baking phase is comparable for both dough systems. Therefore, fermentation itself does not change the level of extractable protein. The differences occur in the latter baking step when polymerization is induced. As a consequence of the limited mobility of the system, pointed out by the increasing viscosity, only proximate proteins can form exchange reactions (Verbauwheide et al., 2020). As previously discussed in Section 3.3, the reactive volume for the polymerization in yeasted dough decreases as protein strands are extended in the lamella around the expanding gas cells. As the polymerization reaction is limited to adjacent protein strands, extension of the strands reduces the number of crosslinks that can be formed within proteins. These extension processes can be traced back using the microstructural data (see Section 3.2). Due to the higher surface area, a smaller number of molecules is in reactive distance to each other as parts of the protein molecules are adjacent to the gas cell surface. Hence, the entrapped gas cells limit the polymerization process and cause a higher SDS-extractability. This can be supported by the microstructural observations. Next to these sterical limitations, the release of glutathione from lysed yeast cells might contribute to the higher extractability as glutathione interacts with free SH-groups and limits the polymerization of the gluten network. In general, polymerization, quantified by an increase of the molecular weight of gluten polymers, can be made responsible for increasing viscosity above 65 °C or 70 °C according to the obtained results. The comparison of yeasted and non-yeasted dough systems revealed a lower extend of crosslinking in yeasted dough systems in general.

3.4. Impact of hydrothermal treatment and yeast fermentation on the starch gelatinization process

The contribution of starch gelatinization to the changing dough matrix functionality during baking was analyzed using DSC methodology. The extend of the starch gelatinization process was traced by measuring the remaining starch gelatinization enthalpy (ΔH_{gel}) of the pre-heated samples. This reverse approach reveals the extend of starch gelatinization by comparing the remaining ΔH_{gel} with the initial gelatinization enthalpy of an unbaked sample. The obtained data for the

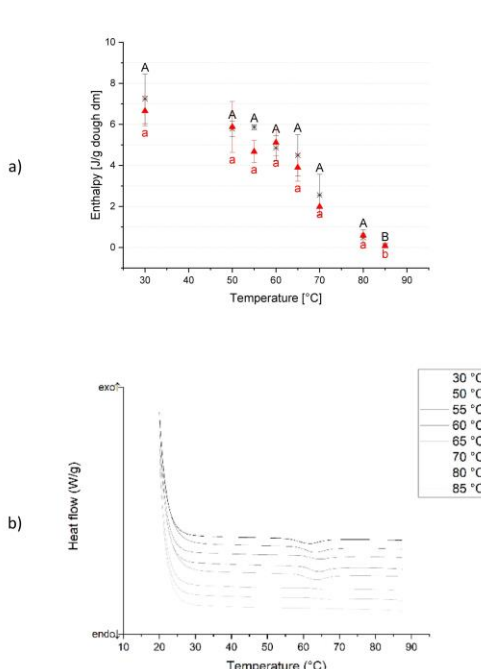


Fig. 4. Effect of thermal treatment on starch crystallinity of yeasted and non-yeasted dough during the baking process. a) Resulting residual enthalpy in dependency of the pre-heating temperature. (●) Reference without additives, (▲) 1% fresh yeast/100 g flour. All doughs were rested/fermented for 1 h at 30 °C prior to the heating process. Different letters indicate significant differences (Kruskal-Wallis and Dunn's test, $\alpha = 0.05$). (n = 3, $\bar{X} \pm \text{STD}$) b) Exemplary DSC heat flow thermogram of dough samples with different thermal pre-treatment.

ΔH_{gel} in dependence of the baking temperature is shown in Fig. 4 a). The main question addressed with this technique was, if yeasted and non-yeasted dough show any difference in the thermal dependency of the starch gelatinization process. In both systems, the phase transition of starch occurred between 50 °C and 70 °C, which is in good agreement with literature with respect to the chosen hydration level. The decrease of ΔH_{gel} with increasing heat pre-treatment of the samples reflect the proceeding starch gelatinization during the baking process. With progressive heating, the peak onset temperature shifts to higher temperatures with longer baking times as a greater amount of starch granules was already gelatinized during the baking process itself (see Fig. 4 b)). Since large A type granules experience a shorter gelatinization period due to the higher amylose content, the remaining crystalline structures are likely to origin from not fully gelatinized amylopectin structures in B type granules (Ao & Jane, 2007). The comparison of both dough systems did not result in significant differences between yeasted and non-yeasted dough. Nevertheless, the starch gelatinization process proceeds slightly faster in yeasted dough. Possible explanations for this could either be based on the presence of yeast metabolites that were released into the dough matrix during the fermentation and baking process or secondary fermentation effects such as the extension of gluten strands or the clustering of starch granules due to the displacement from the thinning lamella. In our current study, a possible effect of the presence of yeast metabolites was therefore analyzed by spiking experiments. By spiking

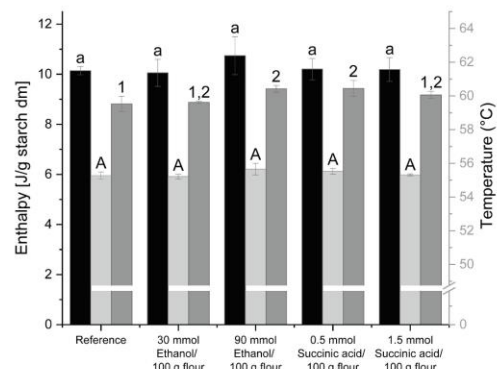


Fig. 5. Impact of ethanol and succinic acid as yeast metabolites on the starch gelatinization process. Wheat starch-water mixtures were incubated with respective amounts of ethanol or succinic acid. Ethanol and succinic acid amounts were chosen according to Jayaram et al. (2013). (■) Enthalpy in J/g wheat starch dm, (■) peak onset temperature in °C, (■) peak temperature in °C. Different letters or numbers indicate significant differences (ANOVA and Tukey test, $\alpha = 0.05$). (n = 3, $\bar{X} \pm \text{STD}$).

yeast-like concentrations of ethanol and succinic acid to starch solutions, the interaction with the starch gelatinization process was assessed. Both metabolites show a limited interaction with the starch gelatinization process (see Fig. 5).

Succinic acid increased the gelatinization peak temperature for a succinic acid concentration of 0.5 mmol/100 g flour, which corresponds to succinic acid concentrations in yeasted doughs (Jayaram et al., 2013). The gelatinization enthalpy is not significantly affected by the presence of acid for the short period of dough fermentation. Hydrolysis or acid-thinning was formerly reported by other authors to increases the gelatinization temperature due to a relative increase of crystalline structures (Ulbrich et al., 2014). A reliable impact of succinic acid on the starch gelatinization process is even though doubted, as this effect was not repeatable with higher succinic acid concentrations (see Fig. 5). Ethanol and succinic acid are therefore not believed to be responsible for changes in the endothermic starch transition process. The low concentrations and the limited exposure time cause significant ambiguity on possible effects of these yeast metabolites on the starch gelatinization process.

However, the abovementioned theory hypothesized the occurrence of direct and indirect effects of yeast metabolites affecting the starch gelatinization process. The release of CO_2 causes an increase of the gas void fraction in fermenting dough and induces structural rearrangements, which could probably cause a decreased initiating temperature for the starch transition process as a secondary effect. As the fermentation causes the extension of the gluten structure (see Section 3.2), starch is known to be displaced from the thinning lamella around the growing gas cells. Therefore, starch is less embedded within the proteins and might be better accessible for water. With more water available for the starch transition process, this process might be accelerated in yeasted doughs. Low field ^1H NMR will be used to reveal possible changes in the hydration equilibrium of the dough matrix caused by yeast fermentation during the fermentation and baking process. Based on the results discussed in this section, starch gelatinization can be regarded as the driving force for an increasing viscosity between 50 °C and 65 °C/70 °C in both dough systems.

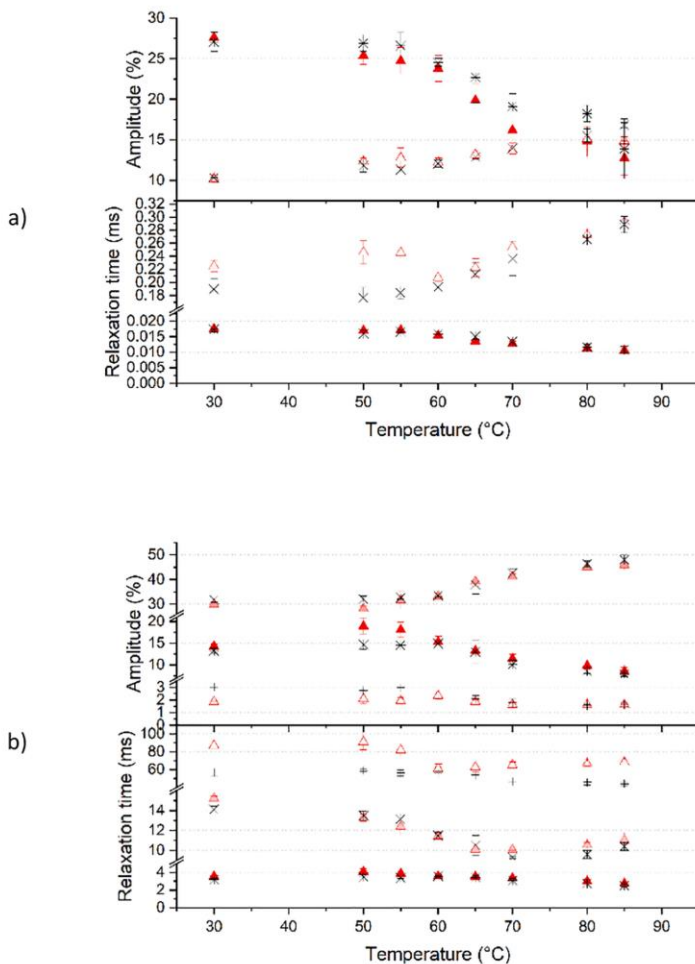


Fig. 6. T_2 relaxation times and amplitudes of yeasted and non-yeasted dough during the baking process. a) FID relaxation times ($T_{2,1}$) and amplitudes ($A_{2,1}$): (●) $T_{2,1}$ and $A_{2,1}$ reference without additives, (x) $T_{2,2}$ and $A_{2,2}$ reference without additives, (▲) $T_{2,1}$ and $A_{2,1}$ 1% fresh yeast/100 g flour (▲) $T_{2,2}$ and $A_{2,2}$ 1% fresh yeast/100 g flour. b) CPMG relaxation times ($T_{2,3}$) and amplitudes ($A_{2,3}$): (●) $T_{2,3}$ and $A_{2,3}$ reference without additives (x) $T_{2,4}$ and $A_{2,4}$ reference without additives, (▲) $T_{2,3}$ and $A_{2,3}$ 1% fresh yeast/100 g flour, (▲) $T_{2,4}$ and $A_{2,4}$ 1% fresh yeast/100 g flour. All doughs were rested/fermented for 1 h at 30 °C prior to the heating process. ($n = 3$, $\bar{X} \pm \text{STD}$).

3.5. Impact of hydrothermal treatment on the water mobility and hydration equilibrium of cereal polymers

The intended use of the low field ^1H NMR technique was mainly to reveal yeast induced changes in the mobility and quantity of different proton populations in the dough matrix. Therefore, a yeasted dough system and a non-yeasted dough system were analyzed by ^1H NMR along the whole baking process. More specific, a combined free induction decay (FID) and the Carr-Purcell-Meiboom-Gill (CPMG) pulse sequence can be used to characterize protons of the polymers itself and water populations as suggested by Rondeau-Mourou et al. (2015). Based on the results of these authors and the data of Pojić et al. (2016), a summarizing schematic (see Fig. A.2) has been developed in order to make the data obtained in our current study more available. According to those

authors, five proton fractions can be distinguished in wheat dough systems: Population 1 and 2 represent fast relaxing FID populations and Population 3–5 are believed to represent water populations with increasing mobility within the dough system (Pojić et al., 2016; Rondeau-Mourou et al., 2015). Relaxation times and amplitudes of these populations are shown in Fig. 6 a) and b). The results of the statistical evaluation are presented in Table A.1).

Population 1 is characterized by a markedly decreasing amplitude ($A_{2,1}$) with increasing thermal treatment. The amplitude drops significantly, beginning from 65 °C. This effect can be explained by the diminishing presence of crystalline structures due to the melting of crystalline starch structures. The increasing hydration of starch caused by the ongoing pasting process and the leaching of amylose into the extra-granular space increases the hydration level of starch polymers.

The formerly unhydrated starch protons quantified within population 1 are therefore now quantified with the increasing population 2 ($A_{2,2}$) of hydrated starch protons (Pojic et al., 2016; Rondeau-Mouro et al., 2015). Further, the relaxation time decreases significantly throughout the baking process. The shorter relaxation times are likely to be caused by the leaching of amylose (Rondeau-Mouro et al., 2015). As the leached amylose is no longer unhydrated, it will no longer be quantified within population 1. Therefore, the population is dominated by crystalline amylopectin with shorter relaxation times. The measured relaxation times and amplitudes do not differ significantly between reference and yeasted dough, even though the amplitude of yeasted doughs appears lower than the one of the reference wheat doughs for temperatures ranging from 50 °C to 70 °C. This drop might indicate a slightly accelerated starch gelatinization as less unhydrated starch in a crystalline structure can be quantified in yeasted doughs.

The relaxation time of the second population ($T_{2,2}$) increases along the baking process. This can be attributed to the unfolding of protein regions as hydrogen bonds break and inner protein regions get exposed. These conformational changes are likely to cause a higher mobility as weaker molecular interactions could contribute to the longer time required to return to the equilibrium. An interesting observation is the markedly higher relaxation time of population 2 of yeasted doughs during the initial baking phase. This might be related to a higher mobility of polymers in yeast-leavened doughs caused by the ongoing gluten destabilization and depolymerization processes. During the later baking phase, the relaxation times of both dough systems increase again to a comparable level. The increase in temperature could entropically favor the opening of relatively larger gluten polymers and therefore induce interactions with other protein chains, according to a mechanism proposed by Kontogiorgos et al. (2010). Therefore, interactions of small protein fragments with larger structures could lead to the reduction of the relaxation times of yeasted doughs. Regarding the amplitude of the second population, an increase can be seen along the baking process. This can be attributed to the heat facilitated pasting of starch granule, as an uptake of water is facilitated.

As shown in Fig. 6 b), the amplitude of population 3 ($A_{2,3}$) decreases during the baking process. This might be related to the degradation of the granular structure of starch, leading to the release of more polymers to the extragranular space and therefore decreasing the intensity of the signal of the intragranular water protons. In regard to the relaxation time, a slight decrease can be observed. This drop is indicating a more rigid binding of water, probably caused by the overall decrease of the matrix viscosity as an increasing amount of water is transferred into the remaining starch granules. Comparing yeasted and non-yeasted dough systems, the amplitude for yeasted doughs appears higher for temperatures of 50 °C and 55 °C. A possible explanation for this phenomenon might be, that smaller gluten fragments, formed due to the degrading impact of yeast on the gluten network, are easier to hydrate. The less complex structure might favor the extent of hydration as less inner, water-inaccessible protein sites exist.

The trend of decreasing water mobility can also be observed for water protons quantified in population 4 and 5. The relaxation time decreases due to the overall matrix viscosity increase as more water is absorbed by the starch granules. Furthermore, the amplitude of population 4 ($A_{2,4}$) shows a markedly increase. This increase has formerly been described by Pojic et al. (2016) and Rondeau-Mouro et al. (2015) and has been attributed to the increasing amount of extragranular starch polymers. The decreasing values of the amplitude of population 1 confirm these assumptions. In contrast to that, the amplitude of population 5 ($A_{2,5}$) shows a decrease due to the ongoing starch swelling

process. For both populations (4 + 5), yeasted dough shows higher relaxation times compared to reference wheat dough. This can be attributed to the higher mobility of polymers due to the degradation of the gluten network. Therefore, the relaxation times of the hydrating water appear to be longer.

Findings of hydrothermally treated starch-gluten systems are in agreement with the previous findings of Engelsen et al. (2001), Pojic et al. (2016) and Rondeau-Mouro et al. (2015) who observed the main changes for temperatures around 55 °C. The overall proton relaxation time was shown to increase up to 55 °C and then decreases due to the initiation of the gelatinization process. Yeasted doughs depict an altered gelatinization behavior as a slightly accelerated starch gelatinization was observed in population 1. Further, a higher mobility of polymers quantified in population 2 indicates weaker molecular interactions (Assifaoui et al., 2006). Higher mobility of protons in population 3, 4 and 5 is further assumed to indicate the degradation of the gluten network as the hydrating water shows longer relaxation times in a more mobile network (Assifaoui et al., 2006; Guo et al., 2021).

4. Conclusion

The current study generated new knowledge on the dependency of the rheological behavior of dough on thermally induced polymer transitions. Like hypothesized, the degrading impact of yeast fermentation on the gluten network favored the formation of a wider meshed, less branched network through the entrapment of gas cells. As this tendency was observed over the whole baking process, a lower level of polymerization of the proteins in yeasted doughs was concluded and verified by a higher SDS-extractability of proteins in yeasted dough samples. The limited polymerization ability of the yeasted dough system was related to the formation of low molecular weight fragments due to the rupturing of the gluten network upon the extensional stress and a sterical prevention of the formation of (SH)-SS exchanges due to the presence of gas cells entrapped in the dough matrix. Furthermore, the observed microstructural degradation lead to secondary effects such as an impact on the starch gelatinization process, as indicated by DSC and NMR techniques. To identify the impact of the yeast-induced changes in the transitional behavior of dough's biopolymers on the rheological behavior of the dough systems upon thermal treatment, elongational rheology was used. The behavior of non-yeasted dough systems was clearly impacted by starch functionality, whereas leavened dough systems were overshadowed by gluten functionality. In case of biologically or chemically leavened dough systems, the rheological behavior was mainly affected by the presence of gas as the pre-extension of gluten strands during fermentation impacted the stress memory of gluten and caused strain hardening. The resulting steady increase in viscosity throughout the entire baking process might further have been enhanced by the observed changes in the course of the starch gelatinization process. As the dough matrix solidified earlier in case of yeasted doughs, a higher gas holding capacity might have been favored by the higher viscosity of the system. The increased gas void fraction increases the occurrence of strain hardening, leading to a self-enforcing system. Overall, promising results have been obtained using elongational rheometry, imitating the deformation occurring during the baking process. However, a closer look on the rheological behaviour in dependency of the applied deformation could be beneficial to gain more sophisticated knowledge on the effect of individual thermally induced polymer transitions on the changing material's properties during the baking process in the future studies.

Funding

This research received no external funding.

CRediT authorship contribution statement

Thekla Alpers: Conceptualization, Methodology, Investigation, Writing – original draft. **Johanna Olma:** Methodology, Investigation. **Mario Jekle:** Conceptualization, Supervision, Writing – review & editing. **Thomas Becker:** Supervision, Writing – review & editing.

Declaration of Competing Interest

The authors declare that they have no known competing financial interests or personal relationships that could have appeared to influence the work reported in this paper.

Appendix

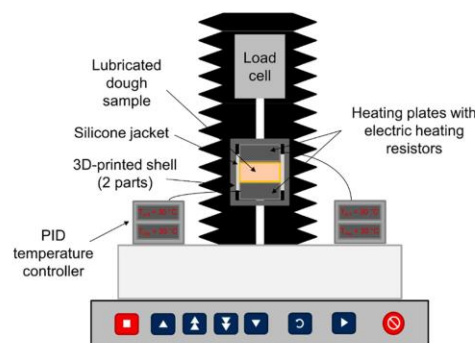


Fig. A1. Simplified scheme of the inline fermentation and baking setup designed for the lubricated squeezing flow measurements using the texture analyzer.

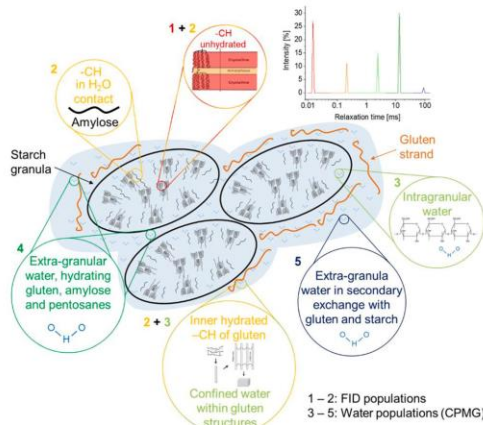


Fig. A2. Schematic model of T2 populations quantified by a combined FID and CPMG pulse sequence based on the previous work of Pojić et al. (2016) and Rondeau-Mourou et al. (2015). Population 1 and 2 represent fast relaxing FID populations and population 3–5 represent water populations with higher mobility assessed by the CPMG sequence. Scheme partly contains figures from Kontogiorgos and Kasapis (2010) and Wang et al. (2014).

Table A1

T_2 relaxation times ($T_{2,i}$) and amplitudes ($A_{2,i}$) of yeasted and non-yeasted dough during the baking process. All doughs were rested/fermented for 1 h at 30 °C prior to the heating process. Different letters indicate significant differences (Kruskal-Wallis and Dunn's test, $\alpha = 0.05$). (n = 3, $\bar{X} \pm \text{STD}$).

| | Temperature [°C] | $T_{2,1}$ [ms] | $A_{2,1}$ [%] | $T_{2,2}$ [ms] | $A_{2,2}$ [%] | $T_{2,3}$ [ms] | $A_{2,3}$ [%] | $T_{2,4}$ [ms] | $A_{2,4}$ [%] | $T_{2,5}$ [ms] | $A_{2,5}$ [%] |
|---------------|------------------|--------------------------------|-----------------------------|----------------------------|-----------------------------|----------------------------|-----------------------------|-----------------------------|-----------------------------|-----------------------------|----------------------------|
| Yeasted dough | 30 | 0.0175 ± 0.0003 ^a | 27.62 ± 0.79 ^a | 0.22 ± 0.01 ^{a,b} | 10.22 ± 0.43 ^a | 3.56 ± 0.07 ^{a,b} | 14.28 ± 0.50 ^{a,b} | 15.21 ± 0.24 ^a | 29.94 ± 0.51 ^{a,b} | 87.18 ± 3.50 ^a | 1.85 ± 0.03 ^a |
| | 50 | 0.0170 ± 0.0003 ^{a,b} | 25.37 ± 1.10 ^{a,b} | 0.25 ± 0.02 ^{a,b} | 12.33 ± 0.40 ^{a,b} | 4.10 ± 0.33 ^a | 18.97 ± 1.86 ^a | 13.27 ± 0.34 ^{a,b} | 28.09 ± 1.07 ^a | 91.16 ± 8.77 ^a | 2.09 ± 0.39 ^a |
| | 55 | 0.0172 ± 0.0003 ^{a,b} | 24.75 ± 1.63 ^{a,b} | 0.25 ± 0.01 ^a | 12.82 ± 1.16 ^{a,b} | 3.88 ± 0.18 ^{a,b} | 18.09 ± 1.78 ^a | 12.42 ± 0.84 ^{a,b} | 31.70 ± 3.58 ^{a,b} | 82.09 ± 7.30 ^a | 1.93 ± 0.25 ^a |
| | 60 | 0.0154 ± 0.0003 ^{a,b} | 23.77 ± 1.61 ^{a,b} | 0.21 ± 0.01 ^{a,b} | 12.22 ± 0.56 ^{a,b} | 3.57 ± 0.18 ^{a,b} | 15.27 ± 1.34 ^{a,b} | 11.41 ± 1.20 ^{a,b} | 33.27 ± 1.75 ^{a,b} | 60.89 ± 1.75 ^{a,b} | 2.33 ± 0.39 ^a |
| | 65 | 0.0136 ± 0.0008 ^{a,b} | 19.89 ± 2.01 ^{a,b} | 0.22 ± 0.01 ^{a,b} | 13.18 ± 0.41 ^{a,b} | 3.55 ± 0.10 ^{a,b} | 13.28 ± 0.88 ^{a,b} | 10.11 ± 0.26 ^{a,b} | 39.23 ± 1.95 ^{a,b} | 62.66 ± 5.23 ^a | 1.85 ± 0.18 ^a |
| | 70 | 0.0127 ± 0.0008 ^{a,b} | 16.19 ± 1.60 ^{a,b} | 0.25 ± 0.01 ^{a,b} | 13.67 ± 0.40 ^{a,b} | 3.35 ± 0.16 ^{a,b} | 11.45 ± 0.97 ^{a,b} | 10.08 ± 0.08 ^{a,b} | 41.18 ± 1.11 ^{a,b} | 65.29 ± 3.15 ^a | 1.63 ± 0.18 ^a |
| | 80 | 0.0113 ± 0.0007 ^b | 14.78 ± 1.85 ^{a,b} | 0.27 ± 0.00 ^{a,b} | 15.09 ± 1.05 ^{a,b} | 3.00 ± 0.20 ^{a,b} | 9.89 ± 0.98 ^{a,b} | 10.56 ± 0.23 ^{a,b} | 45.08 ± 1.04 ^{a,b} | 66.53 ± 2.69 ^a | 1.65 ± 0.19 ^a |
| | 85 | 0.0106 ± 0.0013 ^b | 12.75 ± 2.12 ^b | 0.29 ± 0.00 ^b | 14.83 ± 0.55 ^b | 2.76 ± 0.26 ^b | 8.52 ± 0.88 ^b | 11.02 ± 0.77 ^b | 45.95 ± 1.90 ^b | 68.08 ± 3.26 ^a | 1.60 ± 0.12 ^a |
| | 30 | 0.0174 ± 0.0009 ^a | 27.06 ± 1.19 ^a | 0.19 ± 0.02 ^{a,b} | 10.32 ± 0.06 ^a | 3.20 ± 0.10 ^{a,b} | 13.21 ± 0.59 ^{a,b} | 14.11 ± 0.32 ^a | 31.75 ± 0.92 ^a | 56.79 ± 4.28 ^{a,b} | 3.02 ± 0.15 ^a |
| | 50 | 0.0160 ± 0.0011 ^{a,b} | 26.91 ± 1.04 ^{a,b} | 0.18 ± 0.02 ^{a,b} | 11.87 ± 0.02 ^{a,b} | 3.50 ± 0.28 ^{a,b} | 14.67 ± 1.10 ^{a,b} | 13.49 ± 0.44 ^{a,b} | 31.99 ± 1.33 ^{a,b} | 58.73 ± 1.75 ^a | 2.75 ± 0.18 ^{a,b} |
| | 55 | 0.0166 ± 0.0006 ^{a,b} | 26.60 ± 1.61 ^{a,b} | 0.18 ± 0.01 ^{a,b} | 11.33 ± 0.37 ^{a,b} | 3.37 ± 0.09 ^{a,b} | 14.55 ± 0.57 ^{a,b} | 13.14 ± 0.56 ^{a,b} | 32.65 ± 0.53 ^{a,b} | 56.17 ± 3.26 ^{a,b} | 2.99 ± 0.27 ^{a,b} |
| | 60 | 0.0159 ± 0.0005 ^{a,b} | 24.53 ± 0.51 ^{a,b} | 0.19 ± 0.01 ^{a,b} | 12.07 ± 0.40 ^{a,b} | 3.56 ± 0.11 ^a | 14.90 ± 0.49 ^a | 11.48 ± 0.33 ^{a,b} | 33.43 ± 0.33 ^{a,b} | 55.95 ± 2.64 ^{a,b} | 2.30 ± 0.16 ^{a,b} |
| | 65 | 0.0151 ± 0.0009 ^{a,b} | 22.68 ± 3.12 ^{a,b} | 0.21 ± 0.02 ^{a,b} | 12.89 ± 0.28 ^{a,b} | 3.44 ± 0.21 ^{a,b} | 13.00 ± 0.21 ^{a,b} | 10.51 ± 1.00 ^{a,b} | 37.87 ± 3.77 ^{a,b} | 53.87 ± 6.32 ^{a,b} | 2.10 ± 0.27 ^{a,b} |
| | 70 | 0.0134 ± 0.0013 ^{a,b} | 19.11 ± 1.57 ^{a,b} | 0.24 ± 0.03 ^{a,b} | 13.99 ± 0.28 ^{a,b} | 3.07 ± 0.21 ^{a,b} | 10.09 ± 0.98 ^{a,b} | 9.31 ± 0.21 ^{a,b} | 42.67 ± 0.98 ^{a,b} | 46.47 ± 3.25 ^{a,b} | 1.78 ± 0.35 ^{a,b} |
| | 80 | 0.0117 ± 0.0009 ^b | 18.22 ± 1.00 ^{a,b} | 0.27 ± 0.01 ^{a,b} | 15.55 ± 0.80 ^{a,b} | 2.77 ± 0.23 ^{a,b} | 8.62 ± 0.60 ^{a,b} | 9.61 ± 0.60 ^{a,b} | 46.35 ± 1.25 ^{a,b} | 45.79 ± 1.25 ^{a,b} | 1.53 ± 0.10 ^b |
| | 85 | 0.0106 ± 0.0012 ^{a,b} | 13.89 ± 3.69 ^b | 0.29 ± 0.01 ^b | 16.80 ± 0.29 ^b | 2.50 ± 0.14 ^b | 7.87 ± 0.54 ^b | 10.42 ± 0.41 ^{a,b} | 48.09 ± 0.41 ^{a,b} | 43.96 ± 1.89 ^b | 1.61 ± 0.19 ^{a,b} |

References

Alpers, T., Tauscher, V., Steglich, T., Becker, T., & Jekle, M. (2021). The self-enforcing starch-gluten system – Strain-dependent effects of yeast metabolites on the polymeric matrix. *Polymers*, 23(1), 1–15. <https://doi.org/10.3390/polym13010030>

Amemiyama, J. I., & Menjivar, J. A. (1992). Comparison of Small and Large Deformation Measurements to Characterize the Rheology of Wheat Flour Doughs. In *Rheology of Foods* (Vol. 16, pp. 91–108). Elsevier. <https://doi.org/10.1016/B978-1-85166-877-9.50011-0>.

Ao, Z., & Jane, J. lin. (2007). Characterization and modeling of the A- and B-granule starches of wheat, triticale, and barley. *Carbohydrate Polymers*, 67(1), 46–55. <https://doi.org/10.1016/j.carbpol.2006.04.013>

Assifaoui, A., Champion, D., Chiotelli, E., & Verel, A. (2006). Rheological behaviour of biscuit dough in relation to water mobility. *International Journal of Food Science and Technology*, 41(SUPPL. 2), 124–128. <https://doi.org/10.1111/j.1365-2621.2006.01469.x>

Bernklau, I., Lucas, L., Jekle, M., & Becker, T. (2016). Protein network analysis - A new approach for quantifying wheat dough microstructure. *Food Research International*, 89, 812–819. <https://doi.org/10.1016/j.foodres.2016.10.012>

Bosmans, G. M., Lagrain, B., Deleu, L. J., Fierens, E., Hills, B. P., & Delcour, J. A. (2012). Assignments of proton populations in dough and bread using NMR relaxometry of starch, gluten, and flour model systems. *Journal of Agricultural and Food Chemistry*, 60(21), 5461–5470. <https://doi.org/10.1021/jf3008508>

Chatraei, S., Macosko, C. W., & Winter, H. (1981). Lubricated squeezing flow: A new biaxial extensional rheometer. *Journal of Rheology*, 25(4), 433–443. <https://doi.org/10.1122/1.549648>

Engelsen, S. B., Jensen, M. K., Pedersen, H. T., Nørsgaard, L., & Munck, L. (2001). NMR-baking and multivariate prediction of instrumental texture parameters in bread. *Journal of Cereal Science*, 33(1), 59–69. <https://doi.org/10.1006/jcres.2000.0343>

Fukukawa, M., Ohta, K. I., & Watanabe, H. (2002). Determination of the terminal extent of starch gelatinization in a limited water system by DSC. *Journal of Food Engineering*, 53(1), 39–42. [https://doi.org/10.1016/S0260-8774\(01\)00137-6](https://doi.org/10.1016/S0260-8774(01)00137-6)

Graumlich, T. R., & Stevenson, K. E. (1979). Respiration and viability of thermally injured *Saccharomyces cerevisiae*. *Applied and Environmental Microbiology*, 38(3), 461–465. <https://doi.org/10.1128/aem.38.3.461-465.1979>

Guo, L., Fang, F., Zhang, Y., Xu, D., Jin, Z., & Xu, X. (2021). Glutathione affects rheology and water distribution of wheat dough by changing gluten conformation and protein depolymerisation. *International Journal of Food Science and Technology*, 56(7), 3157–3165. <https://doi.org/10.1111/ijfs.14806>

Jayaram, V. B., Cuyvers, S., Lagrain, B., Verstrepen, K. J., Delcour, J. A., & Courtin, C. M. (2013). Mapping of *Saccharomyces cerevisiae* metabolites in fermenting wheat

straight-dough reveals succinic acid as pH-determining factor. *Food Chemistry*, 136 (2), 301–308. <https://doi.org/10.1016/j.foodchem.2012.08.039>

Jekle, M., Mühlberger, K., & Becker, T. (2016). Starch-gluten interactions during gelatinization and its functionality in dough like model systems. *Food Hydrocolloids*, 54, 196–201. <https://doi.org/10.1016/j.foodhyd.2015.10.005>

Keetels, C. J. A. M., Van Vliet, T., & Walstra, P. (1996). Gelation and retrogradation of concentrated starch systems: I. Gelation. *Food Hydrocolloids*, 10(3), 343–353.

Kontogiorgos, V., & Kasapis, S. (2010). Temperature dependence of relaxation spectra for highly hydrated gluten networks. *Journal of Cereal Science*, 52(1), 100–105. <https://doi.org/10.1016/j.jcs.2010.04.001>

Lagrain, B., Brijns, K., Veraverbeke, W. S., & Delcour, J. A. (2005). The impact of heating and cooling on the physico-chemical properties of wheat gluten-water suspensions. *Journal of Cereal Science*, 42(2), 327–333. <https://doi.org/10.1016/j.jcs.2005.06.005>

Lagrain, B., Thewissen, B. G., Brijns, K., & Delcour, J. A. (2008). Mechanism of gliadin-glutenin cross-linking during hydrothermal treatment. *Food Chemistry*, 107(2), 753–760. <https://doi.org/10.1016/j.foodchem.2007.08.082>

López-Malo, A., Guerrero, S., & Alzamora, S. M. (1999). *Saccharomyces cerevisiae* thermal inactivation kinetics combined with ultrasound. *Journal of Food Protection*, 62(10), 1215–1217. <https://doi.org/10.4315/0362-028X.62-10.1215>

Lucas, I., Stauner, B., Jekle, M., & Becker, T. (2018). Staining methods for dough systems - Impact on microstructure and functionality. *LWT – Food Science and Technology*, 88 (June), 139–145. <https://doi.org/10.1016/j.lwt.2017.10.010>

Meerts, M., Ramirez Cervera, A., Struyf, N., Cardinaels, R., Courtin, C. M., & Moldenaers, P. (2018). The effects of yeast metabolites on the rheological behaviour of the dough matrix in fermented wheat flour dough. *Journal of Cereal Science*, 82 (February), 183–189. <https://doi.org/10.1016/j.jcs.2018.06.006>

Paulik, S., Yu, W. W., Flanagan, B., Gilbert, R. G., Jekle, M., & Becker, T. (2019). Characterizing the impact of starch and gluten-induced alterations on gelatinization behavior of physically modified model dough. *Food Chemistry*, 301(July), Article 12576. <https://doi.org/10.1016/j.foodchem.2019.12576>

Pojić, M., Musse, M., Rondeau, C., Hadnadvé, M., Grenier, D., Mariette, F., ... Lucas, T. (2016). Overall and local bread expansion, mechanical properties, and molecular structure during bread baking: Effect of emulsifying starches. *Food and Bioprocess Technology*, 9(8), 1287–1305. <https://doi.org/10.1007/s11947-016-1713-2>

Redl, A., Guillet, S., & Morel, M. H. (2003). Heat and shear mediated polymerisation of plasticized wheat gluten protein upon mixing. *Journal of Cereal Science*, 38(1), 105–114. [https://doi.org/10.1016/S0733-5210\(03\)00003-1](https://doi.org/10.1016/S0733-5210(03)00003-1)

Reveron, I. M., Barreiro, J. A., & Sandoval, A. J. (2003). Thermal Resistance of *Saccharomyces cerevisiae* in Pilser Beer. *Journal of the Institute of Brewing*, 109(2), 120–123. <https://doi.org/10.1002/j.2050-0416.2003.tb00140.x>

Rondeau-Moura, C., Cambert, M., Kovrlija, R., Musse, M., Lucas, T., & Mariette, F. (2015). Temperature-associated proton dynamics in wheat starch-based model

systems and wheat flour dough evaluated by NMR. *Food and Bioprocess Technology*, 8 (4), 777–790. <https://doi.org/10.1007/s11947-014-1445-0>

Rouillé, J., Bonny, J. M., Della Valle, G., Devaux, M. F., & Renou, J. P. (2005). Effect of flour minor components on bubble growth in bread dough during proofing assessed by magnetic resonance imaging. *Journal of Agricultural and Food Chemistry*, 53(10), 3986–3994. <https://doi.org/10.1021/jf047953r>

Salvador, A., Sanz, T., & Fiszman, S. M. (2006). Dynamic rheological characteristics of wheat flour-water doughs. Effect of adding NaCl, sucrose and yeast. *Food Hydrocolloids*, 20(6), 780–786. <https://doi.org/10.1016/j.foodhyd.2005.07.009>

Schietd, B., Baumann, A., Conde-Pérez, B., & Vilgis, T. A. (2013). Short- and long-range interactions governing the viscoelastic properties during wheat dough and model dough development. *Journal of Texture Studies*, 44(4), 317–332. <https://doi.org/10.1111/jtxs.12027>

Tsai, M. L., Li, C. F., & Lii, C. Y. (1997). Effects of granular structures on the pasting behaviors of starches. *Cereal Chemistry*, 74(6), 750–757. <https://doi.org/10.1094/CCHEM.1997.74.6.750>

Ulbrich, M., Natan, C., & Flotet, E. (2014). Acid modification of wheat, potato, and pea starch applying gentle conditions - Impacts on starch properties. *Standardization News*, 66(9–10), 903–913. <https://doi.org/10.1002/star.201400089>

Vanin, F. M., Lucas, T., Trystram, G., & Michon, C. (2018). Biaxial extensional viscosity in wheat flour dough during baking. *Journal of Food Engineering*, 236, 29–35. <https://doi.org/10.1016/j.jfooding.2018.05.007>

Verbauwedge, A. E., Lambrecht, M. A., Jekle, M., Lucas, I., Fierens, E., Shegay, O., ... Delcour, J. A. (2020). Microscopic investigation of the formation of a thermoset wheat gluten network in a model system relevant for bread making. *International Journal of Food Science and Technology*, 55(2), 891–898. <https://doi.org/10.1111/ijfs.14359>

Verheyen, C., Albrecht, A., Becker, T., & Jekle, M. (2016). Destabilization of wheat dough: Interrelation between CO₂ and glutathione. *Innovative Food Science and Emerging Technologies*, 34, 320–325. <https://doi.org/10.1016/j.ifset.2016.03.006>

Wang, K., Henry, R. J., & Gilbert, R. G. (2014). Causal relations among starch biosynthesis, structure, and properties. *Springer Science Reviews*, 2(1–2), 15–33. <https://doi.org/10.1007/s40362-014-0016-0>

Wang, K. Q., Luo, S. Z., Zhong, X. Y., Cai, J., Jiang, S. T., & Zheng, Z. (2016). Changes in chemical interactions and protein conformation during heat-induced wheat gluten gel formation. *Food Chemistry*, 214, 393–399. <https://doi.org/10.1016/j.foodchem.2016.07.037>

Weegels, P. L., de Groot, A. M. G., Verhoek, J. A., & Hamer, R. J. (1994). Effects on gluten of heating at different moisture contents. II. Changes in physico-chemical properties and secondary structure. *Journal of Cereal Science*, 19(1), 39–47. <https://doi.org/10.1006/jcrs.1994.1006>

Wilderjans, E., Kerckhofs, G., Lagrain, B., Brijls, K., Wevers, M., & Delcour, J. A. (2010). Baking gradients cause heterogeneity in starch and proteins in pound cake. *Cereal Chemistry*, 87(5), 475–480. <https://doi.org/10.1094/CCHEM-05-10-0048>

Wilderjans, E., Pareyt, B., Goesaert, H., Brijls, K., & Delcour, J. A. (2008). The role of gluten in a pound cake system: A model approach based on gluten-starch blends. *Food Chemistry*, 110(4), 909–915. <https://doi.org/10.1016/j.foodchem.2008.02.079>

Xu, F., Hu, H., Liu, Q., Dai, X., & Zhang, H. (2017). Rheological and microstructural properties of wheat flour dough systems added with potato granules. *International Journal of Food Properties*, 20(1), 1145–1157. <https://doi.org/10.1080/10942912.2017.1337791>

Zudaire, E., Gambardella, L., Kurcz, C., & Vermeren, S. (2011). A computational tool for quantitative analysis of vascular networks. *PLoS ONE*, 6(11), Article e27385. <https://doi.org/10.1371/journal.pone.0027385>

3.4 Strain-dependent assessment of dough's polymer structure and functionality during the baking process

PLOS ONE

RESEARCH ARTICLE

Strain-dependent assessment of dough's polymer structure and functionality during the baking process

Thekla Alpers¹*, Thomas Becker¹, Mario Jekle²

1 Research Group Cereal Technology and Process Engineering, Chair of Brewing and Beverage Technology, Technical University of Munich, Freising, Germany, **2** Department of Plant-Based Foods, Institute of Food Science and Biotechnology, University of Hohenheim, Stuttgart, Germany

* thekla.alpers@tum.de

Abstract



OPEN ACCESS

Citation: Alpers T, Becker T, Jekle M (2023) Strain-dependent assessment of dough's polymer structure and functionality during the baking process. PLOS ONE 18(3): e0282670. <https://doi.org/10.1371/journal.pone.0282670>

Editor: Khalil Abdelrazeq Khalil, University of Sharjah, UNITED ARAB EMIRATES

Received: December 15, 2022

Accepted: February 19, 2023

Published: March 7, 2023

Copyright: © 2023 Alpers et al. This is an open access article distributed under the terms of the Creative Commons Attribution License, which permits unrestricted use, distribution, and reproduction in any medium, provided the original author and source are credited.

Data Availability Statement: All underlying data is presented in the manuscript.

Funding: The authors received no specific funding for this work.

Competing interests: The authors have declared that no competing interests exist.

During the baking process, the functionality of the heterogeneous dough matrix changes as the composing polymers experience conformational transition processes. The thermally induced structural changes affect the involvement and functionality of the polymers in the dough matrix. With the main hypothesis being that different types and magnitudes of strain exerted during the measurement would provide information on different structural levels and interactions, SAOS rheology in multiwave mode and large deformation extensional rheometry were applied to two microstructurally different systems. The functionality of the two systems, a highly connected standard wheat dough ($\phi \approx 1.1$) and an aerated, yeasted wheat dough ($\phi \approx 2.3$), depicting limited connectivity and strength of interactions, was accessed under different deformations and types of strains. Applying SAOS rheology, starch functionality prevailed on the behavior of the dough matrix. In contrast, gluten functionality prevailed on the large deformation behavior. Using an inline fermentation and baking LSF technique, the heat-induced gluten polymerization was shown to increase strain hardening behavior above 70°C. In the aerated system, the strain hardening effect became already evident under small deformation testing, as the expansion of gas cells caused a pre-expansion of the gluten strands. The expanded dough matrix of yeasted dough was further shown to be substantially subjected to degradation once the network reached beyond its maximal gas holding capacity. Using this approach, the combined impact of yeast fermentation and thermal treatment on the strain hardening behavior of wheat dough was revealed for the first time by LSF. Furthermore, the rheological properties were successfully linked to oven rise behavior: a decreasing connectivity combined with the initiation of strain hardening by fast extension processes occurring in the yeasted dough matrix during the final baking phase was linked to limited oven rise functionality prematurely around 60°C.

1 Introduction

The functionality of wheat dough is defined by the interactions of starch and protein, the main polymers constituting the dough matrix. Hydration and mechanical energy input lead to the

formation of a network structure with viscoelastic behavior. The complex rheological behavior changes during the thermal treatment during baking. The dough-to-crumb-transition is initiated by conformational changes of the consisting matrix polymers. This unique behavior has been used in bread making for centuries. In particular, the viscoelastic properties of the non-Newtonian fluid crucially impact the behavior of dough during shaping, proofing and baking. The properties of the dough matrix are enabled by the interactions of the dough's biopolymers on different structural scales. The matrix consists of suspended starch granules, which are located in a 3-dimensional gluten network together with minor dough components such as lipids, arabinoxylans and enzymes [1]. Therefore, decisive interactions appear in between starch granules, between starch granules and proteins, and between the supramolecular protein assemblies [2–4]. Depending on the deformation applied to the dough system, relevant interactions respond in a strain-dependent manner. In this way, primarily short- and long-range interactions are distinguished. Short-range interactions (mainly starch-starch interactions) respond at low strains, whereas increasing strains have to be applied to cause a response of gluten-starch and gluten-gluten interactions [2]. Some authors further highlighted the importance of the type of strain applied, as the functionality of gluten is mainly exposed upon extensional deformation [5–8]. Accordingly, extensional deformation has been used to quantify e.g. strain hardening behavior of dough [9–11]. Translating this strain-dependent behavior to the production process, kneading, shaping, proofing and oven rise processes may be considered large deformation processes, which might primarily cause the response of long-range interactions.

Besides the diverse interactions on different structural scales within the dough phase, thermal treatment during the baking process initiates an even more complex behavior by initiating conformational transition processes of the dough's polymers. Therefore, quantification of the changing material properties by rheological measurements upon thermal treatment is of special importance. Small amplitude oscillatory shear rheology has been commonly used to quantify those rheological changes during the baking process using temperature sweeps. As is the case during kneading, shaping, proofing and oven rise, the viscoelastic dough system is also subjected to large deformation. Hence, large deformation experiments can also provide (and presumably better) relevant information. In shear rheology, this behavior can be accessed using LAOS rheology [12].

Recently, extensional techniques have gained increasing popularity in cereal technology as the dough matrix mainly undergoes biaxial extension during the bread making process. This deformation is responded by specific functionalities, originating from the polymerized character of the gluten proteins. Here, strain hardening behavior is important, which is widely known in polymer science and defined as a phenomenon that the stress required to deform a material increases more than proportional to the strain at a constant strain rate [13]. Therefore, elongational rheology can provide further information on the behavior of dough during process-relevant deformation types [11]. In this way, extensional techniques, such as lubricated squeezing flow, capillary breakup elongational rheometry, filament stretching rheometry, sentmanat extension rheometry or hyperbolic contraction flow can principally be applied [9,11,14–17]. Especially in order to access gluten (or zein) functionality, these techniques are state-of-the-art [7,10,17–19].

So far, little research has been conducted on the impact of thermal treatment on the elongational rheological behavior of wheat dough. Recently, Vanin et al. (2018) successfully conducted LSF measurements to trace the changing rheological behavior of non-yeasted wheat bread dough during thermal treatment and observed marked differences in the shear rheological behavior of dough during heating [17]. So far, research has focused on the behavior of highly connected polymeric wheat dough systems under elongational deformation upon

thermal treatment. Conversely, the integrity of the wheat dough network cannot be granted in practice, as yeast metabolites, generated during the fermentation process, affect the functionality of the gluten network along the bread making process [10,20]. The impact of the degradation of the well branched structure on wheat dough functionality has not been quantified yet and will be the focus of this work.

Hence, this paper aims to elucidate the link between dough structure and oven rise behavior by shedding light on the polymers' functionality in relation to the changes in the dough's molecular and microstructure. Therefore, two dough systems will be characterized using different shear and extensional rheological methodologies. Both systems will be studied with different rheological methods to access their structural and functional changes during the dough-to-crumb-transition. It is hypothesized that different types and magnitudes of strain exerted during the measurement will provide structural information on different scales. The dough systems used in this work are standard non-yeasted wheat dough and yeasted wheat dough. In comparison to the standard wheat dough system, the microstructure of yeasted dough has been shown to be less branched, as the microstructure of yeasted dough is markedly affected by the degrading effects of yeast fermentation [10,21]. Beside this, secondary yeast metabolites were not shown to affect the network structure or functionality significantly [10]. Therefore, yeast represents an optimal tool to implement structural changes, while the functionality of the dough matrix polymers itself remains constant. However, concerning the drawbacks, the measurement of yeasted doughs has been shown to cause major difficulties. Due to the expansion caused by the CO_2 production and dissolution from the liquid dough phase, the dough structure becomes very sensitive to external forces and a sample transfer to the measuring device after fermentation is likely to cause structural damage. Therefore, it would be desirable to ferment the samples in the measurement device itself (which will subsequently be referred to as inline fermentation) to overcome these disadvantages. In inline fermentation, uniaxial expansion of the sample must be enabled to avoid overfilling effects. In extensional rheology, a suitable technique for inline fermentation, heating and rheometry using lubricated squeezing flow was formerly suggested by Alpers et al. (2021) [21]. Regarding shear rheology, inline fermentation is even more desirable, as sample transfer—and especially sample loading—can cause a degassing of the fermented dough sample. During inline fermentation and baking, normal force driven measurement gap adjustment allows the progressive expansion without erroneous sample compression or loss of sample contact. Furthermore, the implementation of multiwave oscillatory shear rheological techniques favor the measurement of yeasted dough samples. Applying multiwave rheology, more information can be extracted out of a reduced measurement time [22,23]. This is beneficial for accessing the time-dependent functionality of dough during fermentation and temperature-dependent behavior during the baking process. In case of yeasted dough, multiwave rheology is further advantageous due to the short measurement times at the same information content. As normal force adjustment should not be active during shear rheological measurements, a short measurement time comes together with lower downtimes for the normal force adjustment, hence avoiding the biaxial sample expansion. Overall, the knowledge gained on strain-dependent dough functionality in different matrices during the baking process will be linked to the dependency of oven rise behavior on the structure and functionality of the polymeric dough system.

2 Materials and methods

2.1 Dough preparation

The experiments were performed using a German commercial wheat flour Type 550. Standard flour characterization resulted in a quantified moisture content of 13.30 ± 0.17 g moisture per

100 g flour (AACCi 44-01, $n = 3$, $\bar{X} \pm \text{STD}$), a protein content of 11.26 ± 0.10 g per 100 g dry flour (AACCi 46-16, $N \times 5.7$, $n = 3$, $\bar{X} \pm \text{STD}$), 0.55 ± 0.05 g ash per 100 g dry flour (ICC 104/1, $n = 3$, $\bar{X} \pm \text{STD}$) and 30.5 ± 0.1 g wet gluten per 100 g flour (AACCi 38-12A, $n = 3$, $\bar{X} \pm \text{STD}$). The kneading was performed in a 50 g scale Z-kneader at 63 rpm using 49.60 g flour, 3 g white sugar/100 g flour (EC category II quality, Bako, Nürnberg, Germany) and 29.25 ml demineralized water. The kneading procedure was adjusted to the optimum dough development protocol which was previously determined using a Z-kneader doughLAB (Perten Instruments AB, Hägersten, Sweden) following AACCi 54-70.01. Sugar was added to provide sufficient fermentable sugars for the yeast fermentation. Yeasted doughs were prepared using fresh compressed yeast (*Saccharomyces cerevisiae*, F.X. Wieninger GmbH, Passau, Germany) at a level of 1 g yeast/100 g flour.

2.2 Elongation properties by lubricated squeezing flow

The sample preparation was performed similar to [21] and will be described in the following section. After the kneading process, the dough samples were sheeted to the desired sample height and cut using a cylindrical cutter (45 mm diameter). Standard non-yeasted wheat dough was sheeted to a final height of 20 mm, whereas in yeasted wheat dough the final height was decreased to 10 mm to compromise for volume expansion during fermentation and baking. Pre-tests confirmed comparable heights of the yeasted and non-yeasted dough samples prior to the compression step using this protocol. Furthermore, no significant difference ($\alpha = 0.05$) has been shown between $\eta_b(\dot{\epsilon} = 0.1)$ derived from wheat dough samples of 20, 30 and 40 mm height, proofing the validity of the used approach. The cylindrical samples were then lubricated using paraffin oil (viscous, Merck KGaA, Darmstadt, Germany) and afterwards immediately transferred to a self-constructed rig for a texture analyzer (TA.XT.Plus, Stable Micro Systems Ltd, Godalming, United Kingdom) equipped with a 50 kg load cell. The setup was developed based on the procedure described by Chatraei et al. (1981) [14]. The original setup was refined by integrating a heating unit to allow in-line fermentation and heat treatment of the dough samples. This approach was used to prevent any external stress of the fermented dough samples, which could lead to a degassing and the collapsing of the structure. Therefore, the setup consisted of two lubricated metal plates of 45 mm diameter, which were tempered using electric heating resistors (aluminum housed fixed power wirewound resistor, $1 \text{ k}\Omega$, 25 W, ATE Electronics, Giaveno, Italy) connected to a PID temperature controller (SYL-2342P, Auber Instruments, Alpharetta, GA, USA). The samples were fermented for 60 min at 30 °C to allow the release of sufficient gas and secondary yeast metabolites into the dough matrix. During the fermentation and baking step, the samples could expand uniaxially as the upper plate was adjusted in order to keep the normal force at a constant level of 10 g. Uniaxial extension of the dough samples was achieved using a silicone jacket (0.5 mm, Sahltac, Bremen, Germany) and a customized, 3D-printed shell (GreenTec Pro, Extrudr FD3D GmbH, Lauterach, Austria). Using these coatings and applying a paraffin layer, the dehydration of the samples was prevented during this time. After fermenting/resting, the dough samples were heated to the desired temperatures. Initial time-temperature calibration of the heating step was performed in terms of pre-tests using an external 1-wire digital thermometer (DS18B20, Maxim Integrated Products Inc., San Jose, CA, USA) connected to an Arduino microprocessor (Arduino Mega 2560, Arduino AG, Turin, Italy), which tracked the dough's core temperature. These pre-tests were performed in triplicate, both for yeasted and non-yeasted doughs. In the final setup, the dough samples were heat-treated according to the previously measured heating times to ensure the structural integrity of the samples. After reaching the desired baking temperature (30; 50, 60, 70, 80, 85 °C, respectively), the silicon jacket and 3D printed shell were

removed to allow a free squeeze flow. The cylindrical samples were compressed to 90% of their initial height by displacing the upper plate. The compression was performed using five different displacement speeds (0.1, 1, 2, 5 and 10 mm/s). The true compression speed was adjusted according to the final sample height of each sample and corrected to reach comparable strain-strain rate combinations. The resulting force-displacement-curves were used to calculate the biaxial strain ϵ_b , the biaxial strain rate $\dot{\epsilon}_b$, and the apparent biaxial viscosity η_b^* according to [10]. Further, the strain hardening index was calculated by extracting the stress values for deformations of 0.3, 0.4, 0.5, 0.6, 0.7 0.8, 0.9 and 1.0 for each displacement speed and temperature. The stress read values were plotted against the biaxial strain rate using a double logarithmic scale. The data was fitted using a linear model, which was then used to calculate the stress values for two biaxial strain rates (0.01 and 1.00 s^{-1}), exemplarily representing rather slow and fast extension processes within the limits of the method. The obtained stress values were plotted against the deformation on a logarithmic scale. According to Rouille et al. (2005), the slope of the linear model expresses the strain hardening index, defined as the increase in stress with increasing extension at a constant extension rate [9]. All measurements were performed in triplicate and the average values are presented with the standard deviation.

2.3 Shear rheological behavior accessed by multiwave rheology

The oscillatory shear rheological measurements were performed using a Modular Compact Rheometer (MCR 502, Anton Paar GmbH, Graz, Austria). The rheometer was equipped with parallel cross-hatched plates (25 mm diameter). The temperature and humidity of the samples were controlled by a CTD 180 HR chamber (Anton Paar GmbH, Graz, Austria) connected to a modular humidity generator (MHG 100, ProUmid GmbH & Co. KG, Ulm, Germany). After kneading, 4 g dough were transferred to the rheometer and centered within the measurement geometries. Subsequently, the sample was compressed to an initial height of 2 mm in case of standard non-yeasted wheat dough and to 1 mm in case of yeasted wheat dough (to compensate for volume extension effects) by setting the measurement gap. After removing excess dough, the cutting surface was covered with paraffin oil (viscous, Merck KgaA, Darmstadt, Germany) to prevent dehydration. The samples were then allowed to rest/ferment for 60 min. Applying normal force controlled gap adjustment ($F_N = 0.01$ N), a uniaxial extension of the dough samples was achieved during the fermentation step. Using this gap adjustment, it was possible to maintain the sample diameter equal to the diameter of the plate-plate geometry at any time. This is normally achieved by trimming the sample to a cylindrical shape prior the measurement so it should not be harmed during the subsequent equilibration or measurement steps. The highly sensitive normal force control enabled a free uniaxial expansion of the sample during a 60 min fermentation step and the consecutive heating process. Fermentation was performed at 30 °C and 80% relative humidity. Subsequently, a temperature sweep was performed from 30 – 95 °C at a heating rate of 4.5 °C/min. During the heating steps, normal force control was activated ($F_N = 0.01$ N), whereas the gap was kept constant during the measurement intervals. Measurements were conducted every 5 °C at a frequency of 1 Hz and a deformation of 0.05% at a fixed measurement time of 25 s. The deformation was applied as multiwave strain according to Vidal et al. (2022) [23], enabling the simultaneous measurement of multiple frequencies within a single measurement point. Besides the fundamental frequency of 1 Hz, harmonics being the 2nd, 3rd, 5th, 7th, 8th and 10th multiple of the fundamental frequency, were performed simultaneously. The resulting amplitude totaled 0.082%, which was still in line with the determined LVE region of yeasted and non-yeasted dough. The Fourier transformation of the superimposed resulting torque/stress functions was automatically evaluated by RheoCompass (Version 1.25, Anton Paar GmbH, Graz, Austria). The obtained values for complex

module data ($|G^*|$) were then fitted to the power law equation (c.f. Eq (1)).

$$G^*(\omega) = A_f \omega^{1/z} \quad (1)$$

where ω is the frequency (s^{-1}), A_f refers to the network strength ($Pa s^{1/2}$) and z to the network connectivity (-) [24]. All measurements were performed in triplicate and average values are presented with standard deviation.

3 Results and discussion

3.1 Impact of thermal treatment on the shear rheological behavior of dough

Shear rheology was used to access the functionality of yeasted and non-yeasted wheat flour dough under small deformation. As it can be seen in Fig 1, the initial behavior of both dough samples differs in the absolute value of $|G^*|$, as $|G^*|$ of non-yeasted standard wheat dough is higher compared to yeasted wheat dough. This drop in $|G^*|$ for yeasted doughs has been observed previously and was related to the entrapped gas cells [18,25–27]. Besides CO_2 , previous work of the authors has shown that secondary yeast metabolites like ethanol or succinic acid only have a minor impact on the rheological behavior of the dough matrix under a small amplitude oscillatory strain [10]. Therefore, the increased gas void fraction, inducing micro-structural changes in the protein network (reduced protein strand length and connectivity [10]), of yeasted wheat dough can be regarded as being the decisive factor for the reduction of $|G^*|$. The dependency of $|G^*|$ on the gas void fraction can be generally observed in aerated systems, for example in rigid polyurethane foams. For example, Saint-Michel et al. (2006) showed

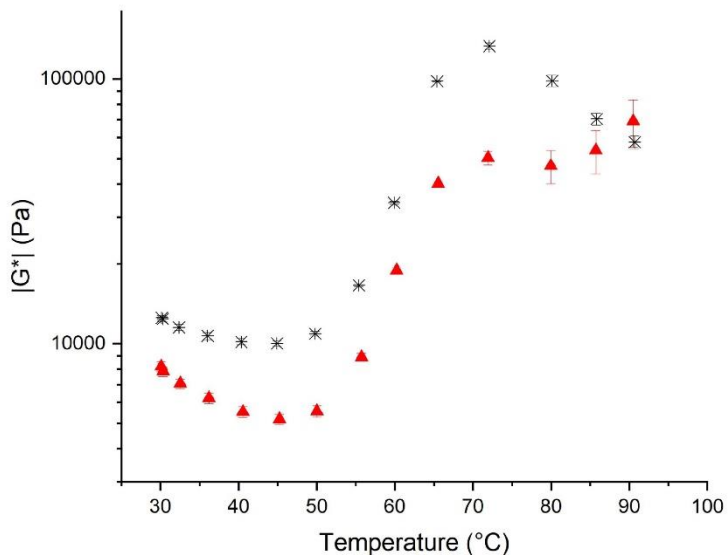


Fig 1. Complex modulus retrieved from shear rheological measurements at $\gamma = 0.03\%$ at 1 Hz after 60 min resting/fermenting at 30°C and subsequent heating. (*) Standard non-yeasted wheat dough and (▲) yeasted wheat dough (1 g fresh yeast/100 g flour). ($n \geq 3$, $\bar{X} \pm STD$).

<https://doi.org/10.1371/journal.pone.0282670.g001>

that G' increases with an increasing density of these foams [28]. This effect can be explained by a higher material density, causing the interaction of particles to become more probably. This mechanism can be applied to dough matrices with different gas void fractions as well, as dough can be considered as a foamed material [29].

Upon baking, $|G^*|$ decreases during the initial heating phase, to a temperature of $46.35 \pm 0.04^\circ\text{C}$ or $45.27 \pm 0.11^\circ\text{C}$ in case of non-yeasted and yeasted doughs, respectively, followed by a steep increase for both systems. A peak viscosity is reached at 70°C for both dough systems, with $|G^*|$ of yeasted doughs being markedly lower than in the non-yeasted system. After this peak viscosity, the behavior differs markedly between the dough systems. The complex modulus of non-yeasted standard wheat dough decreases steadily with increasing temperature, which can mainly be related to the loss of the granular starch structure upon gelatinization. Contrarily, the complex modulus of yeasted dough decreases slightly after the $|G^*|_{\max}$ and increases again during the final baking phase. This behavior can be explained by the ongoing gas expansion, which is known to cause strain hardening of the extended gluten strands (see Section 3.3). At the end of the baking process, the final behavior resulting from yeasted and non-yeasted dough systems present comparable $|G^*|$ values. Therefore, the reinforcing effect of strain hardening is seen to accomplish for the effects of the higher gas void fraction in yeasted dough. Additional knowledge, underlining the yeast-induced extension of the protein network during the early baking phase in terms of a decreasing protein strand width and increasing average protein strand length, has been reported earlier by accessing the protein network structure by Confocal Laser Scanning Microscopy [21]. The strain hardening effect might further be supported by additional effects, such as altered structures in the dough matrix itself. Here, one reason could be the formation of a denser starch network due to the exclusion of starch granules from the lamella during fermentation and oven rise process. It is therefore hypothesized that the material of the gas cell-surrounding lamellae is mainly composed of gluten strands. Hence, the establishment of starch clusters in the nodes enables a higher extent of starch-starch interactions. It is furthermore hypothesized that starch, being clustered in nodes, might be more accessible to water as the granules are not further embedded in the gluten network. Thus, an accelerated starch gelatinization process could take place in yeasted doughs and the formation of a continuous network of gelatinized starch is more likely to be formed in the nodes [21]. Confirmatory indications were found by accessing the extend of the starch gelatinization process in yeasted and non-yeasted wheat dough systems using Differential Scanning Calorimetry during thermal treatment, where a slightly accelerated starch gelatinization process was observed in yeasted dough systems [21]. Furthermore, the displacement of starch granules changes the strain hardening process, as it is no longer affected by the presence of particles.

More detailed structural information can be extracted from the applied multiwave approach. The frequency dependent behavior was accessed using a power law fit of the $|G^*|$ multiwave data to extract more sophisticated structural information. The obtained values for the network connectivity z are presented in Fig 2. As already assumed previously, the initial non-yeasted standard wheat dough appears to be higher connected, as z of non-yeasted dough is higher than z of yeasted dough. Thus, the yeasted standard wheat dough appears to have a network configuration with less connection points. In this case, the release of CO_2 is believed to cause a degradation of the network due to a fracture of the dough matrix caused by the expansion of gas cells. This has been observed in the protein microstructures of yeasted dough during the fermentation [10,21]. Upon baking, the z value of non-yeasted standard wheat dough increases steadily due to starch gelatinization and heat induced gluten polymerization [21]. In case of yeasted dough, an abnormal decrease in connectivity was observed for temperatures above 80°C . Above these temperatures, protein polymerization appears to be limited in

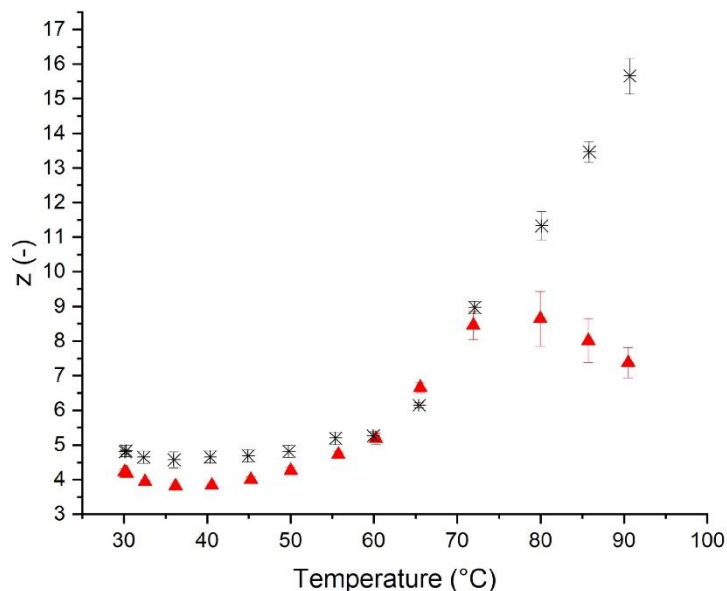


Fig 2. Effect of yeast on the dough structure accessed by shear rheological measurements during the baking process after 60 min resting/fermenting at 30°C. Network connectivity z describing quantity of interactions. (*) Standard non-yeasted wheat dough and (▲) yeasted wheat dough (1 g fresh yeast/100 g flour) [24,31]. ($n \geq 3$, $\bar{X} \pm \text{STD}$).

<https://doi.org/10.1371/journal.pone.0282670.g002>

yeasted dough. As expanding gas cells partially hinder the interaction of protein-protein binding sites, less adjacent proteins can react in gluten polymerization reactions [30]. This can further be supported by the fact that yeasted doughs showed a higher protein extractability, which was formerly related to a limited extent of polymerization in leavened dough systems [21]. Furthermore, the increasing contribution of the thermal expansion of the entrapped gas cells might potentially cause the occurrence of small gluten fragments due to strand rupture. In this case, the initiated degradation counteracts the heat-induced polymerization and leads to a decreasing network connectivity.

3.2 Impact of thermal treatment on the extensional rheological behavior of dough

Besides SAOS rheology, large deformation extensional rheology has been used to access the behavior of the dough matrixes. The biaxial viscosity of non-yeasted standard wheat dough and yeasted dough was accessed by LSF. The viscosity values presented do not qualify for an absolute comparison, as the sample masses of non-yeasted and yeasted dough differ. The sample masses used for the measurements were adjusted in order to keep strain-strain rate progression comparable. Therefore, the following section will focus on the dependency of the biaxial viscosity on the temperature rather than focus on a comparison of the absolute values in between dough systems. As can be seen in Fig 3 for an extension rate of 0.01 s^{-1} , the viscosity

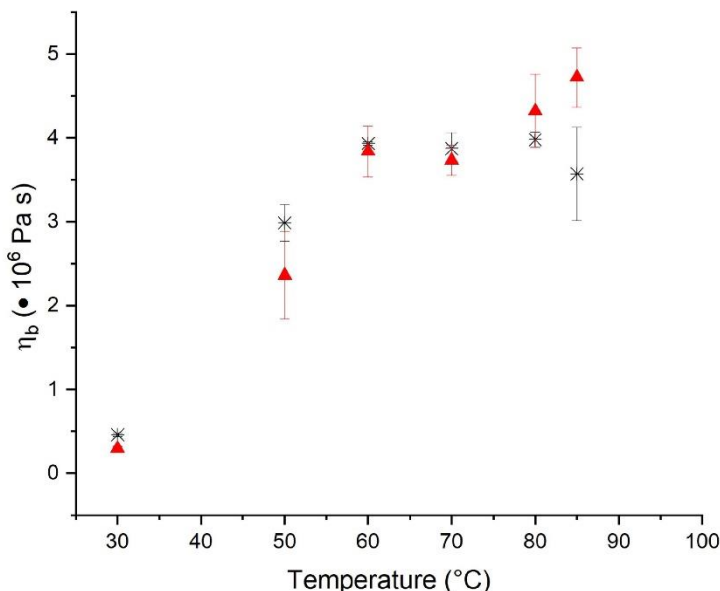


Fig 3. Effect of yeast on the extensional rheological behavior of wheat dough measured at $\dot{\epsilon}_0 = 0.01 \text{ s}^{-1}$ after 60 min resting/fermentation at 30°C and heating to the specified temperature. Viscosities of different dough systems are not quantitatively comparable as the mass varied between the different dough systems in order to reach comparable strain-strain rate combinations. (*) Standard non-yeasted wheat dough and (▲) yeasted wheat dough (1 g fresh yeast/100 g flour). ($n \geq 3$, $\bar{X} \pm \text{STD}$).

<https://doi.org/10.1371/journal.pone.0282670.g003>

of yeasted dough increases steadily during the whole baking process, whereas non-yeasted dough reaches a plateau viscosity value during the latter baking phase. Thus, the observed behavior differs markedly from the rheological behavior observed for shear rheological testing. While the course of $|G''|$ for SAOS rheology is reminiscent of the course of starch suspensions during heating, the course of η_b lacks in the final loss of consistency. As suggested earlier by Turbin-Orger et al. (2016), extensional rheology emphasizes gluten functionality by mainly addressing long-range interactions [32]. It can therefore be concluded that the observed changes of η_b are mainly related to changes in the gluten structure and the associated gluten functionality. Overall, the strongest changes in gluten functionality can be observed within 50°C and 70°C, where conformational changes occur due to fewer hydrophobic interactions [30]. For temperatures above 70°C only minor changes appear. Contrarily, yeasted dough systems present a different behavior for η_b above 70°C. A further increase of η_b until the final baking temperature became evident instead of reaching a plateau value. As discussed above, this might be related to a re-enforcing effect of strain hardening due to the extension of gluten strands in leavened dough or changes in the dough matrix viscosity, such as an altered starch gelatinization behavior. The contribution of strain hardening to the rheological behavior of yeasted dough will be discussed in Section 3.3.

A sophisticated structural interpretation is possible by using the power law model to describe the strain rate dependency of η_b : $\eta_b = K \cdot \dot{\epsilon}^{(n-1)}$, where K (Pa sⁿ) is the consistency

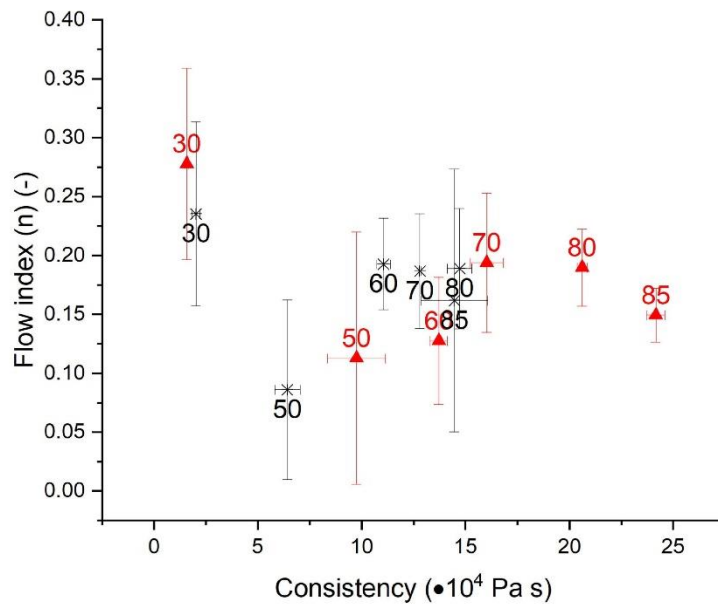


Fig 4. Impact of fermentation and heating on the flow index and consistency for $\varepsilon_b = 1.00$. (*) Standard non-yeasted wheat dough and (▲) yeasted wheat dough (1 g fresh yeast/100 g flour). The numbers in each value represent the related treatment temperature of the sample. Data of different dough systems is not quantitatively comparable, as the mass varied between the different dough systems in order to reach comparable strain-strain rate combinations. ($n = 3, X \pm \text{STD}$).

<https://doi.org/10.1371/journal.pone.0282670.g004>

index and n (-) is the flow index [32]. The results in terms of the consistency index K and the flow index n are presented in Fig 4 for non-yeasted and yeasted wheat dough systems for temperatures from 30°C to 85°C. In general, the data points of both dough systems are shown to shift to higher consistency index values with increasing temperature. The consistency index K of yeasted doughs increases steadily from 30°C to 85°C, whereas in non-yeasted doughs, K increases only slightly from 60°C to 80°C and decreases from 80°C to 85°C. The flow index n of standard non-yeasted wheat dough drops initially with a temperature increase from 30°C to 50°C, while K increases for these temperatures. The reduced flow index can be explained using the Arrhenius-like temperature dependency, which states a higher mobility of the polymers with increasing temperature. These initial changes are followed by a steady increase of n with K till final values for n (final flow index reached at 60°C) and K (final value reached at 80°C) are reached. Therefore, the flow index seems to be limited by the onset of the starch gelatinization process, which was formerly shown to occur within 50°C and 70°C [21]. Regarding the consistency index, a leveling off only after the setting in of the protein polymerization process can be observed. The onset of the polymerization process has been located earlier by protein extractability measurements and was found to set in at temperatures above 65°C or 70°C [21,30].

Contrarily, the behavior of the yeasted wheat dough has been shown to be markedly affected by the presence of growing gas cells. After the likewise appearing initial drop, n shows

the highest flow indices at 70 and 80°C, followed by a steady decrease of the flow index. This can be explained by an increasing crosslinking, which is then limited by an increasing network degradation due to growing gas cells and the accompanied overextension of the lamella. Contrarily, K of yeasted wheat doughs shows a steady increase, even during the final baking phase. As this behavior cannot be observed in non-yeasted doughs, this behavior is therefore likely to be explained by the strain hardening phenomena triggered by the extending gas cells. Therefore, the presented results suggest different mechanisms behind the solidification behavior of non-yeasted and yeasted dough matrices. While pure polymerization appears to dominate the solidification process in non-yeasted dough systems, yeasted dough undergoes limited polymerization, but more pronounced strain hardening due to the expansion of gas cells. This hypothesis can be underlined by the results of SDS-supported protein extraction of heat-treated wheat dough systems as presented by Alpers et al. (2022). The study revealed a lower extend of protein polymerization in yeasted wheat dough for temperatures above 65°C, compared to non-yeasted wheat dough. This was explained by a higher gas void fraction in yeasted dough, which limits the connectivity of the protein strands and, therefore, the amount of proteins in reactive distance for polymerization [21,30]. On the other hand, as discussed above, microstructural data on the protein network reveals a decreasing protein strand width, indicating gas cell growth during the initial baking process [21]. Therefore, initialization of strain hardening behavior is likely to be more pronounced in yeasted wheat dough, counteracting the functional effects of a lower extend of protein polymerization.

3.3 Impact of thermal treatment on the strain hardening behavior of dough

To further elucidate the ability of both matrices for stabilization by strain hardening during the baking process, this phenomenon was quantified. The dependency of the strain hardening functionality on the extent of the thermal treatment is presented in Fig 5. Up to a temperature of 50°C, a strong increase of the SHI for both dough systems can be observed. This can mainly be related to the thermally induced changes in protein conformation and interactions. The decreasing strength of hydrogen bonds limits the ability of the gluten strands to interact via short-range interactions. Due to this, the slippage of proteins along each other without intermediate stabilization is more likely to cause strain hardening. Furthermore, the initiation of conformational changes causes the aggregation of proteins and changes the ability of extension of loop regions upon elongation. This might explain the early triggering of strain hardening due to the reaching of the extensibility limit. For temperatures below 50°C, the pasting process of starch is also known to reduce the overall mobility of the system and therefore causes a decreasing plasticization of the polymers [33]. With progressive thermal treatment, a decreasing strain hardening index can be observed within 50°C and 70°C. Here, the gelatinization of starch decreases the rigidity of starch granules and leads to the development of a continuous starch-gluten network. Additional binding sites might therefore support the extension processes and enable intermediate stabilization. Additionally, dissociating starch granules are hypothesized to cause less friction on the extending gluten strands and therefore induce less pronounced strain hardening, which can explain the decreasing SHI as well. During the final baking phase, the SH index is shown to increase again, whereby the yeasted dough system presents a more pronounced SHI increase. At the molecular level, the polymerization process of gluten proteins has been reported to initiate at temperatures above 70°C [30]. Increasing molecular interactions [30] could therefore decrease the amount of extendable loop regions. The extension process is therefore hypothesized to be limited due to the limited expendability of the protein strands. Thus, the strain hardening process is triggered already at a lower overall extension and the measured SHI is increasing.

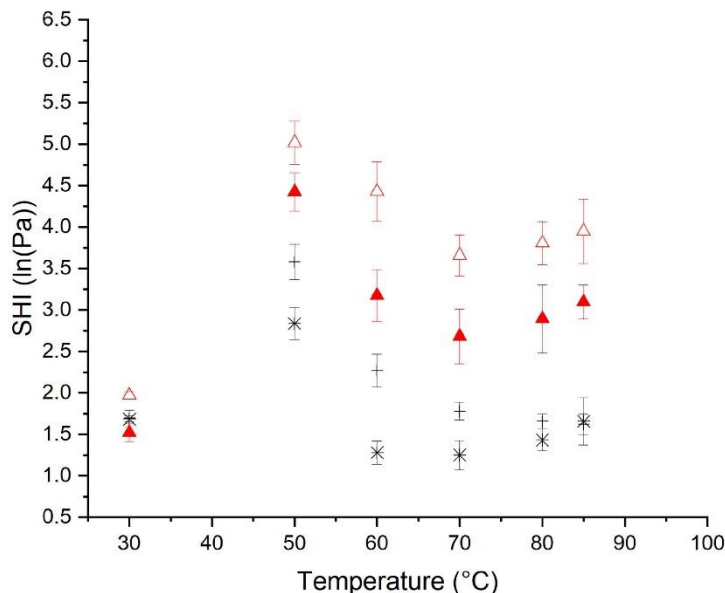


Fig 5. Strain hardening behavior of non-yeasted and yeasted dough after 60 min fermentation and subsequent heating to the specified temperatures. (*) Standard non-yeasted wheat dough, $\dot{\epsilon}_b = 0.01 \text{ s}^{-1}$, (—) standard non-yeasted wheat dough, $\dot{\epsilon}_b = 1.00 \text{ s}^{-1}$, (▲) yeasted wheat dough (1 g fresh yeast/100 g flour), $\dot{\epsilon}_b = 0.01 \text{ s}^{-1}$ and (△) yeasted wheat dough (1 g fresh yeast/100 g flour), $\dot{\epsilon}_b = 1.00 \text{ s}^{-1}$. (n = 3, $\bar{X} \pm \text{STD}$).

<https://doi.org/10.1371/journal.pone.0282670.g005>

Additional information can be obtained by comparing the strain hardening behavior of the dough systems at different strain rates. Furthermore, the strain rate dependent behavior can be used to predict the behavior of the dough systems under different deformations along the bread making process. For this reason, the current study uses two strain rates to predict the behavior of the dough systems at slow and fast extension processes. At an extension rate of $\dot{\epsilon} = 0.01 \text{ s}^{-1}$, the SHI of both dough systems was found to be lower than at the fast extension rate of $\dot{\epsilon} = 1.00 \text{ s}^{-1}$. This behavior has previously been observed by the authors and was explained by the enabling of rearrangement, slippage and intermediate stabilization along protein strands at slow extension rates [10]. These processes were hypothesized to lower the strain hardening index for dough systems at low extension rates. In case of high extension rates, gluten strands might remain entangled due to the fast extension process. In this case, no free slippage and missing stabilization by intermediate polymer–filler-interactions are hypothesized to contribute to an intensified strain hardening behavior. Additionally, friction occurring within starch granules or starch granules and protein strands might raise the strain hardening behavior. The observation that the SHI is particularly high around 50°C, where starch is still in its granular structure, enforces the hypothesis of friction contributing to strain hardening behavior. Considering the SHI at fast extension rates, a more pronounced strain hardening behavior becomes evident for yeasted dough systems. The pre-extended protein strands of the yeasted dough system seem to cause an earlier onset of strain hardening, which leads to an overall increase of the SHI for yeasted dough systems. This proves the previously considered

explanation of a higher strain hardening character of yeasted dough systems, which was used to explain the observed differences in shear and elongational rheological behavior of both dough systems, especially at higher temperatures.

3.4 Oven rise behavior and macroscopic quantification of extension processes

Using the knowledge on strain-dependent dough functionality in different matrices gained during the baking process, the oven rise behavior of both matrices during the baking process will be discussed in the following section. For this reason, the course of the relative dough volume for yeasted and non-yeasted wheat dough during fermentation and baking are presented in Fig 6. It becomes evident that the yeast dough system is subjected to a significant volume expansion during the fermentation process (Fig 6A). The course of the increase of the relative volume is similar to the course reported by Chevallier et al. (2012) [34]. As stated by those authors, the growth can be divided into different phases. During an initial lag phase, the incorporated yeast cells produce CO_2 , which migrates in the liquid dough matrix and remains solubilized. This phase is followed by an initial growth phase. After the solubility limit of the liquid dough phase has been reached, CO_2 starts to dissolve and dissipates into the entrapped gas cells. The increasing gas fraction causes the expansion of the gas cells. This leads to the establishment of a linear growth rate, with which the expansion process continues throughout the whole 60 min of fermentation [34]. During this period, no stationary phase is reached and hence, the gas holding limit of the dough systems is not exceeded. Consequently, the produced CO_2 can still be entrapped and stabilized within the dough matrix and does not escape yet. Contrarily, the non-yeasted dough is not subjected to any considerable volume expansion processes. The relative volume of the system is rather inert during the resting phase, which indicates no initial inoculation and no microbial contamination of the flour with relevance for gas formation.

After the fermentation phase, the yeasted dough starts with a higher initial relative volume into the baking process. During the baking phase, further expansion processes can be observed (Fig 6B). This expansion is referred to as oven rise, which is defined as the volume expansion of dough during the thermally induced dough to crumb transition. In case of yeasted dough, a

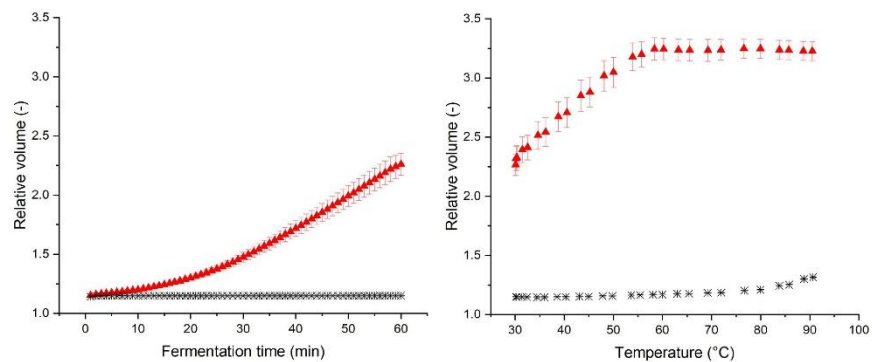


Fig 6. Relative volume of yeasted dough and non-yeasted standard wheat dough during 60 min fermentation at 30°C and subsequent heating to 90°C. a) Time dependency of the relative volume during the fermentation process. b) Temperature dependency of the relative volume during the heating process. (*) Standard non-yeasted wheat dough and (▲) yeasted wheat dough (1 g fresh yeast/100 g flour). (n ≥ 3, X ± STD).

<https://doi.org/10.1371/journal.pone.0282670.g006>

steep initial oven rise behavior can be observed up to 50°C. The maximum relative volume is then reached at 60°C and retained until the end of the baking process. The initial expansion can be explained by the CO₂ production of yeast cells till the death of yeast cells sets in at ~50°C [35–37]. During this initial baking phase, an expansion rate of 0.104 min⁻¹ was determined by a linear model (relative volume-baking time), which is markedly higher compared to the gas production rate during the fermentation phase. During this phase, the expansion rate was quantified to 0.027 min⁻¹. The differences can be explained by the well-known thermal dependency of yeast activity. Due to this dependency, a higher gas fermentation rate can be observed at elevated temperatures up to a temperature of 50°C, where yeast cells are subjected to thermal damage. Additionally, thermally driven expansion processes promote the volumetric expansion of the matrix while baking. The yeast-driven oven rise is followed by another short expansion phase till 60°C. The appearing expansion can now be clearly related to further expansion of the already incorporated gas phase, evaporating water and ethanol, dissolution of CO₂ and thermal expansion of the liquid dough phase within 50°C and 60°C. Beyond 60°C, no further expansion can be observed. As previously observed in the quantification of the shear and elongational rheological behavior, yeasted dough has a limited network connectivity and enhanced strain hardening behavior. This could lead to a limited gas holding capacity and repressed final oven rise as the viscosity increases in a more pronounced way due to strain hardening.

Contrarily, oven rise in standard wheat dough was found to be comparably low due to the limited amount of gas entrapped in the dough matrix. A significantly retarded oven rise can be observed (starting at 70°C). The end of the expansion process was not recorded within the conducted experimental setup. The rheological characterization revealed a softening of the dough matrix for temperatures above 70°C, quantified in terms of a decreasing |G*|. This might promote an expansion during the latter baking phase. Additionally, no decrease in network branching was quantified (n and z remained constant or increased). Therefore, there is no indication for a limited gas holding capacity in case of standard non-yeasted wheat dough which could limit further oven rise as it was shown for the yeasted system, which suffered remarkable damage on a microstructural level. The oven rise of the standard wheat dough system, which is induced by evaporation processes, results in an expansion rate of 0.035 min⁻¹. As the expansion process proceeds slower than in yeasted dough, less strain hardening is to be expected due to the fact that slow extension processes cause less strain hardening compared to fast extension processes (see Section 3.3). The lower resistance to extension of the dough matrix might therefore contribute to the occurrence of oven rise even at high temperatures, even though the lower relative volume has to be taken into account, favoring oven rise during the final baking phase as well.

4 Strain-dependent functionality of the dough's polymers during the baking process: A structural model

The major focus of this work was the identification of different functional structures within the dough matrix, which respond to certain types and magnitudes of exerted strain. As the bread making process involves deformations of various types and strengths, the response of the dough matrix composing polymers to these stresses is important so the behavior of the system during the production process can be understood. Especially during the baking step, where conformational transition processes of the dough's composing polymers are initiated, the changing functionality of each component is of great interest. Therefore, SAOS rheology and large deformation extensional rheology (LSF) were applied to a non-yeasted standard wheat dough system and a yeasted wheat dough system during thermal treatment.

Our results show that the response to the application of small deformations is markedly different to the response to large deformations. While small strains mainly resulted in the response of filler-filler interactions, large deformations gave rise to more pronounced gluten functionality. This agrees with the observations of Turbin-Orger et al. (2016) [32]. With this knowledge, the contradicting behavior and structural evolution of both systems ((i) highly connected standard wheat dough and (ii) pre-extended and structurally degraded yeasted wheat dough under conventional shear rheology) can be explained: The standard wheat dough system (i) mainly depicts starch functionality upon thermal treatment. Starch pasting and gelatinization initiated a first raise in viscosity around 45°C and lead to a maximum peak viscosity around 70°C, where starch gelatinization was formerly shown to be fairly concluded. Continued thermal treatment led to a viscosity drop due to the increased mobility of starch molecules. Structural information obtained by the application of the multiwave technique revealed an increasing structural connectivity during this final heating phase, which may be attributed to increased interactions within starch molecules in the new-formed continuous starch phase. Besides this, the heat-induced gluten polymerization contributes to the increased connectivity. The increasing connectivity of the standard wheat dough system during the final baking phase also becomes evident when looking at the behavior of standard wheat dough under large elongational deformation: Even though starch functionality would cause a viscosity drop in the final baking phase, this behavior is strongly reduced when considering η_b . By evaluating the SHI, even a hardening above 80°C becomes obvious due to heat-induced gluten polymerization.

In yeasted dough systems (ii), a higher share of gluten functionality was shown to be initiated as the leavening of the system caused additional deformation. These internal forces caused a pre-extension of the system (as quantified on a microstructural level by [21]) and therefore favored the occurrence of large deformation behavior. Therefore, the behavior of yeasted doughs under a small deformation showed a comparable course to the behavior observed under a large extensional deformation. The usage of small as well as large deformation techniques further provided good insights into the effect of yeast fermentation on the dough matrix structure. In general, yeasted wheat dough appeared to be less well connected, which gave rise to a reduced matrix strength (lower complex modulus) This observation can be supported by comparative data on the extend of protein polymerization in yeasted and non-yeasted wheat dough as reported by Alpers et al. (2022), which indicates a higher level of non-crosslinked, low molecular weight gluten in yeasted wheat dough during the final baking process. The fitting of the observed rheological behavior under both, small and large deformation, by structural models revealed a strong impact of the expanding gas cells on the course of the connectivity of the dough matrix during the baking procedure. Starting with an already less connected network, the expanding gas cells were further shown to impact starch gelatinization and heat-induced gluten polymerization. In case of gluten functionality (quantified by large deformation rheology), the polymerization (especially above 70°C) was shown to be limited, as the mobility of the system seemed to be rather reduced by an increasing consistency (e.g. strain hardening) than by an increase in connectivity. The opposite was observed in starch functionality under small deformations: Upon the expansion of gas cells, starch granules are hypothesized to be excluded from the lamella and clustered in the connecting nodes. The clustering of starch in nodes gave rise to an earlier and more extensive starch gelatinization process in yeasted doughs (slight shift in the inflection point to a lower temperature). Further, the aggregated starch polymers were shown to be more likely to form a continuous network within the nodes when the granular structure breaks up in succession of the gelatinization process as the strength of the network under small deformations increased during the final baking step, while the connectivity itself was shown to decrease.

The importance of starch and gluten functionality for the oven rise process became evident when the gained knowledge on structural changes is related to the functionality of the systems. In case of yeasted dough, a strong oven rise behavior was observed during the initial baking phase. This can mainly be related to the thermal activation of yeast, which causes the more rapid production and dissolution of CO_2 . As gluten functionality is strongly preserved (high connectivity (z and n), strong strain hardening behavior), the released gas can be stabilized in the dough matrix. During the latter baking process (above 60°C), no further expansion can be observed. Based on the elucidated structural changes within the system, structural degradation dominates in this point. Here, decreasing connectivity indicates rupture of the network, together with the presence of smaller, highly mobile gluten fragments [21]. Consequently, the SHI strongly decreases and any further gas released (e.g. by dissolution, evaporation or expansion processes) can no longer be stabilized by the dough matrix. Besides this, the expansion of yeasted wheat dough can be considered a rather fast expansion process as a high amount of gas stabilized in the system expands and considerable amounts of dissolving CO_2 cause a fast increase of the gas void fraction. The occurring fast expansion rates therefore initiate a higher resistance (SHI) of the system towards further expansion, which might limit the extensibility during the final baking phase additionally. Contrarily, in non-yeasted dough, expansion processes are rather slow, as the gas cell expansion is mainly based on evaporation and thermal expansion processes. During slow expansion processes, intermediate stabilization mechanisms were previously shown to be active and able to stabilize the matrix expansion [10]. Furthermore, starch functionality should be considered different during slow expansion processes, as the occurring friction is low and rather a stabilizing effect was hypothesized due to the possibility of intermediate stabilization within starch and gluten upon the reformation of short range interactions upon expansion. As starch functionality was shown to dominate the small deformation response of the system, a stabilizing effect can be attributed to starch during the expansion process of non-yeasted dough during the final baking phase. The low viscosity measured under small deformation processes during the final baking phase and the limited strain hardening functionality for slow extension processes are both attributed to the preserved oven rise functionality above temperatures of 80°C in non-yeasted dough. Hence, it is necessary to quantify the rheological behavior of dough systems according to the type and strength occurring during the production process to extract reliable data.

5 Conclusion

By elaborating inline fermentation and baking techniques, allowing the assessment of both—yeasted and non-yeasted dough systems—, it was possible to determine the effect of structural changes of the main dough's polymers on their changing functionality in the dough matrix during the baking step. In this framework, yeast was used as a tool to implement structural changes in the dough matrix without changing the functionality of the dough's polymers itself. Subjecting these systems to different types and magnitudes of strain upon thermal treatment, a structural model was proposed for the dough's polymers during baking. The contribution of the functionality of the polymers to accomplish an oven rise has been elucidated by differentiating the functionality of the polymeric system in dependency of the experienced thermal treatment and deformation occurring within the dough matrix. Overall, SAOS multiwave rheology was shown to be a powerful tool to analyze starch functionality in non-yeasted systems. Contrarily, large deformation techniques, initiated either by external or internal forces, have been shown to be more impacted by gluten functionality due to the enhanced strain hardening behavior, caused by gluten extension or the stress memory of gluten.

Author Contributions

Conceptualization: Thekla Alpers, Mario Jekle.

Formal analysis: Thekla Alpers.

Investigation: Thekla Alpers.

Methodology: Thekla Alpers.

Project administration: Thekla Alpers.

Supervision: Mario Jekle.

Visualization: Thekla Alpers.

Writing – original draft: Thekla Alpers.

Writing – review & editing: Thomas Becker, Mario Jekle.

References

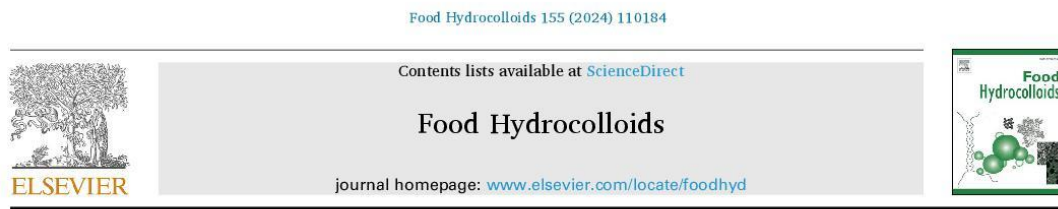
1. Jekle M., Mühlberger K., and Becker T., "Starch-gluten interactions during gelatinization and its functionality in dough like model systems," *Food Hydrocoll.*, vol. 54, pp. 196–201, 2016, <https://doi.org/10.1016/j.foodhyd.2015.10.005>
2. Schiedt B., Baumann A., Conde-Petit B., and Vilgis T. A., "Short- and long-range interactions governing the viscoelastic properties during wheat dough and model dough development," *J. Texture Stud.*, vol. 44, no. 4, pp. 317–332, 2013, <https://doi.org/10.1111/jtxs.12027>
3. Aramendi J. I. and Menjivar J. A., Comparison of Small and Large Deformation Measurements to Characterize the Rheology of Wheat Flour Doughs, vol. 16. ELSEVIER SCIENCE PUBLISHERS LTD, 1992.
4. Kontogiorgos V., Shah P., and Bills P., "Influence of supramolecular forces on the linear viscoelasticity of gluten," *Rheol. Acta*, vol. 55, no. 3, pp. 187–195, 2016, <https://doi.org/10.1007/s00397-015-0901-8>
5. Martín-Alfonso J., Cuadri A., Berta M., and Stading M., "Relation between concentration and shear-extensional rheology properties of xanthan and guar gum solutions," *Carbohydr. Polym.*, vol. 181, pp. 63–70, 2018, <https://doi.org/10.1016/j.carbpol.2017.10.057> PMID: 29254016
6. Mccann T. H., Le Gall M., and Day L., "Extensional dough rheology—Impact of flour composition and extension speed," *J. Cereal Sci.*, vol. 69, pp. 228–237, 2016, <https://doi.org/10.1016/j.jcs.2016.03.012>
7. Andersson H., Öhgren C., Johansson D., Kniola M., and Stading M., "Extensional flow, viscoelasticity and baking performance of gluten-free zein-starch doughs supplemented with hydrocolloids," *Food Hydrocoll.*, vol. 25, no. 6, pp. 1587–1595, 2011, <https://doi.org/10.1016/j.foodhyd.2010.11.028>
8. Van Vliet T., "Strain hardening as an indicator of bread-making performance: A review with discussion," *J. Cereal Sci.*, vol. 48, pp. 1–9, 2008, <https://doi.org/10.1016/j.jcs.2007.08.010>
9. Rouillé J., Della Valle G., Lefebvre J., Sliwinski E., and VanVliet T., "Shear and extensional properties of bread doughs affected by their minor components," *J. Cereal Sci.*, vol. 42, no. 1, pp. 45–57, 2005, <https://doi.org/10.1016/j.jcs.2004.12.008>
10. Alpers T., Tauscher V., Steglich T., Becker T., and Jekle M., "The self-enforcing starch–gluten system—strain-dependent effects of yeast metabolites on the polymeric matrix," *Polymers (Basel.)*, vol. 23, no. 1, pp. 1–15, 2021, <https://doi.org/10.3390/polym13010030> PMID: 33374760
11. Ng T. S. K., McKinley G. H., and Padmanabhan M., "Linear to non-linear rheology of wheat flour dough," *Appl. Rheol.*, vol. 16, no. 5, pp. 265–274, 2006, <https://doi.org/10.1515/arh-2006-0019>
12. Hyun K. et al., "A review of nonlinear oscillatory shear tests: Analysis and application of large amplitude oscillatory shear (LAOS)," *Prog. Polym. Sci.*, vol. 36, no. 12, pp. 1697–1753, 2011, <https://doi.org/10.1016/j.progpolymsci.2011.02.002>
13. van Vliet T., Janssen A. M., Bloksma A. H., and Walstra P., "Strain Hardening of Dough As a Requirement for Gas Retention," *J. Texture Stud.*, vol. 23, no. 4, pp. 439–460, 1992, <https://doi.org/10.1111/j.1745-4603.1992.tb00033.x>
14. Chatrael S., Macosko C. W., and Winter H. H., "Lubricated squeezing flow: A new biaxial extensional rheometer," *J. Rheol. (N. Y. N. Y.)*, vol. 25, no. 4, pp. 433–443, 1981, <https://doi.org/10.1122/1.549648>
15. Wikström K. and Bohlin L., "Extensional Flow Studies of Wheat Flour Dough. I. Experimental Method for Measurements in Contraction Flow Geometry and Application to Flours Varying in Breadmaking

Performance," *J. Cereal Sci.*, vol. 29, no. 3, pp. 217–226, May 1999, <https://doi.org/10.1006/jcrs.1999.0251>

16. Stading M., "Determination of extensional rheological properties by hyperbolic contraction flow," *AIP Conf. Proc.*, vol. 1027, pp. 1114–1116, 2008, <https://doi.org/10.1063/1.2964484>
17. Vanin F. M., Lucas T., Trystram G., and Michon C., "Biaxial extensional viscosity in wheat flour dough during baking," *J. Food Eng.*, vol. 236, pp. 29–35, 2018, <https://doi.org/10.1016/j.foodeng.2018.05.007>
18. Meerts M., Vaes D., Botteldoorn S., Courtin C. M., Cardinaels R., and Moldenaers P., "The time-dependent rheology of fermenting wheat flour dough: Effects of salt and sugar," *Rheol. Acta*, vol. 57, pp. 813–827, 2018, <https://doi.org/10.1007/s00397-018-1113-9>
19. Rouillé J., Della Valle G., Lefebvre J., Sliwinski E., and van Vliet T., "The role of minor components in shear and extensional viscosities of wheat flour dough," *Conf. Pap.*, no. November 2014, 2002.
20. Meerts M., Ramirez Cervera A., Struyf N., Cardinaels R., Courtin C. M., and Moldenaers P., "The effects of yeast metabolites on the rheological behaviour of the dough matrix in fermented wheat flour dough," *J. Cereal Sci.*, vol. 82, no. February, pp. 183–189, 2018, <https://doi.org/10.1016/j.jcs.2018.06.006>
21. Alpers T., Olma J., Becker T., and Jekle M., "Relation between polymer transitions and the extensional viscosity of dough systems during thermal stabilization assessed by lubricated squeezing flow," *Unpubl. manuscript/Manuscript Submitte*, Publ., vol. Chair of B, no. TUM School of Life Science, p. Technical University of Munich, 2021.
22. Holly E. E., Venkataraman S. K., Champon F., and Henning Winter H., "Fourier transform mechanical spectroscopy of viscoelastic materials with transient structure," *J. NonNewton. Fluid Mech.*, vol. 27, no. 1, pp. 17–26, 1988, [https://doi.org/10.1016/0377-0257\(88\)80002-8](https://doi.org/10.1016/0377-0257(88)80002-8)
23. Vidal L. M., Braun A., Jekle M., and Becker T., "Micro-Scale Shear Kneading—Gluten Network Development under Multiple Stress–Relaxation Steps and Evaluation via Multrowave Rheology," *Polymers (Basel)*, vol. 14, no. 4, 2022, <https://doi.org/10.3390/polym14040846> PMID: 35215759
24. Gabriele D., de Cindio B., and D'Antona P., "A weak gel model for foods," *Rheol. Acta*, vol. 40, no. 2, pp. 120–127, Mar. 2001, <https://doi.org/10.1007/s003970000139>
25. Lee S., Pyrak-Nolte L. J., and Campanella O., "Determination of ultrasonic-based rheological properties of dough during fermentation," *J. Texture Stud.*, vol. 35, no. 1, pp. 33–52, May 2004, <https://doi.org/10.1111/j.1745-4603.2004.tb00821.x>
26. Lee S. and Campanella O., "Impulse viscoelastic characterization of wheat flour dough during fermentation," *J. Food Eng.*, vol. 118, no. 3, pp. 266–270, 2013, <https://doi.org/10.1016/j.foodeng.2013.04.024>
27. Verheyen C., Jekle M., and Becker T., "Effects of *Saccharomyces cerevisiae* on the structural kinetics of wheat dough during fermentation," *LWT—Food Sci. Technol.*, vol. 58, no. 1, pp. 194–202, 2014, <https://doi.org/10.1016/j.lwt.2014.02.050>
28. Saint-Michel F., Chazeau L., Cavallé J., and Chabert E., "Mechanical properties of high density polyurethane foams: I. Effect of the density," *Compos. Sci. Technol.*, vol. 66, no. 15, pp. 2700–2708, Dec. 2006, <https://doi.org/10.1016/j.compscitech.2006.03.009>
29. Campbell G. M. and Mougeot E., "Creation and characterisation of aerated food products," *Trends Food Sci. Technol.*, vol. 10, no. 9, pp. 283–296, 1999, [https://doi.org/10.1016/S0924-2244\(00\)00008-X](https://doi.org/10.1016/S0924-2244(00)00008-X)
30. Verbauwedge A. E. et al., "Microscopic investigation of the formation of a thermoset wheat gluten network in a model system relevant for bread making," *Int. J. Food Sci. Technol.*, vol. 55, no. 2, pp. 891–898, 2020, <https://doi.org/10.1111/ijfs.14359>
31. Lucas I., Petermeier H., Becker T., and Jekle M., "Definition of network types—Prediction of dough mechanical behaviour under shear by gluten microstructure," *Sci. Rep.*, no. March, pp. 1–13, 2019, <https://doi.org/10.1038/s41598-019-41072-w> PMID: 30886245
32. Turbin-Orger A., Shehzad A., Chaunier L., Chiron H., and Della Valle G., "Elongational properties and proofing behaviour of wheat flour dough," *J. Food Eng.*, vol. 168, pp. 129–136, 2016, <https://doi.org/10.1016/j.foodeng.2015.07.029>
33. Schirmer M., Jekle M., and Becker T., "Starch gelatinization and its complexity for analysis," *Starch/Stärke*, vol. 67, no. 1–2, pp. 30–41, 2015, <https://doi.org/10.1002/star.201400071>
34. Chevallier S., Zúñiga R., and Le-Bail A., "Assessment of Bread Dough Expansion during Fermentation," *Food Bioprocess Technol.*, vol. 5, no. 2, pp. 609–617, 2012, <https://doi.org/10.1007/s11947-009-0319-3>
35. Graumlich T. R. and Stevenson K. E., "Respiration and viability of thermally injured *Saccharomyces cerevisiae*," *Appl. Environ. Microbiol.*, vol. 38, no. 3, pp. 461–465, 1979, <https://doi.org/10.1128/aem.38.3.461-465.1979> PMID: 394681

36. López-Malo A., Guerrero S., and Alzamora S. M., "Saccharomyces cerevisiae thermal inactivation kinetics combined with ultrasound," *J. Food Prot.*, vol. 62, no. 10, pp. 1215–1217, 1999, <https://doi.org/10.4315/0362-028x-62.10.1215> PMID: 10528730
37. Reveron I. M., Barreiro J. A., and Sandoval A. J., "Thermal Resistance of *Saccharomyces cerevisiae* in Pilsen Beer," *J. Inst. Brew.*, vol. 109, no. 2, pp. 120–123, 2003, <https://doi.org/10.1002/j.2050-0416.2003.tb00140.x>

3.5 New insights into crumb formation in model systems: Effects of yeast metabolites and hydration level by means of multiwave rheology



New insights into crumb formation in model systems: Effects of yeast metabolites and hydration level by means of multiwave rheology



Thekla Alpers ^a, Daniela Panoch ^a, Mario Jekle ^{b,*}, Thomas Becker ^a

^a Research Group Cereal Technology and Process Engineering, Chair of Brewing and Beverage Technology, TUM School of Life Sciences, Technical University of Munich, Freising, Germany

^b Department of Plant-Based Foods, Institute of Food Science and Biotechnology, University of Hohenheim, Stuttgart, Germany

ARTICLE INFO

Keywords:
Yeast fermentation
Polymer transitions
Low-field NMR
Small amplitude oscillatory shear rheology (SAOS)
Multiwave rheology

ABSTRACT

The solidification of wheat dough is induced by a complex sequence of polymer transition processes. The extend of the polymer transitions is thereby strongly dependent on the hydration level of each constituent. Further, yeast metabolites, resulting from the fermentation of dough, are hypothesized to impact the functionality of dough's polymers in their thermal transitional behavior. Hence, the aim of this work was to elucidate the occurrence of polymer transitions in dependency of (i) the amount of water available for hydration and (ii) the presence of yeast metabolites. An approach of reduced complexity was chosen to reveal the interactions during the hydro-thermal treatment by multiwave SAOS rheology together with basic physicochemical characterization methods (DSC, ¹H NMR). By excluding single dough polymers from the solidification cascade, their functionality in the polymeric system was elucidated. In combination with a non-invasive yeast inactivation method, sophisticated information on the dependence of the matrix solidification on the matrix hydration level and presence of yeast metabolites were established. Water shortage was shown to limit the extend of starch gelatinization, resulting in a reduced overall matrix solidification, whereas the extend of gluten polymerization was not affected by water shortage. In contrast, a water surplus favored the progression of starch gelatinization, which was also shown to be induced indirectly by yeast metabolites. Therefore, the water availability and accessibility of starch were shown to be decisive for the solidification of the dough matrix. The knowledge obtained contributes to the elucidation of the impact of baker's yeast on the dough matrix.

1. Introduction

The complexity of the dough matrix becomes evident especially during the thermal processing during baking. During the dough-crumb transition, the functionality of the dough matrix changes drastically due to the ongoing phase transitions and structural changes of the polymeric cereal matrix. Being a complex polymeric system, the impact of single polymers gives rise to manifold changes in interactions of these polymers and phases on different structural levels. These interactions shape the complex rheological changes of dough during the baking process. Many researchers have addressed this topic in order to trace the importance of each individual polymer to the diverse shifts in functionality (Addo, Xiong, & Blanchard, 2001; Dreese, Faubion, & Hoseney, 1988; Jekle, Mühlberger, & Becker, 2016; Rouillé, Della Valle, Lefebvre, Sliwinski, & VanVliet, 2005). But major problems had to be faced due to the complexity of the matrix. Here, the ratio of the flour constituents as

well as the hydration level have been shown to be decisive factors for the course of the solidification process (Dreese et al., 1988; Fukuoka, Ohira, & Watanabe, 2002; Jekle et al., 2016; Masi, Cavella, & Sepe, 1998; Weegels, de Groot, Verhoek, & Hamer, 1994).

As water is a limited factor in the dough system, especially the hydration level of flour has been shown to majorly impact the dough-to-crumb transformation. The water distribution in the dough matrix is based on the water retention capacity (WRC) of each cereal polymer and the water binding kinetics. Here, gluten has been shown to be the main water absorber in the unheated dough matrix. It can absorb a multifold amount of water of its own weight (average WRC of vital gluten from multiple suppliers = 131%) (Schiedt, Baumann, Conde-Petit, & Vilgis, 2013). Upon hydration, gluten particles have been shown to swell and further to form a continuous phase (Roman-Gutierrez, Guilbert, & Cug, 2002). In contrast to that, the hydration of pure wheat starch does not result in extensive water absorption by the starch granules (WRC \approx 65%

* Corresponding author.

E-mail address: mario.jekle@uni-hohenheim.de (M. Jekle).

<https://doi.org/10.1016/j.foodhyd.2024.110184>

Received 20 February 2024; Received in revised form 28 April 2024; Accepted 12 May 2024

Available online 16 May 2024

0268-005X/© 2024 The Authors. Published by Elsevier Ltd. This is an open access article under the CC BY license (<http://creativecommons.org/licenses/by/4.0/>).

([Jakobi, Jekle, & Becker, 2018](#)). In starch-based systems, water has been shown to be stabilized by capillary forces ([Schiedt et al., 2013](#)) and has been shown to be mainly extragranular beyond a basic minimum hydration level ([Assifaoui, Champion, Chiotelli, & Verel, 2006](#)). Upon heating, the water distribution between the dough constituents shifts towards an hydration equilibrium in favor of starch ([Eliasson, 1983](#)), provoking the cascade of solidification processes during the dough-crumb transition. Several researchers have shown that, depending on the availability of water and starch/gluten ratio, the solidification process can vary intensely. [Jekle et al. \(2016\)](#) used artificial systems with different starch/gluten ratios and concluded that the hydration level itself and the accessibility of starch are decisive factors for the solidification process ([Jekle et al., 2016](#)). [Champenois, Rao, and Walker \(1998\)](#) followed the same approach but with water in excess, which limits the transferability of the results to dough systems with limited water availability for the polymeric system ([Champenois et al., 1998](#)).

The extend of the hydration of the dough's polymers has been shown to be of particular interest when it comes to yeast fermentation. In general, a destabilizing effect of yeast on the dough matrix has been reported by several authors in the dough phase itself ([Alpers, Tauscher, Steglich, Becker, & Jekle, 2021](#); [Meerts, Vaes, et al., 2018](#); [Newberry, Phan-Thien, Larroque, Tanner, & Larsen, 2002](#); [Rezaei, Jayaram, Verstrepen, & Courtin, 2016](#); [Verheyen, Jekle, & Becker, 2014](#)), as well as during the thermal treatment upon baking ([Salvador, Sanz, & Fiszman, 2006](#)). Earlier research of the authors indicated that yeast fermentation has an impact on the hydration equilibrium of the cereal matrix, which might impact the solidification process provoked during baking. Based on the fact that (i) secondary yeast metabolites such as ethanol or succinic acid in yeast-like amounts do not directly influence the functionality of the dough matrix itself after short fermentation times ([Alpers et al., 2021](#)) and (ii) a changed proton distribution and a slightly accelerated starch gelatinization process in yeasted doughs upon the thermal processing, an indirect effect of yeast fermentation on the polymer transitions during baking has been hypothesized ([Alpers, Olma, Jekle, & Becker, 2022](#)). Specifically, the hydration level of starch was hypothesized to be slightly increased due to the expansion of gas cells. This is believed to be caused by the increased mobility of gluten fragments due to the degrading effect of yeast fermentation on the protein microstructure of yeasted doughs caused by the leavening of the dough on the one hand. Furthermore, a clustering of starch granules in the nodes at the end of the protein lamellas around the expanded gas cells has been hypothesized to cause a higher accessibility of starch granules for water ([Alpers et al., 2022](#)). As these findings have been made in the complex polymeric dough matrix, there is a demand for clarification on the effect of yeast fermentation on each individual compound.

Therefore, the aim of the paper is to elucidate the impact of the hydration level of dough systems on the contribution of single polymer transitions to the dough-crumb transition. Further, the impact of yeast metabolites on these transition processes is meant to be also elucidated. The gained insights should explain the contribution of yeast metabolites on the crumb formation processes by direct and indirect effects. Based on the previous findings, it is hypothesized that secondary yeast metabolites do not impact directly the occurrence of polymer transitions in dough, nor impact their functional relevance ([Alpers et al., 2021](#)). In contrast, the effects of a changing hydration level and distribution of water within the dough polymers is hypothesized to affect the extent and sequence of polymer transitions in dough contributing to the solidification process during the crumb formation process. This is of particular interest for the clarification of the impact of the water availability on the dough solidification process itself and in presence of yeast, where direct and indirect effects of the yeast fermentation could impact the dough-to-crumb transformation process as well. In order to reduce the complexity, different model systems were used in this study. Following the idea of a re-engineered dough matrix, single polymers were aimed to be excluded from the solidification process. Using this approach, it is possible to trace back the impact of single polymers on the structural and

functional changes of cereal biopolymers. Additionally, combining the simplified systems with baker's yeast contributes to the elucidation of the impact of yeast metabolites on the rheological changes of the dough matrix during the baking process. Using this approach, comprehensive knowledge on the impact of yeast fermentation on the formation of an altered crumb structure is gained. As the presence of yeast during baking intensifies the difficulties in terms of an increase of complexity by the time- and temperature-dependent release of metabolites into the dough matrix and by causing major difficulties in terms of measurement, an approach suggested by [Newberry et al. \(2002\)](#) was followed, where yeast was thermally inactivated by a freeze-thawing schedule ([Newberry et al., 2002](#)). Using this approach, the impact of the yeast cells itself and their metabolites can be captured in terms of their impact on dough's functionality, but the continued production of metabolites during the measurement is inhibited. Therefore, the inactivation leads to a steadier measurement, as the measurement procedure is not subjected to further time-dependent release of metabolites.

2. Material and methods

2.1. Preparation of the (semi-inert) dough matrix

The flour used in this study was standard German wheat flour type 550 (Rosenmühle, Ergolding, Germany). An initial characterization resulted in a moisture content of $11.33\% \pm 0.07\%$ (AACCi 44-01, $\bar{x} \pm \text{STD}$, $n = 3$), a starch content of $77.4\% \pm 1.0\%$ on dry base matter (AACCi 76-13.01, $\bar{x} \pm \text{range}$, $n = 2$), a protein content of $12.46\% \pm 0.07\%$ on dry base matter (AACCi 46-30 using an automated Dumas system ($N \times 5.7$, VarioMax Cube N, Elementar Analysensysteme GmbH, Hanau, Germany), $\bar{x} \pm \text{STD}$, $n = 3$), a fat content of $1.29\% \pm 0.02\%$ on dry base matter (AACCi 30-25, $\bar{x} \pm \text{STD}$, $n = 3$) and a mineral content of $0.59\% \pm 0.04\%$ on dry base matter (AACCi 08-12, $\bar{x} \pm \text{STD}$, $n = 3$). The optimal dough development parameters for a dough containing 1.5% white sugar (referred to the total flour amount corrected to 14% moisture content, EC category II quality, Bäko, Nürnberg, Germany) were analyzed by a Z-kneader (50 g bowl, DoughLAB, Perten Instruments AB, Hägersten, Sweden) according to ICC 115/1 and resulted in an optimal kneading time of 5.22 min and a hydration level of 61.8 %, based on 14% flour moisture. The flour systems were prepared based on these kneading parameters.

The artificial wheat starch-vital gluten system was composed of 80% commercial wheat starch (Food star, Kröner Stärke GmbH, Ibbenbüren, Germany) and 20% native vital gluten, based on the starch content determined for the flour used in this study. Native vital gluten was retrieved from the flour used in this study by a washing process suggested by [Wehrli et al. \(2023\)](#). 1 kg of flour was hydrated and kneaded to a dough and subsequently soaked in distilled water for 30 min. The softened dough was then washed out under a distilled water flow for 16 min following a fixed sequence of kneading speed and time. The separation of starch was reached by using an 80 µm polyester sieve cloth (PES-80/120, Schwegmann Filtrationstechnik GmbH, Grafschaft-Ringen, Germany). Additionally, water insoluble fibers were removed at two points in intermediate cleaning steps. The washed-out gluten was then frozen at -20°C in preparation for subsequent freeze drying. The freeze-dried vital gluten was then milled using a ball mill under the flow of liquid nitrogen (Cyromill, Retsch GmbH, Haan, Germany) to avoid any thermal induced effects on the protein. The purified vital gluten had a moisture content of $4.77\% \pm 0.07\%$ (AACCi 44-01, $\bar{x} \pm \text{STD}$, $n = 3$) and a protein content of $84.73\% \pm 0.31\%$ ($N \times 5.7$, AACCi 46-30 using an automated Dumas system, $\bar{x} \pm \text{STD}$, $n = 3$). The native character was validated by accessing the denaturation behavior by Differential Scanning Calorimetry (see [Fig. A1](#)).

To reconstitute an (semi)-inert system which would not be subjected to starch gelatinization ([Brandner, Becker, & Jekle, 2018](#)), the starch content of the artificial system was replaced by glass beads of comparable particle size distribution. Glass beads (Micropel, Sovitec, kindly

provided by Bassermann minerals GmbH & Co. KG) of two different sizes were mixer in an 80:20 ratio (20 μm and 5 μm , respectively). A comparable particle size distribution of wheat starch and the artificial glass beads system was validated by particle size measurement (Mastersizer 3000, Hydro EV, Malvern Instruments Ltd, Worcestershire, UK), resulting in the particle size distribution data shown in Table 1.

The reengineered systems were prepared under the same conditions as the wheat flour-based dough using a z-kneader and a kneading time of 5.22 min. Due to the marked differences in the water absorption between the wheat flour-based and semi-artificial system, the water addition needed to be standardized based on functionality rather than on total water level. Thus, to enhance comparability between the different systems, the hydration level of the systems was defined based on a comparable rheological behavior. This was achieved by adjusting the hydration level of the systems to the same $|G^*|_{20^\circ\text{C}}$ at 1 Hz and 0.2% deformation to 10000 Pa, being roughly the $|G^*|_{20^\circ\text{C}}$ of standard wheat flour dough. The resulting hydration levels were 72.0% for the wheat starch – vital gluten system and 38.9% for the glass beads – vital gluten system, based on 14% moisture of the dry matter. A second standardization was performed with the wheat flour system to reach a comparable maximum $|G^*|$ in course of the heating procedure described in 2.3. The resulting hydration level for the wheat flour doughs standardized for $|G^*|_{\text{max}}$ was 47.0%, based on 14% flour moisture. When native vital gluten was used for the dough preparation, the powder was hydrated with 2/3 of the total water added to the system prior to the kneading step. To reduce the initial degree of polymerization of gluten in selected systems, commercial reduced glutathione (GSH, VWR International GmbH, Darmstadt, Germany) was added during the dough preparation step at a level of 43 ppm (referred to total solids amount, corrected to 14% moisture content). Yeasted systems were prepared with fresh compressed yeast (*S. cerevisiae*, F.X. Wiesinger GmbH, Passau, Germany) using 1 g yeast/100 g flour. To enable fermentation even in absence of starch and allow comparability between different systems, all systems contained a white sugar level of 1.5% (referred to the total solids amount corrected to 14% moisture content). The yeasted samples were subsequently fermented for 60 min at 30 $^\circ\text{C}$ before the inactivation process was performed.

2.2. Dough inactivation

The yeast inactivation was performed according to a modified procedure suggested by Newberry et al. (2002). As suggested by the authors, 4 g samples of the prepared dough systems were shock-frozen by immersion in liquid nitrogen. After a transfer into a sealed container, the samples were subjected to a two-staged thawing process, first at -18 $^\circ\text{C}$ for at least 22 h and subsequently at 20 $^\circ\text{C}$ for 2 h right before the measurements. The successful inactivation was proven in preliminary tests by measuring the yeast gassing power. To access this, the inactivated dough samples were equilibrated for 1 h at 30 $^\circ\text{C}$ in a plate-plate geometry in a rotational rheometer (AR-G2, TA Instruments, New Castle, WA, USA) while the automated gap adjustment was activated to reach a constant normal force of 0.01 N. As no increasing gap and, thus, no sample expansion was observed for the inactivated yeasted dough but for non-inactivated yeasted dough, the inactivation method was regarded as successful. The success of the inactivation method has been

attributed to the combined effects of a fast freezing process and a slow thawing process. Due to the fast freezing, the cells are not able to adjust their internal water amount and are subjected to intracellular freezing. As the slow thawing process favors the occurrence of recrystallization, the intracellular ice is further subjected to growth of ice crystals by recrystallization. The tendency to form spherical, thermodynamic more stable ice crystals, is thought to cause cell injury, therefore beneficiating the lethality of freeze-thawing with fast cooling and slow warming rates (Mazur & Schmidt, 1968). Even though the inactivation method was shown to impact the dough only minimally, all dough systems were treated with the freeze-thawing procedure to enhance comparability between yeasted and non-yeasted dough systems.

2.3. Shear rheological measurements

A Modular Compact Rheometer (MCR 502, Anton Paar GmbH, Graz, Austria) was used to perform the oscillatory shear rheological measurements. The measurement was performed on thaw dough samples, which were clamped between parallel cross-hatched plates (25 mm diameter). During the measurement, temperature and humidity control was achieved by a CTD 180 HR chamber (Anton Paar GmbH, Graz, Austria) connected to a modular humidity generator (MHG 100, ProUmid GmbH & Co. KG, Ulm, Germany). After compressing the sample to the desired sample height of 2 mm, excess dough was removed using a scalpel and the cutting surface was covered with paraffin oil (viscous, Merck KGaA, Darmstadt, Germany) to prevent dehydration. Prior to the measurement, the samples were allowed to equilibrate for 10 min at 30 $^\circ\text{C}$. Subsequently, a temperature sweep from 30 $^\circ\text{C}$ to 90 $^\circ\text{C}$ was performed at a heating rate of 4.5 $^\circ\text{C}/\text{min}$. Multiwave measurements were performed every 5 $^\circ\text{C}$ based on a frequency of 1 Hz and a deformation of 0.2% at a fixed measurement time of 25 s. Based on the fundamental frequency, additional harmonics being the 2nd, 3rd, 5th, 7th, 8th and 10th multiples of the fundamental frequency, were performed simultaneously. Due to the multiwave mode, the resulting amplitude summed up to 0.328%, which agreed with the previously accessed linear visco-elastic region for all analyzed dough systems. Within the measurement steps, heating of the dough samples was performed using the normal force controlled gap adjustment ($F_H = 0.01 \text{ N}$). By allowing an uniaxial extension of the dough samples, additional torque on the upper geometry is avoided (Cardinaels, Reddy, & Clasen, 2019; Meerts, Vaes, et al., 2018). Data evaluation was conducted by using the Fourier transformation of the superimposed resulting torque/stress functions provided by Anton Paar (RheoCompass version 1.25, Anton Paar GmbH, Graz, Austria). The obtained values for complex module data ($|G^*|$) were then fitted to the power law equation (c.f. Equation (1)).

$$G^*(f) = A_f f^{1/z} \quad \text{Equation 1}$$

where f is the frequency (Hz), A_f refers to the network strength ($\text{Pa s}^{1/z}$) and z to the network connectivity (-) (Gabriele, de Cindio, & D'Antona, 2001). All measurements were performed in triplicate and average values are presented with standard deviation.

2.4. Gelatinization behavior

Differential Scanning Calorimetry (DSC250, TA Instruments, New Castle, WA, USA) equipped with a RCS40 cooler system with nitrogen flow rate of 50 mL/min was used to study the gelatinization behavior of the different dough systems. The temperature was calibrated at 10 $^\circ\text{C}/\text{min}$ by the melting point of pre-melted indium in hermetically sealed Tzero aluminum pans and lids. For the assessment of the gelatinization enthalpy of starch, the dough samples were homogenized with water in excess (dough/water ration = 1/3) using an Ultra-Turrax (T25, IKA Labor-technik, Staufen, Germany) at 13500 rpm for 30 s. An aliquot of 10–20 mg was then loaded to the instrument at 20 $^\circ\text{C}$. For the measurement, the

Table 1
Particle size distribution of commercial wheat starch and the glass bead mixture. Particle sizes are presented as D-values for volume distribution. $D_{3,10}$, $D_{3,50}$, and $D_{3,90}$ are percentiles, which are defined as the maximum particle diameter, to which 10%, 50% or 90% of the sample volume exists, respectively. ($n = 3$, $\bar{X} \pm \text{STD}$).

| Characterized system | $D_{3,10}$ (μm) | $D_{3,50}$ (μm) | $D_{3,90}$ (μm) |
|----------------------|------------------------------|------------------------------|------------------------------|
| Wheat starch | 12.00 ± 0.53 | 21.10 ± 0.71 | 34.10 ± 1.14 |
| Glass bead system | 6.66 ± 0.76 | 22.60 ± 1.33 | 47.70 ± 2.69 |

sample and an empty reference were heated at 10 °C/min to 90 °C in an inert nitrogen atmosphere. The obtained heat flow diagrams were analyzed using the Trios software (V5.1.1, TA Instruments, New Castle, WA, USA) in terms of onset temperature, peak temperature and enthalpy change ΔH . The enthalpy was normalized to the dry mass of starch in the sample. Moisture measurements were performed by using a moisture analyzer (DAB 100-3/MLB 50-3, KERN & SOHN GmbH, Balingen, Germany). Measurements were performed in triplicate and average values are presented with standard deviation. To study the extend of starch gelatinization in baked samples, 4 g of the dough samples were reduced to a sample thickness of approximately 4 mm and hermetically sealed in PE plastic bags. The samples were heated from 20 °C to 90 °C in a water bath with a temperature ramp close to 4 °C/min. The heated samples were immediately removed after the core of the samples reached the desired temperature and were subsequently cooled to room temperature and freeze stored at -20 °C till the measurements were performed. The heat treatment was performed in triplicate. The sample preparation for the DSC measurement was performed as described above.

2.5. Quantification of freezable water

To characterize the ratio of free water in the systems, the amount of freezable water was accessed by Differential Scanning Calorimetry. The device was used as described above but the temperature calibration was performed with a heating rate of 5 °C/min to fit the heating rate applied in the measurement used. 20 mg dough sample were transferred into Tzero aluminum pans and hermetically sealed. The samples were loaded to the device at 20 °C and subsequently cooled down to -30 °C at a cooling rate of 5 °C/min. After an isothermal step at -30 °C for 1 min, the samples were heated to 25 °C at a heating rate of 5 °C/min. The peak area at 0 °C was accessed (ΔH_{DSC}) and applied in the following formula to calculate the amount of freezable water (Equation (2)) (Yang & Mather, 2014, pp. 1–4).

$$\text{Freezable water} = \frac{\Delta H_{DSC}}{\Delta H_{m,H_2O}^0 \bullet MC} \bullet 100\% \quad \text{Equation 2}$$

where ($\Delta H_{m,H_2O}^0$) is the enthalpy of fusion of pure water (333.5 J/g) and MC is the moisture content of the analyzed dough samples.

2.6. Protein extractability

The amount of SDS-extractable protein was accessed by homogenizing 2 g of dough in 40 ml SDS buffer solution (0.05M sodium phosphate buffer (VWR LLC, Solon, OH, USA) with 2.0% (w/v) sodium dodecyl sulfate (VWR bvba, Leuven, Belgium), pH 6.8). The homogenization was performed as described in section 2.4. The extraction was performed for 30 min, followed by a centrifugation step (4600×g, 10 min, 20 °C, Rotina 420 R, Hettich GmbH & Co. KG, Tuttlingen, Germany). After the first extraction step, the procedure was repeated with the pellet as described above. The supernatants of both consecutive extraction steps were combined, and the protein content was determined by Kjeldahl analysis. Extractions were performed in triplicate and protein determination was performed in technical duplicates. Results, given as percentage of SDS-extractable protein of the total protein content in the dough/crumb samples, are presented as average values with standard deviation.

2.7. Time domain NMR

Carr-Purcell-Meiboom-Gill (CPMG) measurements were performed using a low field 1H NMR (inQ 20 NMR analyzer, Bruker BioSpin GmbH, Rheinstetten, Germany). An aliquot of 1 g of dough samples was weighted in 8 mm inlays for 10 mm NMR tubes and equilibrated in the instrument till a temperature of 37 °C in the core of the sample was reached. The echo time in the CPMG sequence was 175 µs between the

90° and 180° pulses and 15000 echoes were recorded. For an optimal signal-to-noise ratio, sixteen scans were performed with a recycle delay of 1 s. The obtained data were normalized for the actual sample weight and moisture content and processed using an exponential fit (c.f. Equation (3)).

$$I(t) = A_{2,1} e^{-\frac{t}{T_{2,1}}} + A_{2,2} e^{-\frac{t}{T_{2,2}}} + A_{2,3} e^{-\frac{t}{T_{2,3}}} + I_0 \quad \text{Equation 3}$$

Measurements were performed in triplicate and average values are presented with standard deviation.

2.8. Statistical analysis

Mathematical evaluation and statistical testing were performed using OriginPro (Version 2021 (9.80), OriginLab Corporation, Northampton, MA, USA). Kruskal-Wallis test as a non-parametric test followed by Dunn's Test as a post-hoc test were used to detect significant differences between groups on a significance level of $\alpha = 0.05$.

3. Results and discussion

3.1. Impact of flour hydration and yeast metabolites on the solidification process during baking

The solidification behavior of wheat flour dough during baking was accessed by SAOS rheology. The multiwave method was used due to the advantage of gaining more sophisticated structural information in shorter measurement time. The resulting $|G^*|$ at the fundamental frequency of 1 Hz of wheat flour dough at different hydration levels during the baking process is shown in Fig. 1 a. All different hydration levels present the characteristic solidification course of heat-treated starch containing systems. The course of $|G^*|$ is strongly influenced by starch functionality, indicated by a strong increase of $|G^*|$ at around 60 °C, followed by a decrease upon exceeding temperatures of 80 °C. Before entering the starch gelatinization process, $|G^*|$ follows an Arrhenius-like relation, as with increasing temperature, the interactions within the network structure are weakened, leading to a decrease of $|G^*|$ (Doğan, 2002; Migliori, Gabriele, Baldino, Lupi, & De Cindio, 2011; Rubio-Merino & Rubio-Hernández, 2019; Salvador et al., 2006). In this initial heating step, a strong dependency on the hydration level of the flour can be observed. The highest hydration level (72.0%) resulted in the lowest initial $|G^*|$ values. This can be explained by the enhanced plasticization of the system, leading to an increased mobility of the polymers (Masi et al., 1998; Upadhyay, Ghosal, & Mehra, 2012). Furthermore, a higher water content is known to retard the network formation upon kneading, which would lead to an additional decrease of $|G^*|$ as the kneading time was kept constant for all systems. This assumption is further supported by the fact, that the dough with the highest hydration level resulted in the lowest initial z-value (see Fig. 1 b), which can be interpreted as a lower number of interactions within the dough network compared to the medium and low hydration level. Upon heating, an increasing hydration level, from water shortage to optimum hydration, was found to significantly decrease the inflection point of the course of $|G^*|$. The inflection points were determined by calculating the zero points of the second derivative of a third-degree polynomial fit of the region of interest of $|G^*|$ and are subsequently referred to as solidification temperatures. Depending on the hydration level, the solidification temperatures were found to be 65.7 ± 0.6 °C, 62.9 ± 0.2 °C and 60.8 ± 0.6 °C for a hydration level of 47.0%, 61.8% and 72.0%, respectively. Furthermore, a higher hydration level was found to provoke a stronger increase of $|G^*|$ and an earlier reaching of $|G^*|_{\max}$. In contrast, the absolute values of $|G^*|_{\max}$ were on a comparable level. It was therefore concluded that a higher hydration level facilitates a higher extend of starch gelatinization. Further, this interpretation is

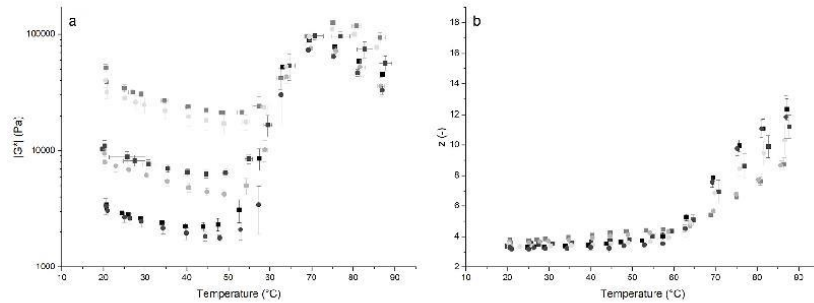


Fig. 1. Effect of the hydration level and yeast on the dough structure accessed by shear rheological measurements during the baking process of inactivated dough. a) Course of $|G^*|$ at 1 Hz during the baking process. b) Network connectivity z describing quantity of interactions derived from the power law fit of a frequency sweep performed in multiwave mode during the baking process (Gabriele et al., 2001). Standard wheat dough with a hydration level of (■) 47.0%, (■) 61.8% and (■) 72.0% and yeast-treated wheat doughs with a hydration level of (○) 47.0% (●) 61.8% and (●) 72.0%. ($n \geq 3$, $\bar{X} \pm \text{STD}$).

supported by the fact, that the final drop of $|G^*|$ was observed to increase with a higher hydration level of wheat flour. As the extend of the starch gelatinization process is linked to an increase with an increasing amount of available water (Fukuoka et al., 2002; Schirmer, Jekle, & Becker, 2011), the dissociation of starch granules and leaching might also occur to a higher extend and provoke a higher degree of polymer mobility. Furthermore, a higher flour hydration level was shown to intensify the increasing connectivity during the baking process as the z -value of the dough with the highest hydration level increased from the lowest initial value to the highest network connectivity at the end of the baking process. It is therefore assumed that a higher hydration level is benefiting interactions within the dough polymers during the heating process. The contribution of this process to the solidification of the dough matrix is meant to be further accessed in section 3.2.

Besides the impact of the hydration level, the main scope of this study was to elucidate the effect of yeast metabolites on the heat induced solidification process. To be able to neglect the impact of the time- and temperature dependent production of yeast metabolites during the measurement, the yeast cells were inactivated after a fermentation period of 1 h prior to the baking process. The level of yeast metabolites formed was therefore limited to the amount of metabolites released during the fermentation period. Regarding the formed gaseous CO_2 , it must be considered that the samples were compressed during the measurement preparation, so that the incorporated gas content did not influence the measurement results extensively, even though no active degassing was conducted. Overall, the presence of yeast metabolites was shown to decrease the initial $|G^*|$ values of each dough system, whereas the general course of $|G^*|$ was not shown to be affected. The decreased strength of the system might be related to the weakening impact of yeast metabolites on the protein microstructure as the density of the doughs decreased with fermentation, which was previously observed for yeast fermented wheat flour dough (Alpers et al., 2021). The extend of the destabilizing effect of yeast was the strongest at an optimal hydration level and in presence of a water surplus, whereas only a minor destabilizing impact of yeast metabolites was quantified for the system with water shortage. In this case, the firmer network structure is thought to be a limiting factor for the leavening effect. The suppressed yeast fermentation led to a reduced dough expansion and therefore a limited destabilizing effect on the dough matrix. This observation is encouraged by the findings regarding the connectivity value z . Here, the highest impact of yeast metabolites was also found on the optimal developed dough with a hydration level of 61.8% as the z -value was markedly decreased upon yeast addition. The observed impact of yeast metabolites is assumed to be the sum of (i) extensional stress caused by growing gas

cells during the initial fermentation period and (ii) the secondary yeast metabolites that remained in the dough matrix. The potentially marked impact of secondary yeast metabolites differs from previously published findings of the authors (Alpers et al., 2021). The authors reported previously that secondary yeast metabolites in yeast-equivalent amounts were not found to impact the dough functionality markedly, whereas the current results indicate an effect on the rheological behavior of the dough matrix. This might be related to the fact that the inactivation method increased the permeability of the yeast cell walls and might cause the leakage of yeast metabolites in a higher amount into the surrounding dough matrix. This might have increased the level of metabolites diffusing into the dough matrix and might have caused impacts on the dough structure and functionality as reported earlier by several researchers, who accessed the effect of yeast metabolites in multifold amounts (Aslankoohi, Rezaei, Vervoort, Courtin, & Verstrepen, 2015; Jayaram, Cuyvers, Verstrepen, Delcour, & Courtin, 2014; Jayaram, Rezaei, et al., 2014; Meerts, Ramirez Cervera, et al., 2018; Meerts, Vaes, et al., 2018; Rezaei et al., 2016). Furthermore, the inactivation process might have caused the release of glutathione into the dough system, which is known to cause a weakening of the dough structure (Verheyen, Albrecht, Becker, & Jekle, 2016).

As abovementioned, the secondary metabolites, that were released into the dough matrix during the fermentation period, did not appear to impact the general course of $|G^*|$. The inflection points of the $|G^*|$ courses were not shown to be affected by the presence of yeast metabolites in a significant manner. Therefore, secondary metabolites do not appear to impact the solidification-inducing polymer transition processes in the dough matrix. To validate this observation, a subdivision of the matrix into its single polymer systems was needed to overcome mixed matrix effects and strengthen the validity of the results. Therefore, re-engineered dough systems have been used to elucidate the impact of yeast metabolites on the independent polymer transition processes rather than on the complex dough matrix.

3.2. Impact of hydration of dough polymers and presence of yeast metabolites on the solidification process in (semi-)inert systems during baking

Following this idea, different model systems were used in this study. Re-engineered dough matrices were created, where single polymers were aimed to be excluded from the solidification process by inhibition or replacement to reduce complexity. The impact of single polymers on the solidification behavior during baking can therefore be accessed and their dependency on the hydration level and presence of yeast

metabolites can be traced back. The basic re-engineered matrix itself is composed of native vital gluten and wheat starch. By combining the isolated native vital gluten with commercial wheat starch, a well-defined re-engineered dough system was established. The temperature-dependent behavior of $|G^*|$ follows the course of a normal wheat flour dough as can be seen in Fig. 2 a. The dependency on the hydration level is similar to the behavior observed in wheat flour dough as an increasing water content decreases the initial $|G^*|$. Upon heating, the initial difference in $|G^*|$ aligned as both systems showed comparable inflection points (59.35 ± 0.52 °C and 59.16 ± 0.54 °C for a hydration level of 61.8% and 72.0%, respectively), reached equal $|G^*|_{max}$ values and showed the same extent of drop in $|G^*|$ upon further heating. The final drop in $|G^*|$ appeared to be more pronounced than in the wheat flour systems. As a higher water content tends to facilitate a higher extend of starch gelatinization, the overproportioned increase of $|G^*|$ could be explained by the intensified pasting behavior of starch and, after reaching the $|G^*|_{max}$ value, a higher extend of dissociation of the granular structure. This behavior is in line with the previously observed behavior of the wheat dough systems. Furthermore, the presence of yeast was shown to increase the mobility of the polymers in the system in a similar manner as in wheat dough systems. The start of the solidification process, as well as the kinetics, were not affected by the presence of yeast. But, unlike as in the wheat flour-based systems, the extent of the solidification process in terms of the relative increase of $|G^*|$ was observed to increase upon yeast addition. As previously reported, the changes in the microstructure of the fermented dough matrix were believed to facilitate the accessibility of starch granules for water

(Alpers et al., 2022). As starch granules are displaced from the thinning protein-based lamella around the expanding gas cells, clusters of starch are formed in the connecting nodes (Grenier, Rondeau-Mourot, Dede, Morel, & Lucas, 2021). These clusters were believed to facilitate the accessibility of starch for water and, therefore, favor the gelatinization process.

To further address the importance of single dough polymer transitions to the overall solidification behavior of the dough matrix in dependence of yeast and hydration level, the importance of gluten polymerization was accessed by inhibiting the crosslinking by adding glutathione to the system, acting as a -SH blocker. Glutathione is known to inhibit the formation of -S-S-bonds, as it interacts with gluten by sulphydryl/disulphide interchange reactions (Hüttner & Wieser, 2001). The presence of GSH during the dough mixing step causes a reduced polymerization degree of gluten and leads to the formation of a weaker network structure (Guo et al., 2021; Verheyen et al., 2016). To counteract the contribution of gluten to the solidification process of the dough matrix, the initial gluten polymerization was therefore inhibited to a certain extent. The overall course of the GSH-supplemented systems appears comparable to wheat starch – vital gluten systems (see Fig. 2 b). The impact of the hydration level is equal to the one described previously. Therefore, it becomes evident that GSH is only inhibiting the polymerization of gluten in the dough phase, whereas its effect diminishes when the heat-induced gluten polymerization sets in.

In a subsequent reduction step, wheat starch was replaced by inert glass beads, having a comparable particle size distribution as starch granules. Hence, the role of starch gelatinization is eliminated from the

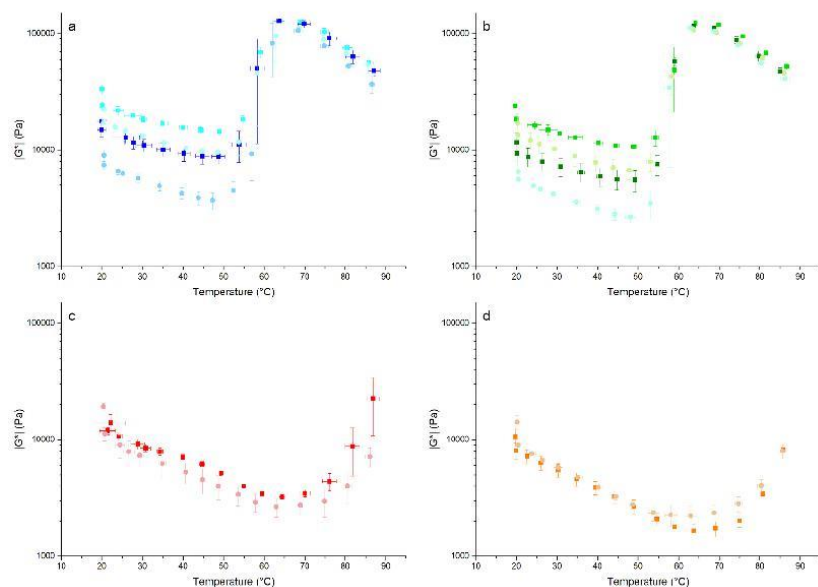


Fig. 2. Effect of the hydration level of the dough polymers and yeast metabolites on the solidification process in inactivated (semi-)inert systems assessed by shear rheological measurements during the baking process. The data is shown as course of $|G^*|$ at 1 Hz during the baking process. a) Wheat starch – vital gluten at a hydration level of (●) 61.8% and (■) 72.0% and yeast-treated wheat starch – vital gluten at a hydration level of (○) 61.8% and (○) 72.0%. b) Wheat starch – vital gluten and GSH at a hydration level of (□) 61.8% and (□) 72.0% and yeast-treated wheat starch – vital gluten and GSH at a hydration level of (○) 61.8% and (○) 72.0%. c) Glass beads – vital gluten at a hydration level of (■) 38.0% and yeast-treated glass beads – vital gluten at a hydration level of (○) 38.0%. d) Glass beads – vital gluten and GSH at a hydration level of (□) 38.0% and yeast-treated glass beads – vital gluten and GSH at a hydration level of (○) 38.0% ($n \geq 3$, $\bar{x} \pm \text{STD}$).

solidification process. By following the approach formerly described by Brandner et al. (2018), only the heat-induced gluten polymerization process will contribute to the solidification process of dough during baking. The resulting course of $|G^*|$ differs markedly from the course of starch-containing systems (see Fig. 2 c). The initial drop of $|G^*|$ with increasing temperature (Arrhenius-like relation) is followed by a steady increase until $|G^*|_{\max}$ is reached at T_{end} . As starch dissociation is responsible for the previously observed final viscosity drop, the starch-free system is not subjected to this phenomenon. $|G^*|$ of the glass beads – vital gluten system follows the Arrhenius-like relation till a temperature of 55 °C–65 °C, whereas a remarkable solidification starts around 70°. This solidification point is in line with the solidification temperature previously observed by Wehlhi et al. (2021) and can be explained by the thermally induced restructuring of the denaturing proteins (Verbauwheide et al., 2020). In presence of yeast, $|G^*|$ was shown to decline, which can be attributed to the same degrading impact of yeast metabolites on the gluten microstructure as described above (see section 3.1).

By limiting the initial extend of -S-S-bonds with the addition of GSH to the system, the heat-induced protein polymerization was shown to be only slightly affected (see Fig. 2 d). The inflection point of the GSH-treated system was found to be 67.73 ± 0.02 °C, which did not significantly differ from the pure glass beads-gluten system (69.07 ± 0.79 °C). Therefore, it can be finally concluded, that GSH is only limiting the extend of -S-S-bonds during the network formation, but does not affect the heat-induced polymerization process. The presence of yeast did cause a different impact in the GSH-containing system than in the previously described glass beads-based systems. In case of the GSH-containing system, the initial $|G^*|$ of the yeasted and non-yeasted systems were comparable, but $|G^*|$ was shown to be increased around the solidification point in the yeasted protein-based system. As the GSH-treated glass bead-vital gluten system was generally less strongly connected, the weakening impact of yeast might not have the same importance as in the strongly connected gluten systems. As GSH is interacting with gluten by sulphydryl/disulphide interchange reactions (Hüttner & Wieser, 2001), the gluten network structure is based on a higher number of hydrogen bonds and hydrophobic interactions rather than on -S-S-bonds. The weaker network might lead to a reduced gas holding capacity and consequently a less weakening impact of yeast metabolites on the network microstructure. Hence, the yeast-treated and yeast-free glass beads – vital gluten systems share a comparable absolute $|G^*|$.

3.3. Contribution of polymer transitions to the solidification process of the dough matrix during baking

To trace the importance of single polymer transitions on the overall solidification behavior of the dough matrix, a rheological approach was followed. The above-described systems were standardized to the same initial $|G^*|$ at 20 °C (at 1 Hz and the deformation described above, see section 2.3) by adjusting the hydration level to enable the comparability of the extend of the solidification behavior between the different systems (see Fig. 3 a). All five systems show the same initial drop in $|G^*|$ during baking. By comparing starch- and glass beads-based systems, the impact of starch on the solidification becomes evident in terms of the initial rise and final decrease of $|G^*|$. In general, the solidification of the wheat flour-based systems occurs at higher temperatures than in the re-engineered wheat starch – vital gluten mixtures. Apparently, other constituents in the wheat flour dough either absorb water, which is therefore not available for the starch gelatinization, or hinder the accessibility of the starch granules for water (Döring, Nuber, Stukenborg, Jekle, & Becker, 2015; Guo, Yang, & Zhu, 2018). The artificial character of the wheat starch – vital gluten system might further favor the hydration of the starch granules, as they are less embedded and therefore more accessible for water (Jekle et al., 2016). It seems that the starch gelatinization can proceed easier, which is further supported by the fact that the kinetics of the solidification process appear faster. Additionally, the observation that the decrease in $|G^*|$ after $|G^*|_{\max}$ is more pronounced in the re-engineered wheat starch – vital gluten system implies a dissociation of starch granules caused by a higher extend of starch gelatinization. The presence of GSH was not shown to affect the solidification process in the starch-based system. Besides a lower initial $|G^*|$, the solidification behavior appears similar to the uninhibited system. As aforementioned, it can be concluded that GSH only affects the initial connectivity of the gluten network but does not inhibit the heat-induced protein polymerization. In comparison to the GSH-free system, the overall increase of $|G^*|$ in this system appears higher, which might indicate a higher availability of water for starch gelatinization as the gluten polymers are less connected. Here, the looser network structure might also favor the accessibility of starch for water in general due to the higher mobility of the gluten strands. This is further supported by the connectivity measure z (see Fig. 3 b), which starts at a lower level but increases more rapidly to a higher level than in the GSH-free system towards the end of the baking process. The stronger increase in connectivity for GSH-containing wheat starch – vital gluten systems might further be favored by the difference in the general network structure. As the GSH-supplemented system relays to a greater

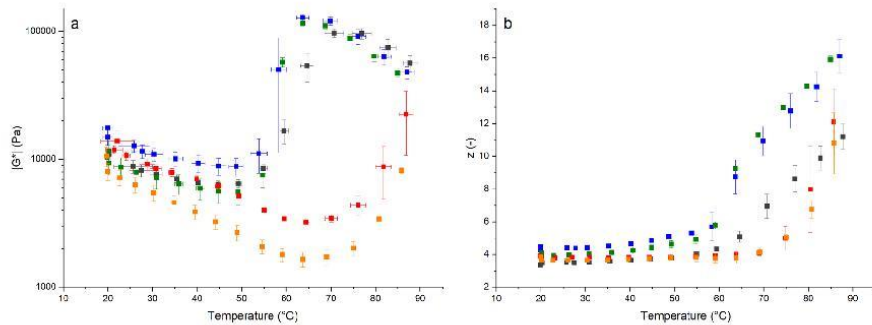


Fig. 3. Impact of polymer transitions on the solidification process of the dough matrix during the baking process. All systems are standardized to the same initial $|G^*|_{20\text{ }^{\circ}\text{C}}$ by adjusting the hydration level. a) Course of $|G^*|$ at 1 Hz during the baking process. b) Network connectivity z describing the quantity of interactions derived from the power law fit of a frequency sweep performed in multiwave mode during the baking process (Gabriele et al., 2001). (■) Wheat flour at a hydration level of 61.8%, (■) wheat starch – vital gluten at a hydration level of 72.0%, (■) wheat starch – vital gluten and GSH at a hydration level of 72.0%, (■) glass beads – vital gluten at a hydration level of 38.0% and (■) glass beads – vital gluten and GSH at a hydration level of 38.0%. ($n \geq 3$, $\bar{X} \pm \text{STD}$).

degree on the formation of hydrogen and hydrophobic interactions rather than on the formation of *S-S* bonds, the modified initial network conformation might favor the heat-induced polymerization. In general, the increase of connectivity during the baking process can be attributed to an increasing amount of the following interactions, as described by other researches earlier: starch-starch (gelatinization and increasing hydrophobic interactions due to the denaturation of starch surface proteins), gluten-gluten (thermal-induced polymerization) and starch-gluten interactions (hydrogen bondings between gluten and starch) (Dreese et al., 1988; Mann, Schiedt, Baumann, Conde-Petit, & Vilgis, 2014; Schiedt et al., 2013). The highest overall connectivity can be found in the wheat starch – vital gluten systems, which are more likely to interact. In contrast, the *z*-values of the wheat flour dough are markedly reduced and subjected to a less steep increase while heating. This might be attributed to a limited hydration level of the starch polymers, as secondary constituents of wheat flour, such as pentosanes, decrease the amount of water available for the hydration of starch and gluten and therefore their plasticization (Döring et al., 2015; Guo et al., 2018). Furthermore, some of these constituents are known to interfere with the gluten network development, and thus, lead to a reduced amount of interactions formed in the wheat flour-based systems.

As it can be observed from Fig. 3 a, the course of $|G^*|$ in glass beads – vital gluten systems differs greatly from the starch-based behavior described before. The solidification point appears to be retarded compared to the inflection point quantified for the wheat flour system. In case of the glass beads – vital gluten system, the addition of GSH leads to a reduction of $|G^*|$ during the whole baking process. As these systems are not subjected to any starch transitions, the weakening effect of GSH on the gluten network remains present during the whole baking process even though the heat-induced polymerization-based solidification remains clearly visible in both systems. From Fig. 3 b it becomes evident that the connectivity measure *z* can be seen as a measure for the contribution of gluten to the solidification process. The heat-induced gluten polymerization process can be seen to cause a steep increase of *z* in the glass beads-based systems around 70 °C. This increase is also observed in the starch-based systems, whereas the $|G^*|$ data of starch-based systems is dominated by the increasing polymer mobility (decreasing $|G^*|$), induced by the dissociation of starch granules. Therefore, the use of multiwave measurements has been shown to reveal more sophisticated structural data compared to the conventional temperature-sweep measurements as the contribution of the heat-induced gluten polymerization becomes evident through frequency dependent data evaluation. In contrast, the consideration of $|G^*|$ data only reveals the sum function of gluten and starch functionality, whereas

gluten functionality prevails the frequency-dependent viscoelastic response of the system.

To validate the hypothesis of a better hydration of starch in the re-engineered system, a second standardization of $|G^*|$ was performed for the flour system and re-engineered wheat starch – vital gluten systems. A standardized $|G^*|_{\max}$ was used to elucidate the kinetics of the different solidification processes in detail (see Fig. 4 a). It is apparent that the solidification process of the wheat flour matrix sets in at a higher temperature. Further, it appears that the solidification of the flour-based system requires more time as the increase in $|G^*|$ is less steep. This cannot be overcome by a higher initial firmness of the dough system in general and is therefore rather linked to a limited water accessibility of starch. Contrarily, in this case the limited hydration of the starch granules rather retards the gelatinization process and therefore the whole solidification process. Considering the other side, the higher water content of the wheat starch – vital gluten systems enabled a better starch hydration, resulting in a higher extend of starch gelatinization. This becomes further evident when comparing the network connectivity values *z* (see Fig. 4 b). The limited extend of starch gelatinization in wheat flour systems with water shortage results in a lower final network connectivity. This can be attributed to the competitive hydration in wheat flour systems, where secondary constituents, such as pentosanes, decrease the available amount of water for starch hydration and, therefore, the extend of starch gelatinization. There, the setup highlights the important role of secondary constituents to the solidification processes occurring during baking. The initial difference within wheat starch – vital gluten and wheat starch – vital gluten + GSH systems can be attributed to the reducing effect of GSH. As abovementioned, the softening effect of GSH diminishes as with higher temperatures gluten polymerization reactions are intensified.

3.4. Physicochemical analysis of the polymer transitions occurring during the solidification process during baking

3.4.1. Gelatinization enthalpy

The physicochemical characterization of the systems enforces the observations made by the rheological characterizations. The quantification of the amount of starch that would be able to gelatinize in case of unlimited water supply, revealed the comparability of all starch-based system (see Fig. 5). The slight increase of enthalpy per gram of starch dry matter in the wheat starch-based systems might be related to the artificial character of the systems and the preceding pre-treatments of the wheat starch used. In the heat-treated systems, the impact of water shortage is seen to strongly limit the extend of starch gelatinization. In

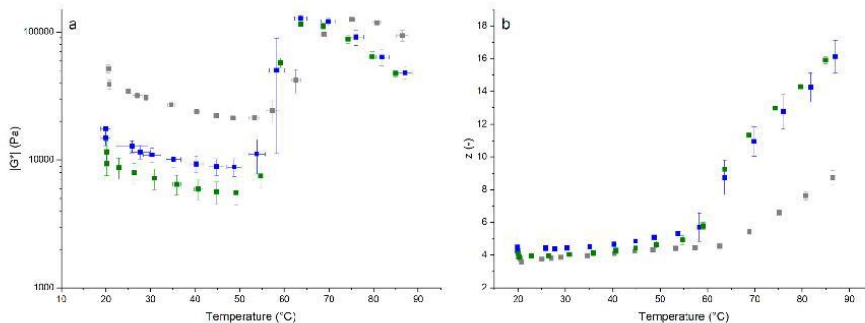


Fig. 4. Impact of polymer transitions on the solidification process of the dough matrix during the baking process. All systems are standardized to the same maximal $|G^*|_{\max}$ by adjusting the hydration level. a) Course of $|G^*|$ at 1 Hz during the baking process. b) Network connectivity *z* describing the quantity of interactions derived from the power law fit of a frequency sweep performed in multiwave mode during the baking process (Gabriele et al., 2001). (■) Wheat flour at a hydration level of 47.0%, (■) wheat starch - vital gluten at a hydration level of 72.0% and (■) wheat starch – vital gluten and GSH at a hydration level of 72.0%. ($n \geq 3$, $\bar{x} \pm \text{STD}$).

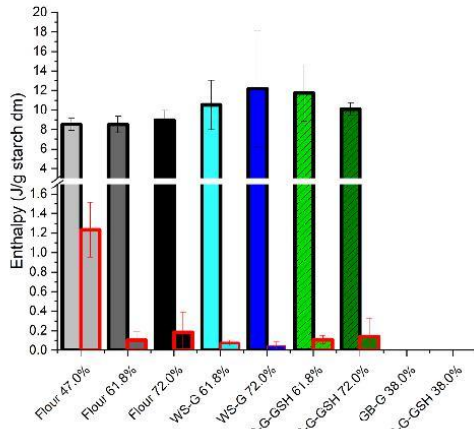


Fig. 5. Resulting (residual) enthalpy in dependency of the polymeric system and hydration level. The results are presented as enthalpy per g starch dry mass (dm). Black bordered bars represent samples measured at 20 °C, whereas red bordered bars represent samples that have been previously heat treated to 90 °C. (n = 3, $\bar{X} \pm \text{STD}$).

wheat flour-based systems, the enthalpy of the heat-treated system was reduced by $85.6 \pm 2.1\%$ compared to the non-baked wheat-flour system for a hydration level of 47.0%, whereas in presence of a higher hydration level the reduction was quantified to reach to $98.7 \pm 1.2\%$ or $98.1 \pm 2.0\%$ (61.8% and 72.0% hydration level, respectively). This can be observed for the wheat flour-based systems as well as for the re-engineered wheat starch – vital gluten systems. The presence of GSH was not shown to significantly affect the extend of the gelatinization process, indicating that the observed differences in the solidification behavior of these systems can more likewise be attributed to the differences in the connectivity of the systems in the dough phase rather than on the differences in polymer transition processes.

3.4.2. Protein extractability

In terms of protein extractability, the most significant effect was observed upon the thermal treatment of the systems, which was shown to decrease the SDS-extractability by at least half (see Fig. 6). SDS-soluble proteins involve the fraction of low molecular weight proteins, wherefore the extractability decreases upon heat treatment as the heat-induced polymerization increases the polymers' sizes. This can be regarded as a proof of concept as the heat-induced polymerization was shown to be induced in all system types. The hydration level was not shown to significantly affect the extend of extractability neither in the dough, nor in the crumb phase. Therefore, heat-induced polymerization was shown to not be suppressed by water shortage (restricted to the hydration levels used in this study). Furthermore, the extend of protein polymerization was shown to occur to the greatest extend in non-starch-based systems. This can be explained by the absence of interrupting starch polymers, which would limit the extend of interactions within neighboring gluten strands. As starch granules are subjected to intense swelling during the baking process, the spacial impact of starch is increasing upon baking. Thus, a bigger volume fraction is taken by starch and the potential for interactions within protein polymers is reduced. This results in a reduced extend of polymerization in the starch-based systems. However, the presence of GSH in starch-based and non-starch-based systems was not shown to decrease the extractability in the GSH treated systems. The applied method is therefore not sensitive to GSH-induced effects on the protein polymerization. Contrarily, Guo

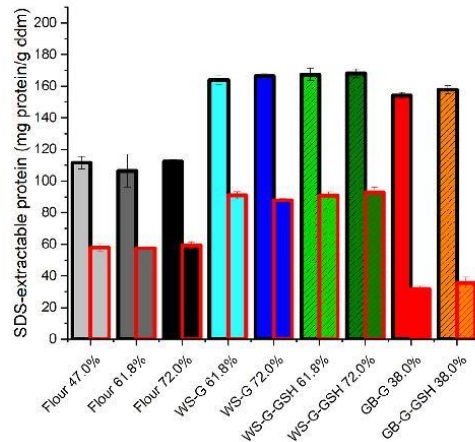


Fig. 6. Effect of thermal treatment on protein extractability of yeasted and non-yeasted dough during the baking process in different polymeric systems. Black bordered bars represent samples measured at 20 °C, whereas red bordered bars represent samples that have been previously heat treated to 90 °C. (n = 3, $\bar{X} \pm \text{STD}$).

et al. (2020) detected an increasing amount of depolymerization with an increasing amount of GSH in wheat dough. Departing from this study, the authors used a higher amount of GSH ($>0.01\%$ GSH), which could explain the contrasting results in terms of SDS-extractability (Guo et al., 2021).

3.4.3. Hydration properties

Since the solidification process is strongly interconnected to the changes in the hydration of the individual dough polymers, the hydration properties of the investigated systems were accessed for further insights. Therefore, polymeric systems with different hydration levels and polymers were analyzed in terms of their freezable water content and for the quantification of the protein populations by ^1H NMR for unheated samples (20 °C) and heat-treated samples (90 °C) (see Fig. 7 a and b). Overall, the amount of freezable water was found to increase with systems' hydration levels. Additionally, in the re-engineered systems, the presence of GSH slightly increased the amount of freezable water in the 20 °C systems, which supports the abovementioned hypothesis of a higher availability of water for the starch gelatinization in those systems. As GSH limits the polymerization of the gluten network, the hydrating water was shown to be less tightly bound and in some cases even released to the surrounding as free water (Guo et al., 2021). Upon baking, the amount of freezable water was shown to decrease in general as more water is in exchange with the polymers after the polymer transitions. The only exceptions from this observation are the optimal hydrated flour dough system (61.8% hydration level) and the glass beads - vital gluten system. Using NMR spectroscopy, these systems were further investigated. Using a CPMG pulse sequence, three proton populations were quantified. These results are in line with the observations of various other researchers (Kovrlija, Goubin, & Rondeau-Mouro, 2020; Kovrlija & Rondeau-Mouro, 2017; Lu & Seetharaman, 2013; Rondeau-Mouro et al., 2015). It appeared that the water mobility of the first and second quantified CPMG population increased with an increasing hydration level of the flour samples, whereas the relaxation time of the third population did only increase from water shortage to optimum hydration. The increasing mobility, which can be quantified in terms of an increasing relaxation time, is related to the increased plasticization of the polymers as more water is

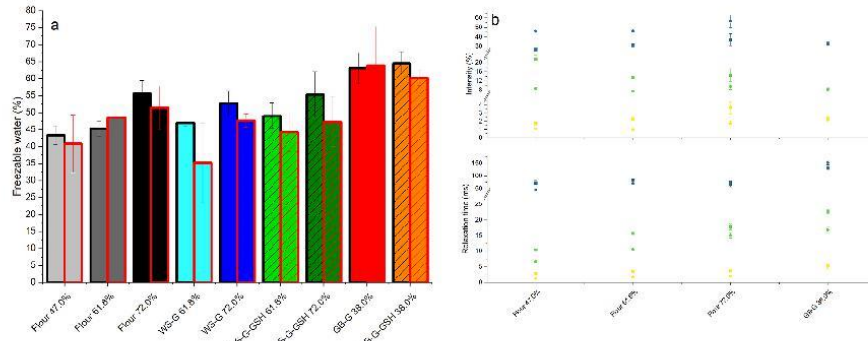


Fig. 7. Hydration properties of different polymeric system in dependence of the hydration level. a) Freezeable water content as percentage of the total water content. Black bordered bars represent samples measured at 20 °C, whereas red bordered bars represent samples that have been previously heat treated to 90 °C. b) CPMG-Populations accessed by ^1H NMR. Results presented in terms of relaxation time ($T_{2,2}$) and Intensity ($A_{2,2}$) $T_{2,1}$ and $A_{2,1}$ of (■) 20 °C and (●) 90 °C samples, $T_{2,2}$ and $A_{2,2}$ of (■) 20 °C (●) 90 °C samples and $T_{2,3}$ and $A_{2,3}$ of (■) 20 °C (●) 90 °C samples. ($n \geq 2$, $\bar{X} \pm \text{STD}$).

available in the systems. Upon baking, the relaxation time of all populations were shown to decrease in wheat flour systems of all hydration levels. This behavior can be explained by the overall solidification of the systems, which reduces the mobility of the polymers in general.

Regarding the intensities of the signal of each population, the observed behavior depicts the general changes occurring in wheat flour doughs (Kovljija & Rondeau-Mouou, 2017; Rondeau-Mouou et al., 2015). Particularly worth mentioning is the behavior observed in absence of starch. In contrast to the wheat starch-based systems, the glass beads - vital gluten system shows a rather constant hydration behavior. The intensities quantified for population 1–3 are not markedly affected by the heat treatment. A comparable observation is reported by Bosmans et al. (2012), where only minor differences were observed within unheated and heated vital gluten samples (Bosmans et al., 2012). Therefore, it can be concluded that starch is the decisive factor for changes in the hydration equilibrium as the gluten system itself remains rather constant throughout the baking process.

4. Conclusion

The level and kinetics of starch gelatinization were shown to clearly determine the solidification process of dough during the baking step. Our results are in general agreement to previous studies, where the availability of water has been clearly found to determine the extent of starch gelatinization and dissociation. Using the existing knowledge combined with the approach of inactivated yeast-fermented dough, a new framework was established to elucidate the effects of yeast metabolites on the solidification behavior of yeast-fermented dough. Our approach, based on polymeric dough matrices with reduced complexity, clearly revealed the effects of metabolites on the different polymers in the dough matrix. An effect of yeast fermentation on the extend of starch gelatinization was observed in the solidification behavior. The release of CO_2 by fermenting yeast cells causes the occurrence of extensional stress on the dough matrix. This effect provokes a higher accessibility of starch for water due to a weakened network structure or the clustering of starch granules in nodes. As already reported by other researchers and also quantified in this study, the accessibility of starch for water is decisive for the kinetics and extend of the dough matrix' solidification behavior. Therefore, it has been concluded that also yeast fermentation provokes a higher water availability for starch and impacts the solidification behavior of dough on a molecular level.

Regarding the contribution of gluten to the solidification behavior, a dependency on the initial network connectivity of the system was

shown. Differences in the initial network connectivity by either (i) the extend of connectivity, affected by the hydration level, yeast fermentation or GSH, or (ii) the type of interactions were shown to impact the course of the solidification during heating. The presented results further revealed that a frequency-dependent measure is needed for the quantification of the contribution of gluten-gluten interactions to the solidification process. The used multiwave setup enabled a distinguishing between starch- and gluten-induced changes in the rheological behavior of the dough matrix. In general, the process of the heat-induced gluten polymerization was shown to be fairly independent of the hydration level of the systems, at least for the hydration levels investigated in this study. Furthermore, the water equilibrium in the polymeric matrix has been shown to be mainly affected by starch, which is a water absorbent upon thermal treatment and no evidence has been found for an active water transfer from gluten to starch during the heat treatment. Using the described approach of reduced complexity together with the in-situ production of yeast metabolites followed by a non-invasive yeast inactivation method, new insights on the impact of yeast metabolites on the dough solidification behavior during baking were generated. Active decoupling of the polymeric dough system allowed conclusions to be reached about the impact of yeast fermentation on the individual dough constituents. The newly gained information can be used to predict baking performance of yeasted dough systems and to further control the final bread properties.

Funding

This research did not receive any specific grant from funding agencies in the public, commercial, or not-for-profit sectors.

CRediT authorship contribution statement

Thekla Alpers: Writing – original draft, Visualization, Methodology, Investigation, Formal analysis, Conceptualization. **Daniela Panoch:** Writing – review & editing, Investigation, Data curation. **Mario Jekle:** Writing – review & editing, Supervision, Conceptualization. **Thomas Becker:** Writing – review & editing.

Declaration of competing interest

The authors declare that they have no known competing financial interests or personal relationships that could have appeared to influence the work reported in this paper.

Data availability

Data will be made available on request.

Appendix A. Supplementary data

Supplementary data to this article can be found online at <https://doi.org/10.1016/j.foodhyd.2024.110184>.

References

Addo, K., Xiong, Y. L., & Blanchard, S. P. (2001). Thermal and dynamic rheological properties of wheat flour fractions. *Food Research International*, 34(4), 329–335. [https://doi.org/10.1016/S0963-9969\(00\)00171-X](https://doi.org/10.1016/S0963-9969(00)00171-X)

Alpers, T., Olma, J., Jekle, M., & Becker, T. (2022). Relation between polymer transitions and the extensional viscosity of dough systems during thermal stabilization assessed by lubricated squeezing flow. *Food Chemistry*, 389, Article 133048. <https://doi.org/10.1016/j.foodchem.2022.133048>

Alpers, T., Tauscher, V., Steglich, T., Becker, T., & Jekle, M. (2021). The self-enforcing starch-gluten system—strain-dependent effects of yeast metabolites on the polymeric matrix. *Polymers*, 23(1), 1–15. <https://doi.org/10.3390/polym13010030>

Astankooi, E., Rezaei, M. N., Vervoort, Y., Coutin, C. M., & Verstrepen, K. J. (2015). Glycerol production by fermenting yeast cells is essential for optimal bread dough fermentation. *PLoS One*, 10(3), 1–13. <https://doi.org/10.1371/journal.pone.019364>

Assifaoui, A., Champion, D., Chiotelli, E., & Verel, A. (2006). Rheological behaviour of biscuit dough in relation to water mobility. *International Journal of Food Science and Technology*, 41(SUPPL. 2), 124–128. <https://doi.org/10.1111/j.1365-2621.2006.01469.x>

Bosmans, G. M., Lagrain, B., Deleu, L. J., Fiersens, E., Hills, B. P., & Delcour, J. A. (2012). Assignments of proton populations in dough and bread using NMR relaxometry of starch, gluten, and flour model systems. *Journal of Agricultural and Food Chemistry*, 60(21), 5461–5470. <https://doi.org/10.1021/f30085508>

Brandner, S., Becker, T., & Jekle, M. (2018). Wheat dough imitating artificial dough system based on hydrocolloids and glass beads. *Journal of Food Engineering*, 223, 144–151. <https://doi.org/10.1016/j.jfooodeng.2017.12.014>

Cardinaels, R., Reddy, N. K., & Clasen, C. (2019). Quantifying the errors due to overfilling for Newtonian fluids in rotational rheometry. *Rheologica Acta*, 58(8), 525–538. <https://doi.org/10.1007/s00397-019-01153-z>

Champonois, Y., Rao, M. A., & Walker, L. P. (1998). Influence of α -amylase on the viscoelastic properties of starch-gluten pastes and gels. *Journal of the Science of Food and Agriculture*, 78(1), 127–133. [https://doi.org/10.1002/\(sici\)1097-0010\(199809\)78:1<127::aid-jsof99>3.0.co;2-k](https://doi.org/10.1002/(sici)1097-0010(199809)78:1<127::aid-jsof99>3.0.co;2-k)

Doğan, I. S. (2002). Dynamic rheological properties of dough as affected by amylases from various sources. *Nahrung-Food*, 46(6), 399–403. [https://doi.org/10.1002/1521-3803\(200211\)46:6<399::aid-food399>3.0.co;2-1](https://doi.org/10.1002/1521-3803(200211)46:6<399::aid-food399>3.0.co;2-1)

Döring, C., Huber, C., Stukenborg, F., Jekle, M., & Becker, T. (2015). Impact of arabinoxylan addition on protein microstructure formation in wheat and rye dough. *Journal of Food Engineering*, 154, 10–16. <https://doi.org/10.1016/j.jfooodeng.2014.12.019>

Dreese, P. C., Faubion, J. M., & Hosney, R. C. (1988). Dynamic rheological properties of flour, gluten, and gluten-starch doughs. I. Temperature-dependent changes during heating. *Cereal Chemistry*, 65(4), 348–353.

Eliasson, C. G. (1983). Differential scanning calorimetry studies on wheat starch—gluten mixtures: I. Effect of gluten on the gelatinization of wheat starch. *Journal of Cereal Science*, 1(3), 199–205. [https://doi.org/10.1016/S0733-5210\(83\)80021-6](https://doi.org/10.1016/S0733-5210(83)80021-6)

Fukukawa, M., Ohta, K. I., & Watanabe, H. (2002). Determination of the terminal extent of starch gelatinization in a limited water system by DSC. *Journal of Food Engineering*, 53(1), 39–42. [https://doi.org/10.1016/S0260-8774\(01\)00137-6](https://doi.org/10.1016/S0260-8774(01)00137-6)

Gabriele, D., de Cindio, B., & D'Antona, P. (2001). A weak gel model for foods. *Rheologica Acta*, 40(2), 120–127. <https://doi.org/10.1007/s003970000139>

Gremet, D., Rondeau-Mouro, C., Dedej, K. B., Morel, H. B., & Lucas, T. (2021). Gas cell opening in bread dough during baking. *Trends in Food Science and Technology*, 109 (December 2019), 482–498. <https://doi.org/10.1016/j.tifs.2021.01.032>

Guo, L., Fang, F., Zhang, Y., Xu, D., Jin, Z., & Xu, X. (2021). Glutathione affects rheology and water distribution of wheat dough by changing gluten conformation and protein depolymerisation. *International Journal of Food Science and Technology*, 56(7), 3157–3165. <https://doi.org/10.1111/jifs.14806>

Guo, X. N., Yang, S., & Zhu, K. X. (2018). Impact of arabinoxylan with different molecular weight on the thermo-mechanical, rheological, water mobility and microstructural characteristics of wheat dough. *International Journal of Food Science and Technology*, 53(9), 2150–2158. <https://doi.org/10.1111/jifs.13802>

Hüttner, S., & Wieser, H. (2001). Studies on distribution and binding of endogenous glutathione in wheat dough and gluten. I. Distribution of glutathione in Osborne fractions. *European Food Research and Technology*, 213(4–5), 329–334. <https://doi.org/10.1007/s0021000387>

Jakobi, S., Jekle, M., & Becker, T. (2018). Direct link between specific structural levels of starch and hydration properties. *Carbohydrate Polymers*, 181(June 2017), 159–166. <https://doi.org/10.1016/j.carbpol.2017.10.062>

Jayaram, V. B., Cuypers, S., Verstrepen, K. J., Delcour, J. A., & Coutin, C. M. (2014). Succinic acid in levels produced by yeast (*Saccharomyces cerevisiae*) during fermentation strongly impacts wheat bread dough properties. *Food Chemistry*, 151, 421–428. <https://doi.org/10.1016/j.foodchem.2013.11.025>

Jayaram, V. B., Rezaei, M. N., Cuypers, S., Verstrepen, K. J., Delcour, J. A., & Coutin, C. M. (2014). Ethanol at levels produced by *Saccharomyces cerevisiae* during wheat dough fermentation has a strong impact on dough properties. *Journal of Agricultural and Food Chemistry*, 62(38), 9326–9335. <https://doi.org/10.1021/jf502547a>

Jekle, M., Mühlberger, K., & Becker, T. (2016). Starch-gluten interactions during gelatinization and its functionality in dough like model systems. *Food Hydrocolloids*, 54, 190–201. <https://doi.org/10.1016/j.foodhyd.2015.10.005>

Kovrilia, R., Gonbin, E., & Rondeau-Mouro, C. (2020). TD-NMR studies of starches from different botanical origins: Hydrothermal and storage effects. *Food Chemistry*, 308 (April 2019). <https://doi.org/10.1016/j.foodchem.2019.125675>

Kovrilia, R., & Rondeau-Mouro, C. (2017). Hydrothermal changes of starch Monitored by combined NMR and DSC methods. *Food and Bioprocess Technology*, 10(3), 445–461. <https://doi.org/10.1007/s11947-016-1832-9>

Lu, Z., & Seetharaman, K. (2013). 1 H nuclear magnetic resonance (NMR) and differential scanning calorimetry (DSC) studies of water mobility in dough systems containing barley flour. *Cereal Chemistry*, 90(2), 120–126. <https://doi.org/10.1094/CHEM-09-12-0116-R>

Mann, J., Schiedt, B., Baumann, A., Conde-Petit, B., & Vilgis, T. A. (2014). Effect of heat treatment on wheat dough rheology and wheat protein solubility. *Food Science and Technology International*, 20(5), 341–351. <https://doi.org/10.1177/1082013213468381>

Masi, P., Cavella, S., & Sepe, M. (1998). Characterization of dynamic viscoelastic behavior of wheat flour dough at different moisture contents. *Cereal Chemistry*, 75 (4), 428–432. <https://doi.org/10.1094/CHEM.1998.75.4.428>

Mazur, P., & Schmidt, J. J. (1968). Interactions of cooling velocity, temperature, and warming velocity on the survival of frozen and thawed yeast. *Cryobiology*, 5(1), 1–17. [https://doi.org/10.1016/S0003-2651\(68\)80138-5](https://doi.org/10.1016/S0003-2651(68)80138-5)

Meerts, M., Ramirez Cervera, A., Struyf, N., Cardinaels, R., Coutin, C. M., & Moldenaers, P. (2018). The effects of yeast metabolites on the rheological behaviour of the dough matrix in fermented wheat flour dough. *Journal of Cereal Science*, 82, 183–189. <https://doi.org/10.1016/j.jcs.2018.06.006>

Meerts, M., Vaes, D., Botteldoorn, S., Coutin, C. M., Cardinaels, R., & Moldenaers, P. (2018). The time-dependent rheology of fermenting wheat flour dough: Effects of salt and sugar. *Rheologica Acta*, 57, 813–827. <https://doi.org/10.1007/s00397-018-1113-9>

Migliori, M., Gabriele, D., Baldino, N., Lupi, F. R., & De Cindio, B. (2011). Rheological properties of bread dough: Effect of egg level. *Journal of Food Process Engineering*, 34 (4), 1266–1281. <https://doi.org/10.1111/j.1745-4530.2009.00410.x>

Newberry, M. P., Phan-Thien, N., Larroque, O. R., Tanner, R. I., & Larsen, N. G. (2002). Dynamic and Elongation rheology of yeasted bread doughs. *Cereal Chemistry*, 79(6), 874–879. <https://doi.org/10.1094/CHEM-2002.79.6.874>

Rezaei, M. N., Jayaram, V. B., Verstrepen, K. J., & Coutin, C. M. (2016). The impact of yeast fermentation on dough matrix properties. *Journal of the Science of Food and Agriculture*, 97(1), 1–10. <https://doi.org/10.1002/jfa.7562>, May 2015.

Roman-Gutierrez, A. D., Guilbert, S., & Cuq, B. (2002). Description of microstructural changes in wheat flour and flour components during hydration by using environmental scanning electron microscopy. *LWT - Food Science and Technology*, 35 (8), 730–740. <https://doi.org/10.1006/fstl.2002.0932>

Rondeau-Mouro, C., Camber, M., Kovrilia, R., Musse, M., Lucas, T., & Mariette, F. (2015). Temperature-associated proton dynamics in wheat starch-based model systems and wheat flour dough evaluated by NMR. *Food and Bioprocess Technology*, 8 (4), 777–790. <https://doi.org/10.1007/s11947-014-1445-0>

Rouillé, J., Della Valle, G., Lefebvre, J., Sliwinski, E., & Van Vliet, T. (2005). Shear and extensional properties of bread doughs affected by their minor components. *Journal of Cereal Science*, 42, 45–57. <https://doi.org/10.1016/j.jcs.2004.12.008>

Rubio-Merino, J., & Rubio-Hernández, F. J. (2019). Activation energy for the viscoelastic flow: Analysis of the microstructure-at-rest of (water- and milk-based)fruit beverages. *Food Chemistry*, 293(May), 486–490. <https://doi.org/10.1016/j.foodchem.2019.05.012>

Salvador, A., Sanz, T., & Fiszman, S. M. (2006). Dynamic rheological characteristics of wheat flour-water doughs. Effect of adding NaCl, sucrose and yeast. *Food Hydrocolloids*, 20(6), 780–786. <https://doi.org/10.1016/j.foodhyd.2005.07.009>

Schiedt, B., Baumann, A., Conde-Petit, B., & Vilgis, T. A. (2013). Short- and long-range interactions governing the viscoelastic properties during wheat dough and model dough development. *Journal of Texture Studies*, 44(4), 317–332. <https://doi.org/10.1111/jtxs.12027>

Schirmer, M., Jekle, M., & Becker, T. (2011). Quantification in starch microstructure as a function of baking time. *Procedia Food Science*, 1(May), 145–152. <https://doi.org/10.1016/j.profoo.2011.09.023>

Upadhyay, R., Ghosal, D., & Mehra, A. (2012). Characterization of bread dough: Rheological properties and microstructure. *Journal of Food Engineering*, 109(1), 104–113. <https://doi.org/10.1016/j.jfooodeng.2011.09.028>

Verbanwheide, A. E., Lambrecht, M. A., Jekle, M., Lucas, T., Fiersens, E., Shegai, O., et al. (2020). Microscopic investigation of the formation of a thermoset wheat gluten network in a model system relevant for bread making. *International Journal of Food Science and Technology*, 55(2), 891–896. <https://doi.org/10.1111/ijfs.14359>

Verheyen, C., Albrecht, A., Becker, T., & Jekle, M. (2016). Destabilization of wheat dough: Interrelation between CO₂ and glutathione. *Innovative Food Science and Emerging Technologies*, 34, 320–325. <https://doi.org/10.1016/j.ifset.2016.03.006>

Verheyen, C., Jekle, M., & Becker, T. (2014). Effects of *Saccharomyces cerevisiae* on the structural kinetics of wheat dough during fermentation. *LWT - Food Science and Technology*, 58(1), 194–202. <https://doi.org/10.1016/j.lwt.2014.02.050>

Weegels, P. L., de Groot, A. M. G., Verhoek, J. A., & Hamer, R. J. (1994). Effects of gluten of heating at different moisture contents. II. Changes in physico-chemical properties

and secondary structure. *Journal of Cereal Science*, 19(1), 39–47. <https://doi.org/10.1006/jcres.1994.1006>

Wehrli, M. C., Ini, S., Jekle, M., Kratky, T., & Becker, T. (2023). Resilience study of wheat protein networks with large amplitude oscillatory shear rheology. *LWT*, 114596. <https://doi.org/10.1016/j.lwt.2023.114596>

Wehrli, M. C., Kratky, T., Schopf, M., Scheif, K. A., Becker, T., & Jekle, M. (2021). Thermally induced gluten modification observed with rheology and spectroscopies. *International Journal of Biological Macromolecules*, 173, 26–33. <https://doi.org/10.1016/j.ijbiomac.2021.01.008>

Yang, P., & Mather, P. T. (2014). Thermal analysis to determine various forms of water present in Hydrogels. TA Instruments. <http://molbiol.ru/forums/index.php?act=Altha&type=post&id=220252>.

4 Discussion

Understanding the structure and functionality of foods is vital to adequate processing. Wheat dough displays a multiphase system with a non-Newtonian rheological behavior. Accordingly, the flow behavior depends on the type, amplitude, and rate of the applied strain. Throughout bread making, multiple stressors are well-documented to influence the mechanical properties of the dough matrix. One such stressor is baker's yeast, a primary source for a time-dependent transformation of the dough matrix along the bread making process. However, although it is used daily, the impact of its respective metabolites on the overall functionality of yeasted wheat dough remains unclear. Another major stressor occurs during baking, where thermal stress changes the structure and functionality of the wheat dough matrix. This final step of bread making exposes the matrix to thermal stress, inducing a cascade of physicochemical changes to the wheat dough's polymers. While the effects of individual yeast metabolites in the dough matrix and the occurrence of thermally induced polymer transitions have generated considerable research interest, few researchers have addressed the interactions within both effects. Therefore, this work investigated the effect of yeast metabolites (mechanical and chemical stressors) on the wheat dough's structure and rheological behavior during the cold stage and during baking.

A common approach in food science is to extract information on the processibility of food matrices by applying process-imitating deformations (Berta et al., 2016; Ng et al., 2006). During bread making, the dough is subjected to various types of strain and strain rates (see Chapter 1.2). With a focus on proofing and baking, biaxial extension represents the dominating strain type (Della Valle et al., 2014). However, it is important to note that both the amplitude and the rate of strain can vary drastically depending on the specific process (Bloksma, 1990; Della Valle et al., 2014; Peter L. Weegels et al., 2003). In the case of wheat dough, another consideration must be borne in mind, as the wheat dough's polymers exhibit a strain-dependent response (Schiedt et al., 2013). Thus, the strain applied for functional or structural characterization of the wheat dough's matrix must be carefully chosen to match the magnitude of interest, meeting two distinct requirements (Hyun et al., 2011).

No one-suits-it-all-solution exists to characterize the processibility and structure of yeasted wheat dough throughout proofing and baking. Thus, several techniques must be combined to extract all relevant information on the flow behavior and structure of the dough matrix. As mentioned, special consideration must be given to (i) the types of strain and strain rates occurring, and thus to be imitated, during proofing and baking and (ii) the strain-dependent response of the dough's polymers. With regard to the former, biaxial deformation should be applied at low strain rates and moderate deformation to characterize the rheological behavior under conditions relevant for proofing and baking. LSF was applied as one promising technique, exerting large amplitude biaxial extension on the dough matrix and, thus, imitating the type of deformation occurring during the proofing and baking process. Restrictions in this approach occur as the strain rates reached with LSF ($\dot{\epsilon}_b = 10^{-3} \text{ s}^{-1}$ to 10^{-1} s^{-1}) (Launay & Michon,

2008)) are in a different order of magnitude compared to the strain rates occurring during proofing ($\dot{\varepsilon}_b = 10^{-4} \text{ s}^{-1}$ to 10^{-3} s^{-1} (Babin et al., 2006; Turbin-Orger et al., 2015)). However, the application of such slow strain rates poses also other challenges. Given slow deformations, the flow behavior and the extent of SH are difficult to access for wheat dough as problems occur due to long measurement times, within which the dough's properties undergo time-dependent changes due to the ongoing fermentation and, thus, the release of yeast metabolites. Therefore, assumptions and approximations must be made to assess the rheological behavior of yeasted dough during proofing and baking, leaving LSF as a suitable technique to characterize yeasted wheat dough's processibility.

When considering the second scope of the rheological characterization, being structural elucidation, LSF is limited to the application of relatively large deformations and, thus, the characterization of large range interactions. Thus, a second technique must be applied to shed light on the interactions of the dough's polymers only sensitive to small amplitude strain. In this regard, SAOS rheometry has received considerable attention, revealing small range interactions (e.g., starch-starch and starch-protein interactions (Amemiya & Menjivar, 1992)). As one major aim of this work was to characterize the impact of yeast metabolites or thermal stress on the dough structure within short measurement times, multiwave rheology was applied. This technique represents a superior approach, allowing the extraction of more information during a short measurement time. Applying this technique within the framework of this thesis, the impact of yeast metabolites on the solidification kinetics of the wheat dough matrix during thermal processing was revealed. Beyond the initial expectations, being the characterization of short range interactions between starch polymers and starch as well as starch and protein polymers, the application of the multiwave measurement mode was also shown to represent a suitable tool for extracting long range gluten-related functionality behavior via SAOS rheometry (Alpers et al., 2023). The analysis of the frequency-dependent material behavior revealed an increasing amount of interactions of flow units with increasing temperature. While the simple stress response of wheat dough and wheat dough-like starch-gluten-systems was dominated by the effects of the dissociation of the granular structure of starch (Alpers et al., 2023, 2024), a structural parameter fitting the frequency-dependent deformation behavior of the material suggested an increasing connectivity of the dough matrix above 60 °C (Alpers et al., 2023). Thus, this measure of interactions obtained from the multiwave measurements unveiled the increasing extent of protein polymerization during baking, while the stress response served as a tool to analyze the progression of starch gelatinization.

Aside from SAOS testing's potential to reveal structural information on both starch-starch- and protein-protein-interactions, extensional testing is inevitable to quantify SH. SH, a phenomenon commonly depicted by branched polymers, has been intrinsically linked to good baking properties (Kokelaar et al., 1996). In this context, LSF was chosen as a suitable tool to quantify SH for slow and fast extension processes, as they have been reported to appear during the proofing and baking step of the bread making process (Alpers et al., 2021, 2023).

Although the use of LSF is controversial due to the requirement for material incompressibility, it has been applied elsewhere to yeasted and leavened dough systems (Chin et al., 2005; Formato & Pepe, 2005; Jødal & Larsen, 2021; Yue et al., 2020). Thus, the use of LSF for yeasted dough can be advocated, especially when applied to systems with limited gas void fractions in the form of close-cell foams (Launay & Michon, 2008), assuming the incompressibility of the wheat dough itself (Kouassi-Koffi et al., 2010; Vanin et al., 2018). Following this assumption, Yue et al. (2020) applied LSF to fermented dough made from flours of 16 different Chinese wheat varieties. The authors analyzed the correlations between the rheological measures of yeasted dough before or after fermentation and the parameters describing the bread quality through a principal component analysis. The authors achieved a higher correlation using the data of the fermented dough, indicating the need for the rheometrical characterization of fermented wheat dough instead of the respective unleavened dough. Furthermore, the loading plot revealed a marked correlation between $\eta_b(\dot{\varepsilon})$ and the quality parameters describing the crumb texture indicating the suitability of the use of LSF measurements on the fermented dough to predict bread quality parameters (Yue et al., 2020). Thus, SAOS and LSF rheometry represent suitable tools for investigating the impact of chemical, physical, and thermal stress on the wheat dough matrix under process-relevant deformations.

Based on the definition of suitable rheological techniques, the contribution of single yeast metabolites to the overall dough functionality during proofing was assessed. As fermented wheat dough represents a multi-component system composed of various polymers and yeast metabolites in increasing concentrations, added value was seen in reducing its complexity. In this context, achieving defined amounts of yeast metabolites in the dough matrix to determine the impact of single yeast metabolites has been the subject of many studies. For instance, Razeai et al. (2015) used *S. cerevisiae* strains with different metabolomes, leading to shifts towards higher levels of several metabolites. Significant differences in glycerol, acetic acid, and succinic acid levels were observed depending on the employed strain (Rezaei, Verstrepen, et al., 2015). Another method relied on harvesting cells at different growth phases, which was shown to be a suitable control tool for defining the level at which different metabolites are produced during proofing (Rezaei et al., 2014). Using this approach, the concentrations of ethanol, glycerol, and organic acid levels differed by a factor of two to four after comparable fermentation times. The metabolome differed significantly, especially between cells harvested during the (early) exponential growth phase and after the diauxic shift. A third method used mutants to overexpress or suppress individual metabolites (Aslankoohi et al., 2015). However, although all the abovementioned methods can induce shifts in the metabolome, causal relations are challenging to identify due to the induction of manifold changes in the metabolome. Hence, several researchers have followed the spiking of single yeast metabolites (Jayaram, Cuyvers, et al., 2014; Jayaram, Rezaei, et al., 2014; Meerts, Ramirez Cervera, et al., 2018). Although this approach has already provided comprehensive insights into the effects of individual yeast metabolites, a comparative assessment of the

impact of the individual metabolites with regard to the overall effect of the yeast metabolome still needs to be completed. Therefore, the following hypothesis has been followed:

The non-yeasted dough can behave similarly to its yeasted counterpart by spiking the primary (CO_2 and ethanol) and secondary (succinic acid) metabolites in their respective concentrations. The spiking of yeast metabolites is hypothesized to affect the rheological behavior of wheat dough in dependency on the applied type and rate of strain. Thus, the individual impact of single yeast metabolites on the functionality during the individual bread making sub-processes can be determined.

As discussed above, spiking single yeast metabolites represents a promising approach for the sake of practicality. Despite its advantages, the chemical incorporation of metabolites (e.g., spiking) brings the influence of the metabolites on the dough matrix forward in time in comparison to the gradual release of metabolites during the biological incorporation of metabolites (e.g., yeast fermentation). Thus, spiked metabolites can already impact the network formation during kneading. To analyze the impact of ethanol and succinic acid on dough development in this work, the course of the torque during kneading was recorded in the presence and absence of these metabolites in different concentrations. As shown in Figure 3a, increasing ethanol concentrations cause a decrease in the maximum torque and favor the development of a second peak during the dough development. Although this effect was majorly contributed to an increased amount of plasticizer, a more pronounced softening was observed for ethanol rather than for a surplus of water. From these large amplitude deformation experiments, it is suggested that the presence of ethanol causes the formation of a less developed and less stable network. This effect can be attributed to the presence of a solvent for gliadins, as suggested by Jayaram et al. (2014). Nevertheless, significant effects were limited to concentrations greater than 30 mmol/100 g flour in this work ($H = 20.403$, $p < 0.005$). However, it is relevant to remark that such concentrations are only reached after comparable long fermentation times or in the presence of high yeast levels. For example, Jayaram et al. (2013) quantified such concentrations after 3 h of fermentation with 2% (w/flour weight) compressed yeast or after approximately 1.5 h with 5.3% (w/flour weight) compressed yeast. In the case of succinic acid, marked effects, such as the stiffening of the dough, were only present for concentrations as high as 1.5 mmol/100 g flour, which is three times above the maximum concentration later used in this work. A concentration of 1.5 mmol succinic acid/100 g flour was only quantified after 3 h of proofing in the presence of 5.3% (w/flour weight) compressed yeast (Jayaram et al., 2013). The stiffening effect of succinic acid can be attributed to conformational changes of the gluten proteins upon acidification.

On the margin of this thesis, the contribution of dissolved CO_2 to the acidification of yeasted wheat dough was elucidated. Until now, researchers have reported that succinic acid and acetic acid are responsible for the pH drop during proofing (Jayaram et al., 2013, Rezaei, Verstrepen, et al., 2015). However, the effect of CO_2 and, thus, carbonic acid might be underestimated. To elucidate the contribution of each acidifying compound, both the effect of the saturation of the wheat dough matrix with CO_2 and the effect of the presence of succinic

and acetic acid, as well as the binary effect, were analyzed (see Figure 3b). The concentrations of succinic acid and acetic acid were quantified after 3 h of fermentation with 2% (w/flour weight) compressed yeast ($\text{pH} = 5.25 \pm 0.01$) using a LC-MS/MS-based quantification method to ensure comparable concentrations in the re-engineered systems. Following this, the resulting concentrations (succinic acid = 0.52 ± 0.01 mmol/100 g flour, acetic acid = 0.50 ± 0.04 mmol/100 g flour) were added to a non-yeasted wheat dough (pH of the untreated wheat dough = 5.73 ± 0.02). Saturation of the wheat dough matrix with CO_2 using modified headspace atmosphere mixing resulted in a pH of 5.54 ± 0.01 . The combined addition of both organic acids resulted in a pH of 5.26 ± 0.02 . Interestingly, adding both organic acids together with the saturation with CO_2 only resulted in a pH of 5.20 ± 0.02 , suggesting that the dough matrix's buffer capacity avoids further acidification. Thus, both organic acids and carbonic acid cause a marked pH drop. However, as CO_2 is formed in much higher quantities in the yeasted dough than organic acids, CO_2 could be regarded as responsible for an initial pH drop. In contrast, organic acids only contributed to additional acidification.

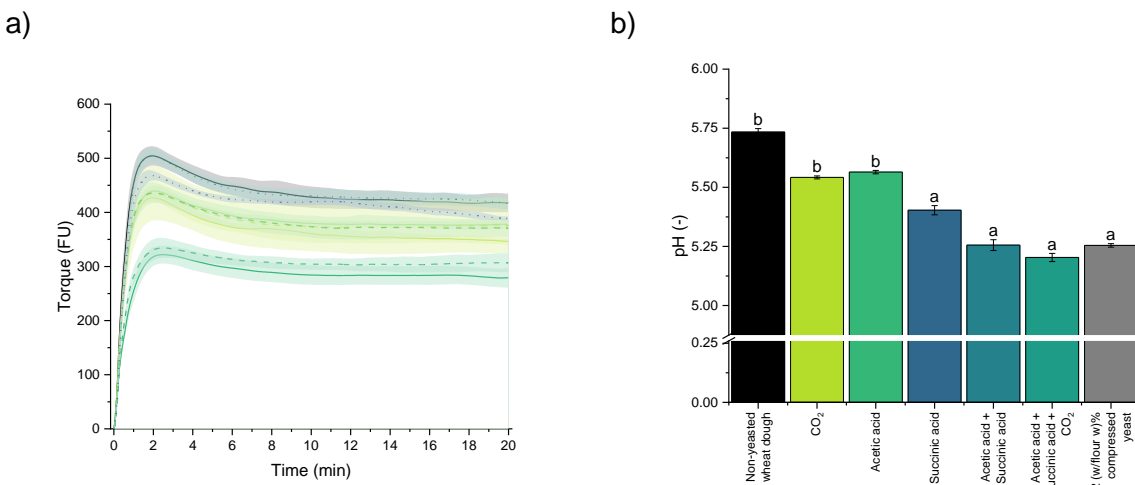


Figure 3: Effect of yeast metabolites on the dough development and the pH value of wheat dough. (a) Development of the torque required during kneading for a non-yeasted wheat dough (—), wheat dough spiked with 15 mmol ethanol/100 g flour (—), 30 mmol ethanol/100 g flour (—), 90 mmol ethanol/100 g flour (—), 0.5 mmol succinic acid/100 g flour (···) and 1.5 mmol succinic acid/100 g flour (···). Additionally, water was added in amounts similar to the respective ethanol additions to differentiate between the impact of additional plasticizer and the presence of a new solvent. Results are shown for water representing an addition of 15 mmol ethanol/100 g flour (—), 30 mmol ethanol/100 g flour (—) and 90 mmol ethanol/100 g flour (—). ($n = 3, \bar{X} \pm \text{standard deviation}$). (b) pH of wheat dough after spiking various acidifying compounds in yeast-equivalent concentrations in comparison to (non-)yeasted wheat dough. ($n = 3, \bar{X} \pm \text{standard deviation}$)

Despite its impact on the network formation, spiking yeast metabolites is considered the most reliable approach for incorporating single yeast metabolites. Attempts conducted in the early phase of this work to coat the metabolites in particles with waxy shells or ethyl cellulose shells were neglected due to the possible impact of the coating material on the dough matrix and the risk of an inhomogeneous distribution of yeast metabolites in the dough matrix. To replicate the homogeneous distribution of yeast metabolites, such as when released during proofing, comparably small amounts of metabolites would need to be coated and spiked, leading to a high concentration of coating material in the wheat dough matrix.

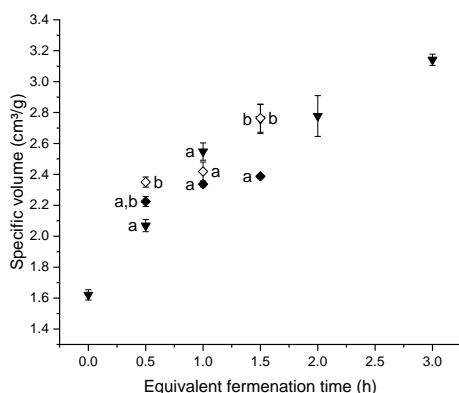
Given the previously described minor effects on dough development, the direct spiking approach was further used to elucidate the contribution of single yeast metabolites to the structural and functional changes in proofing wheat dough in this work. Following the previously introduced rheological approach, SAOS and LSF testing was applied to the yeasted and spiked doughs to understand the impact of single yeast metabolites on the dough's structure and processability. The impact of metabolites in yeast-like concentrations on the structure of the wheat dough matrix was accessed using SAOS rheometry. The data was evaluated using a power law model for structural elucidation. Additionally, the functionality of the non-yeasted, yeasted, and spiked wheat dough matrix was quantified under process-relevant biaxial deformation in terms of the SHI. The structure and processability of wheat dough were significantly impacted in the presence of gaseous CO₂. The mechanical stress exerted by gaseous CO₂ was further found to account for the major changes, which reached the extent of structural and functional changes observed in the yeasted dough itself. Compared to the significant changes occurring in the leavened and yeasted wheat dough, chemical stressors (ethanol and succinic acid) were found to cause only minor re-enforcing effects under small and large amplitude deformations (Alpers et al., 2021). Results from other researchers encourage these findings. Newberry et al. (2002) found no significant impact of chemical stressors using SAOS rheometry. Similarly, Meerts et al. (2018) reported that the simultaneous addition of ethanol, succinic acid, and glycerol as chemical stressors in yeast-like amounts is not solely responsible for the changes observed in the SAOS rheological behavior of degassed fermented wheat dough. The authors hypothesized the origin of the discrepancy in the nature of the incorporation of the metabolites into the dough matrix, where the instant addition of a high concentration of metabolites during the development of the dough matrix differs markedly from the successive release of metabolites from yeast cells during the fermentation process (Meerts, Ramirez Cervera, et al., 2018).

However, new insights were generated regarding the impact of the chemical stressors succinic acid and ethanol on the processability of wheat dough. Up to now, chemical stressors have been reported to account for major changes in the rheological behavior of yeasted wheat dough. Newberry et al. (2002) and Meerts et al. (2018) observed a significant impact of chemical stressors on the rheological behavior under large amplitude deformation using uniaxial extension and a Sentmanat extensional rheometer-like technique, respectively. The authors reported a decrease in the extensional viscosity and the extensibility while being subjected to uni- or biaxial extensional deformation. However, the results of this work indicate a predominant effect of CO₂ compared to ethanol and succinic acid as chemical stressors. Claiming a dominating impact of CO₂ as a mechanical stressor is possible due to the comparative approach taken. With this approach, it became evident that CO₂ governs the behavior of proofing wheat dough under small and large amplitude deformations (Alpers et al., 2021). This was concluded because chemically and biologically leavened dough behaved similarly at comparable gas void fractions. Independent of the applied leavening method, the doughs were characterized by a lower extent of interactions and a lower matrix strength with

increasing gas void fraction at a small strain amplitude. Contrarily, upon large range deformation, SH was pronounced, indicating a higher resistance to extension. The reasons for this discrepancy will be elucidated later in this work (p. 103 ff.). Thus, the mechanical stress exerted by gaseous CO₂ has a dominating structural and functional impact on the wheat dough matrix, while ethanol and succinic acid, as chemical stressors, only minorly affected the abovementioned.

Although the dominating impact of CO₂ on the structure and processibility of yeasted wheat dough became evident within this work, little is yet known about potential interactions within different yeast metabolites. Thus, the impact of binary or more complex mixtures of spiked yeast metabolites should be analyzed in future works. Also, results on the attempt to completely imitate a yeasted wheat dough matrix still need to be published. Reasons for the lack of research might be related to the difficulties arising from the relatively high gas void fraction for rheological testing. However, initial attempts have been made within this work to combine chemical and mechanical stressors during bread making trials, providing a further indication of the validity of the spiking approach. Figure 4 a) and b) shows the specific volume and crumb firmness of pan-baked wheat bread with either 2 g/100 g flour compressed yeast or yeast metabolites in equivalent concentrations. When comparing the three systems, similar bread characteristics can be achieved with the sole presence of gaseous CO₂, a combination of gaseous CO₂ and ethanol in yeast-like amounts, or yeast metabolites themselves. In most cases, gaseous CO₂ was sufficient to replicate the effect of biological leavening. In cases of longer fermentation times, the specific volume of the yeasted formulations was only reached in case of simultaneous presence of gaseous CO₂ and ethanol in yeast-equivalent amounts. It is suggested that ethanol increased protein-protein interactions within the dough matrix and, thus, the SHI (Alpers et al., 2021) at higher concentrations. Hence, considerable amounts of ethanol might have favored a better gas holding capacity of the dough matrix.

a)



b)

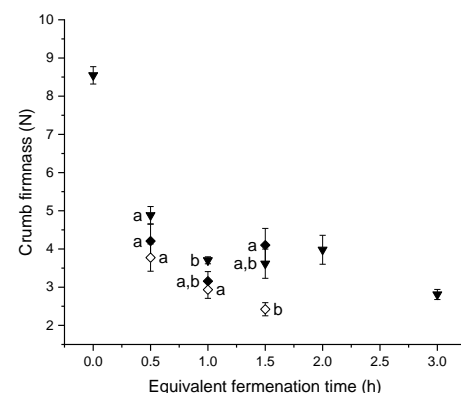


Figure 4: Specific volume and crumb firmness of pan baked wheat bread containing compressed yeast or yeast metabolites in equivalent concentrations. a) Specific volume. b) crumb firmness. (▼) 2 g compressed yeast/ 100 g flour, (◆) CO₂ in yeast-equivalent amounts or (◇) CO₂ and ethanol in yeast-equivalent amounts. Non-parametric Kruskal-Wallis test, followed by a Dunn's Post Hoc test was used for statistical evaluation. (n = 3, $\bar{X} \pm$ standard error).

Summarizing the effect of the individual yeast metabolites on the rheological behavior of the wheat dough matrix, it can be concluded that chemical and mechanical stressors must be considered in a differentiated way. As shown in Figure 3 and by other authors, chemical stressors predominantly affect the behavior of the dough matrix under large amplitude deformation (Jayaram, Cuyvers, et al., 2014; Jayaram, Rezaei, et al., 2014; Newberry et al., 2002). Under small amplitude strain, the impact only becomes apparent for high concentrations present after long fermentation times (Alpers et al., 2021; Meerts, Ramirez Cervera, et al., 2018; Newberry et al., 2002). Contrarily, the mechanical stressor CO_2 revealed its functional impact on the rheological behavior under small and large deformations (Alpers et al., 2021, 2024). Regarding the weighing of different yeast metabolites, CO_2 predominates during short proofing times, whereas ethanol and succinic acid as chemical stressors increase their relevance with increasing concentration during longer proofing times. Thus, the original hypothesis can be confirmed, whereby it must be restricted as the functionality of yeasted dough was predominated by the primary yeast metabolite CO_2 during short proofing times. Subsequently, the exertion of mechanical stress on the dough matrix has a major functional impact, whereas the effect of chemical stressors became apparent only at higher concentrations as present after long proofing times. The latter might originate from higher concentrations or longer exposure times, where analyzing the latter remains challenging due to simultaneously occurring time-dependent endogenous changes in the dough structure due to enzymatic activity or relaxation processes.

Additionally, a dependency of the impact of yeast metabolites on the exerted type and rate of strain became evident within this work (Alpers et al., 2021; Yue et al., 2020). Until now, yeasted dough was mainly characterized as a destabilized, fragile dough matrix (Casutt et al., 1984; Salvador et al., 2006; Verheyen et al., 2014). Comparable observations were made in this work under SAOS characterization (Alpers et al., 2021, 2023, 2024). Contrarily, an emphasized SH character was observed for systems with a higher gas void fraction. Thus, a yeasted dough was interpreted as a self-enforcing system (Alpers et al., 2021). This finding may explain the unique stability of yeasted wheat dough systems. The origin of this discrepant behavior will be further discussed in the following section, focusing on the causes of the functional differences between yeast-leavened and non-yeast-leavened systems. Thereby, the following hypothesis was followed:

The yeast metabolite-induced changes in the rheological behavior of yeasted dough matrix are based to the alteration of protein structure on a molecular and microscopic length scale by *S. cerevisiae* metabolites.

The relation between the protein microstructure of wheat dough and its rheological behavior is well known. Correlations have been observed independent of the type and amplitude of strain (Alpers et al., 2021; M. Dufour et al., 2024; Lucas et al., 2019). Furthermore, links between the molecular structure of gluten or the gluten composition and the wheat (or related species) dough's rheological properties are also widely known and are exploited towards their potential to improve bread quality (Bauer et al., 2003; Geisslitz et al., 2018; Scherf & Köhler, 2016;

Thanhaeuser et al., 2014; Herbert Wieser et al., 2009). Few researchers could also relate gluten composition to wheat dough's protein microstructure (Vidal et al., 2023). In contrast to these endogenous factors, the effect of processing during bread making and yeast fermentation on the wheat dough's different structural length scales has gained little attention. Microstructural changes in the proofing wheat dough matrix have been investigated using SEM and CLSM. The qualitative observations upon proofing comprise the expansion of gas cells and the appearance of discontinuities within the gluten matrix, a thinning of the dough matrix, and relocation of dough matrix constituents (Gan et al., 1990; Pomeranz et al., 1984; Rojas et al., 2000). Quantitative approaches revealed a decreasing connectivity and increasing looseness of the protein network during proofing (Bernklau et al., 2017). Other authors described a transformation of the protein network configuration into a coarse and clustered structure upon proofing (Alpers et al., 2021). A strong link between yeast-induced structural alterations and the wheat dough's resulting extensional flow behavior should be highlighted (Alpers et al., 2021). Apart from the protein structure, Alvarez-Ramirez (2019) describes a re-localization of wheat dough constituents on a microstructural length scale in the presence of yeast as these cells were reported to cluster around starch granules. However, other authors highlighted difficulties in differentiating between yeast cells and B granules (Rojas et al., 2000). Correspondingly, Wang et al. found the surface of starch granules to be considerably modified after 2 h of fermentation. The authors related the appearance of pores and cracks to wheat-endogenous amylolytic activity and structural degradation induced by yeast metabolites (H. Wang et al., 2024).

Comparatively, little information has been reported on the effect of yeast fermentation on the molecular structure of gluten. While Newberry et al. (2002) and Wang et al. (2016) consistently reported that the polymerization of proteins directly after kneading is markedly decreased in the presence of dry yeast, discrepant observations were made during proofing: Newberry et al. (2002) reported an increase in polymerization, whereas Wang et al. found the extractability of glutenins to increase during proofing, indicating further depolymerization during this sub-process (X. Y. Wang et al., 2016). A potential explanation for these contradictory observations was given by Borneo and Khan, who found the effect of proofing on the protein extractability along the bread making process to depend on the wheat cultivar (Borneo & Khan, 1999). The authors suspected the origin of these inconsistent results in the individual wheat cultivar's gluten composition, determining the extent of gluten degradation during proofing.

Concerning the secondary structure of gluten, slight indicators for yeast-induced changes were observed by Wang et al. (2017). The authors used FT-IR to investigate the effects of yeast fermentation on the conformation of the glutenin macropolymer (GMP). The percentage of α -helical structures decreased slightly, whereas the percentage of β -sheet, β -turn, and random coil structures did not markedly differ from the control sample. However, these differences in the secondary structure of gluten were not significant between a non-yeasted control dough and a yeasted dough (1%(w/flour w) compressed yeast) (J. Wang et al., 2017). Using higher yeast levels, Alvarez-Ramirez (2019) observed a significant decrease of α -helices upon

proofing. The reason for the increase of the percentage of α -helices quantified with increasing yeast concentrations remains, however, unexplainable. In general, transitions of α -helical to β -sheet structures have been widely monitored upon stretching of protein-based materials (Church et al., 1998; L. Kreplak et al., 2004; Laurent Kreplak et al., 2008; Litvinov et al., 2012; Qin et al., 2009). The uncoiling of α -helices is known to allow the extension of molecules at a constant force level (Qin et al., 2009). The occurrence of such mechanisms in gluten-based systems was shown by Wellner et al. (2005), who reported a decrease in β -turns and α -helices after repetitive extensions. Assuming that this mechanical extension is also the primary consequence of the release of CO_2 into the wheat dough matrix, this mechanical stressor is responsible for the decoiling of α -helices and the associated increasing proportion of β -sheets during proofing. The extension of the gluten strands would, thus, reduce the capacity of the gluten matrix to respond to additional deformation with low resistance to extension. Consequently, a yeast-induced reduction of α -helical structures in the gluten protein conformation would result in a higher SHI. This hypothesis was confirmed within this work, as the extent of SH was observed to increase with increasing gas void fractions for biologically and chemically leavened wheat dough systems (Alpers et al., 2021). Nevertheless, the source of this change in functionality was not traced back to its structural origins within this thesis. However, it is hypothesized that it can be found in an altered secondary structure of the gluten proteins.

Until now, the question of which *S. cerevisiae* metabolite causes the described changes in the molecular structure and microstructure of proteins remained unanswered. While a stronger incorporation of gliadins in the gluten network due to the presence of ethanol was shown by Jayaram et al., a weakening effect on interactions between gluten proteins has been reported in the presence of succinic acid (Jayaram et al., 2013). Both observations were made on a functional level, as the extent of gluten aggregation was accessed in the presence of the metabolites in yeast-like amounts. Contrarily, the effect of gaseous CO_2 on the protein structure was widely unknown on a molecular and microscopic length scale. Using a structural rheological model, the effect of gaseous CO_2 on the wheat dough matrix was successfully described on a microscopic length scale, where CO_2 was shown to impede interactions of flow units in the wheat dough matrix and to reduce the network strength (Alpers et al., 2021). The magnitude of structural changes quantified by this approach prevails over the effects of ethanol and succinic acid, especially during short proofing times. Therefore, it could be assumed that CO_2 is the major metabolite, shaping the molecular structure and microstructure of the wheat dough proteins. A final verification is, however, pending. A possible approach would involve applying spectroscopic techniques to metabolite-spiked wheat dough matrices. FT-IR could reveal a potential effect of these secondary metabolites on the secondary structure. Furthermore, the application of Raman spectroscopy could further help to elucidate the contribution of disulfide bonds to the polymerization of gluten proteins *in situ* (Lancelot et al., 2021).

Tracing back the origin of the altered rheological behavior to changes in the microstructure of the protein network, further attention was drawn to the impact of a partially degraded gluten network on the processibility during the subsequent bread making process. Besides yeast-induced mechanical and chemical stresses, thermal stress also occurs during baking. During this process, yeasted and non-yeasted dough show a distinct solidification behavior during thermal treatment (Alpers et al., 2023). The solidification process is well-known to be induced by a cascade of physicochemical changes in wheat dough's macropolymers, as previously reviewed in Chapter 1.4.3. Within the scope of this work, the presence of yeast metabolites on the onset and extent of the occurrence of these polymer transitions was meant to be differentiated. Based on the insights gained on the effect of yeast metabolites on the structure and functionality of the wheat dough matrix, the following hypothesis was formulated regarding the impact on the baking process.

The yeast-induced modification of the polymeric structures in wheat dough are further hypothesized to alter the thermally induced polymer transition processes. Consequently, the changes on the molecular and microstructural length scale alter the thermal dependency of the flow behavior and the solidification behavior of the wheat dough matrix during baking.

The mechanical stress exerted by gaseous CO₂ was previously identified to significantly alter the wheat dough protein microstructure. Gaseous CO₂ was thus identified as the most influential yeast metabolite within this work compared to the alterations induced by succinic acid and ethanol as chemical stressors. Consequently, the influence of mechanical and chemical stressors was hereinafter considered separately regarding their effect on the dough-to-crumb transition. This individual consideration revealed a major impact of gaseous CO₂, while chemical stressors alone did not affect the course of the solidification process induced throughout baking (Alpers et al., 2024). Furthermore, the occurrence of thermally induced polymer transitions, such as starch gelatinization, did not depend on the presence of yeast-like amounts of ethanol or succinic acid in the dough matrix (Alpers et al., 2022). This was related to the fact that thermal transitions of wheat polymers are predominantly affected by the extent of the hydration of the polymers (Eliasson, 1983; Jekle et al., 2016) and the spatial proximity of reaction partners (Verbauwhede et al., 2020). Contrary observations to the ones made within this work were reported by Wang et al. (2024). The authors found the hierarchical structure of native starch to be increasingly disordered during short fermentation times, resulting in an earlier onset of starch gelatinization. However, it must be mentioned that the authors did not distinguish between the effects induced by the endogenous amylolytic activity and the yeast metabolites.

Comparing the impact of chemical and mechanical stressors, the role of CO₂ on the abovementioned pacemakers for solidification was emphasized during the baking process (Alpers et al., 2023). This was verified by studying the progress of the thermally induced transition process in a non-yeasted, dense, and highly branched dough structure in comparison to a yeasted wheat dough with a partially degraded protein network. This approach revealed a limited ability for heat-induced polymerization of proteins in yeasted wheat dough

(Alpers et al., 2022). This interpretation is based on the quantitative assessment of the change in the microstructural protein network and the degree of crosslinking of the proteins at the molecular level during the baking process. (Alpers et al., 2021). For the sake of further clarification, a re-engineering approach was additionally followed. Within this scope, re-engineered wheat dough matrices, composed of native vital gluten and wheat starch or wheat starch-imitating glass beads, were employed to differentiate between the impact of yeast metabolites on the gluten- or starch-induced solidification processes. The before-mentioned glass beads are a shape-imitating substitute for wheat starch, which is, other than starch, thermally inert during the baking process (Brandner et al., 2018). In this re-engineered system, the formation of yeast metabolites was limited to the proofing step using a non-structurally invasive, thermal yeast-inactivation method. An additional partial degassing of the samples minimized the impact of gaseous CO₂ on the measurement. The reduction of the gas void fraction of the dough samples allowed to emphasize the potential effect of the remaining metabolites, whose concentration was not affected by the degassing procedure. Although a weakening effect of the mechanical stress exerted during proofing became evident from the reduced initial stiffness of the gluten-glass bead matrix, the further course of the solidification process was not affected in the presence of the remaining non-mechanical stressors (Alpers et al., 2024). This emphasizes the minor influence of chemical stressors on the polymerization of gluten proteins during baking. Contrarily, the whole yeast metabolome's was shown to be impeded gluten polymerization (Alpers et al., 2022). Thus, an obstructive effect of gaseous CO₂ on this heat-induced process can be concluded.

In fermented wheat dough, the course of solidification was further affected due to the progression of the starch gelatinization. Starch gelatinization was slightly accelerated in yeasted wheat dough matrices compared to the progression of starch gelatinization in non-yeasted wheat dough (Alpers et al., 2022). As the comparable effect became evident for non-yeasted re-engineered dough systems as well as wheat dough systems containing a higher water level, the accessibility and the hydration level of starch are held responsible for this effect. Together with the abovementioned observations of a negligible impact of chemical stressors on the onset of the starch gelatinization process, the effect of chemical stressors is considered as minor compared to the microstructural changes induced by mechanical intervention due to the release of CO₂ into the dough matrix.

To summarize, gaseous CO₂ is suspected to represent the main factor influencing the course of the dough matrix during the baking process, as it affects the accessibility and, consequently, the hydration of starch. The improved accessibility of starch is hypothesized to result in an earlier onset of starch gelatinization. In contrast, gluten polymerization was shown to be limited due to the reduced availability of proximate reaction partners. The origin of these effects is assumed to be related to the microstructure of wheat dough after proofing. As the composition of the gas cell-surrounding matrix changes during proofing (David Grenier et al., 2021), a cascade of different processes is initiated. Initially, the extension of the gas cell-surrounding lamella causes starch depletion in the lamella. The resulting clustering of starch in the nodes

will likely enable higher accessibility of starch granules for hydration. This higher hydration level of the starch granules might explain the earlier solidification of yeasted wheat dough, as the hydration level is a decisive factor for the progression of starch gelatinization. A degraded protein network could additionally serve as an accelerator for starch gelatinization. Comparable effects have been observed for undeveloped dough (Campos et al., 1997) and in re-engineered starch–gluten–systems (Alpers et al., 2024; Eliasson, 1983; Jekle et al., 2016). Besides its impact on the course of the starch gelatinization process, CO₂ interfered with the gluten polymerization. This was related to the growth of the gas cells, which causes the decrease of the proximity of gluten proteins and, thus, the extent of heat-induced protein polymerization to be limited in yeasted wheat doughs. Also other researchers have already employed the limited availability of reaction partners to explain limitations in the polymerization of gluten proteins (Verbauwheide et al., 2020).

Consequences of the altered course and extent of starch gelatinization and gluten polymerization were shown to alter the extensional flow behavior of wheat dough along the baking process. Within this work, a general elucidation of the polymer transition processes being relevant for changes in the SH behavior of the wheat dough matrix during baking was carried out. The SHI generally increased for temperatures ranging from 30 °C to 50 °C. Due to the weakening hydrogen bonds (Verbauwheide et al., 2020), an increase in protein-protein interactions is induced, leading to a lower ability for extension. Georget and Belton (2006) further observed the irreversible formation of β -sheets for hydrothermal treatment at 35 °C – 45 °C, suggesting a hardening of the structure and a reduced extensibility. Above 50 °C, a decrease in the SHI can then be observed for wheat dough. This can be linked to the reinforcing role of starch granules in the polymeric gluten matrix, which diminishes when gelatinization sets in and pasting is induced (S. Wang et al., 2016). Additionally, the extent of the Payne effect could further contribute to the decreasing SH behavior. In general, smaller particles have also a higher reinforcing effect on particle-filled polymeric systems due to their higher specific surface area (Warasitthinon et al., 2019). Thus, the reinforcing effect of starch on the particle-filled gluten matrix decreases during baking as starch granules swell. Furthermore, it was observed that an increasing temperature decreases the extent of the Payne effect (Mujtaba et al., 2012). Therefore, the decreasing Payne effect might also contribute to the decrease of the SHI above 50 °C.

The SHI increased during the latter baking phase, when the dough matrix was heated above 70 °C. A connection with the onset temperature of the gluten protein polymerization (Schofield et al., 1983) is suspected. Besides an increased crosslinking of glutenins via disulfide bonds (Lagrain et al., 2005; Schofield et al., 1983), an irreversible increase of intermolecular β -sheets is known to occur above 75 °C (Georget & Belton, 2006). These conformational changes serve as an explanation for an increased SHI above 70 °C (Alpers et al., 2023). Additionally, an increasing chain length of the polymers is also known to increase the emergence of the Payne effect, as shown by Sarvestani using a numerical approach (Sarvestani, 2016). At the same time, branching was reported to resemble an essential prerequisite for enhanced SH (Hepperle

& Münstedt, 2006). Thus, the increasing branching of the gluten proteins explains the increase of the SHI with increasing protein polymerization in a direct and indirect manner via the reinforcement of the Payne effect. Interestingly, the increase of the SHI above 70 °C is more abundant in yeasted dough systems, presumably caused by the mechanical stretching of the network. Thus, CO₂ as a mechanical stressor also majorly shapes the thermal dependency of the SH ability of the wheat dough matrix during baking. Remarkably, the extent of SH was not affected by the abovementioned reduced protein connectivity observed on a molecular and microstructural length scale. Thus, the self-enforcing nature of the yeasted wheat dough matrix can compensate for this degradation. In terms of the behavior of the wheat dough matrix during processing, the enhanced SH occurring for yeasted dough was shown to terminate oven rise prematurely around 60 °C when compared to non-yeasted wheat dough systems.

In conclusion, the above-stated hypothesis can be confirmed by deliberating a yeast-induced modification of the polymeric structures in wheat dough to alter the thermally induced polymer transition processes. However, chemical stressors were again found to have only a minor influence on the course of the solidification process. Instead, indirect steric effects, induced by the mechanical expansion of the wheat dough matrix due to the expansion of gas cells, were shown to determine the onset and extent of polymer transition processes in the yeasted wheat dough. Nevertheless, the extent of SH was mainly driven by the system's gas void fraction rather than yeast-induced differences in the solidification behavior of the wheat dough matrix.

5 Outlook

The initial question of this work was to identify the impact of individual yeast metabolites on the structure and functionality of the wheat dough matrix. Within this scope, gaseous CO₂ was identified as the most relevant metabolite due to its effect on the structure and processibility of wheat dough. Despite its disruptive impact on the protein's structure on a molecular- and microscopic length scale, the dough matrix-stabilizing strain hardening behavior increased due to the pre-extension of gluten strands around the growing gas cells. As discussed earlier, the structural origin of the discrepancy between a less branched protein network and the occurrence of SH at an increased degree was not resolved within this thesis. Thus, further elucidation should be fostered. This research question could be further accompanied by additional investigations of the potential limitations of this "pre-stabilization" by pre-extension of the gluten strands. Following this approach, an identification of the ideal extent of structural stabilization by extension resulting in strain hardening on the one hand and, on the other hand, structural breakdown due to overextension of gluten strands on a molecular length scale could be reached.

New promising insights could also be gained by resolving the spatial distribution of yeast metabolites in the dough matrix. Further research could be inspired by Huen et al.'s approach, who applied confocal Raman microscopy to frozen wheat dough to study the microstructure of frozen bread dough (Huen et al., 2014). Shifting the focus from the author's objective to analyze the spatial distribution of dough components (ice, starch, gluten, and yeast) to the localization of individual yeast metabolites could help to identify their impact on wheat dough polymers. By resolving the spatial distribution of yeast metabolites in the fermenting wheat dough matrix, structural effects on the dough's polymers could be resolved with spatial resolution. Linking this approach, e.g., with the spectroscopic assessment of the gluten conformation in dependency of the exposure to yeast metabolites, could pave the way to an in-depth understanding of the origin of structural and functional changes in the wheat dough matrix.

Aside from the need to clarify the observed changes on a molecular length scale, a closer look should be taken at the kinetics of the yeast metabolite formation. The strain rate dependency of SH indicates a need for consecutive research in this direction. Increased matrix stability could be expected for higher CO₂ production rates as faster gas formation rates result in a faster extension of the wheat dough matrix, leading to an enhanced SH (Alpers et al., 2021). Promising indications for the existence of a relation between the CO₂ formation rate and the gas retention capacity can be found in the literature. For example, Verheyen and Verheyen et al. reported the total gas volume in the wheat dough matrix to increase linearly with the CO₂ formation rate using an increasing amount of chemical leavening agents and, interestingly, increasing amounts of CO₂ to be stabilized in the dough matrix (Verheyen, 2016; Verheyen et al., 2016). This macroscopic trend was valid regardless of any potential destabilization on a molecular length scale. Also, the results of Rezaei et al. (2014) indicate the existence of such

a self-enforcing effect of the dough matrix upon high gas formation rates. The authors analyzed the effect of the gas formation rate on the gas retention capacity of wheat dough using *S. cerevisiae* harvested at different physiological phases. As expected, a negative linear correlation was observed between the maximum gas formation rate and the time of porosity (Tx) during proofing. For low and intermediate gas formation rates, a linear relation was also observed between the maximum gas formation rate, the lost amount of CO₂, and the maximum dough height (Rezaei et al., 2014). A detailed analysis revealed that the linear relation was interrupted at the highest gas formation rates. However, limited interpretability is given due to the origin of the yeast cells employed for fermentation from different physiological growth phases, as, due to this circumstance, the CO₂ formation rate and the concentration of secondary yeast metabolites varies. Thus, a final relation of the CO₂ production rate to the gas retention capacity cannot be deduced from this dataset. Like Rezaei et al. (2014), Verheyen et al. (2015) modulate the gas formation rate in wheat dough by yeast cell count per 100 g flour. From this data, an exponential decay can be observed for the dependency of Tx on the CO₂ production rate, likewise indicating the occurrence of a potential stabilization mechanism at high CO₂ formation rates. Furthermore, Verheyen et al. (2015) report a favorable effect of shorter fermentation periods on the specific bread volume. However, potential relations between the protein conformation and, consequently, the extent of strain hardening remain to be investigated. Taking all these indicators into account, a detailed study of the effect of the extension rate on the strain hardening behavior of wheat dough would be recommended. Applications of this study's outcomes could be given regarding the transition towards lower protein contents in German wheat flour, which could induce a development towards wheat flour doughs with limited gas retention potential. Enhancing strain hardening to compensate for protein networks with reduced connectivity could be a promising approach to enhance the processability of weak wheat flours.

Limitations towards elucidating the relation between the CO₂ formation rate and the extent of SH are currently given due to the intrinsic link of the CO₂ formation rate to the concentration of the biological or the chemical leavening agent in the wheat dough matrix. Thus, a model system could reduce the complexity. A promising approach is seen when applying Rheo-FT-IR, as conducted by Wellner et al. (2005), who elucidated the effect of extension on the protein conformation. This approach could give insights into the impact of the applied strain rate on the changes occurring in the secondary protein structure upon extension. Regarding industrial application, the benefits of the potential usage of non-conventional yeast strains could be explored. *S. cerevisiae* strains have already been selected due to their potential to form high amounts of CO₂ in a short time (Birch et al., 2013). However, research mainly focused on the total amount of CO₂ produced rather than the kinetics of CO₂ formation when screening non-conventional yeast strains (Bell et al., 2001; Timmermans et al., 2023), despite marked differences in the CO₂ formation rate are already well documented for non-conventional yeast strains (Aslankoohi et al., 2016; Zhou et al., 2017). Hence, great potential resides in studying non-conventional yeast strain's ability to form CO₂ at higher kinetics.

Looking beyond the relation of gas retention capacity and the structure of the gluten matrix, the impact of yeast metabolites on the stabilization of gas cells by liquid thin films should also be considered. This way of gas cell stabilization is of particular interest after longer fermentation times when defects in the gluten network occur. Under these circumstances, the stabilization of the gas cells is not just supported by the existence of the 3D gluten network but is increasingly dependent on alternative foam stabilization mechanisms. In this regard, Sroan et al. (2009) highlighted the existence of thin liquid films around the gas cells, which are stabilized by substances with interfacial activity. Following this line of thinking, another follow-up research question occurs when considering the impact of yeast fermentation on the capacity of the dough matrix to stabilize gas cells with thin liquid films. This capacity could be expected to be affected due to (i) the release of surface-active yeast metabolites into the dough matrix or (ii) the effect of yeast metabolites on the solubility of conformation of endogenous surfactants in the wheat dough. Initial work in this field has been conducted by Song et al. (2024). The authors investigated the effect of yeast or sourdough fermentation on the interfacial activity of dough liquor. This liquid, extracted by ultracentrifugation of wheat dough, is assumed to resemble the liquid of the thin liquid film surrounding lamella. In a mixed wheat-buckwheat system, yeast fermentation did not affect the properties of the dough liquor, which was characterized by surface hydrophobicity, foaming properties, and absorption kinetics at the air-water interface (Song et al., 2024). Thus, it can be concluded that no surface active substances were released or formed during yeast fermentation using conventional *S. cerevisiae*. Regardless of these findings, a potential effect of single yeast metabolites in superior quantities as released by non-conventional processing conditions or yeast strains cannot yet be excluded. Further research would be needed to support this hypothesis. In this regard, applying spectroscopic methods focusing on the air-water interface, such as Infrared Reflection-Absorption Spectroscopy, could be considered beneficial (e.g., as shown earlier for the case of antibodies (Koepf et al., 2018)). Consequently, the potential effects of yeast metabolites on the secondary structure of soluble wheat proteins at the air-water interface could be elucidated and related to a potential effect on foam stability. Given the successful identification of either stabilization mechanism, such an alternative foam stabilization mechanism could be beneficial to compensate for an increased gluten strand rupturing (e.g., due to higher CO₂ formation rates or quantities) or adverse wheat qualities (e.g., low protein and gluten contents). This could contribute to the potential elucidation of alternative fermentation parameters tailored to improve the foam stabilization during the proofing and baking step.

6 References

Abang Zaidel, D. N., Chin, N. L., Abdul Rahman, R., & Karim, R. (2008). Rheological characterisation of gluten from extensibility measurement. *Journal of Food Engineering*, 86(4), 549–556. <https://doi.org/10.1016/j.jfoodeng.2007.11.005>

Ai, Y., & Jane, J. (2015). Gelatinization and rheological properties of starch. *Starch - Stärke*, 67(3–4), 213–224. <https://doi.org/10.1002/star.201400201>

Alpers, T., Becker, T., & Jekle, M. (2023). Strain-dependent assessment of dough's polymer structure and functionality during the baking process. *PLoS ONE*, 18(3), e0282670. <https://doi.org/https://doi.org/10.1371/journal.pone.0282670>

Alpers, T., Olma, J., Jekle, M., & Becker, T. (2022). Relation between polymer transitions and the extensional viscosity of dough systems during thermal stabilization assessed by lubricated squeezing flow. *Food Chemistry*, 389, 133048. <https://doi.org/10.1016/j.foodchem.2022.133048>

Alpers, T., Panoch, D., Jekle, M., & Becker, T. (2024). New insights into crumb formation in model systems: Effects of yeast metabolites and hydration level by means of multiwave rheology. *Food Hydrocolloids*, 155, 110184. <https://doi.org/10.1016/j.foodhyd.2024.110184>

Alpers, T., Tauscher, V., Steglich, T., Becker, T., & Jekle, M. (2021). The self-enforcing starch–gluten system—Strain–dependent effects of yeast metabolites on the polymeric matrix. *Polymers*, 13(1), 30. <https://doi.org/10.3390/polym13010030>

Alvarez-Ramirez, J., Carrera-Tarela, Y., Carrillo-Navas, H., Vernon-Carter, E. J., & Garcia-Diaz, S. (2019). Effect of leavening time on LAOS properties of yeasted wheat dough. *Food Hydrocolloids*, 90, 421–432. <https://doi.org/10.1016/j.foodhyd.2018.12.055>

Amann, L. S., Frank, O., Dawid, C., & Hofmann, T. F. (2022). The Sensory-Directed Elucidation of the Key Tastants and Odorants in Sourdough Bread Crumb. *Foods*, 11(15). <https://doi.org/10.3390/foods11152325>

Amemiya, J. I., & Menjivar, J. A. (1992). Comparison of small and large deformation measurements to characterize the rheology of wheat flour doughs. *Journal of Food Engineering*, 16(1–2), 91–108. [https://doi.org/https://doi.org/10.1016/0260-8774\(92\)90022-X](https://doi.org/https://doi.org/10.1016/0260-8774(92)90022-X)

Ao, Z., & Jane, J. Iin. (2007). Characterization and modeling of the A- and B-granule starches of wheat, triticale, and barley. *Carbohydrate Polymers*, 67(1), 46–55. <https://doi.org/10.1016/j.carbpol.2006.04.013>

Apichartsrangkoon, A., Ledward, D. A., Bell, A. E., & Brennan, J. G. (1998). Physicochemical properties of high pressure treated wheat gluten. *Food Chemistry*, 63(2), 215–220. [https://doi.org/10.1016/S0308-8146\(98\)00004-1](https://doi.org/10.1016/S0308-8146(98)00004-1)

Arufe, S., Chiron, H., Doré, J., Savary-Auzeloux, I., Saulnier, L., & Della Valle, G. (2017). Processing and rheological properties of wheat flour dough and bread containing high levels of soluble dietary fibres blends. *Food Research International*, 97, 123–132. <https://doi.org/10.1016/j.foodres.2017.03.040>

Aslankoohi, E., Herrera-Malaver, B., Rezaei, M. N., Steensels, J., Courtin, C. M., & Verstrepen, K. J. (2016). Non-conventional yeast strains increase the aroma complexity of bread. *PLOS ONE*, 11(10), e0165126. <https://doi.org/10.1371/journal.pone.0165126>

Aslankoohi, E., Rezaei, M. N., Vervoort, Y., Courtin, C. M., & Verstrepen, K. J. (2015). Glycerol production by fermenting yeast cells is essential for optimal bread dough fermentation. *PLoS ONE*, 10(3), e0119364. <https://doi.org/10.1371/journal.pone.0119364>

Babin, P., Della Valle, G., Chiron, H., Cloetens, P., Hoszowska, J., Pernot, P., Réguerre, A. L., Salvo, L., & Dendievel, R. (2006). Fast X-ray tomography analysis of bubble growth and foam setting during breadmaking. *Journal of Cereal Science*, 43(3), 393–397. <https://doi.org/10.1016/j.jcs.2005.12.002>

Babin, P., Della Valle, G. D., Chiron, H., Cloetens, P., Hoszowska, J., Pernot, P., Réguerre, A. L., Salvo, L., & Dendievel, R. (2008). In situ fast x-ray tomography study of the evolution of cellular structure in bread dough during proving and baking. In *Bubbles in Food 2: Novelty, Health and Luxury* (Vol. 7). AACC International, Inc. <https://doi.org/10.1016/B978-1-891127-59-5.50030-4>

Baldwin, P. M. (2001). Starch granule-associated proteins and polypeptides: A review. *Starch/Staerke*, 53(10), 475–503. [https://doi.org/10.1002/1521-379X\(200110\)53:10<475::AID-STAR475>3.0.CO;2-E](https://doi.org/10.1002/1521-379X(200110)53:10<475::AID-STAR475>3.0.CO;2-E)

Barber, B., Ortolá, C., Barber, S., & Fernández, F. (1992). Storage of packaged white bread. *Zeitschrift Für Lebensmittel-Untersuchung Und -Forschung*, 194(5), 442–449. <https://doi.org/10.1007/BF01197726>

Bauer, N., Koehler, P., Wieser, H., & Schieberle, P. (2003). Studies on effects of microbial transglutaminase on gluten proteins of wheat. II. Rheological properties. *Cereal Chemistry*, 80(6), 787–790. <https://doi.org/10.1094/CCHEM.2003.80.6.787>

Bell, P. J. L., Higgins, V. J., & Attfield, P. V. (2001). Comparison of fermentative capacities of industrial baking and wild-type yeasts of the species *Saccharomyces cerevisiae* in different sugar media. *Letters in Applied Microbiology*, 32(4), 224–229. <https://doi.org/10.1046/j.1472-765X.2001.00894.x>

Belton, P. S. (1999). On the elasticity of wheat gluten. *Journal of Cereal Science*, 29(2), 103–107. <https://doi.org/10.1006/jcrs.1998.0227>

Belton, P. S. (2005). New approaches to study the molecular basis of the mechanical properties of gluten. *Journal of Cereal Science*, 41(2), 203–211. <https://doi.org/10.1016/j.jcs.2004.06.003>

Bernklau, I., Lucas, L., Jekle, M., & Becker, T. (2016). Protein network analysis — A new approach for quantifying wheat dough microstructure. *Food Research International*, 89, 812–819. <https://doi.org/10.1016/j.foodres.2016.10.012>

Bernklau, I., Neußer, C., Moroni, A. V., Gysler, C., Spagnolello, A., Chung, W., Jekle, M., & Becker, T. (2017). Structural, textural and sensory impact of sodium reduction on long fermented pizza. *Food Chemistry*, 234, 398–407. <https://doi.org/10.1016/j.foodchem.2017.04.188>

Berta, M., Muskens, E., Schuster, E., & Stading, M. (2016). Rheology of natural and imitation mozzarella cheese at conditions relevant to pizza baking. *International Dairy Journal*, 57, 34–38. <https://doi.org/10.1016/j.idairyj.2016.02.038>

Birch, A. N., van den Berg, F. W. J., & Hansen, Å. S. (2013). Expansion profiles of wheat doughs fermented by seven commercial baker's yeasts. *Journal of Cereal Science*, 58(2), 318–323. <https://doi.org/10.1016/j.jcs.2013.05.009>

Bloksma, A. H. (1972). Rheology of wheat flour doughs. *Journal of Texture Studies*, 3, 3–17. [https://doi.org/10.1016/0255-2701\(93\)80030-k](https://doi.org/10.1016/0255-2701(93)80030-k)

Bloksma, A. H. (1979). Effect of heating rate on viscosity of wheat flour doughs. *Journal of Texture Studies*, 10(3), 261–269. <https://doi.org/10.1111/j.1745-4603.1980.tb00252.x>

Bloksma, A. H. (1990). Rheology of the breadmaking process. *Cereal Foods World*, 35, 228–236.

Bloksma, A. H., & Nieman, W. (1975). The effect of temperature on some rheological properties of wheat flour doughs. *Journal of Texture Studies*, 6(3), 343–361. <https://doi.org/10.1111/j.1745-4603.1975.tb01130.x>

Borneo, R., & Khan, K. (1999). Protein changes during various stages of breadmaking of four spring wheats: Quantification by size-exclusion HPLC. *Cereal Chemistry*, 76(5), 711–717. <https://doi.org/10.1094/CCHEM.1999.76.5.711>

Bösl, M., Dunkel, A., Hartl, D., Dollinger, A., Spaccasassi, A., Stark, T. D., Dawid, C., & Hofmann, T. F. (2023). Toward High-Throughput Analysis of Aroma Compounds Using Ultrahigh-Performance Liquid Chromatography-Tandem Mass Spectrometry: Screening of Key Food Odorants in Various Foods. *Journal of Agricultural and Food Chemistry*, 71(22), 8622–8632. <https://doi.org/10.1021/acs.jafc.3c00935>

Bosmans, G. M., Lagrain, B., Deleu, L. J., Fierens, E., Hills, B. P., & Delcour, J. A. (2012). Assignments of proton populations in dough and bread using NMR relaxometry of starch, gluten, and flour model systems. *Journal of Agricultural and Food Chemistry*, 60(21), 5461–5470. <https://doi.org/10.1021/jf3008508>

Brandner, S., Becker, T., & Jekle, M. (2018). Wheat dough imitating artificial dough system based on hydrocolloids and glass beads. *Journal of Food Engineering*, 223, 144–151. <https://doi.org/10.1016/j.jfoodeng.2017.12.014>

Brandner, S., Becker, T., & Jekle, M. (2022a). Instantaneous wheat dough relaxation by alternating current electric fields. *Journal of Food Engineering*, 315, 110818. <https://doi.org/10.1016/j.jfoodeng.2021.110818>

Brandner, S., Becker, T., & Jekle, M. (2022b). Gluten–starch interface characteristics and wheat dough rheology—Insights from hybrid artificial systems. *Journal of Food Science*, 87(4), 1375–1385. <https://doi.org/10.1111/1750-3841.16115>

Broach, J. R. (2012). Nutritional control of growth and development in yeast. *Genetics*, 192(1), 73–105. <https://doi.org/10.1534/genetics.111.135731>

Camarasa, C., Grivet, J. P., & Dequin, S. (2003). Investigation by ¹³C-NMR and tricarboxylic acid (TCA) deletion mutant analysis of pathways of succinate formation in *Saccharomyces cerevisiae* during anaerobic fermentation. *Microbiology*, 149(9), 2669–2678. <https://doi.org/10.1099/mic.0.26007-0>

Campos, D. T., Steffe, J. F., & Ng, P. K. W. (1997). Rheological behavior of undeveloped and developed wheat dough. *Cereal Chemistry Journal*, 74(4), 489–494. <https://doi.org/10.1094/CCHEM.1997.74.4.489>

Caramanico, R., Marti, A., Vaccino, P., Bottega, G., Cappa, C., Lucisano, M., & Pagani, M. A. (2018). Rheological properties and baking performance of new waxy lines: Strengths and weaknesses. *LWT - Food Science and Technology*, 88, 159–164. <https://doi.org/10.1016/j.lwt.2017.09.035>

Casutt, V., Preston, K. R., & Kilborn, R. H. (1984). Effects of fermentation time, inherent flour strength, and salt level on extensigraph properties of full-formula remix-to-peak processed doughs. *Cereal Chemistry*, 61(5), 454–459.

Champenois, Y., Rao, M. A., & Walker, L. P. (1998). Influence of α -amylase on the viscoelastic properties of starch-gluten pastes and gels. *Journal of the Science of Food and Agriculture*, 78(1), 127–133. [https://doi.org/10.1002/\(sici\)1097-0010\(199809\)78:1<127::aid-jsfa99>3.0.co;2-k](https://doi.org/10.1002/(sici)1097-0010(199809)78:1<127::aid-jsfa99>3.0.co;2-k)

Charalambides, M. N., Wanigasooriya, L., Williams, G. J., & Chakrabarti, S. (2002). Biaxial deformation of dough using the bubble inflation technique. I. Experimental. *Rheologica Acta*, 41(6), 532–540. <https://doi.org/10.1007/s00397-002-0242-2>

Charalambides, M., Wanigasooriya, L., & Williams, G. (2002). Biaxial deformation of dough using the bubble inflation technique. II. Numerical modelling. *Rheologica Acta*, 41(6), 541–548. <https://doi.org/10.1007/s00397-002-0243-1>

Chatraei, S., Macosko, C. W., & Winter, H. H. (1981). Lubricated Squeezing Flow: A new biaxial extensional rheometer. *Journal of Rheology*, 25(4), 433–443. <https://doi.org/10.1122/1.549648>

Chin, N. L., Martin, P. J., & Campbell, G. M. (2005). Dough aeration and rheology: Part 3. Effect of the presence of gas bubbles in bread dough on measured bulk rheology and work input rate. *Journal of the Science of Food and Agriculture*, 85(13), 2203–2212. <https://doi.org/10.1002/jsfa.2238>

Chiotelli, E., & Le Meste, M. (2002). Effect of small and large wheat starch granules on thermomechanical behavior of starch. *Cereal Chemistry*, 79(2), 286–293. <https://doi.org/10.1094/CCHEM.2002.79.2.286>

Chiotellis, E., & Campbell, G. M. (2003). Proving of bread dough II. *Food and Bioproducts Processing*, 81(3), 207–216. <https://doi.org/10.1205/096030803322437974>

Church, J. S., Corino, G. L., & Woodhead, A. L. (1998). The effects of stretching on wool fibres as monitored by FT-Raman spectroscopy. *Journal of Molecular Structure*, 440(1–3), 15–23. [https://doi.org/10.1016/S0022-2860\(97\)00227-5](https://doi.org/10.1016/S0022-2860(97)00227-5)

Clarke, C. I., Schober, T. J., Dockery, P., O'Sullivan, K., & Arendt, E. K. (2004). Wheat sourdough fermentation: effects of time and acidification on fundamental rheological properties. *Cereal Chemistry*, 81(3), 409–417. <https://doi.org/10.1094/CCHEM.2004.81.3.409>

Connelly, R. K., & Kokini, J. L. (2006). 3D numerical simulation of the flow of viscous newtonian and shear thinning fluids in a twin sigma blade mixer. *Advances in Polymer Technology*, 25(3), 182–194. <https://doi.org/10.1002/adv.20071>

Dedey, K. B., Grenier, D., & Lucas, T. (2021). Mathematical modelling of uniaxial extension of a heterogeneous gas cell wall in bread dough: Stress fields and stress concentration analysis relating to the proving and baking steps. *Journal of Food Engineering*, 308(May), 110669. <https://doi.org/10.1016/j.jfoodeng.2021.110669>

Defaye, A. B., Ledward, D. A., MacDougall, D. B., & Tester, R. F. (1995). Renaturation of metmyoglobin subjected to high isostatic pressure. *Food Chemistry*, 52(1), 19–22. [https://doi.org/10.1016/0308-8146\(94\)P4175-F](https://doi.org/10.1016/0308-8146(94)P4175-F)

Della Valle, G., Chiron, H., Cicerelli, L., Kansou, K., Katina, K., Ndiaye, A., Whitworth, M., & Poutanen, K. (2014). Basic knowledge models for the design of bread texture. *Trends in Food Science and Technology*, 36(1), 5–14. <https://doi.org/10.1016/j.tifs.2014.01.003>

Dobraszczyk, B. J., & Morgenstern, M. P. (2003). Rheology and the breadmaking process. *Journal of Cereal Science*, 38(3), 229–245. [https://doi.org/10.1016/S0733-5210\(03\)00059-6](https://doi.org/10.1016/S0733-5210(03)00059-6)

Doppler, F., Jelonkiewicz, L., Rezaei, M. N., Lesens, C., Toussaint, R., & Durand-Dubief, M. (2022). Viability of *Saccharomyces cerevisiae* during baking of bread dough by flow cytometry. *Journal of Microbiological Methods*, 200(June), 106556. <https://doi.org/10.1016/j.mimet.2022.106556>

Döring, C., Nuber, C., Stukenborg, F., Jekle, M., & Becker, T. (2015). Impact of arabinoxylan addition on protein microstructure formation in wheat and rye dough. *Journal of Food Engineering*, 154, 10–16. <https://doi.org/10.1016/j.jfoodeng.2014.12.019>

Dornez, E., Gebruers, K., Cuyvers, S., Delcour, J. A., & Courtin, C. M. (2007). Impact of wheat flour-associated endoxylanases on arabinoxylan in dough after mixing and resting. *Journal of Agricultural and Food Chemistry*, 55(17), 7149–7155. <https://doi.org/10.1021/jf071363m>

Dörr, D., Kuhn, U., & Altstädt, V. (2020). Rheological study of gelation and crosslinking in chemical modified polyamide 12 using a multiwave technique. *Polymers*, 12(4), 7–9. <https://doi.org/10.3390/POLYM12040855>

Dreese, P. C., Faubion, J. M., & Hosene, R. C. (1988). Dynamic rheological properties of flour, gluten, and gluten-starch doughs. II. Effect of various processing and ingredient changes. *Cereal Chemistry*, 65(4), 354–359.

Dufour, M., Chaunier, L., Lourdin, D., Réguerre, A. L., Hugon, F., Dugué, A., Kansou, K., Saulnier, L., & Della Valle, G. (2024). Unravelling the relationships between wheat dough extensional properties, gluten network and water distribution. *Food Hydrocolloids*, 146, 109214. <https://doi.org/10.1016/j.foodhyd.2023.109214>

Dufour, Maude, Chaunier, L., Hugon, F., Dugué, A., Kansou, K., Saulnier, L., & Della Valle, G. (2024). From Alveograph test to extensional behavior of wheat flour dough. *Rheologica Acta*, 63(3), 179–190. <https://doi.org/10.1007/s00397-024-01430-6>

Dunnewind, B., Sliwinski, E. L., Grolle, K., & Van Vliet, T. (2003). The Kieffer dough and gluten extensibility rig - An experimental evaluation. *Journal of Texture Studies*, 34(5–6), 537–560. <https://doi.org/10.1111/j.1745-4603.2003.tb01080.x>

Dzialo, M. C., Park, R., Steensels, J., Lievens, B., & Verstrepen, K. J. (2017). Physiology, ecology and industrial applications of aroma formation in yeast. *FEMS Microbiology Reviews*, 41(Supp_1), S95–S128. <https://doi.org/10.1093/femsre/fux031>

Eliasson, A. C. (1983). Differential scanning calorimetry studies on wheat starch—gluten mixtures: I. Effect of gluten on the gelatinization of wheat starch. *Journal of Cereal Science*, 1(3), 199–205. [https://doi.org/10.1016/S0733-5210\(83\)80021-6](https://doi.org/10.1016/S0733-5210(83)80021-6)

Eliasson, A. C., & Karlsson, R. (1983). Gelatinization properties of different size classes of wheat starch granules measured with differential scanning calorimetry. *Starch - Stärke*, 35(4), 130–133. <https://doi.org/10.1002/star.19830350406>

Elmehdi, H. M., Page, J. H., & Scanlon, M. G. (2003). Monitoring dough fermentation using acoustic waves. *Food and Bioproducts Processing: Transactions of the Institution of Chemical Engineers, Part C*, 81(3), 217–223.
<https://doi.org/10.1205/096030803322437983>

Engmann, J., Servais, C., & Burbidge, A. S. (2005). Squeeze flow theory and applications to rheometry: A review. *Journal of Non-Newtonian Fluid Mechanics*, 132(1–3), 1–27.
<https://doi.org/10.1016/j.jnnfm.2005.08.007>

Færgestad, E. M., Molteberg, E. L., & Magnus, E. M. (2000). Interrelationships of Protein Composition, Protein Level, Baking Process and the Characteristics of Hearth Bread and Pan Bread. *Journal of Cereal Science*, 31(3), 309–320.
<https://doi.org/10.1006/jcrs.1999.0304>

Fischer, P., & Windhab, E. J. (2011). Rheology of food materials. *Current Opinion in Colloid and Interface Science*, 16(1), 36–40. <https://doi.org/10.1016/j.cocis.2010.07.003>

Formato, A., & Pepe, O. (2005). Pizza dough differentiation by principal component analysis of alveographic, microbiological, and chemical parameters. *Cereal Chemistry*, 82(4), 356–360. <https://doi.org/10.1094/CC-82-0356>

Fu, J., Mulvaney, S. J., & Cohen, C. (1997). Effect of added fat on the rheological properties of wheat flour doughs. *Cereal Chemistry*, 74(3), 304–311.
<https://doi.org/10.1094/CCHEM.1997.74.3.304>

Gabriele, D., de Cindio, B., & D'Antona, P. (2001). A weak gel model for foods. *Rheologica Acta*, 40(2), 120–127. <https://doi.org/10.1007/s003970000139>

Galal, A. M., Varriano-Marston, E., Johnson, J. A., Varriano-Marston, E., & Johnson, J. A. (1978). Rheological dough properties as affected by organic acids and salt. *Cereal Chemistry*, 55(5), 683–691.

Gan, Z., Angold, R. E., Williams, M. R., Ellis, P. R., Vaughan, J. G., & Galliard, T. (1990). The microstructure and gas retention of bread dough. *Journal of Cereal Science*, 12(1), 15–24. [https://doi.org/10.1016/S0733-5210\(09\)80153-7](https://doi.org/10.1016/S0733-5210(09)80153-7)

Geisslitz, S., Wieser, H., Scherf, K. A., & Koehler, P. (2018). Gluten protein composition and aggregation properties as predictors for bread volume of common wheat, spelt, durum wheat, emmer and einkorn. *Journal of Cereal Science*, 83, 204–212.
<https://doi.org/10.1016/j.jcs.2018.08.012>

Georget, D. M. R., & Belton, P. S. (2006). Effects of temperature and water content on the secondary structure of wheat gluten studied by FTIR spectroscopy. *Biomacromolecules*, 7(2), 469–475. <https://doi.org/10.1021/bm050667j>

Georgopoulos, T., Larsson, H., & Eliasson, A. C. (2004). A comparison of the rheological properties of wheat flour dough and its gluten prepared by ultracentrifugation. *Food Hydrocolloids*, 18(1), 143–151. [https://doi.org/10.1016/S0268-005X\(03\)00059-6](https://doi.org/10.1016/S0268-005X(03)00059-6)

Goesaert, H., Brijs, K., Veraverbeke, W. S., Courtin, C. M., Gebruers, K., & Delcour, J. A. (2005). Wheat flour constituents: How they impact bread quality, and how to impact their functionality. *Trends in Food Science and Technology*, 16(1–3), 12–30.
<https://doi.org/10.1016/j.tifs.2004.02.011>

Grenier, D., Lucas, T., & Le Ray, D. (2010). Measurement of local pressure during proving of bread dough sticks: Contribution of surface tension and dough viscosity to gas pressure in bubbles. *Journal of Cereal Science*, 52(3), 373–377.
<https://doi.org/10.1016/j.jcs.2010.06.016>

Grenier, David, Rondeau-Mourot, C., Dede, K. B., Morel, M. H., & Lucas, T. (2021). Gas cell opening in bread dough during baking. *Trends in Food Science and Technology*, 109, 482–498. <https://doi.org/10.1016/j.tifs.2021.01.032>

Guerrieri, N., Alberti, E., Lavelli, V., & Cerletti, P. (1996). Use of spectroscopic and fluorescence techniques to assess heat-induced molecular modifications of gluten. *Cereal Chemistry*, 73(3), 368–374.

Haward, S. J., Varchanis, S., McKinley, G. H., Alves, M. A., & Shen, A. Q. (2023). Extensional rheometry of mobile fluids. Part II: Comparison between the uniaxial, planar and biaxial extensional rheology of dilute polymer solutions using numerically-optimized stagnation point microfluidic devices. *Journal of Rheology*, 67(5), 1011–1030.
<https://doi.org/https://doi.org/10.1122/8.0000660>

He, J., Penson, S., Powers, S. J., Hawes, C., Shewry, P. R., & Tosi, P. (2013). Spatial patterns of gluten protein and polymer distribution in wheat grain. *Journal of Agricultural and Food Chemistry*, 61(26), 6207–6215. <https://doi.org/10.1021/jf401623d>

Heitmann, M., Zannini, E., & Arendt, E. (2018). Impact of *Saccharomyces cerevisiae* metabolites produced during fermentation on bread quality parameters: A review. *Critical Reviews in Food Science and Nutrition*, 58(7), 1152–1164. <https://doi.org/10.1080/10408398.2016.1244153>

Hepperle, J., & Münstedt, H. (2006). Rheological properties of branched polystyrenes: Nonlinear shear and extensional behavior. *Rheologica Acta*, 45(5), 717–727. <https://doi.org/10.1007/s00397-005-0031-9>

Hohmann, S. (2002). Osmotic stress signaling and osmoadaptation in yeasts. *Microbiology and Molecular Biology Reviews*, 66(2), 300–372. <https://doi.org/10.1128/mmbr.66.2.300-372.2002>

Holly, E. E., Venkataraman, S. K., Chambon, F., & Henning Winter, H. (1988). Fourier transform mechanical spectroscopy of viscoelastic materials with transient structure. *Journal of Non-Newtonian Fluid Mechanics*, 27(1), 17–26. [https://doi.org/10.1016/0377-0257\(88\)80002-8](https://doi.org/10.1016/0377-0257(88)80002-8)

Hong, L., & Lei, J. (2009). Scaling law for the radius of gyration of proteins and its dependence on hydrophobicity. *Journal of Polymer Science Part B: Polymer Physics*, 47(2), 207–214. <https://doi.org/10.1002/polb.21634>

Huen, J., Börsmann, J., Matullat, I., Böhm, L., Stukenborg, F., Heitmann, M., Zannini, E., & Arendt, E. K. (2018). Pilot scale investigation of the relationship between baked good properties and wheat flour analytical values. *European Food Research and Technology*, 244(3), 481–490. <https://doi.org/10.1007/s00217-017-2975-2>

Huen, J., Weikusat, C., Bayer-Giraldi, M., Weikusat, I., Ringer, L., & Lösche, K. (2014). Confocal Raman microscopy of frozen bread dough. *Journal of Cereal Science*, 60(3), 555–560. <https://doi.org/10.1016/j.jcs.2014.07.012>

Hwang, C. H., & Gunasekaran, S. (2001). Determining wheat dough mixing characteristics from power consumption profile of a conventional mixer. *Cereal Chemistry*, 78(1), 88–92. <https://doi.org/10.1094/CCHEM.2001.78.1.88>

Hyun, K., Wilhelm, M., Klein, C. O., Cho, K. S., Nam, J. G., Ahn, K. H., Lee, S. J., Ewoldt, R. H., & McKinley, G. H. (2011). A review of nonlinear oscillatory shear tests: Analysis and application of large amplitude oscillatory shear (LAOS). *Progress in Polymer Science*, 36(12), 1697–1753. <https://doi.org/10.1016/j.progpolymsci.2011.02.002>

Jakobi, S., Jekle, M., & Becker, T. (2018). Direct link between specific structural levels of starch and hydration properties. *Carbohydrate Polymers*, 181, 159–166. <https://doi.org/10.1016/j.carbpol.2017.10.062>

Janssen, A. M., Van Vliet, T., & Vereijken, J. M. (1996). Fundamental and empirical rheological behaviour of wheat flour doughs and comparison with bread making performance. *Journal of Cereal Science*, 23(1), 43–54. <https://doi.org/10.1006/jcrs.1996.0004>

Janssen, A. M., Vliet, T. Van, & Vereijken, J. M. (1996). Rheological behaviour of wheat glutens at small and large deformations. Comparison of two glutens differing in bread making potential. *Journal of Cereal Science*, 23(1), 19–31.

Jayaram, V. B., Cuyvers, S., Lagrain, B., Verstrepen, K. J., Delcour, J. A., & Courtin, C. M. (2013). Mapping of *Saccharomyces cerevisiae* metabolites in fermenting wheat straight-dough reveals succinic acid as pH-determining factor. *Food Chemistry*, 136(2), 301–308. <https://doi.org/10.1016/j.foodchem.2012.08.039>

Jayaram, V. B., Cuyvers, S., Verstrepen, K. J., Delcour, J. A., & Courtin, C. M. (2014). Succinic acid in levels produced by yeast (*Saccharomyces cerevisiae*) during fermentation strongly impacts wheat bread dough properties. *Food Chemistry*, 151, 421–428. <https://doi.org/10.1016/j.foodchem.2013.11.025>

Jayaram, V. B., Rezaei, M. N., Cuyvers, S., Verstrepen, K. J., Delcour, J. A., & Courtin, C. M. (2014). Ethanol at levels produced by *Saccharomyces cerevisiae* during wheat dough fermentation has a strong impact on dough properties. *Journal of Agricultural and Food Chemistry*, 62(38), 9326–9335. <https://doi.org/10.1021/jf502547a>

Jekle, M., & Becker, T. (2015). Wheat dough microstructure: The relation between visual structure and mechanical behavior. *Critical Reviews in Food Science and Nutrition*, 55(3), 369–382. <https://doi.org/10.1080/10408398.2012.656476>

Jekle, M., Mühlberger, K., & Becker, T. (2016). Starch-gluten interactions during gelatinization and its functionality in dough like model systems. *Food Hydrocolloids*, 54, 196–201. <https://doi.org/10.1016/j.foodhyd.2015.10.005>

Jenkins, P. J., Cameron, R. E., & Donald, A. M. (1993). A universal feature in the structure of starch granules from different botanical sources. *Starch - Stärke*, 45(12), 417–420. <https://doi.org/10.1002/star.19930451202>

Ji, H. K., Maeda, T., & Morita, N. (2005). Application of polished-graded wheat grains for sourdough bread. *Cereal Chemistry*, 82(2), 144–151. <https://doi.org/10.1094/CC-82-0144>

Jødal, A. S. S., & Larsen, K. L. (2021). Alveograph characterization of industrial samples of Danish pastry dough. *Cereal Chemistry*, 98(6), 1271–1281. <https://doi.org/10.1002/cche.10479>

Jongen, T. R. G., Bruschke, M. V., & Dekker, J. G. (2003). Analysis of dough kneaders using numerical flow simulations. *Cereal Chemistry*, 80(4), 383–389. <https://doi.org/10.1094/CCHEM.2003.80.4.383>

Joye, I. J., Draganski, A., Delcour, J. A., & Ludescher, R. D. (2012). Monitoring molecular oxygen depletion in wheat flour dough using erythrosin B phosphorescence: A biophysical approach. *Food Biophysics*, 7(2), 138–144. <https://doi.org/10.1007/s11483-012-9251-6>

Keetels, C. J. A. M., Van Vliet, T., & Walstra, P. (1996). Gelation and retrogradation of concentrated starch systems: 1. Gelation. *Food Hydrocolloids*, 10(3), 343–353. [https://doi.org/10.1016/S0268-005X\(96\)80011-7](https://doi.org/10.1016/S0268-005X(96)80011-7)

Khatkar, B. S., & David Schofield, J. (2002). Dynamic rheology of wheat flour dough. I. Non-linear viscoelastic behaviour. *Journal of the Science of Food and Agriculture*, 82(8), 827–829. <https://doi.org/10.1002/jsfa.1109>

Kieffer, R., Wieser, H., Henderson, M. H., & Graveland, A. (1998). Correlations of the Breadmaking Performance of Wheat Flour with Rheological Measurements on a Micro-scale. *Journal of Cereal Science*, 27(1), 53–60.

Kim, Y. R., Cornillon, P., Campanella, O. H., Stroshine, R. L., Lee, S., & Shim, J. Y. (2008). Small and large deformation rheology for hard wheat flour dough as influenced by mixing and resting. *Journal of Food Science*, 73(1), 1–8. <https://doi.org/10.1111/j.1750-3841.2007.00599.x>

Koepf, E., Richert, M., Braunschweig, B., Schroeder, R., Brezesinski, G., & Friess, W. (2018). Impact of formulation pH on physicochemical protein characteristics at the liquid-air interface. *International Journal of Pharmaceutics*, 541(1–2), 234–245. <https://doi.org/10.1016/j.ijpharm.2018.02.009>

Kokelaar, J. J., Van Vliet, T., & Prins, A. (1996). Strain hardening properties and extensibility of flour and gluten doughs in relation to breadmaking performance. *Journal of Cereal Science*, 24(3), 199–214. <https://doi.org/10.1006/jcrs.1996.0053>

Koksel, F., Aritan, S., Strybulevych, A., Page, J. H., & Scanlon, M. G. (2016). The bubble size distribution and its evolution in non-yeasted wheat flour doughs investigated by synchrotron X-ray microtomography. *Food Research International*, 80, 12–18. <https://doi.org/10.1016/j.foodres.2015.12.005>

Koksel, F., & Scanlon, M. G. (2016). Kinetics of bubble growth in bread dough and crust formation. In *Imaging Technologies and Data Processing for Food Engineers* (pp. 129–167). https://doi.org/10.1007/978-3-319-24735-9_5

Kouassi-Koffi, J. D., Launay, B., Davidou, S., Kouamé, L. P., & Michon, C. (2010). Lubricated squeezing flow of thin slabs of wheat flour dough: Comparison of results at constant plate speed and constant extension rates. *Rheologica Acta*, 49(3), 275–283. <https://doi.org/10.1007/s00397-009-0414-4>

Kreplak, L., Doucet, J., Dumas, P., & Briki, F. (2004). New aspects of the α -helix to β -sheet transition in stretched hard α -keratin fibers. *Biophysical Journal*, 87(1), 640–647. <https://doi.org/10.1529/biophysj.103.036749>

Kreplak, Laurent, Herrmann, H., & Aebi, U. (2008). Tensile properties of single desmin intermediate filaments. *Biophysical Journal*, 94(7), 2790–2799. <https://doi.org/10.1529/biophysj.107.119826>

Lagrain, B., Brijs, K., Veraverbeke, W. S., & Delcour, J. A. (2005). The impact of heating and cooling on the physico-chemical properties of wheat gluten–water suspensions. *Journal of Cereal Science*, 42(3), 327–333. <https://doi.org/10.1016/j.jcs.2005.06.005>

Lagrain, B., Rombouts, I., Wieser, H., Delcour, J. A., & Koehler, P. (2012). A reassessment of the electrophoretic mobility of high molecular weight glutenin subunits of wheat. *Journal of Cereal Science*, 56(3), 726–732. <https://doi.org/10.1016/j.jcs.2012.08.003>

Lagrain, B., Thewissen, B. G., Brijs, K., & Delcour, J. A. (2008). Mechanism of gliadin–glutenin cross-linking during hydrothermal treatment. *Food Chemistry*, 107(2), 753–760. <https://doi.org/10.1016/j.foodchem.2007.08.082>

Lahue, C., Madden, A. A., Dunn, R. R., & Smukowski Heil, C. (2020). History and domestication of *Saccharomyces cerevisiae* in bread baking. *Frontiers in Genetics*, 11, 584718. <https://doi.org/10.3389/fgene.2020.584718>

Lancelot, E., Fontaine, J., Grua-Priol, J., Assaf, A., Thouand, G., & Le-Bail, A. (2021). Study of structural changes of gluten proteins during bread dough mixing by Raman spectroscopy. *Food Chemistry*, 358. <https://doi.org/10.1016/j.foodchem.2021.129916>

Launay, B., Bure, J., & Praden, J. (1977). Use of the Chopin Alveographe as a rheological tool. I. Dough deformation measurements. *Cereal Chemistry*, 54(5), 1042–1048.

Launay, B., & Michon, C. (2008). Biaxial extension of wheat flour doughs: Lubricated Squeezing Flow and stress relaxation properties. *Journal of Texture Studies*, 39(5), 496–529. [https://doi.org/https://doi.org/10.1111/j.1745-4603.2008.00156.x](https://doi.org/10.1111/j.1745-4603.2008.00156.x)

Lee, S., & Campanella, O. (2013). Impulse viscoelastic characterization of wheat flour dough during fermentation. *Journal of Food Engineering*, 118(3), 266–270. <https://doi.org/10.1016/j.jfoodeng.2013.04.024>

Lee, S., Pyrak-Nolet, L. J., & Campanella, O. (2004). Determination of ultrasonic-based rheological properties of dough during fermentation. *Journal of Texture Studies*, 35(1), 33–52. <https://doi.org/10.1111/j.1745-4603.2004.tb00821.x>

Lefebvre, J., Popineau, Y., Deshayes, G., & Lavenant, L. (2000). Temperature-induced changes in the dynamic rheological behavior and size distribution of polymeric proteins for glutens from wheat near-isogenic lines differing in HMW glutenin subunit composition. *Cereal Chemistry*, 77(2), 193–201. <https://doi.org/10.1094/CCHEM.2000.77.2.193>

Leon, A., Rosell, C. M., & De Barber, C. B. (2003). A differential scanning calorimetry study of wheat proteins. *European Food Research and Technology*, 217(1), 13–16. <https://doi.org/10.1007/s00217-003-0699-y>

Létang, C., Piau, M., & Verdier, C. (1999). Characterization of wheat flour–water doughs. Part I: Rheometry and microstructure. *Journal of Food Engineering*, 41(2), 121–132. [https://doi.org/https://doi.org/10.1016/S0260-8774\(99\)00082-5](https://doi.org/https://doi.org/10.1016/S0260-8774(99)00082-5)

Li, M., Yue, Q., Liu, C., Zheng, X., Hong, J., Li, L., & Bian, K. (2021). Comparative study of rheology and steamed bread quality of wheat dough and gluten: Starch doughs. *Journal of Food Processing and Preservation*, 45(2). <https://doi.org/10.1111/jfpp.15160>

Liao, L., Liu, T. X., Zhao, M. M., Cui, C., Yuan, B. E., Tang, S., & Yang, F. (2010). Functional, nutritional and conformational changes from deamidation of wheat gluten with succinic acid and citric acid. *Food Chemistry*, 123(1), 123–130. <https://doi.org/10.1016/j.foodchem.2010.04.017>

Lin, L., Huang, J., Zhao, L., Wang, J., Wang, Z., & Wei, C. (2015). Effect of granule size on the properties of lotus rhizome C-type starch. *Carbohydrate Polymers*, 134, 448–457. <https://doi.org/10.1016/j.carbpol.2015.08.026>

Linlaud, N., Ferrer, E., Puppo, M. C., & Ferrero, C. (2011). Hydrocolloid interaction with water, protein, and starch in wheat dough. *Journal of Agricultural and Food Chemistry*, 59(2), 713–719. <https://doi.org/10.1021/jf1026197>

Litvinov, R. I., Faizullin, D. A., Zuev, Y. F., & Weisel, J. W. (2012). The α -helix to β -sheet transition in stretched and compressed hydrated fibrin clots. *Biophysical Journal*, 103(5), 1020–1027. <https://doi.org/10.1016/j.bpj.2012.07.046>

Loveday, S. M., & Winger, R. J. (2008). Simultaneous extraction and enzymatic quantification of glucose, sucrose, and ethanol in fermenting yeasted dough. *Cereal Chemistry*, 85(4), 530–533. <https://doi.org/10.1094/CCHEM-85-4-0530>

Lucas, I., Petermeier, H., Becker, T., & Jekle, M. (2019). Definition of network types – Prediction of dough mechanical behaviour under shear by gluten microstructure. *Scientific Reports*, 9(1), 4700. <https://doi.org/10.1038/s41598-019-41072-w>

Lynch, D. M., & Bamforth, C. W. (2002). Measurement and characterization of bubble nucleation in beer. *Journal of Food Science*, 67(7), 2696–2701. <https://doi.org/10.1111/j.1365-2621.2002.tb08801.x>

Ma, J., Lin, Y., Chen, X., Zhao, B., & Zhang, J. (2014). Flow behavior, thixotropy and dynamical viscoelasticity of sodium alginate aqueous solutions. *Food Hydrocolloids*, 38, 119–128. <https://doi.org/10.1016/j.foodhyd.2013.11.016>

Mann, J., Schiedt, B., Baumann, A., Conde-Petit, B., & Vilgis, T. A. (2014). Effect of heat treatment on wheat dough rheology and wheat protein solubility. *Food Science and Technology International*, 20(5), 341–351. <https://doi.org/10.1177/1082013213488381>

Matta, J., & Tytus, R. (1990). Liquid stretching using a falling cylinder. *Journal of Non-Newtonian Fluid Mechanics*, 35(2–3), 215–229. [https://doi.org/10.1016/0377-0257\(90\)85050-9](https://doi.org/10.1016/0377-0257(90)85050-9)

Mccann, T. H., Gall, M. Le, & Day, L. (2016). Extensional dough rheology - Impact of flour composition and extension speed. *Journal of Cereal Science*, 69, 228–237. <https://doi.org/10.1016/j.jcs.2016.03.012>

Meerts, M., Cardinaels, R., Oosterlinck, F., M. Courtin, C., & Moldenaers, P. (2017). The interplay between the main flour constituents in the rheological behaviour of wheat flour dough. *Food and Bioprocess Technology*, 10(2), 249–265. <https://doi.org/10.1007/s11947-016-1810-2>

Meerts, M., Ramirez Cervera, A., Struyf, N., Cardinaels, R., Courtin, C. M., & Moldenaers, P. (2018). The effects of yeast metabolites on the rheological behaviour of the dough matrix in fermented wheat flour dough. *Journal of Cereal Science*, 82, 183–189. <https://doi.org/10.1016/j.jcs.2018.06.006>

Meerts, M., Vaes, D., Botteldoorn, S., Courtin, C. M., Cardinaels, R., & Moldenaers, P. (2018). The time-dependent rheology of fermenting wheat flour dough: effects of salt and sugar. *Rheologica Acta*, 57(12), 813–827. <https://doi.org/10.1007/s00397-018-1113-9>

Mehta, K. L., Scanlon, M. G., Sapirstein, H. D., & Page, J. H. (2009). Ultrasonic investigation of the effect of vegetable shortening and mixing time on the mechanical properties of bread dough. *Journal of Food Science*, 74(9). <https://doi.org/10.1111/j.1750-3841.2009.01346.x>

Meißner, J. (1969). Rheometer zur Untersuchung der deformationsmechanischen Eigenschaften von Kunststoff-Schmelzen unter definierter Zugbeanspruchung. *Rheologica Acta*, 8(1), 78–88. <https://doi.org/10.1007/BF02321358>

Mennah-Govela, Y. A., & Bornhorst, G. M. (2021). Food buffering capacity: quantification methods and its importance in digestion and health. *Food and Function*, 12(2), 543–563. <https://doi.org/10.1039/d0fo02415e>

Miller, R. A., Graf, E., & Hoseney, R. C. (1994). Leavened dough pH determination by an improved method. *Journal of Food Science*, 59(5), 1086–1087. <https://doi.org/10.1111/j.1365-2621.1994.tb08196.x>

Mills, E. N. C., Wilde, P. J., Salt, L. J., & Skeggs, P. (2003). Bubble formation and stabilization in bread dough. *Food and Bioproducts Processing: Transactions of the Institution of Chemical Engineers, Part C*, 81(3), 189–193. <https://doi.org/10.1205/096030803322437956>

Morel, M. H., Redl, A., & Guilbert, S. (2002). Mechanism of heat and shear mediated aggregation of wheat gluten protein upon mixing. *Biomacromolecules*, 3(3), 488–497. <https://doi.org/10.1021/bm015639p>

Mujtaba, A., Keller, M., Ilisch, S., Radusch, H. J., Thurn-Albrecht, T., Saalwächter, K., & Beiner, M. (2012). Mechanical properties and cross-link density of styrene-butadiene model composites containing fillers with bimodal particle size distribution. *Macromolecules*, 45(16), 6504–6515. <https://doi.org/10.1021/ma300925p>

Newberry, M. P., Phan-Thien, N., Larroque, O. R., Tanner, R. I., & Larsen, N. G. (2002). Dynamic and elongation rheology of yeasted bread doughs. *Cereal Chemistry*, 79(6), 874–879. <https://doi.org/10.1094/CCHEM.2002.79.6.874>

Ng, T. S. K., McKinley, G. H., & Padmanabhan, M. (2006). Linear to non-linear rheology of wheat flour dough. *Applied Rheology*, 16(5), 265–274. <https://doi.org/10.1515/arh-2006-0019>

Noda, T., Takigawa, S., Matsuura-Endo, C., Kim, S. J., Hashimoto, N., Yamauchi, H., Hanashiro, I., & Takeda, Y. (2005). Physicochemical properties and amylopectin structures of large, small, and extremely small potato starch granules. *Carbohydrate Polymers*, 60(2), 245–251. <https://doi.org/10.1016/j.carbpol.2005.01.015>

Oliveira, R., Lages, F., Silva-Graça, M., & Lucas, C. (2003). Fps1p channel is the mediator of the major part of glycerol passive diffusion in *Saccharomyces cerevisiae*: Artefacts and re-definitions. *Biochimica et Biophysica Acta - Biomembranes*, 1613(1–2), 57–71. [https://doi.org/10.1016/S0005-2736\(03\)00138-X](https://doi.org/10.1016/S0005-2736(03)00138-X)

Palla, C., de Vicente, J., Carrín, M. E., & Gálvez Ruiz, M. J. (2019). Effects of cooling temperature profiles on the monoglycerides oleogel properties: A rheo-microscopy study. *Food Research International*, 125, 108613. <https://doi.org/10.1016/j.foodres.2019.108613>

Pandiella, S. S., Garcia, L. A., & Diaz, M. (1999). Evolution of CO₂ bubbles during brewery fermentation. In *Bubbles in Food* (pp. 33–43). Eagan Press.

Payne, A. R. (1962). The dynamic properties of carbon black-loaded natural rubber. *Journal of Applied Polymer Science*, 11(19), 57–63.

Pérez, S. J., Rojas, C. C., Eliasson, A.-C., & Sjöö, M. E. (2019). Phase separation , water and thermal properties of andean grain flours and their effect on wheat flour dough. *Journal of Food Processing and Technology*, 10(2). <https://doi.org/10.4172/2157-7110.1000779>

Perry, P. A., & Donald, A. M. (2000). The role of plasticization in starch granule assembly. *Biomacromolecules*, 1(3), 424–432. <https://doi.org/10.1021/bm0055145>

Petrie, C. J. S. (2006). Extensional viscosity: A critical discussion. *Journal of Non-Newtonian Fluid Mechanics*, 137(1–3), 15–23. <https://doi.org/10.1016/j.jnnfm.2006.01.011>

Pomeranz, Y., Meyer, D., & Seibel, W. (1984). Wheat, wheat-rye, and rye dough and bread studied by scanning electron-microscopy. *Cereal Chemistry*, 61(1), 53–59.

Qin, Z., Kreplak, L., & Buehler, M. J. (2009). Hierarchical structure controls nanomechanical properties of vimentin intermediate filaments. *PLoS ONE*, 4(10). <https://doi.org/10.1371/journal.pone.0007294>

Raab, A. M., & Lang, C. (2011). Oxidative versus reductive succinic acid production in the yeast *Saccharomyces cerevisiae*. *Bioengineered Bugs*, 2(2). <https://doi.org/10.4161/bbug.2.2.14549>

Ratnayake, W. S., & Jackson, D. S. (2007). A new insight into the gelatinization process of native starches. *Carbohydrate Polymers*, 67(4), 511–529. <https://doi.org/10.1016/j.carbpol.2006.06.025>

Redl, A., Guilbert, S., & Morel, M. H. (2003). Heat and shear mediated polymerisation of plasticized wheat gluten protein upon mixing. *Journal of Cereal Science*, 38(1), 105–114. [https://doi.org/10.1016/S0733-5210\(03\)00003-1](https://doi.org/10.1016/S0733-5210(03)00003-1)

Remize, F., Andrieu, E., & Dequin, S. (2000). Engineering of the pyruvate dehydrogenase bypass in *Saccharomyces cerevisiae*: Role of the cytosolic Mg²⁺ and mitochondrial K⁺ acetaldehyde dehydrogenases Ald6p and Ald4p in acetate formation during alcoholic fermentation. *Applied and Environmental Microbiology*, 66(8), 3151–3159. <https://doi.org/10.1128/AEM.66.8.3151-3159.2000>

Rezaei, M. N., Aslankoohi, E., Verstrepen, K. J., & Courtin, C. M. (2015). Contribution of the tricarboxylic acid (TCA) cycle and the glyoxylate shunt in *Saccharomyces cerevisiae* to succinic acid production during dough fermentation. *International Journal of Food Microbiology*, 204, 24–32. <https://doi.org/10.1016/j.ijfoodmicro.2015.03.004>

Rezaei, M. N., Dornez, E., Jacobs, P., Parsi, A., Verstrepen, K. J., & Courtin, C. M. (2014). Harvesting yeast (*Saccharomyces cerevisiae*) at different physiological phases significantly affects its functionality in bread dough fermentation. *Food Microbiology*, 39, 108–115. <https://doi.org/10.1016/j.fm.2013.11.013>

Rezaei, M. N., Dornez, E., Verstrepen, K. J., & Courtin, C. M. (2015). Critical assessment of the formation of hydrogen peroxide in dough by fermenting yeast cells. *Food Chemistry*, 168, 183–189. <https://doi.org/10.1016/j.foodchem.2014.07.050>

Rezaei, M. N., Jayaram, V. B., Verstrepen, K. J., & Courtin, C. M. (2016). The impact of yeast fermentation on dough matrix properties. *Journal of the Science of Food and Agriculture*, 96(11), 3741–3748. <https://doi.org/10.1002/jsfa.7562>

Rezaei, M. N., Verstrepen, K. J., & Courtin, C. M. (2015). Metabolite analysis allows insight into the differences in functionality of 25 *Saccharomyces cerevisiae* strains in bread dough fermentation. *Cereal Chemistry*, 92(6), 588–597. <https://doi.org/10.1094/CCHEM-04-15-0061-R>

Roels, S. P., Cleemput, G., Vandewalle, X., Nys, M., & Delcour, J. A. (1993). Bread volume potential of variable-quality flours with constant protein level as determined by factors governing mixing time and baking absorption levels. *Cereal Chemistry*, 70, 318–323.

Rojas, J. A., Rosell, C. M., Benedito De Barber, C., Pérez-Munuera, I., & Lluch, M. A. (2000). The baking process of wheat rolls followed by cryo scanning electron microscopy. *European Food Research and Technology*, 212(1), 57–63. <https://doi.org/10.1007/s002170000209>

Rondeau-Mourot, C., Cambert, M., Kovrlija, R., Musse, M., Lucas, T., & Mariette, F. (2015). Temperature-associated proton dynamics in wheat starch-based model systems and wheat flour dough evaluated by NMR. *Food and Bioprocess Technology*, 8(4), 777–790. <https://doi.org/10.1007/s11947-014-1445-0>

Rouillé, J., Bonny, J. M., Della Valle, G., Devaux, M. F., & Renou, J. P. (2005). Effect of flour minor components on bubble growth in bread dough during proofing assessed by magnetic resonance imaging. *Journal of Agricultural and Food Chemistry*, 53(10), 3986–3994. <https://doi.org/10.1021/jf047953r>

Saccomanno, B., Chambers, A. H., Hayes, A., Mackay, I., McWilliam, S. C., & Trafford, K. (2017). Starch granule morphology in oat endosperm. *Journal of Cereal Science*, 73, 46–54. <https://doi.org/10.1016/j.jcs.2016.10.011>

Saint-Michel, F., Chazeau, L., Cavaillé, J., & Chabert, E. (2006). Mechanical properties of high density polyurethane foams: I. Effect of the density. *Composites Science and Technology*, 66(15), 2700–2708. <https://doi.org/10.1016/j.compscitech.2006.03.009>

Salt, L. J., Wilde, P. J., Georget, D., Wellner, N., Skeggs, P. K., & Mills, E. N. C. (2006). Composition and surface properties of dough liquor. *Journal of Cereal Science*, 43(3), 284–292. <https://doi.org/10.1016/j.jcs.2005.12.013>

Salvador, A., Sanz, T., & Fiszman, S. M. (2006). Dynamic rheological characteristics of wheat flour-water doughs. Effect of adding NaCl, sucrose and yeast. *Food Hydrocolloids*, 20(6), 780–786. <https://doi.org/10.1016/j.foodhyd.2005.07.009>

Sarvestani, A. S. (2016). On the emergence of the Payne effect in polymer melts reinforced with nanoparticles. *Macromolecular Theory and Simulations*, 25(3), 312–321. <https://doi.org/10.1002/mats.201600001>

Schalk, K., Lexhaller, B., Koehler, P., & Scherf, K. A. (2017). Isolation and characterization of gluten protein types from wheat, rye, barley and oats for use as reference materials. *PLOS ONE*, 12(2), e0172819. <https://doi.org/10.1371/journal.pone.0172819>

Scherf, K. A., & Köhler, P. (2016). Weizen und Gluten: Technologische und gesundheitliche Aspekte. *Ernährungs Umschau*, 63(8), 166–175. <https://doi.org/10.4455/eu.2016.035>

Schiedt, B., Baumann, A., Conde-Petit, B., & Vilgis, T. A. (2013). Short- and long-range interactions governing the viscoelastic properties during wheat dough and model dough development. *Journal of Texture Studies*, 44(4), 317–332. <https://doi.org/10.1111/jtxs.12027>

Schmid, M., Wieser, H., & Koehler, P. (2016). Isolation and characterization of high-molecular-weight (HMW) gliadins from wheat flour. *Cereal Chemistry*, 93(6), 536–542. <https://doi.org/10.1094/CCHEM-04-16-0078-R>

Schofield, J. D., Bottomley, R. C., Timms, M. F., & Booth, M. R. (1983). The effect of heat on wheat gluten and the involvement of sulphhydryl-disulphide interchange reactions. *Journal of Cereal Science*, 1(4), 241–253. [https://doi.org/10.1016/S0733-5210\(83\)80012-5](https://doi.org/10.1016/S0733-5210(83)80012-5)

Schopf, M., Wehrli, M. C., Becker, T., Jekle, M., & Scherf, K. A. (2021). Fundamental characterization of wheat gluten. *European Food Research and Technology*, 247(4), 985–997. <https://doi.org/10.1007/s00217-020-03680-z>

Seighalani, F. Z. B., McMahon, D. J., & Sharma, P. (2021). Determination of critical gel-sol transition point of highly concentrated micellar casein concentrate using multiple waveform rheological technique. *Food Hydrocolloids*, 120, 106886. <https://doi.org/10.1016/j.foodhyd.2021.106886>

Sentmanat, M. L. (2004). Miniature universal testing platform: From extensional melt rheology to solid-state deformation behavior. *Rheologica Acta*, 43(6), 657–669. <https://doi.org/10.1007/s00397-004-0405-4>

Shah, P., Campbell, G. M., McKee, S. L., & Rielly, C. D. (1998). Proving of bread dough: Modelling the growth of individual bubbles. *Food and Bioproducts Processing: Transactions of the Institution of Chemical Engineers, Part C*, 76(2), 73–79. <https://doi.org/10.1205/096030898531828>

Shimiya, Y., & Nakamura, K. (1997). Changes in size of gas cells in dough and bread during breadmaking and calculation of critical size of gas cells that expand. *Journal of Texture Studies*, 28(3), 273–288. <https://doi.org/10.1111/j.1745-4603.1997.tb00117.x>

Shimiya, Y., & Yano, T. (1988). Rates of shrinkage and growth of air bubbles entrained in wheat flour dough. *Agricultural and Biological Chemistry*, 52(11), 2879–2883. <https://doi.org/10.1080/00021369.1988.10869152>

Singh, N., & Kaur, L. (2004). Morphological, thermal, rheological and retrogradation properties of potato starch fractions varying in granule size. *Journal of the Science of Food and Agriculture*, 84(10), 1241–1252. <https://doi.org/10.1002/jsfa.1746>

Sliwinski, E. L., van der Hoef, F., Kolster, P., & van Vliet, T. (2004). Large-deformation properties of wheat dough in uni- and biaxial extension. Part II. Gluten dough. *Rheologica Acta*, 43(4), 321–332. <https://doi.org/10.1007/s00397-003-0345-4>

Song, M. K., Guo, X. N., & Zhu, K. X. (2024). Unraveling the impacts of fermentation methods on the protein structural, foaming and air-water interfacial properties of buckwheat steamed bread dough liquor. *Food Bioscience*, 59, 104026. <https://doi.org/10.1016/j.fbio.2024.104026>

Sroan, B. S., Bean, S. R., & MacRitchie, F. (2009). Mechanism of gas cell stabilization in bread making. I. The primary gluten-starch matrix. *Journal of Cereal Science*, 49(1), 32–40. <https://doi.org/10.1016/j.jcs.2008.07.003>

Sroan, B. S., & MacRitchie, F. (2009). Mechanism of gas cell stabilization in breadmaking. II. The secondary liquid lamellae. *Journal of Cereal Science*, 49(1), 41–46. <https://doi.org/10.1016/j.jcs.2008.07.004>

Stading, M. (2008). Determination of extensional rheological properties by hyperbolic contraction flow. *The XVth International Congress on Rheology, The Society of Rheology 80th Annual IngMeet*, 1114–1116. <https://doi.org/10.1063/1.2964484>

Stading, M., & Bohlin, L. (2001). Contraction flow measurements of extensional properties. *Annual Transactions-Nordic Rheology Society*, 8, 181–186.

Steffe, J. F. (1996). *Rheological Methods in Food Process Engineering*. Freeman Press.

Taghizadeh, A., & Favis, B. D. (2013). Effect of high molecular weight plasticizers on the gelatinization of starch under static and shear conditions. *Carbohydrate Polymers*, 92(2), 1799–1808. <https://doi.org/10.1016/j.carbpol.2012.11.018>

Tamás, M. J., Luyten, K., Sutherland, F. C. W., Hernandez, A., Albertyn, J., Valadi, H., Li, H., Prior, B. A., Kilian, S. G., Ramos, J., Gustafsson, L., Thevelein, J. M., & Hohmann, S. (1999). Fps1p controls the accumulation and release of the compatible solute glycerol in yeast osmoregulation. *Molecular Microbiology*, 31(4), 1087–1104. <https://doi.org/10.1046/j.1365-2958.1999.01248.x>

Tang, X. C., Pikal, M. J., & Taylor, L. S. (2002). The effect of temperature on hydrogen bonding in crystalline and amorphous phases in dihydropyrine calcium channel blockers. *Pharmaceutical Research*, 19(4), 484–490. <https://doi.org/10.1023/A:1015199713635>

Thanhaeuser, S. M., Wieser, H., & Koehler, P. (2014). Correlation of quality parameters with the baking performance of wheat flours. *Cereal Chemistry*, 91(4), 333–341. <https://doi.org/10.1094/CCHEM-09-13-0194-CESI>

The Insight Partners. (2023). *Bread Market to Forecast 2030 – COVID-19 Impact and Global Analysis – by Type, Category, Distribution Channel, and Geography*. <https://www.theinsightpartners.com/pr/bread-market>

Timmermans, E., Langie, I., Bautil, A., Brijs, K., Buvé, C., Van Loey, A., Scheirlinck, I., Van der Meulen, R., & Courtin, C. M. (2023). Study of the fermentation characteristics of non-conventional yeast strains in sweet dough. *Foods*, 12(4), 830. <https://doi.org/10.3390/foods12040830>

Tronsmo, K. M., Magnus, E. M., Baardseth, P., Schofield, J. D., Aamodt, A., & Færgestad, E. M. (2003). Comparison of small and large deformation rheological properties of wheat dough and gluten. *Cereal Chemistry*, 80(5), 587–595. <https://doi.org/10.1094/CCHEM.2003.80.5.587>

Tronsmo, K. M., Magnus, E. M., Færgestad, E. M., & Schofield, J. D. (2003). Relationships between gluten rheological properties and hearth loaf characteristics. *Cereal Chemistry*, 80(5), 575–586. <https://doi.org/10.1094/CCHEM.2003.80.5.575>

Tsai, M. L., Li, C. F., & Lii, C. Y. (1997). Effects of granular structures on the pasting behaviors of starches. *Cereal Chemistry*, 74(6), 750–757. <https://doi.org/10.1094/CCHEM.1997.74.6.750>

Turbin-Orger, A., Babin, P., Boller, E., Chaunier, L., Chiron, H., Della Valle, G., Dendievel, R., Réguerre, A. L., & Salvo, L. (2015). Growth and setting of gas bubbles in a viscoelastic matrix imaged by X-ray microtomography: The evolution of cellular structures in fermenting wheat flour dough. *Soft Matter*, 11(17), 3373–3384. <https://doi.org/10.1039/c5sm00100e>

Turbin-Orger, A., Boller, E., Chaunier, L., Chiron, H., Della Valle, G., & Réguerre, A. L. (2012). Kinetics of bubble growth in wheat flour dough during proofing studied by computed X-ray micro-tomography. *Journal of Cereal Science*, 56(3), 676–683. <https://doi.org/10.1016/j.jcs.2012.08.008>

Turbin-Orger, A., Shehzad, A., Chaunier, L., Chiron, H., & Della Valle, G. (2016). Elongational properties and proofing behaviour of wheat flour dough. *Journal of Food Engineering*, 168, 129–136. <https://doi.org/10.1016/j.jfoodeng.2015.07.029>

Udyarajan, C. T., Horne, D. S., & Lucey, J. A. (2007). Use of time-temperature superposition to study the rheological properties of cheese during heating and cooling. *International Journal of Food Science and Technology*, 42(6), 686–698. <https://doi.org/10.1111/j.1365-2621.2006.01468.x>

Ulbrich, M., Natan, C., & Flöter, E. (2014). Acid modification of wheat, potato, and pea starch applying gentle conditions - Impacts on starch properties. *Starch - Stärke*, 66(9–10), 903–913. <https://doi.org/10.1002/star.201400089>

Upadhyay, R., Ghosal, D., & Mehra, A. (2012). Characterization of bread dough: Rheological properties and microstructure. *Journal of Food Engineering*, 109(1), 104–113. <https://doi.org/10.1016/j.jfoodeng.2011.09.028>

Uthayakumaran, S., Newberry, M., Phan-Thien, N., & Tanner, R. (2002). Small and large strain rheology of wheat gluten. *Rheologica Acta*, 41(1), 162–172. <https://doi.org/10.1007/s003970200015>

Van Boeckstaele, F. (2011). *Changes in rheology and microstructure of bread dough*. Ghent University, Belgium.

Van Soest, J. J. G., Bezemer, R. C., De Wit, D., & Vliegenthart, J. F. G. (1996). Influence of glycerol on the melting of potato starch. *Industrial Crops and Products*, 5(1), 1–9. [https://doi.org/10.1016/0926-6690\(95\)00047-X](https://doi.org/10.1016/0926-6690(95)00047-X)

Van Vliet, T., Janssen, A. M., Bloksma, A. H., & Walstra, P. (1992). Strain hardening of dough as a requirement for gas retention. *Journal of Texture Studies*, 23(4), 439–460. <https://doi.org/10.1111/j.1745-4603.1992.tb00033.x>

Vanin, F. M., Lucas, T., Trystram, G., & Michon, C. (2018). Biaxial extensional viscosity in wheat flour dough during baking. *Journal of Food Engineering*, 236, 29–35. <https://doi.org/10.1016/j.jfoodeng.2018.05.007>

Verbauwheide, A. E., Lambrecht, M. A., Jekle, M., Lucas, I., Fierens, E., Shegai, O., Brijs, K., & Delcour, J. A. (2020). Microscopic investigation of the formation of a thermoset wheat gluten network in a model system relevant for bread making. *International Journal of Food Science and Technology*, 55(2), 891–898. <https://doi.org/10.1111/ijfs.14359>

Verheyen, C. (2016). *Structural investigations of yeasted wheat dough - the impact of CO₂ and glutathione*. Technical University of Munich.

Verheyen, C., Albrecht, A., Becker, T., & Jekle, M. (2016). Destabilization of wheat dough: Interrelation between CO₂ and glutathione. *Innovative Food Science and Emerging Technologies*, 34, 320–325. <https://doi.org/10.1016/j.ifset.2016.03.006>

Verheyen, C., Albrecht, A., Herrmann, J., Strobl, M., Jekle, M., & Becker, T. (2015). The contribution of glutathione to the destabilizing effect of yeast on wheat dough. *Food Chemistry*, 173, 243–249. <https://doi.org/10.1016/j.foodchem.2014.10.021>

Verheyen, C., Jekle, M., & Becker, T. (2014). Effects of *Saccharomyces cerevisiae* on the structural kinetics of wheat dough during fermentation. *LWT - Food Science and Technology*, 58, 194–202. <https://doi.org/10.1016/j.lwt.2014.02.050>

Vermeylen, R., Goderis, B., Reynaers, H., & Delcour, J. A. (2005). Gelatinisation related structural aspects of small and large wheat starch granules. *Carbohydrate Polymers*, 62(2), 170–181. <https://doi.org/10.1016/j.carbpol.2005.07.021>

Vidal, L. M., Braun, A., Jekle, M., & Becker, T. (2022). Micro-scale shear kneading—gluten network development under multiple stress–relaxation steps and evaluation via multiwave rheology. *Polymers*, 14(4), 846. <https://doi.org/10.3390/polym14040846>

Vidal, L. M., Ewigmann, H., Schuster, C., Alpers, T., Scherf, K. A., Jekle, M., & Becker, T. (2023). Microscopic analysis of gluten network development under shear load—combining confocal laser scanning microscopy with rheometry. *Journal of Texture Studies*, 54(6), 926–935. <https://doi.org/10.1111/jtxs.12796>

Vilgis, T. A. (2015). Soft matter food physics - The physics of food and cooking. *Reports on Progress in Physics*, 78(12). <https://doi.org/10.1088/0034-4885/78/12/124602>

Vliet, T. van, Janssen, A. M., Bloksma, A. H., & Walstra, P. (1992). Strain hardening of dough as a requirement for gas retention. *Journal of Texture Studies*, 23(4), 439–460. <https://doi.org/10.1111/j.1745-4603.1992.tb00033.x>

Wang, H., Liu, J., Zhang, Y., Li, S., Liu, X., Zhang, Y., Zhao, X., Shen, H., Xie, F., Xu, K., & Zhang, H. (2024). Insights into the hierarchical structure and physicochemical properties of starch isolated from fermented dough. *International Journal of Biological Macromolecules*, 267, 131315. <https://doi.org/10.1016/j.ijbiomac.2024.131315>

Wang, J., Yue, Y., Liu, T., Zhang, B., Wang, Z., & Zhang, C. (2017). Change in glutenin macropolymer secondary structure in wheat sourdough fermentation by FTIR. *Interdisciplinary Sciences – Computational Life Sciences*, 9(2), 247–253. <https://doi.org/10.1007/s12539-016-0206-3>

Wang, P., Zou, M., Tian, M., Gu, Z., & Yang, R. (2018). The impact of heating on the unfolding and polymerization process of frozen-stored gluten. *Food Hydrocolloids*, 85, 195–203. <https://doi.org/10.1016/j.foodhyd.2018.07.019>

Wang, S., Zhang, X., Wang, S., & Copeland, L. (2016). Changes of multi-scale structure during mimicked DSC heating reveal the nature of starch gelatinization. *Scientific Reports*, 6(1), 28271. <https://doi.org/10.1038/srep28271>

Wang, X. Y., Guo, X. N., & Zhu, K. X. (2016). Polymerization of wheat gluten and the changes of glutenin macropolymer (GMP) during the production of Chinese steamed bread. *Food Chemistry*, 201, 275–283. <https://doi.org/10.1016/j.foodchem.2016.01.072>

Warasitthinon, N., Genix, A., Sztucki, M., Oberdisse, J., & Robertson, C. G. (2019). The payne effect: Primarily polymer-related or filler-related phenomenon? *Rubber Chemistry and Technology*, 92(4), 599–611. <https://doi.org/10.5254/rct.19.80441>

Weegels, P.L., Verhoek, J. A., de Groot, A. M. G., & Hamer, R. J. (1994). Effects on gluten of heating at different moisture contents. I. Changes in functional properties. *Journal of Cereal Science*, 19(1), 31–38. <https://doi.org/10.1006/jcrs.1994.1005>

Weegels, Peter L., Groeneweg, F., Esselink, E., Smit, R., Brown, R., & Ferdinando, D. (2003). Large and fast deformations crucial for the rheology of proofing dough. *Cereal Chemistry*, 80(4), 424–426. <https://doi.org/10.1094/CCHEM.2003.80.4.424>

Wehrle, K., Grau, H., & Arendt, E. K. (1997). Effects of lactic acid, acetic acid, and table salt on fundamental rheological properties of wheat dough. *Cereal Chemistry*, 74(6), 739–744. <https://doi.org/https://doi.org/10.1094/CCHEM.1997.74.6.739>

Wehrli, M. C., Ini, S., Jekle, M., Kratky, T., & Becker, T. (2023). Resilience study of wheat protein networks with large amplitude oscillatory shear rheology. *LWT - Food Science and Technology*, 178, 114596. <https://doi.org/10.1016/j.lwt.2023.114596>

Wehrli, M. C., Kratky, T., Schopf, M., Scherf, K. A., Becker, T., & Jekle, M. (2021). Thermally induced gluten modification observed with rheology and spectroscopies. *International Journal of Biological Macromolecules*, 173, 26–33. <https://doi.org/10.1016/j.ijbiomac.2021.01.008>

Wellner, N., Mills, E. N. C., Brownsey, G., Wilson, R. H., Brown, N., Freeman, J., Halford, N. G., Shewry, P. R., & Belton, P. S. (2005). Changes in protein secondary structure during gluten deformation studied by dynamic fourier transform infrared spectroscopy. *Biomacromolecules*, 6(1), 255–261.

Wenhao, L., Yulin, S., Xinlong, X., Qingui, L., Jianmei, Z., Shaohui, O., & Guoquan, Z. (2013). Physicochemical properties of A- and B - starch granules isolated from hard red and soft red winter wheat. *Journal of Agricultural and Food Chemistry*, 61(26), 6477–6484. <https://doi.org/https://doi.org/10.1021/jf400943h>

Wieser, H., & Kieffer, R. (2001). Correlations of the amount of gluten protein types to the technological properties of wheat flours determined on a micro-scale. *Journal of Cereal Science*, 34(1), 19–27. <https://doi.org/10.1006/jcrs.2000.0385>

Wieser, Herbert. (2007). Chemistry of gluten proteins. *Food Microbiology*, 24(2), 115–119. <https://doi.org/10.1016/j.fm.2006.07.004>

Wieser, Herbert, Koehler, P., & Scherf, K. A. (2023a). Chemistry of wheat gluten proteins: Quantitative composition. *Cereal Chemistry*, 100(1), 36–55. <https://doi.org/10.1002/cche.10553>

Wieser, Herbert, Koehler, P., & Scherf, K. A. (2023b). Chemistry of wheat gluten proteins: Qualitative composition. *Cereal Chemistry*, 100(1), 23–35. <https://doi.org/10.1002/cche.10572>

Wieser, Herbert, Mueller, K. J., & Koehler, P. (2009). Studies on the protein composition and baking quality of einkorn lines. *European Food Research and Technology*, 229(3), 523–532. <https://doi.org/10.1007/s00217-009-1081-5>

Wikström, K., & Bohlin, L. (1999a). Extensional flow studies of wheat flour dough. II. Experimental method for measurements in constant extension rate squeezing flow and application to flours varying in breadmaking performance. *Journal of Cereal Science*, 29(3), 227–234. <https://doi.org/10.1006/jcrs.1999.0252>

Wikström, K., & Bohlin, L. (1999b). Extensional flow studies of wheat flour dough. I. Experimental method for measurements in contraction flow geometry and application to flours varying in breadmaking performance. *Journal of Cereal Science*, 29(3), 217–226. <https://doi.org/10.1006/jcrs.1999.0251>

Wilderjans, E., Pareyt, B., Goesaert, H., Brijs, K., & Delcour, J. A. (2008). The role of gluten in a pound cake system: A model approach based on gluten-starch blends. *Food Chemistry*, 110(4), 909–915. <https://doi.org/10.1016/j.foodchem.2008.02.079>

Xu, F., Hu, H., Liu, Q., Dai, X., & Zhang, H. (2017). Rheological and microstructural properties of wheat flour dough systems added with potato granules. *International Journal of Food Properties*, 20(1), 1145–1157. <https://doi.org/10.1080/10942912.2017.1337791>

Yang, P., & Mather, P. T. (2014). Thermal analysis to determine various forms of water present in hydrogels. *TA Instruments*, 1–4.
<http://molbiol.ru/forums/index.php?act=Attach&type=post&id=220252>

Yazar, G., Duvarci, O. C., Tavman, S., & Kokini, J. L. (2016a). Effect of mixing on LAOS properties of hard wheat flour dough. *Journal of Food Engineering*, 190, 195–204.
<https://doi.org/10.1016/j.jfoodeng.2016.06.011>

Yazar, G., Duvarci, O., Tavman, S., & Kokini, J. L. (2016b). Non-linear rheological properties of soft wheat flour dough at different stages of farinograph mixing. *Applied Rheology*, 26(5), 1–11. <https://doi.org/10.3933/ApplRheol-26-52508>

Yıldırım-Mavis, C., Yilmaz, M. T., Dertli, E., Arıcı, M., & Ozmen, D. (2019). Non-linear rheological (LAOS) behavior of sourdough-based dough. *Food Hydrocolloids*, 96, 481–492. <https://doi.org/10.1016/j.foodhyd.2019.05.055>

Yue, Q., Li, M., Liu, C., Li, L., Zheng, X., & Bian, K. (2020). Extensional rheological properties in mixed and fermented/rested dough and relationships with steamed bread quality. *Journal of Cereal Science*, 93, 102968. <https://doi.org/10.1016/j.jcs.2020.102968>

Zhou, N., Schifferdecker, A. J., Gamero, A., Compagno, C., Boekhout, T., Piškur, J., & Knecht, W. (2017). Kazachstanian gamospores and Wickerhamomyces subpelliculosus: Two alternative baker's yeasts in the modern bakery. *International Journal of Food Microbiology*, 250, 45–58. <https://doi.org/10.1016/j.ijfoodmicro.2017.03.013>

Zudaire, E., Gambardella, L., Kurcz, C., & Vermeren, S. (2011). A computational tool for quantitative analysis of vascular networks. *PLoS ONE*, 6(11), e27385.
<https://doi.org/10.1371/journal.pone.0027385>

Zuo, Y., Gu, J., Tan, H., & Zhang, Y. (2015). Thermoplastic starch prepared with different plasticizers: Relation between degree of plasticization and properties. *Journal Wuhan University of Technology, Materials Science Edition*, 30(2), 423–428.
<https://doi.org/10.1007/s11595-015-1164-z>

7 Appendix

7.1 Reviewed paper

1. Alpers, T., Tauscher, V., Steglich, T., Becker, T. & Jekle, M. (2021). The self-enforcing starch–gluten system—Strain–dependent effects of yeast metabolites on the polymeric matrix. *Polymers*. 13(1), 30.
<https://doi.org/10.3390/polym13010030>
2. Alpers, T., Olma, J., Jekle, M. & Becker, T. (2022). Relation between polymer transitions and the extensional viscosity of dough systems during thermal stabilization assessed by lubricated squeezing flow. *Food Chemistry*. 389, 133048.
<https://doi.org/10.1016/j.foodchem.2022.133048>
3. Alpers, T., Becker, T. & Jekle, M. (2023). Strain-dependent assessment of dough's polymer structure and functionality during the baking process. *PLoS One* 18(3), e0282670. <https://doi.org/10.1371/journal.pone.0282670>
4. Alpers, T., Panoch, D., Jekle, M. & Becker, T. (2024). New insights into crumb formation in model systems: Effects of yeast metabolites and hydration level by means of multiwave rheology. *Food Hydrocolloids*. 155, 110184.
<https://doi.org/10.1016/j.foodhyd.2024.110184>

7.2 Oral presentations

1. Alpers, T., Jekle, M., Becker, T. (2017). Hefe im Fokus: Nutzung unscheinbarer Chancen zur Verbesserung der Backwarenqualität. 6. WIG Frühjahrstagung, Freising, Germany.
2. Alpers, T., Jekle, M., Becker, T. (2018). Praxisnahe Erfassung der Verarbeitungseigenschaften fermentierter Teige. 7. WIG Frühjahrstagung, Freising, Germany.
3. Alpers, T., Becker, T., Jekle, M. (2019). Auf dem Weg vom Teig zur Backware – Nutzung des Texture Analysers zur Analyse backprozessrelevanter Parameter. Winopal Hausmesse, Hannover, Germany.
4. Alpers, T., Becker, T., Jekle, M. (2019). Aufklärung des Einflusses strukturrelevanter Hefemetabolite auf das dehnrrheologische Verhalten von Weizenteigen. 5. D-A-CH Tagung für angewandte Getreidewissenschaften, Nyon, Switzerland.
5. Alpers, T., Jekle, M., Becker, T. (2019). Investigation of strain-depended effects of yeast metabolites on the dough matrix. 18th European Young Cereal Scientists and Technologists Workshop, San Benedetto del Tronto, Italy.
6. Alpers, T., Jekle, M., Becker, T. (2019). On traces of yeast – Exploring the structure-functionality of yeast metabolites by fundamental extensional and shear rheology. 19th ICC Conference 2019, Vienna, Austria.

7. Alpers, T., Becker, T., Jekle, M. (2020). Relation between polymer transitions and the temperature-dependent extensional viscosity of dough systems during thermal stabilization accessed by lubricated squeezing flow. 34th EFFoST International Conference, online.
8. Alpers, T., Eichhorn, M., Becker, T., Jekle, M. (2021). Alles nur Gas? – Einblicke zum Einfluss von Hefe auf die Teigstruktur in Theorie und Praxis. WIG Online Edition, online.
9. Alpers, T., Becker, T. (2024). Strain-dependent assessment of dough's polymer structure and functionality during the baking process. 35th VH Yeast Conference, Berlin, Germany.